

PREDICTING DEBRIS YIELD  
USING ARTIFICIAL INTELLIGENCE MODELS

by

Zhiqing Kou

---

A Dissertation Presented to the  
FACULTY OF THE USC GRADUATE SCHOOL  
UNIVERSITY OF SOUTHERN CALIFORNIA  
In Partial Fulfillment of the  
Requirements for the Degree  
DOCTOR OF PHILOSOPHY  
(CIVIL ENGINEERING)

August 2010

Copyright 2010

Zhiqing Kou

## **Dedication**

I dedicate this thesis to my grandma, my parents, and my husband.  
Without their understanding, support, and love, this work cannot be completed.

## **Acknowledgements**

I am very grateful to my supervisor, Professor Jiin-Jen Lee, for his encouragement, guidance and support not just in financial, but morally and spiritually from the initial to the final level. I whole heartedly thank him for his kindness and patience.

I also want to express my gratitude to my colleagues who helped me gather data and needed information to complete this work: Ben Williamdson, Chanin Chaun-Im, Hyoung-Jin Kim, Jay Pak, Jen Chang, Mehrdad Bozorgnia, Xiuying Xing, and Yuan-Hung Tan.

# Table of Contents

Dedication .....	ii
Acknowledgements .....	iii
List of Tables .....	vii
List of Figures .....	x
Abstract .....	xvi
Chapter 1: Introduction .....	1
1.1 General .....	1
1.2 The Estimation of Debris Yield .....	3
1.3 ANN Models to Estimate Debris Yield .....	6
1.4 Neural Fuzzy System and Fuzzy Neural Network to Estimate Debris Yield .....	9
1.5 Objectives of the Present Study .....	10
Chapter 2: Review of Literature .....	12
2.1 Background of Debris Yield Estimation .....	12
2.2 Use of ANN in Hydrologic Applications .....	23
2.2.1 Use of ANN in Rainfall-Runoff Process .....	23
2.2.2 Use of ANN in Streamflow .....	25
2.2.3 Use of ANN in Groundwater .....	26
2.2.4 Use of ANN in Debris Yield .....	27
2.3 Use of Neural Fuzzy System and Fuzzy Neural Network in Hydrologic Modeling .....	29
Chapter 3: Methodology of Modeling .....	33
3.1 Location of Studied Debris Basins and Data Sources .....	33
3.2 ANN Model .....	40
3.2.1 Introduction of ANN Model .....	40
3.2.2 Selection of Input and Output Variables .....	42
3.2.2 Separation of Calibration and Validation Data .....	47
3.2.3 Preprocessing of Data .....	49
3.2.4 Determination of ANN Architecture .....	50
3.2.4.1 Geometry of A Neural Network .....	50
3.2.4.2 Transfer Function .....	53
3.2.4.3 Initial Selection of Connection Weights and Biases .....	54
3.2.5 Training .....	55
3.2.5.1 BP Training Algorithm .....	56

3.2.5.2	Variations of BP Algorithm .....	57
3.3	NFS and FNN Models .....	60
3.3.1	ANFIS Model .....	61
3.3.2	GD-FNN Model .....	65
3.4	Sensitivity Analysis .....	73
Chapter 4: Presentation and Discussion of Results.....		76
4.1	Estimation of Sequent Debris Yield.....	76
4.1.1	Case 1 .....	77
4.1.2	Case 2 .....	81
4.1.3	Case 3 .....	84
4.1.4	Discussion .....	86
4.2	Estimation of Unit Debris Yield.....	89
4.2.1	Case 4 .....	91
4.2.1.1	ANN Model .....	92
4.2.1.2	ANFIS Model.....	97
4.2.1.3	GD-FNN Model .....	100
4.2.2	Case 5 .....	103
4.2.2.1	ANN Model .....	103
4.2.2.2	ANFIS Model.....	108
4.2.2.3	GD-FNN Model .....	110
4.2.3	Case 6 .....	113
4.2.3.1	ANN Model .....	113
4.2.3.2	ANFIS Model.....	117
4.2.3.3	GD-FNN Model .....	120
4.2.4	Case 7 .....	123
4.2.4.1	ANN Model .....	123
4.2.4.2	ANFIS Model.....	127
4.2.4.3	GD-FNN Model .....	130
4.2.5	Overall Discussion.....	132
4.2.5	Case 8 .....	135
4.2.5.1	Case 8(a) .....	136
4.2.5.2	Case 8 (b) .....	139
4.2.5.3	Case 8 (c) .....	141
4.2.5.4	Case 8 (d) .....	143
4.2.6	Case 9 .....	149
4.2.6.1	Case 9(a) .....	150
4.2.6.2	Case 9(b) .....	152
4.2.6.3	Case 9(c) .....	155
4.2.6.4	Case 9(d) .....	157
4.2.7	Case 10 .....	163
4.2.7.1	Case 10(a) .....	164
4.2.7.2	Case 10(b) .....	167

4.2.7.3 Case 10(c) .....	169
4.2.7.4 Case 10(d) .....	171
4.2.8 Case 11 .....	177
4.2.8.1 Case 11(a) .....	178
4.2.8.2 Case 11(b) .....	180
4.2.8.3 Case 11(c) .....	183
4.2.8.4 Case 11(d) .....	185
4.2.9 Case 12 .....	191
4.2.10 Case 13 .....	198
4.2.11 Case 14 .....	203
4.2.12 Case 15 .....	208
 Chapter 5: Summary and Conclusion .....	 213
5.1 Summary and Conclusion .....	213
5.2 Recommendation for Future Study .....	220
 References .....	 221

## List of Tables

Table 1:	Summary of input parameters for each case .....	75
Table 2:	Summary of the performance of ANN models for Case 1 .....	78
Table 3:	Summary of calibration and validation results by two models for Case 1 .....	80
Table 4:	Summary of the performance of ANN models for Case 2 .....	82
Table 5:	Summary of calibration and validation results by two models for Case 2 .....	83
Table 6:	Summary of the performance of ANN models for Case 3 .....	85
Table 7:	Comparison of ANN models performance .....	87
Table 8:	Summary of the performances of ANN models trained by the BRBP algorithm for Case 4 .....	94
Table 9:	Summary of the performances of ANN models trained by the LM algorithm for Case 4 .....	95
Table 10:	Summary of fuzzy rules for Case 4 .....	98
Table 11:	Summary of the performances of ANN models trained by the BRBP algorithm for Case 5 .....	104
Table 12:	Summary of the performances of ANN models trained by the LM algorithm for Case 5 .....	106
Table 13:	Summarization of fuzzy rules for Case 5 .....	108
Table 14:	Summary of the performances of ANN models trained by the BRBP algorithm for Case 6 .....	114
Table 15:	Summary of the performances of ANN models trained by the LM algorithm for Case 6 .....	116
Table 16:	Summary of the performances of ANN models trained by the BRBP algorithm for Case 7 .....	124

Table 17: Summary of the performances of ANN models trained by the LM algorithm for Case 7 .....	126
Table 18: The summary of all model performance from Case 4 to Case 7 .....	133
Table 19: Summary of the performances of ANN models for Case 8(a).....	137
Table 20: Summary of the performances of ANN models for Case 8(b).....	140
Table 21: Summary of the performances of ANN models for Case 8(c) .....	141
Table 22: Summary of the performances of ANN models for Case 8(d).....	143
Table 23: Comparison of ANN models performance for Case 8.....	146
Table 24: Measured, the USACE method, and ANN model (5,6,6,1) estimated unit debris yield for Case 8 .....	147
Table 25: Summary of the performances of ANN models for Case 9(a).....	151
Table 26: Summary of the performances of ANN models for Case 9(b).....	153
Table 27: Summary of the performances of ANN models for Case 9(c) .....	155
Table 28: Summary of the performances of ANN models for Case 9(d).....	157
Table 29: Comparison of ANN models performance for Case 9.....	160
Table 30: Measured, the USACE method, and the best ANN model (7,5,2,1) estimated unit debris yield for Case 9 .....	161
Table 31: Summary of the performances of ANN models for Case 10(a).....	165

Table 32: Summary of the performances of ANN models for Case 10(b).....	167
Table 33: Summary of the performances of ANN models for Case 10(c).....	169
Table 34: Summary of the performances of ANN models for Case 10(d).....	171
Table 35: Comparison of ANN models performance for Case 10.....	173
Table 36: Measured, the USACE method, and the best ANN model (7,5,3,1) estimated unit debris yield for Case 10 .....	174
Table 37: Summary of the performances of ANN models for Case 11(a).....	179
Table 38: Summary of the performances of ANN models for Case 11(b).....	181
Table 39: Summary of the performances of ANN models for Case 11(c).....	183
Table 40: Summary of the performances of ANN models for Case 11(d).....	186
Table 41: Comparison of ANN models performance for Case 11.....	188
Table 42: Measured, the USACE method, and the best ANN model (6,6,1,1) estimated unit debris yield for Case 11 .....	189
Table 43: Summary of the performances of ANN models for Case 12 .....	193
Table 44: Measured, the USACE method, and the best ANN model (4,6,3,1) estimated unit debris yield for Case 12 .....	195
Table 45: Measured, the USACE method, and the best ANN model (4,4,3,1) estimated unit debris yield for Case 13 .....	201
Table 46: Measured, the USACE method, and the best ANN model (4,4,5,1) estimated unit debris yield for Case 14 .....	205
Table 47: Measured, the USACE method, and the best ANN model (4,4,5,1) estimated unit debris yield for Case 15 .....	210

## List of Figures

Figure 1: Location of 14 small debris basins for sequent debris yield .....	37
Figure 2: Location of 36 small debris basins for unit debris yield.....	38
Figure 3: Location of 80 small debris basins for unit debris yield.....	39
Figure 4: Location of 7 large debris basins for unit debris yield .....	40
Figure 5: Schematic diagram of a three layer feed-forward ANN .....	41
Figure 6: Upstream collection area for Brand and Childs debris basin.....	46
Figure 7: Overlay of soil layer and Brand and Childs debris basin watershed.....	47
Figure 8: Basic configuration of fuzzy logic system .....	60
Figure 9: An ANFIS Structure .....	62
Figure 10: The architecture of the GD-FNN model.....	66
Figure 11: The flowchart of GD-FNN algorithm .....	72
Figure 12: Linear regression analysis between measured and ANN model estimated debris yield (a) Calibration Data Set (b). Validation Data Set for Case 1.....	81
Figure 13: Linear regression analysis between measured and ANN model estimated debris yield (a) Calibration Data Set (b) Validation Data Set for Case 2.....	84
Figure 14: Calibration and validation mean square error for (a) Case 1 (b) Case 3.....	88
Figure 15: Linear regression analysis between measured and ANN model (BRBP) estimated debris yield (a) Calibration Data Set (b) Validation Data Set for Case 4.....	96

Figure 16: Linear regression analysis between measured and ANN model (LM) estimated debris yield (a) Calibration Data Set (b) Validation Data Set for Case 4 .....	97
Figure 17: Membership functions for $\log A$ , $T1$ , and $\log I$ (Case 4).....	99
Figure 18: Linear regression analysis between measured and AN-FIS model estimated debris yield (a) Calibration Data Set (b) Validation Data Set for Case 4 .....	99
Figure 19: Membership functions for input variables (Case 4) .....	101
Figure 20: Linear regression analysis between measured and GD-FNN model estimated debris yield (a) Calibration Data Set (b) Validation Data Set for Case 4 .....	102
Figure 21: Linear regression analysis between measured and ANN model (BRBP) estimated debris yield (a) Calibration Data Set (b) Validation Data Set for Case 5.....	107
Figure 22: Linear regression analysis between measured and ANN model (LM) estimated debris yield (a) Calibration Data Set (b) Validation Data Set for Case 5 .....	107
Figure 23: Membership functions for $\log A$ , $\log R_r$ and DDM (Case 5) .....	109
Figure 24: Linear regression analysis between measured and AN-FIS model estimated debris yield (a) Calibration Data Set (b) Validation Data Set for Case 5 .....	109
Figure 25: Membership functions for each input variable (Case 5).....	111
Figure 26: Linear regression analysis between measured and GD-FNN model estimated debris yield (a) Calibration Data Set (b) Validation Data Set for Case 5 .....	112
Figure 27: Linear regression analysis between measured and ANN model (BRBP) estimated debris yield (a) Calibration Data Set (b) Validation Data Set for Case 6.....	116

Figure 28: Linear regression analysis between measured and ANN model (LM) estimated debris yield (a) Calibration Data Set (b) Validation Data Set for Case 6 .....	117
Figure 29: Membership functions for logA and ER (Case 6) .....	118
Figure 30: Linear regression analysis between measured and AN-FIS model estimated debris yield (a) Calibration Data Set (b) Validation Data Set for Case 6 .....	120
Figure 31: Membership functions for input variables (Case 6) .....	121
Figure 32: Linear regression analysis between measured and GD-FNN model estimated debris yield (a) Calibration Data Set (b) Validation Data Set for Case 6 .....	122
Figure 33: Linear regression analysis between measured and ANN model (BRBP) estimated debris yield (a) Calibration Data Set (b) Validation Data Set for Case 7 .....	125
Figure 34: Linear regression analysis between measured and ANN model (LM) estimated debris yield (a) Calibration Data Set (b) Validation Data Set for Case 7 .....	127
Figure 35: Membership functions for logA and TSL (Case 7).....	128
Figure 36: Linear regression analysis between measured and AN-FIS estimated debris yield (a) Calibration Data Set (b) Validation Data Set for Case 7 .....	129
Figure 37: Membership functions for each input variable (Case 7).....	131
Figure 38: Linear regression analysis between measured and GD-FNN estimated debris yield (a) Calibration Data Set (b) Validation Data Set for Case 7 .....	132
Figure 39: Linear regression analysis between measured and ANN model estimated debris yield (a) Calibration Data Set (b) Validation Data Set for Case 8(a) .....	138
Figure 40: Linear regression analysis between measured and ANN model estimated debris yield (a) Calibration Data Set (b) Validation Data Set for Case 8(b) .....	140

Figure 41: Linear regression analysis between measured and ANN model estimated debris yield (a) Calibration Data Set (b) Validation Data Set for Case 8(c).....	143
Figure 42: Linear regression analysis between measured and ANN model estimated debris yield (a) Calibration Data Set (b) Validation Data Set for Case 8(d) .....	145
Figure 43: Comparison between measured USACE and the best ANN model (5,6,6,1) estimated unit debris yield for Case 8.....	149
Figure 44: Linear regression analysis between measured and ANN model estimated debris yield (a) Calibration Data Set (b) Validation Data Set for Case 9(a) .....	152
Figure 45: Linear regression analysis between measured and ANN model estimated debris yield (a) Calibration Data Set (b) Validation Data Set for Case 9(b) .....	154
Figure 46: Linear regression analysis between measured and ANN model estimated debris yield (a) Calibration Data Set (b) Validation Data Set for Case 9(c).....	156
Figure 47: Linear regression analysis between measured and ANN model estimated debris yield (a) Calibration Data Set (b) Validation Data Set for Case 9(d) .....	159
Figure 48: Comparison between measured, USACE, and the best ANN model (7,5,2,1) estimated unit debris yield for Case 9.....	163
Figure 49: Linear regression analysis between measured and ANN model estimated debris yield (a) Calibration Data Set (b) Validation Data Set for Case 10(a) .....	166
Figure 50: Linear regression analysis between measured and ANN model estimated debris yield (a) Calibration Data Set (b) Validation Data Set for Case 10(b) .....	168
Figure 51: Linear regression analysis between measured and ANN model estimated debris yield (a) Calibration Data Set (b) Validation Data Set for Case 10(c).....	170

Figure 52: Linear regression analysis between measured and ANN model estimated debris yield (a) Calibration Data Set (b) Validation Data Set for Case 10(d) .....	172
Figure 53: Comparison between measured, USACE, and the best ANN model (7,5,3,1) estimated unit debris yield for Case 10.....	177
Figure 54: Linear regression analysis between measured and ANN model estimated debris yield (a) Calibration Data Set (b) Validation Data Set for Case 11(a) .....	180
Figure 55: Linear regression analysis between measured and ANN model estimated debris yield (a) Calibration Data Set (b) Validation Data Set for Case 11(b) .....	183
Figure 56: Linear regression analysis between measured and ANN model estimated debris yield (a) Calibration Data Set (b) Validation Data Set for Case 11(c).....	185
Figure 57: Linear regression analysis between measured and ANN model estimated debris yield (a) Calibration Data Set (b) Validation Data Set for Case 11(d) .....	187
Figure 58: Comparison between measured, USACE, and the best ANN model (6,6,1,1) estimated unit debris yield for Case 11.....	192
Figure 59: Linear regression analysis between measured and ANN model estimated debris yield (a) Calibration Data Set (b) Validation Data Set for Case 12.....	195
Figure 60: Comparison between measured, USACE and the best best ANN model (4,6,3,1) estimated unit debris yield for Case 12.....	198
Figure 61: Linear regression analysis between measured and ANN model estimated debris yield (a) Calibration Data Set (b) Validation Data Set for Case 13.....	200
Figure 62: Comparison between measured, USACE, and the best ANN model (4,4,3,1) estimated unit debris yield for Case 13.....	203

Figure 63: Linear regression analysis between measured and ANN model estimated debris yield (a) Calibration Data Set (b) Validation Data Set for Case 14.....	205
Figure 64: Comparison between measured, USACE, and the best ANN model (4,4,5,1) estimated unit debris yield for Case 14.....	207
Figure 65: Linear regression analysis between measured and ANN model estimated debris yield (a) Calibration Data Set (b) Validation Data Set for Case 15.....	209
Figure 66: Comparison between measured, USACE, and the best ANN model (4,4,5,1) estimated unit debris yield for Case 15.....	212

## **Abstract**

Artificial Neural Network is a very powerful computational tool for modeling very complicated and highly nonlinear problems in various fields. In this study, it is first applied to estimate accumulated debris yield in 14 debris basins within Los Angeles County, California as a result of a series of storm events from watersheds partially or totally burned by wildfires from 1984 to 2003. ANN models achieve very satisfactory modeling results as compared to a statistical model.

The ANN technique is then applied to forecast unit debris yield collected from 36 small debris basins within the county resulting from single significant storm events from 1938 to 1983. The same unit debris yield data is simulated by another two artificial intelligence models, Adaptive-Network-Based Fuzzy Inference System (ANFIS) and Generalized Dynamic Fuzzy Neural Network (GD-FNN) model. In addition to four basic input parameters: drainage area, watershed relief ratio, maximum one-hour rainfall intensity, and fire factor, six watershed morphological parameters such as elongation ratio, drainage density, hypsometric index, total stream length, mean bifurcation ratio, and transport efficiency factor are included as input parameters and their relative importance are determined through sensitivity analysis.

ANN models are also developed for modeling unit debris yield at 80 small debris basins. They are classified into five groups based on the relief ratios of their upstream watersheds: mild slope, steep slope, steeper slope, extreme steep

slope, and the steepest slope. In addition to four aforementioned basic input parameters, three soil properties including soil erodibility factor, permeability rate, and liquid limit are considered as input parameter one by one to study their impact on the simulation.

Unit debris yield collected from large watersheds with area between 10 and 25 mi<sup>2</sup>, between 25 and 50 mi<sup>2</sup>, and between 50 and 200 mi<sup>2</sup> are also simulated by neural network models. The modeling results indicate that the accuracy of unit debris yield estimated by ANN models is significantly higher than those obtained from ANFIS, GD-FNN model, and empirical equations developed by US Army Corps of Engineers.

# Chapter 1: Introduction

## 1.1 General

Debris flow is always described as saturated slurries of mud, poorly sorted sediments such as silt, sand, clay, gravel, and boulders, and all kinds of debris that can be washed off and transported through stream channels, or any downhill surfaces. It is one of the most dangerous natural hazards because of its abrupt occurrence without any warning or sign in advance and its catastrophic consequences for both structures and human lives. Although it is not easy to clarify the boundary between debris flow and mud flow, mud flow is distinguished by the relatively low percentage of sediment concentration from 45 to 60 percent in terms of volume and less variation in sediment sizes (Los Angeles County of Department of Public Works (LADPW), 1993). Entrained with water and air, both kinds of flows are multiphase and pick up poorly sorted sediments as they travel downstream (LADPW, 1993). Depending on the size of sediment, debris flow tends to move with a succession of surges with a steep front loaded with boulder-sized fragments, but mud flow transports fine materials with a surge interval from a few seconds to tens of minutes (Mainali and Rajaratnam, 1991). They can be induced by a large storm event on an erosive upland watershed, or even a small storm event on a watershed burned by wildfire, and they might be the outcome of some slope failure such as landslide.

Debris flow and mud flow are very common and widespread phenomena in the western US, and it is a major concern at southern California area where is high erosion area due to very active tectonic activity (Scott and Williams, 1978). The consequence of debris flow and/or mud flow to this highly populated residential and business area is more disastrous. Heavy development on alluvial fans and floodplains, and the frequent occurrence of wildfire in the summer and occasional intense rainfalls during the winter season in this area worsen the situation. In order to reduce economical loss and to protect the lowland areas, debris basins (or sedimentation basins) are built to trap sediments brought by debris flows or mud flows as water is flushed to downstream channels. Just within Los Angeles County, 157 debris basins with a total maximum design capacity of 7,780,900 cubic yards are built until 2005 (Los Angeles Hydrologic Report).

Solid materials such as sand, gravel, boulders, trees, etc., accumulated in a debris basin is called debris or sediment yield which can be roughly counted by cleanout trucks in the unit of volume. The estimation of debris yield is quite complicated and it depends on many factors such as watershed physiographic variables - watershed area and slope, watershed geology, soil condition, runoff, rainfall, vegetative coverage, and so on. However, some factor like runoff is not always available for small watershed (i.e. area less than 3 square miles), and spatial variance of vegetative coverage makes it difficult to be accounted for.

## 1.2 The Estimation of Debris Yield

Since an early documentation of debris and mud flows in 1897 (McGee, 1897), there is a growing interest among hydraulic engineers to study debris yield. Broadly speaking, the existing methods for estimating debris yield can be classified into three categories: empirical, conceptual, and physically-based models.

Empirical models generally identify the relationship between long historical records of inputs (rainfall, runoff, etc.) and sediment yields by using regression techniques. One of the widely used empirical equations, the Universal Soil Loss Equation (USLE), was developed by Williams and Berndt (1972) for the estimation of soil erosion per unit area of a watershed. With the inclusion of empirical constants representing rainfall characteristics, soil properties, and land surface conditions, the USLE was considered to be only good for small-sized areas. Most methods of estimating debris yield for southern California watersheds belong to this category, for example, Tatum's method (1963), debris yield method created by US Army Corps of Engineers, Los Angeles District (USACE) in 2000, and so on. Another recent achievement in this field is the Multi-Sequence Debris Prediction Model (MSDPM), (Pak, 2005; Pak and Lee, 2008). Considering both wildfire and storm impact on watershed erosion, the MSDPM predicts sequent debris yield based on seven parameters: watershed area, relief ratio, dimensionless fire factor, maximum 1-hr rainfall intensity, total rainfall amount, and two newly introduced factors: threshold maximum 1-hr

rainfall intensity and total minimum rainfall amount. If the total rainfall amount for a single storm event is less than the total minimum rainfall amount or the maximum 1-hr rainfall intensity of that event is less than the threshold maximum 1-hr rainfall intensity for that watershed, no debris will be deposited inside a debris basin from this event (Pak, 2005). These two new parameters were introduced to indicate sediment detachment and transport capacity by rainfall, or direct runoff. After calibrated with 17 years data from 1984 to 2000, the model was validated by the recent events after 2000 and showed good agreement with field collected debris yield.

Conceptual models divide the whole watershed into elements and calculate the detachment of soil by rain drops, sediment eroded and transported by overland flow within each element, and then sediment yield is routed from one element to another until finally reaches the concentration point, or the debris basin. The Areal Non-Point-Source Watershed Environment Response Simulation (ANSWERS, Beasley et al. 1980), one of the most commonly referenced conceptual, distributed models, was developed for predicting both runoff and sediment yield by employing five models: a hydrologic model, a sediment detachment/transport model, and three routing components to model overland, subsurface and channel flow. The first part of physically-based models is the same as the conceptual models – the division of whole watershed into elements or grids, but they typically involve solutions of a system of partial differential equations of mass, momentum, and energy conservation within the

watershed. Finite Difference Method (FDM) (Kothyari et al. 1997) and Finite Element Method (FEM) were applied to solve these equations under simplified ground topography and simplified flow condition. Most of the time, due to the lack of field data, the results obtained from physically-based model have to be compared with experimental results and their validity are yet to be definitely confirmed. It is also noteworthy that with the aid of Geographic Information System (GIS) technique the modeling of debris yield has been advanced. For example, Gupta and Solomon's (1977a, b) created distributed numerical model to estimate runoff and sediment discharge of ungaged rivers; Doten and his colleagues (2006) developed spatially distributed model for the dynamic prediction of sediment erosion and transport in mountainous forested watersheds, etc.

Many researchers believe empirical models are too simple to represent such a complicated process. For both conceptual and physically-based models, the prerequisite of huge amount of data at each element is a difficulty. Even if the data are available, physically-based models might suffer numerical modeling problems (e.g. instability and convergence). Artificial intelligence methods such as Artificial Neural Network (ANN) might be a good alternative due to its successful modeling many complicated and highly nonlinear hydrologic problems (ASCE, 2000b; Tokar and Markus, 2006; Jain and Indurthy, 2003; Coppola et al., 2003).

### **1.3 ANN Models to Estimate Debris Yield**

ANN was inspired by the functionality of our own brains and nerve cells. It consists of parallel processing structures that have large numbers of nodes, or neurons and many interconnections between them, which is the source of the power of ANN. Since the introduction of the concept of artificial neuron by McCulloch and Pitts in 1943, it has been used to do the same job as our brains, such as recognizing a familiar face, learning to speak and understand a natural language, and identifying handwritten characters (Dayhoff, 1990). But ANN had not been fully developed until the backpropagation (BP) training algorithm for feed-forward ANN was developed by Rumelhart and McClelland in 1986. Although it cannot be as 'smart' as a biological neuron system, ANN has been well-acknowledged to be able to model highly nonlinear relationship between inputs (i.e. independent variables), and outputs (i.e. dependent variables) and simulate new data to generate satisfactory results.

Without the consideration of explicit physical relations, ANN works well even when the training sets contain noise and measurement errors (ASCE, 2000a). It has been applied in many areas such as physics, biomedical engineering, electrical engineering, computer science, acoustics, image processing, and others. It has also been explored to many hydrology-related problems, for example, rainfall-runoff modeling, streamflow forecasting, water quality simulation and groundwater modeling (ASCE, 2000b). However, the application of ANN technique in sediment yield modeling is one of the recent

applications. In 2006, Raghuwanshi et al. applied ANN method for simulating runoff and sediment yields for a small agriculture watershed in India. Five sets of ANN models were developed; three of them were for daily prediction of runoff and sediment yields with different number of input variables and another two sets were for weekly basis prediction. In all cases, ANN prediction was more accurate than linear regression models and ANN models trained with temperature and rainfall data can achieve better accuracy instead of only including rainfall as input parameter. Another similar study (Lee et al., 2006) calibrated and validated Hydrological Simulation Program FORTRAN (HSPF) first to simulate discharge and sediment yield for three typhoon events at Taiwan. The synthetic data including rainfall intensity at previous time steps and discharge generated by HSPF were applied to train ANN models using the gradient steepest descent algorithm, one kind of BP training algorithms. ANN model was “able to calculate the watershed sediment yield with good accuracy” (Lee et al., 2006) and it was faster and easy to use than the HSPF model. Both HSPF and ANN models are more accurate than an empirical rating-curve method.

To explore the feasibility of ANN technique for debris yield prediction in this study, it is first applied to estimate sequent debris yield using the exactly same input data, same calibration and validation data as used in the MSDPM model (Pak, 2005). Next, it is applied to estimate unit debris yield collected from 36 debris basins within Los Angeles County from 1938 to 1983 and more watershed geomorphologic parameters (i.e. elongation ratio, drainage density,

etc.) are included as input variables in addition to watershed area, watershed relief ratio, maximum one hour precipitation, and fire factor. Soil is a major factor in debris production. Therefore in this study three soil characteristics including soil erodibility factor, soil permeability, and liquid limit are analyzed for each watershed based on the soil data from State Soil Geographic (STATSGO) database developed by U.S. Department of Agriculture Natural Resources Conservation Service (USDA NRCS). In order to prepare three soil characteristics for each watershed, it is necessary to delineate watershed boundaries using Better Assessment Science Integrating Point & Nonpoint Sources (BASINS) software provided by US Environmental Protection Agency (EPA). If a watershed includes more than one soil map units, the soil properties are determined by the weighted average method, i.e. proportioning their values to the percentage of exposure of that soil type. The three soil characteristics are included one by one to study their effects on the estimation of unit debris yield collected from 80 small debris basins (i.e. upstream watershed area is less than 3 square miles). They are divided into five groups based on the relief ratios of their upstream collection watersheds. For example, the first group of data is collected from mild watersheds, the second is from steep watersheds, the third is from watersheds with steeper slope, the fourth is from watersheds with extreme steep slope, and the last group is from watersheds with the steepest slope. Because all the watersheds with the steepest slope have the same value of three soil characteristics, they are not considered as input parameters for the last

group of data. ANN models are also developed for modeling unit debris yield documented at larger watersheds, areas is in range of 10-25 mi<sup>2</sup>, 25-50 mi<sup>2</sup>, and 50-200 mi<sup>2</sup>.

#### **1.4 Neural Fuzzy System and Fuzzy Neural Network to Estimate Debris Yield**

To utilize the interpretable nature of fuzzy logic system to overcome the drawback of ANN – cannot be explained explicitly, there are two possible ways of combining ANN and fuzzy logic system: Neural Fuzzy System (NFS) and Fuzzy Neural Network (FNN). A NFS is a fuzzy logic system capable of using ANN training algorithm to learn and the system is interpretable by fuzzy if-then rules. On the other hand a FNN uses fuzzy method such as fuzzy inputs, fuzzy outputs or fuzzy connection weights, and so on to improve neural network performance.

As one of the earliest NFS methods, Adaptive-Network-Based Fuzzy Inference System (ANFIS, Jang 1993) provides a fuzzy modeling procedure to learn from input/output data pairs through the adjustment and optimization of the membership function parameters by using either BP gradient descent method (BPGDM) or a hybrid learning algorithm - the combination of least squares method (LSM) and BPGDM. Jang (1993) demonstrated that this method can yield remarkable results for modeling nonlinear functions, identifying nonlinear component on-line in a control system, and predicting a chaotic time series. In the last decade, this method has been applied in many fields including hydrologic

modeling, for example, Chau, Wu, and Li (2005) employed ANFIS for flood forecasting in a channel reach of Yangtze River in China. ANFIS is the second artificial intelligence method used in this study to estimate unit debris yield data collected at 36 small debris basins within Los Angeles County.

Generalized Dynamic Fuzzy Neural Network (GD-FNN) algorithm was proposed by Wu and Er (2001) as an improvement on traditional FNNs in the following several aspects: hierarchical on-line learning, automatically recruiting or deleting neurons, and fast learning speed without iterative learning and initialization of structure and parameters. In addition, GD-FNN is able to generate different number of membership function (i.e. Gaussian function) for each input variable, and other improvements such as the number of membership function are not necessarily the same as the number of fuzzy rule, less random parameters involved, and more reasonable methods of refining Gaussian function width. The authors reported satisfactory modeling results for simulating nonlinear dynamic system, time-varying drug delivery system, and multilink robot control. Due to its efficient learning and automatically extraction of fuzzy rules, GD-FNN method is chosen as the third artificial intelligence method for modeling unit debris yields measured at 36 small debris basins within Los Angeles County.

### **1.5 Objectives of the Present Study**

- 1) To examine the efficacy of ANN models for predicting sequent and unit debris yield collected at debris basins from partially or totally burned

watersheds with an area range of 0.1-3 mi<sup>2</sup>, and 10-200 mi<sup>2</sup>, within Los Angeles County, California.

- 2) To examine the feasibility of ANFIS method and GD-FNN method to estimate unit debris yield.
- 3) To analyze the relative importance of input parameters including six watershed geomorphologic parameters such as elongation ratio, drainage density, hypsometric index, total stream length, mean bifurcation ratio, and transport efficiency factor, and three soil properties like soil erodibility factor, permeability rate, and liquid limit.
- 4) To study the effect of ANN architecture on its performance.

## Chapter 2: Review of Literature

### 2.1 Background of Debris Yield Estimation

Estimation of debris yield from watershed has long established itself as an important area of hydrological research due to a number of reasons (e.g. management and maintenance of debris basin, catastrophic consequence to downstream structure and human...). Debris yield modeling is very complicated because the sediment erosion process depends upon many variables such as watershed area and slope, watershed morphologic parameters, rainfall amount, intensity, and duration, soil condition, vegetation and litter cover. The erosion process consists of two major components: detachment and transport of sediment by raindrops which are the major driving force over interrill areas at which the flow depth is shallow, and detachment and transport of sediment are induced by runoff over both interrill and rill areas (Kothyari et al. 1996). It is apparent that sediment yield collected in debris basin is commonly substantially less than the gross erosion within the watershed because most sediments are deposited on the lower lands or in the valley floors during the conveyance of sediment from its source to its lowland concentration point, or debris basin (US Army Corps of Engineers, Los Angeles District (USACE), 2000). The estimation of debris yield, or debris volumes deposited in debris basin, is the major focus in this study. The reason why debris yield is described with the unit of volumes or volumes per unit area is because the volume is 'measured' by cleanout trucks.

Most existing debris yield prediction methods can be classified into three main categories. The first category is empirical models generally achieved by applying regression techniques such as linear regression or multi-regression analysis. One of the well-known empirical models, Universal Soil Loss Equation was developed by Williams and Berndt (1972) for the computation of long term average annual soil loss at agricultural field, and it has the following form

$$A = R * K * LS * C * P \quad (2.1)$$

Where A is estimated average soil loss with the unit of tons per acre per year, R is rainfall-runoff erosivity factor, K is soil erodibility factor (source data is States Soils Geographic Database (STATSGO)), LS is topographic slope length, C is crop coverage factor, and P is erosion-control-practice factor. The factor R can be determined by the annual summation of rainfall energy in every storm relate to raindrop size multiplies its maximum 30-minute intensity. The factor K is a measure of the susceptibility of soil particles to be detached and transported by raindrop and overland flow. The factor LS is a lumped factor of slope and slope length for convenience purpose, and higher slope and longer slope length result in greater erosion potential. The factor C is defined as the ratio of the soil loss from land under a specific crop and management condition to the corresponding loss from continuously fallow and tilled land. It is actually a measure that quantifies the relative effectiveness of soil and crop management systems in terms of preventing soil loss. Finally, the erosion-control-practice factor (P) considers human activities (e.g. contouring, strip cropping, etc.) to reduce runoff

hence minimizing the erosion potential. All these parameters vary spatially except LS, and Williams and Berndt (1972) suggested their weighted average values should be used for the whole watershed. This equation is only applicable for erosion limited by detachment capacity in such fields with negligible curvature and no deposition, and it is applicable for small watershed. Although it was one of the most widely accepted soil loss equations for over 30 years, it cannot be applied to model debris yield resulting from a single storm event and it does not adequately account for the process for watersheds at southern California. In 1963, Mr. Ferrel Tatum created an empirical equation to calculate debris storage requirement for debris basins based on regression and graphical techniques. The equation is

$$S_y = \frac{35,600Q_{csm}^{1.67}Rr^{0.72}}{(5 + VI)^{2.67}} \quad (2.2)$$

In which  $S_y$  is unit sediment yield in cubic yards per square mile,  $Q_{csm}$  is peak discharge with a unit of cubic foot per second per square mile, and  $Rr$  is relief ratio which is defined by the elevation difference between highest and lowest point divided by the horizontal distance parallel to the main channel between the concentration point and the watershed divide, and  $VI$  is called vegetation index and it is the weighted average of the index point of each type of vegetation multiplying the corresponding percentage of area covered by this type of vegetation within the whole watershed (Tatum, 1963). It was developed for watersheds within Los Angeles County and had been used for debris basin

planning, design, and construction for the subsequent 23 years (USACE, 2000). However, with the occurrence of more debris flow events, the update of the equation becomes demanding. Therefore, in 2000, the USACE reevaluated hydrologic variables and selected only those that are important to debris yield and provided five empirical equations with respect to different sizes of watershed area within Los Angeles County. Those five equations cover a range of drainage area from 0.1 to 200 square miles. To give an example, the equation developed for small watershed with an area between 0.1 and 3.0 square miles is:

$$\log D_y = 0.65(\log P) + 0.62(\log RR) + 0.18(\log A) + 0.12(FF) \quad (2.3)$$

Where  $D_y$  is the same as  $S_y$  defined in equation 2.2,  $RR$  is the same as  $R_r$  in equation 2.2 but the unit is ft/mile,  $P$  is 100 times greater than the maximum one hour precipitation with the unit of inch,  $A$  is watershed area in acre,  $FF$  is non-dimensional fire factor and it is a function of burn condition of a watershed by wildfire, watershed area, time after the recent wildfire, and it can be read from the curves provided by USACE. In addition to these empirical equations, a frequency relationship between unit debris yield and the total probability of wildfire and flood were proposed as well.

One of the most recent approaches, Multi-Sequence Debris Prediction Model (MSDPM, Pak, 2005; Pak and Lee, 2008), was developed for predicting sequent debris yield resulting from wildfire and a series of storm events based on precipitation, drainage area, relief ratio, and a non-dimensional fire factor. Two new factors were introduced in the model - threshold maximum 1-hr rainfall

intensity (TMRI) and total minimum rainfall amount (TMRA). MSDPM has the following form.

$$\sum_{i=1}^N (D_y)_i = 0.25 \sum_{i=1}^N \left( 1 + \frac{|(I_m)_i - I_c|}{((I_m)_i - I_c)} \right) \left( 1 + \frac{|(P)_i - P_c|}{((P)_i - P_c)} \right) (I_m)_i^{0.541} S^{0.134} A^{1.023} e^{0.290F} \quad (2.4)$$

Where  $D_y$  = debris yield with unit of  $m^3$ ,  $I_m$  = maximum 1-hr rainfall intensity in unit of mm/hr,  $I_c$  = threshold maximum 1-hr rainfall intensity with the unit of mm/hr,  $P$  = total rainfall amount in millimeter per storm event,  $P_c$  = total minimum rainfall amount in millimeter,  $S$  (m/km) = relief ratio same as that defined earlier,  $A$  = size of drainage area in hectare,  $F$  = fire factor and it is defined in the following equation.

$$F = 6.5 \times (B_p \times B_y^{-0.29} + (1 - B_p) \times (1 - B_y)^{-0.29}) \times (2 - e^{(A_p/200)}) \quad (2.5)$$

In which,  $B_p$  is the percentage of burned area,  $B_y$  is the number of years after the recent wildfire with 10 years as the upper limit,  $A_p$  is the number of antecedent effective precipitation events. The key point of this model is that only and only if maximum 1-hr rainfall intensity and total rainfall amount are greater than TMRI, and TMRA, respectively, there will be some debris deposited in the downstream debris basin. The MSDPM was calibrated by field data collected from 12 debris basins from 1984 to 2000, and validated by the subsequent storm events after 2000. In summary, the MSDPM was developed with the consideration of three main physical processes: the critical condition to entrain

sediment through the inclusion of TMRI, the transport capacity to move sediment toward the concentration point indicated by TMRA, and the antecedent precipitation condition coupled with the subsequent rainfall events (Pak, 2005; Pak and Lee, 2008). The modeling results have been demonstrated to be in good agreement with field collected data.

Empirical equations are criticized for their simplicity to describe such a complicated process, therefore, conceptual models were proposed as an improvement. With assumptions that the process is nonlinear, time-invariant and deterministic, conceptual models simulate the process by using simplified physical laws. The basic study unit is element or grid. Conceptual model considers the detachment of soil by rain drops, erosion and sediment transport by overland flow within each element, and routing of flow and sediment between the elements and finally go to a debris basin. The ANSWERS, one of the earliest and most commonly cited conceptual models, was created by Beasley et al. (1980) to predict both runoff and sediment yield for agricultural watersheds. This model consists of five components: a hydrologic model, a sediment detachment/transport model, and three routing components to model overland, subsurface and channel flow. The hydrologic model is designed to simulate the rainfall-runoff process considering infiltration into the ground, water retention and detention by surface, and subsurface drainage. The infiltration rate was computed by using Holtan's (1961) equation (Equation 2.6).

$$\text{Infiltration rate} = f_c + A\left(\frac{S-F}{T_p}\right)^p \quad (2.6)$$

Where  $f_c$  = steady state infiltration rate,  $A$  = infiltration rate difference between maximum and steady state,  $S$  = storage capacity of a soil,  $F$  = total infiltrated water in terms of volume,  $T_p$  = total porosity, and  $P$  = dimensionless factor relating the rate of decrease in filtration to the increasing in soil moisture content. Potential surface retention was specified in Equation 2.7 (Huggins and Monke, 1966).

$$\frac{\text{The surface Retention Storage Volume}}{\text{The Maximum Possible Retention Volume}} = Ax^B \quad (2.7)$$

In which  $A$  and  $B$  are empirical constants provided for different ground conditions, and  $x$  is the ratio of water depth above a datum to the height of the tallest roughness element. Subsurface drainage was evaluated by using Huggins and Monke's (Equation 2.8, 1966) method.

$$\text{Subsurface Drainage Rate} = f_c \left(1 - \frac{\text{Unsaturated Pore Volume}}{\text{Max. Volume of Gravitational Water}}\right)^b \quad (2.8)$$

$f_c$  is the same as defined in Equation (2.6), and  $b$  is a drainage exponent constant. The impact of rainfall drop or overland flow on the detachment of soil particle was determined by equation 2.9 and 2.10, respectively.

$$\text{Detachment Rate(kg/min)} = 0.027CKA_1I^2 \quad (2.9)$$

$$\text{Detachment Rate(kg/min)} = 0.018CKA_1Sq \quad (2.10)$$

Where  $C$  = cropping and management factor,  $K$  = soil erodibility factor,  $A_1$  = area increment,  $I$  = rainfall intensity in millimeter/minute,  $S$  = slope, and  $q$  = flow rate

per unit width. The transport capacity of overland flow, in kg/min-m, was determined by

$$\begin{cases} 146(S_e q)^{1/2}, q \leq 0.046 \text{ m}^2/\text{min} \\ 14600(S_e q^2), q > 0.046 \text{ m}^2/\text{min} \end{cases} \quad (2.11)$$

The symbol  $S_e$  is the element slope. With the assumption that the flow is uniform, Manning's equation was applied to model overland and channel flow. The routing process was modeled in such a way that runoff and subsurface drainage hydrograph were treated as inflow to the adjacent elements following the direction of steepest slope (Beasley et al., 1980). In 1993, Wu and his colleague estimated runoff and sediment yields for 30 runoff events at three watersheds near Coshocton, Ohio using ANSWERS and two other models, and they reported that the ANSWERS model provided the most consistent results for both variables.

At the beginning of 1980s, many researchers realized that the use of lumped models limited the study of hydrological processes (Abbott et al., 1996a) and recommended that the empirical facts and theoretical knowledge should be combined at a more detailed scale through mathematical synthesis to achieve the correct hydrological scale. In essence it is the path of the development of physically-based models. After dividing whole drainage area into smaller elements or grids and assuming all significant parameters are uniform within each element, physically-based models are set up to solve a system of partial differential equations of mass, momentum, and energy conservation to estimate

sediment yield. In general, the sediment yield process involves two phases, the upland phase and in-channel phase (Bennett, 1974). The complicated nature of the process makes it impossible to solve these equations except under significant simplification. Kothyari et al. (1997) simulated the surface runoff in upland area by using kinematic wave simplification of the Saint Venant equations of flow. With the assumption of one dimensional flow, the first governing equation of overland flow is non-dimensional continuity equation (Kothyari et al., 1997):

$$\frac{\partial Q'}{\partial x'} + \alpha' \beta' Q'^{\beta'-1} \frac{\partial h'}{\partial t'} = w' \times i_e' \quad (2.12)$$

Where  $Q'$  is non-dimensional inflow in x direction,  $\alpha'$  and  $\beta'$  are non-dimensional kinematic wave parameters,  $w'$  is the dimensionless width of an elementary strip (the numerical grids used in this study is the watershed time-area segments within which the concentration time is the same),  $h'$  is the dimensionless flow depth,  $x$  and  $t$  are non-dimensionalized by dividing characteristic length and concentration time, and  $i_e'$  is dimensionless effective rainfall. With the initial and boundary conditions,  $Q'(x', t')$  are solved at each point on the  $(x', t')$  grid by applying a fully implicit four point finite difference scheme. The continuity equation for sediment (Kothyari et al., 1997) is

$$\frac{\partial q_s}{\partial x} + \frac{\partial(q_s / V)}{\partial x} = D_I + D_F \quad (2.13)$$

In this equation,  $q_s$  = sediment load (mass/width/second),  $x$  = distance along the slope,  $V$  = flow velocity,  $D_I$  = interrill erosion rate (mass/area/second),  $D_F$  =

sediment erosion rate from rill areas (mass/area/second). Sediments are mainly detached by rain drops or overland flow. The sediment detachment rate was modeled similar to Equation 2.9 and 2.10 except that the coefficients are determined through calibration process instead of pre-specified values. The sediment transported by overland flow was simulated by Equation 2.11 and the coefficients were optimized by calibration process as well.  $D_I$  and  $D_F$  are known within each element; the solution to Equation 2.13 was procured by using FDM within the same elements as defined in rainfall-runoff modeling. This physical model was applied to 12 small watersheds (area between  $0.002\text{km}^2$  and  $92.5\text{km}^2$ ) considering different climates. The authors concluded that the predicted results were realistic and the model worked better for total sediment yields resulting from more storm events.

The advent of Geographic Information System (GIS) provides a cost-effective means to create, capture, store, query, analyze, display, and output spatially and temporally distributed data at a variety of scales. The current status of sediment modeling has been advanced with the application of GIS. As early as 1977, Gupta developed a distributed model for estimating runoff and sediment discharge for ungaged rivers using GIS. Coupling the meteorological, hydrologic, geophysical, and other related variables from a variety of sources including paper maps, aerial photographs, remote sensing, etc., Gupta's model was claimed to be viable for any sized watershed to obtain runoff and sediment time-series at any point within the watershed. The modeling results at two stations in Canada

indicated an improvement over some simpler techniques such as statistical regression empirical equations. Considered three major sediment generation sources such as mass wasting, hill slope erosion, and road surface erosion, Doten et al. (2006) developed a Distributed Dynamic Hydrology-Soil-Vegetation Model (DHSVM) to estimate erosion and sediment transport in a temperate forested watershed. With the use of stochastically generated soil and vegetation parameters on a grid cell by grid cell basis, the model produced slope failure (i.e. the start of the mass movement) on the basis of a factor-of-safety analysis with an infinite slope model. The eroded sediments from hill slope and road surface were routed to lowland with a rule-based scheme that determines sediment delivery to channel network. Assuming sediment flows into the channel from both upstream and local area, the flow in channel was simulated using a linear reservoir routing scheme. Debris flows were modeled on volumetric basis then converted to mass with respect to different particle sizes and finally sediment yield collected in the basin was determined. Compared with published rates for similar catchments in the Pacific Northwest, the model provided plausible sediment yields and ratios of land sliding to surface erosion for a catchment in the north of Washington State.

All distributed models including conceptual, physically-based and GIS involved models require huge amounts of watershed characteristic data within each element or grid. Most of the time, the availability of these data is a major concern. Even if the data are available, physically-based models tend to have

such problems like numerical instability and convergence. The widely reported successful application of ANN models to a number of hydrological problems inspires this study of applying artificial intelligence models for predicting debris yield.

## **2.2 Use of ANN in Hydrologic Applications**

Most hydrologic processes such as rainfall-runoff process, sediment yield process, streamflow estimation, ground water, and water quality analysis are very complicated. ANN technique is well acknowledged for its high computational power and its ability to learn nonlinear relationship between inputs (i.e. independent variables) and outputs (i.e. dependent variables) for all kinds of problems. The start of the application of ANN in hydrologic areas can be traced back to 1991 (ASCE, 2000b), and more and more researchers claim that the technique is a promising alternative tool for modeling highly nonlinear problem.

### **2.2.1 Use of ANN in Rainfall-Runoff Process**

One of the most important problems faced by hydrologists and engineers is the modeling of rainfall-runoff which is known to be highly nonlinear, temporally and spatially distributed process. There are so many factors affecting runoff except rainfall intensity and duration, such as watershed size and slope, land use, evaporation, soil condition, vegetation cover, and so on. Most existing models for rainfall-runoff process are conceptual models which are reliable in forecasting the important features of the hydrograph, such as the beginning of

the rising limb, the time and the height of the peak, and volume of flow (Kitanidis and Bras, 1980a, b; Sorooshian et al., 1993); however, they were criticized for inclusion of huge amount of parameters and the complicated interaction between those parameters. With the development of ANN technique in modeling nonlinear relationships, many hydrologists conducted research to estimate runoff using ANN models based on rainfall information. A significant amount of applications of ANN technique in the rainfall-runoff modeling were published from 1990 to 2000 (ASCE, 2000b). Most of the studies reported superior prediction accuracy by using ANN model as compared to either conceptual or statistical regression models.

A few recent advancements in the rainfall-runoff modeling by using ANN models are introduced as follows. Tokar and Markus (2006) applied ANN technique to model the monthly streamflow for Fraser River Watershed in Colorado related to streamflow, precipitation, and air temperature in the previous month, and snow water equivalents in the preceding two months. Compared to conceptual water balance model, ANN modeling results are more accurate. Daily runoff in the Racoon River, Iowa, and Little Patuxent River in Maryland was also modeled by using ANN models and the results were better than those obtained by both the Sacramento Soil Moisture Accounting (SAC-SMA) model and Simple Conceptual Rainfall Runoff (SCRR) model. The authors reported that ANN models not only provides high accuracy but also requires shorter training time. Jain and Indurthy (2003) modeled storm event-based rainfall-runoff process for

Salado Creek at San Antonio by using ANN models and then compared to a deterministic model, and a statistical model. The authors reported that ANN models generally outperformed both the deterministic model and the statistical model particularly in terms of peak discharge and time to peak discharge.

### **2.2.2 Use of ANN in Streamflow**

Following the same categorization in ASCE paper (2000b), streamflow forecasting without rainfall information as input parameter is a separate topic here. The focus of this review is the more recent studies of forecasting streamflow using ANN techniques. Jain and Chalisgaonkar (2000) modeled a stage-discharge relation by using three layer feed-forward ANNs trained by BP training algorithm. With input parameters like current and preceding stages and discharge, the performance of ANN models “is much superior as compared to the conventional curve-fitting approach”. The authors also indicated that ANN technique simulated a loop-rating curve (hysteresis effect) much better than a fitting curve. Özgür Kişi (2007) developed ANN models trained by four different training algorithms including BPGSD algorithm, conjugate gradient, cascade correlation, and Levenberg–Marquardt (LM) training algorithm to predict short term (i.e. daily) streamflow of the North Platte River in Colorado. Input parameters used to train ANN models were only preceding discharge with different leading time, for example, one day ahead. The author found that LM algorithm requires much less training time and the prediction accuracy is superior

as compared with the other three training algorithms. In addition, ANN models calibrated by either conjugate gradient or cascade correlation training algorithm outperformed ANN models trained by gradient steepest descent algorithm in terms of streamflow forecast accuracy.

### **2.2.3 Use of ANN in Groundwater**

The modeling of groundwater is another important hydrologic topic around the world. Coppola and his colleagues (2003) examined the potential of ANN in modeling transient water levels at a multilayered ground water system under variable state, pumping, and climate conditions. A three-layered perceptron neural network was trained by BP algorithm for predicting transient water levels at 12 monitoring wells screened in different aquifers under different pumping and climate conditions. The seven physical inputs are temperature, precipitation, initial water levels at the monitoring wells, pumping extractions of the seven production wells, dew point, wind speed condition, and length of stress period. They reported ground water levels predicted by ANN models were more accurate than a calibrated numerical model, and ANN technology can achieve better dynamic water level simulation corresponding to changing pumping and climate conditions. Shigidi and Garcia (2003) estimated aquifer parameters such as transmissivity by using ANN feed-forward model and an inversion model. The authors calibrated and validated an ANN feed-forward model to predict 225 hydraulic heads in 225 uniformly spaced grid in a hypothetical square confined

aquifer with 225 hydraulic conductivity values as inputs. 1,500 hydraulic conductivity fields were generated randomly and the corresponding hydraulic heads were determined by using Modular Three-Dimensional Finite-Difference Ground-Water Flow Model (MODFLOW). 1,000 of them were used for calibration ANN models and the remainder 500 data records for validation. Next, the calibrated network was inverted to estimate the missing parameters – transmissivity in some grids by updating those values until they converge and minimizing the difference between hydraulic head target values and ANN outputs. This paper initiates an interesting approach for using ANN technique to estimate aquifer parameters in groundwater hydrology.

All these research leads to a fact that ANN technique is a suitable and powerful tool in modeling complicated rainfall-runoff process, streamflow forecasting, and groundwater problem.

#### **2.2.4 Use of ANN in Debris Yield**

The adoption of ANN technique for debris yield modeling adds a new dimension to the system theoretical modeling. In 2006, Raghuwanshi et al. applied ANN method for predicting daily and weekly runoff and sediment yield for a small agriculture watershed in India. ANN models were trained by data collected during monsoon seasons within five years and validated by the data collected from the following two years. ANN models with one or two hidden layers were developed to predict both runoff and sediment yield. For daily

prediction, three sets of ANN models were created using different inputs; first set of ANN models was trained only by present day rainfall, second set of ANN models was trained by present day rainfall and the preceding day, and the third set was trained by rainfall, minimum, and maximum temperature. Two sets of inputs were considered in predicting weekly runoff and sediment and first set includes only weekly rainfall, and the second set includes weekly rainfall with mean minimum and maximum temperature. In all these cases, ANN prediction was more accurate than linear regression based models and the inclusion of temperature as ANN models inputs improved the prediction accuracy. Another related study is the estimation of reservoir sedimentation from three typhoon events in Shihmen Reservoir watershed, Taiwan (Lee et al., 2006). The authors used Hydrological Simulation Program FORTRAN (HSPF), a numerical program developed by US Environmental Protection Agency (USEPA), to simulate discharge and sediment yield based on precipitation, discharge, concentration of suspended sediment, and relevant geometric and geologic data such as channel cross section. Among all these parameters, only those parameters that were most sensitive to the results were calibrated by using HSPF to a desired level of accuracy and then saved to model discharge and sediment yield. The correlation coefficients for calibration and validation between observed and simulated results were 0.86 and 0.85, respectively. Due to the lack of complete data sets of concentrations of suspended sediment, the inputs and target outputs for ANN models were synthetic data generated from the calibrated and verified HSPF

model. The optimal inputs for the modeling of sediment yield were found to be rainfall intensity up to the previous four time steps and discharge at the same time step. Trained by GSD algorithm, ANN models with one hidden layer achieved accurate prediction since the correlation coefficients improved to 0.96, and 0.93 for training and testing data (Lee et al., 2006). Both HSPF and ANN approaches were more accurate than empirical rating-curve method.

### **2.3 Use of Neural Fuzzy System and Fuzzy Neural Network in Hydrologic**

#### **Modeling**

Although ANN technique has gained more and more popularity and exhibits promising capability for modeling nonlinear relationship, it was classified as one of empirical models or 'black box' due to the lack of physical concepts and explanation of relations between inputs and outputs. Another kind of artificial intelligence – fuzzy logic system, addresses the linguistic, uncertainty and imprecise knowledge by using fuzzy sets for gradual qualities, and represents if-then rules by fuzzy antecedent and consequent parameters through which human knowledge can be directly implemented (Mitra and Hayashi, 2000). Since fuzzy logic system is not able to learn from examples, that is, the parameters within fuzzy logic system cannot be determined through learning or calibration; many researchers have been exploring the possibility of fusing ANN technique and fuzzy logic system, named Neural Fuzzy System (NFS) or Fuzzy Neural Network (FNN). The NFS is a combination of ANN and fuzzy logic in such a way

that neural network learning algorithms are applied to enhance fuzzy system characteristics in terms of its flexibility, speed, and adaptability (Mitra and Hayashi, 2000). On the other hand a FNN is still basically a neural network but the input signals and/or connection weights and/or the outputs are fuzzy subsets or a set of membership values of fuzzy sets.

As a benchmark method of NFS, Adaptive-Network-based fuzzy inference system (ANFIS, Jang 1993) was employed for numerous problems. Chau et al. (2005) applied ANFIS to forecast downstream water levels of Yangtze River in China. For comparison purpose, an empirical linear regression model and genetic algorithm-based ANN (ANN-GA) model were tested as well based on the known water levels at upstream station, same inputs as for the ANFIS model. The authors reported that both ANFIS and ANN-GA model forecasted flooding levels between two stations on Yangtze River more accurate than the linear regression model, although both methods involved the determination of many parameters. ANFIS model was suggested to be a better suited tool for flood forecasting.

Deka and Chandramouli (2005) introduced their approach to predict stream discharge at one gauge station using a FNN model based on discharge at other gauging stations on Brahmaputra River in India. They reported that the FNN model was superior to ANN model in terms of simulation accuracy for very low, low, and high flow regions. With other features such as flexibility, ease of building and interpreting, FNN approach was believed to be a potential tool for a

wide range of hydrological problems. One of the recent advancements in water resources area is the application of FNN model trained stochastically (SFNN) by a genetic algorithm (Chaves and Kojiri, 2007) for deriving the reservoir monthly operational strategies to improve water quality and maximize water usage. The SFNN method were developed based on seven input parameters (i.e. inflow, beginning-of-period storage, dissolved oxygen, biochemical oxygen demand, total nitrogen, total phosphorous, and chlorophyll-a) and the interested output variable was the end-of-period reservoir storage volume. The SFNN model was implemented to Barra Bonita reservoir in Brazil. Trained with water quality related objectives, the SFNN model successfully produced the reservoir operational strategies and meanwhile achieved the objectives of optimizing water quality and maximizing water utilization.

Tayfur et al. (2003) pioneered the application of fuzzy logic algorithm for estimating sediment load induced by runoff from bare soil surfaces. The inputs including rainfall intensity and slope data were fuzzified by using triangular membership functions, and the output fuzzy sets were defuzzified by using weighted average method. The relations between rainfall intensity, slope, and sediment transport can be interpreted by a set of fuzzy rules. The predicted results were in good agreement with the experimental sediment data. The comparison between the fuzzy logic approach, ANN model, and a physically-based model reveals that “fuzzy model performed better under very high rainfall

intensities over different slopes and over very steep slopes under different rainfall intensities” (Tayfur et al., 2003).

Based on the review of many successful applications of ANN technique in a variety of highly nonlinear hydrologic problems, it is the first artificial intelligence model considered in this study for modeling debris yield. Another two artificial intelligence models - ANFIS and GD-FNN model are developed for modeling debris yield because of their initiative to fuse ANN and fuzzy logic system to combine the advantages of both models and overcome the disadvantages. The application of ANFIS in the hydrologic area has been reported, however, it is a creative approach to apply GD-FNN model for estimating debris yield.

## **Chapter 3: Methodology of Modeling**

### **3.1 Location of Studied Debris Basins and Data Sources**

Under the pressure of increasing population, more and more man-made structures are expanded on alluvial fans and floodplains in southern California. Fast-moving and occurring without warning, debris or mud flows are one of the major natural hazards in this area. Indicated by the historical rainfall records and occurrence time of debris flows for southern California area, debris flows can be triggered by intense rainfall or even less intense, briefer storms on wildfire burned areas.

The reason why southern California area has such a high erosion rate is due to its geological condition, special vegetation and climate which can easily induce wildfire, and dramatic rainfall pattern through a year. Broadly speaking, Los Angeles County consists of 25 percent mountainous area, 14 percent coastal plain, and 61 percent hills, valleys, or deserts (Los Angeles Hydrologic Report). Four rivers including Los Angeles River, Rio Hondo, San Gabriel River and Santa Clara River run across the county. The slope is mild at coastal plain but the slopes of main river systems crossing the coastal plain are steep, ranging from 4 to 14 feet per mile. Below the elevation of 5,000 feet, the topography of mountainous area is mainly consisted of deep, V-shaped canyons with 70 percent or more side slopes and separated by sharp dividing ridges (Los Angeles Hydrologic Report). Two primary mountain ranges are the Santa Monica

Mountains and the San Gabriel Mountains where the gradient of principal canyons is from 150 to 850 feet per mile. Formed by highly fractured igneous rock with large areas of exposed granitic rock formation, the San Gabriel Mountains and Verdugo Hills have a shallow soil mantle that accelerates erosion of the fine material. Valley and desert soils “vary from coarse sand and gravel near canyon mouths to silty clay, clay and sand and gravel in lower valleys at the coastal plain” (Los Angeles Hydrologic Report). Chaparral is the principal vegetation on upper mountainous area and it is very flammable under dry, low-humidity weather accompanied by high winds (Los Angeles Hydrologic Report). Wells (1981) studied the effects of brush fires on erosion processes in coastal southern California area and reported an event that the recorded debris yield from a burned small and steep watershed is 100 times greater than that from the watershed under its unburned condition. The main reason might be more rainfall is flooded on the ground as direct runoff resulting from the removal of vegetation cover and the formation of water-repellent soils.

The Los Angeles County is in semi-arid area and seasonal normal rainfall varies from 27.50 inches in the San Gabriel Mountains to 7.83 inches in the desert (Los Angeles Hydrologic Report). In mountain areas, after the soil is wetted to the capacity, direct runoff will be formed very soon due to steep slope. The volume and rates of excess rainfall is much greater and with earlier arrival time to the peak from areas recently denuded by wildfire (Los Angeles Hydrologic Report). Hence, it is able to carry and pick up more sediment to the alluvial fan

areas. Urbanization at hilly and valley areas increases direct runoff in terms of volume and rates although less sediment is available. Debris yield rates from urbanized hill areas are smaller than undeveloped hill areas, and also smaller than those from recently burned areas, assuming the same-sized area.

As an effective engineering solution, debris basin was built up to retain debris and to reduce risk of debris and mud flow, thus minimizing the loss of structures and human lives. Until 2005, within Los Angeles County, there were 157 debris basins located at canyons mouths to collect the solid sediments and to release water to downstream flood control channels. The study of sequent debris yield resulted from a series of storm events during a specific time period and debris yield flushed by a single significant storm event per unit area is of prime importance for the design and maintenance of debris basins. A very powerful nonlinear relationship modeling tool - artificial neural network is applied to predict both sequent debris yield and unit debris yield collected from watersheds totally or partially burned by wildfire in this study.

Los Angeles District of the USACE provides debris yield data collected from 14 small debris basins (Figure 1) with area less than 3 square miles from 1984 to 2003. They are used for predicting sequent debris yield resulting from wildfire and a series of storm events. 200 pairs of data collected from 36 small debris basins (Figure 2) from 1938 to 1983 within Los Angeles County are used for the study of relative importance of watershed morphological parameters for simulating unit debris yield resulting from single storm event in this study. 349

pairs of data from 80 small debris basins (Figure 3) based on which the USACE developed an empirical regression equation (Equation 2.3) are separated into five groups based on watershed relief ratio. For example, first group includes data from watersheds with mild slope, or relief ratio is in a range of [58, 185] m/km, second group is from watersheds with steep slope (i.e. relief ratio ranges from 185 to 250 m/km), third group is from watersheds with steeper slope, or relief ratio is from 250 to 305 m/km, the fourth group is from watersheds with extreme steep slope, or relief ratio is from 305 to 375 m/km, and the fifth group is from watersheds with the steepest slope, or relief ratio is from 375 to 525 m/km. Each group of unit debris yield data was simulated and the impacts of three soil properties including soil erodibility factor, permeability rate, and liquid limit on the simulation were studied. Unit debris yield collected from watersheds with larger area (e.g. from 10 to 25 square miles, from 25 to 50 square miles, and from 50 to 200 square miles) within Los Angeles County are simulated and compared to the three empirical regression equations formulated by the USACE in this study as well. The location of all the studied larger debris basins is shown in Figure 4.

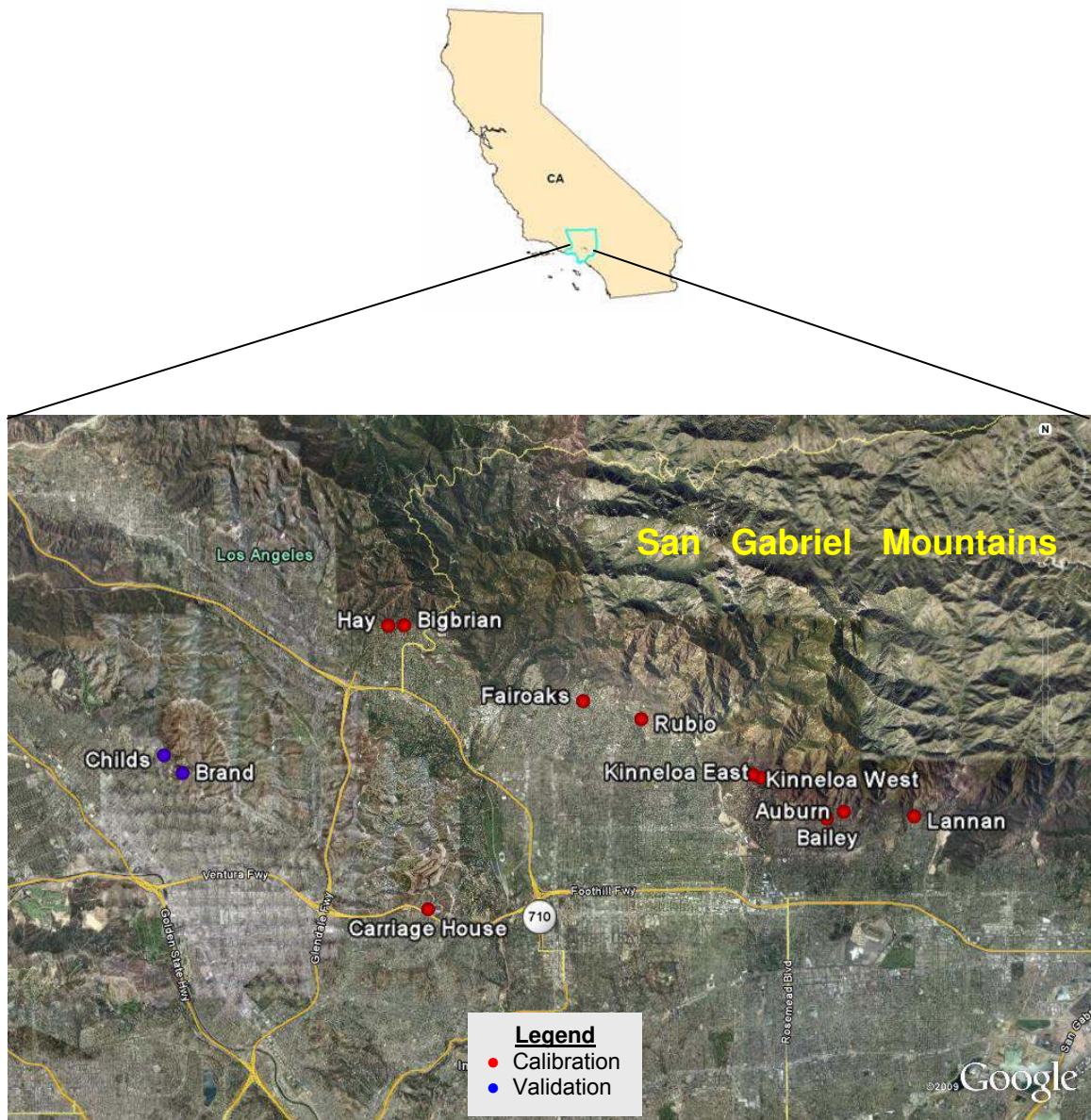


**Figure 1:** Location of 14 small debris basins for sequent debris yield

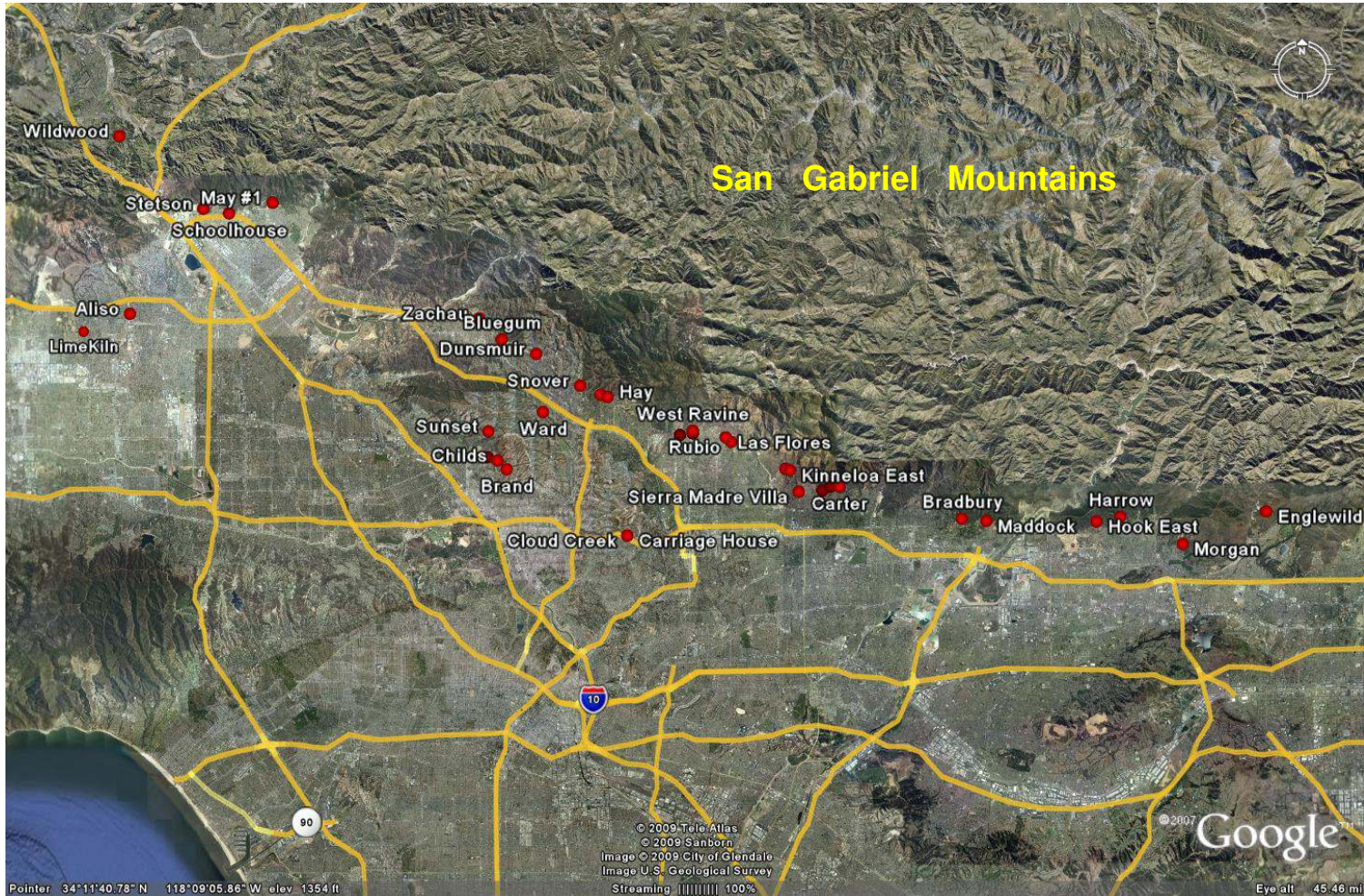


**Figure 2:** Location of 36 small debris basins for unit debris yield

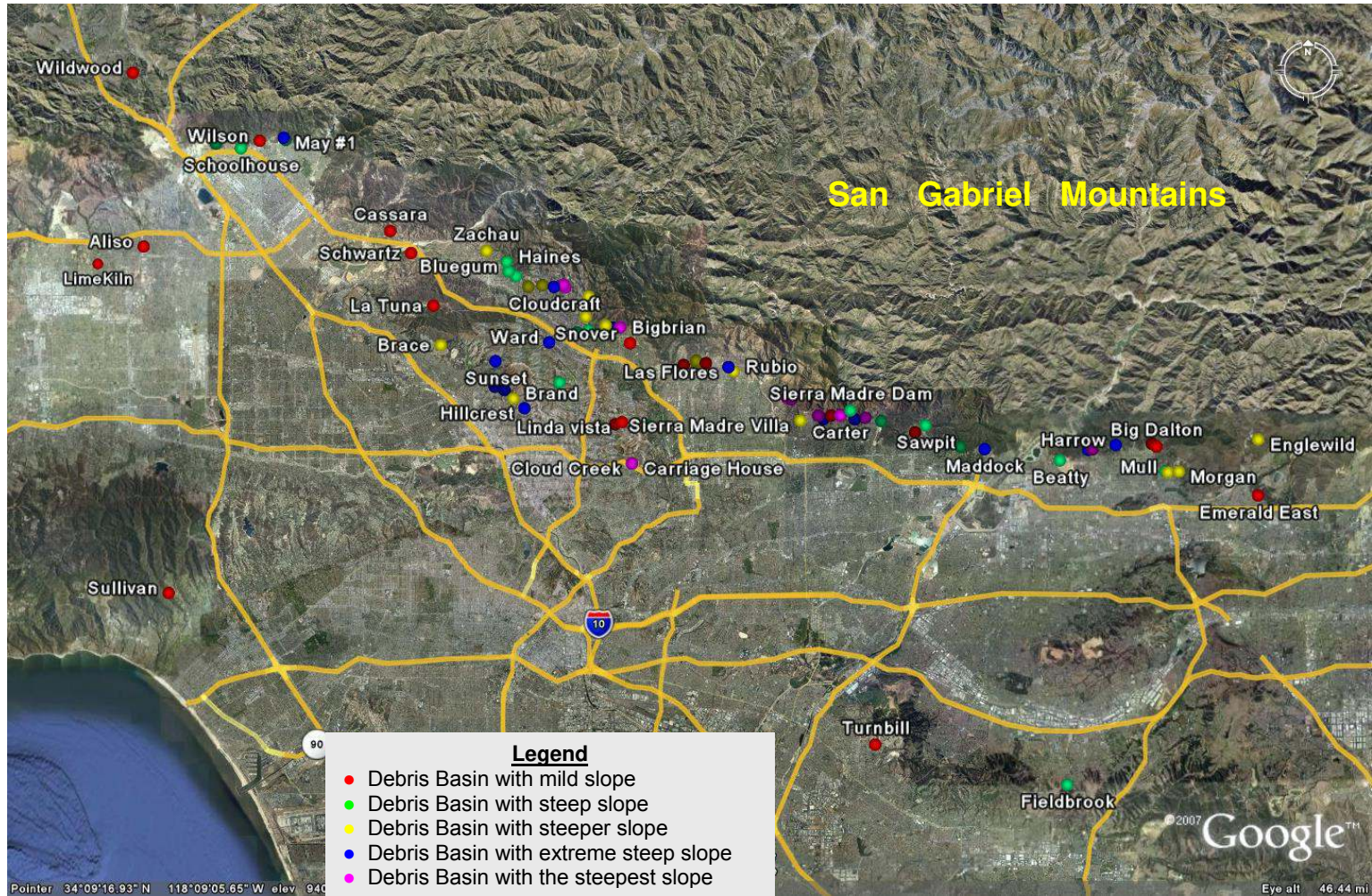


**Figure 3:** Location of 80 small debris basins for unit debris yield

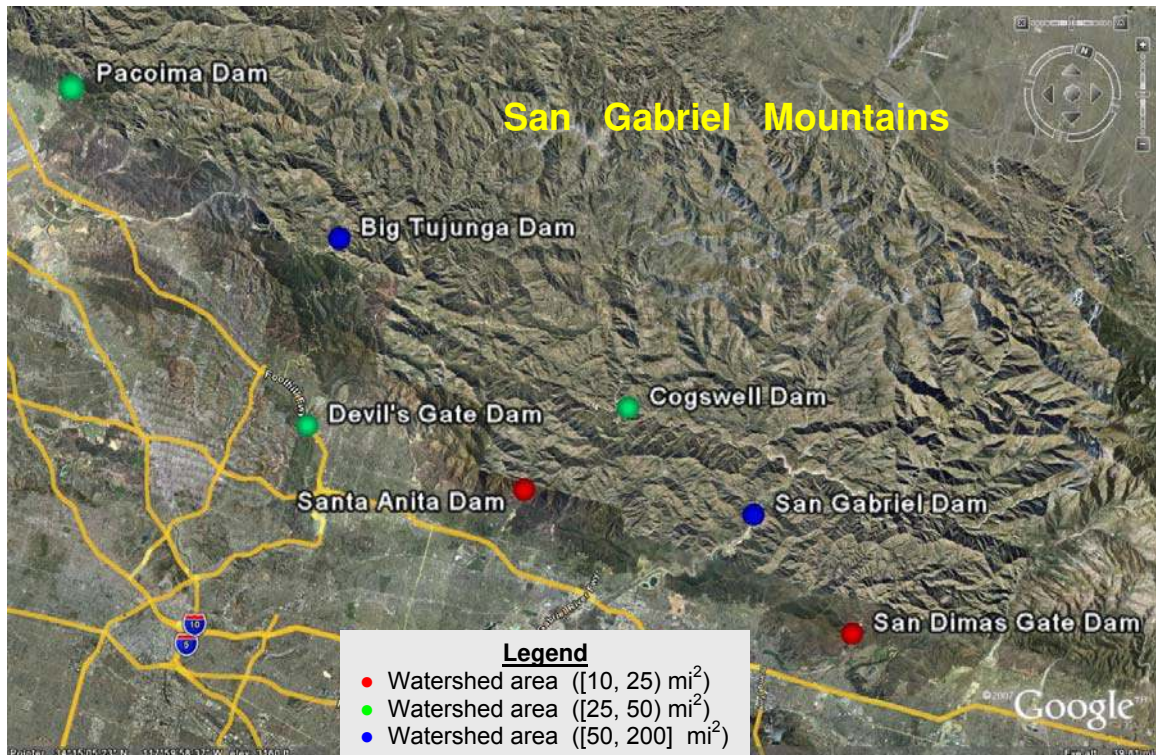


**Figure 4:** Location of 7 large debris basins for unit debris yield

### 3.2 ANN Model

ANN technique is chosen to estimate debris yield for its remarkable capability to identify nonlinear relationship between inputs and outputs for very complicated and highly nonlinear problems which are hard to describe by any explicit equations.

#### 3.2.1 Introduction of ANN Model

It is the power of human brain and nerve system that made people think of the possibility of creating a model for a whole new game of calculation (Dayhoff, 1990). In human brain, a signal is received from another neuron through dendrites, a group of branching fibers, and then the signal passes the cell body

of neuron and flows to the next neuron through the long, branching axon (Dayhoff, 1990). Quite similar to the biological neuron system, the basic processing unit in ANN is called neuron or node, and they are grouped into different layers such as input, hidden, and output layer which are sketched in Figure 5.

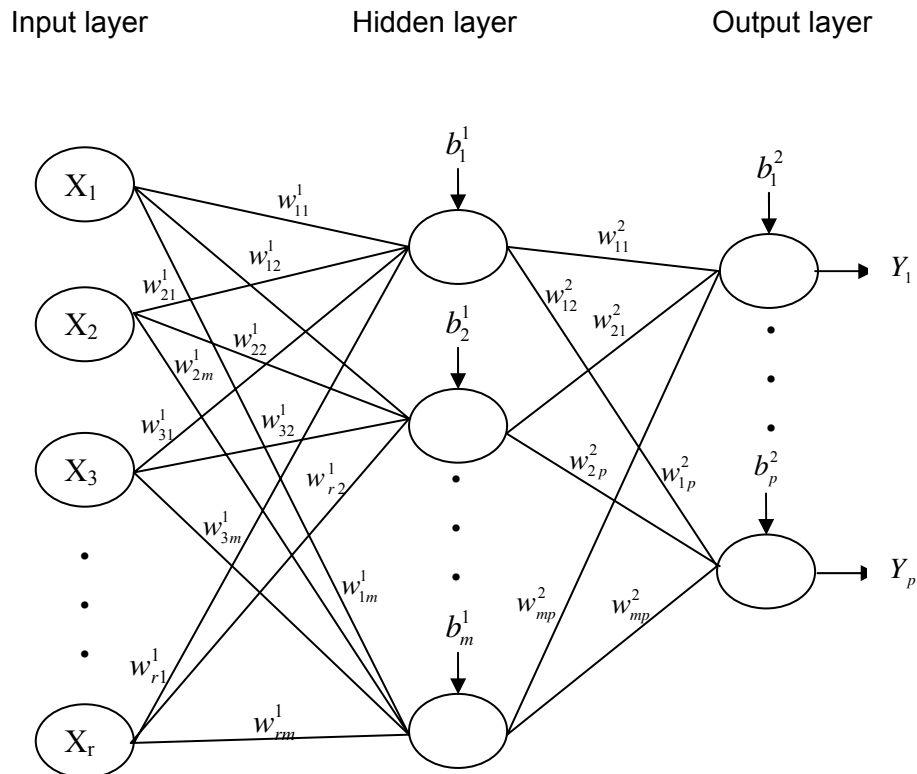


**Figure 5:** Schematic diagram of a three layer feed-forward ANN

$X_1, X_2, \dots,$  and  $X_r$  are  $r$  input parameters, or one input vector. The input vector is connected to each neuron on the hidden layer through connection weights  $w_{ij}^1$ . The superscript 1 indicates the first hidden layer, and the subscripts  $i$  and  $j$  indicate the connection between  $i$ th input variable ( $i = 1, 2, \dots, r$ ) and  $j$ th hidden neuron ( $j = 1, 2, \dots, m$ ). Similarly,  $w_{11}^2, w_{21}^2, \dots, w_{mp}^2$  are connection weights

between the first hidden layer and the output layer with  $p$  neurons.  $b_1^1, b_2^1, \dots, b_m^1$  and  $b_1^2, b_2^2, \dots, b_p^2$  are called biases or threshold values. The values of output variables ( $Y_1, Y_2, \dots, Y_p$ ) are calculated based on the following equation.

$$Y_k = f_2 \left[ \sum_{j=1}^m f_1 \left( \sum_{i=1}^r X_i w_{ij}^1 + b_j^1 \right) * w_{jk}^2 + b_k^2 \right], \quad k = 1, 2, \dots, p \quad (3.1)$$

$f_1$  and  $f_2$  are transfer functions, or activation functions. The functions can be same or different.

Generally speaking, there are five aspects that have impact on ANN model performance and they are input and output variable selection, separation of calibration and validation data sets, data preprocessing, ANN architecture determination, and training algorithm selection (ASCE, 2000b). ANN architecture includes two parts: geometry of the network and internal parameters. The geometry of a network means the number of hidden layer and the number of neuron on each layer. Internal parameters include transfer function, the initial value of connection weights and biases, epoch size, training data error goal, and so on.

### 3.2.2 Selection of Input and Output Variables

Input variable selection is of prime importance to make the “mapping” from the inputs to the outputs efficient and effective (ASCE, 2000a). If the physics in a process is well understood, it is helpful for choosing proper input variables.

Otherwise, sensitivity analysis can be performed to study the relative importance of input parameters (Maier and Dandy, 1996; Ray and Klindworth, 1996).

For the prediction of sequent debris yield, ANN models are trained by five input variables including logarithmic transformed drainage area and relief ratio of the watershed, maximum 1-hr rainfall intensity, total rainfall amount, and fire factor. ANN models are calibrated and validated by the same data applied in the MSDPM model (Pak, 2005). The output is log transformed debris yield resulting from each single storm event generated by the MSDPM model and it is scaled in such a way that the sum of debris yield is equal to the measured accumulated debris yield during that period. Drainage area means the contributing area where debris yield entrapped in debris basin are from, and previous studies reported that it is highly correlated to debris yield (Lustig, 1965). Relief ratio is calculated by the difference between highest and lowest elevation dividing by the maximum stream length. It has been proved to be a very significant variable in most regression equations for simulating debris yield (USACE, 2000).

Other related studies suggest some morphologic parameters also play an important role in unit debris yield simulation, for example, elongation ratio (ER), drainage density (DDR), hypsometric index (HI), total stream length (TSL), mean bifurcation ratio (MBR), and transport efficiency factor (T1). ER is defined as the ratio of diameter of a circle with the area equal to that of the basin to the maximum basin length - from the debris collection site to the watershed boundary along the longest stream. Scott and William (1978) included it in the regression

equations for estimating sediment yield at Transverse Ranges, southern California. DDM is the ratio produced by the sum of all stream lengths divided by drainage area. The stream length is determined by using Morisawa's method that counts not only the length of perennial or ephemeral flow on a standard USGS 1:24,000 scale topographic map but also the extension line into a likely stream or gully indicated by a series of V-shaped contours (USACE, 2000). Strahler (1957) announced a coincidence between maximum drainage density and high debris yield within some watersheds. HI is the relative height, the ground surface area above and under which are the same. It was reported to be a significant factor in Tatum's report (1963). MBR is the average ratio of the number of streams of a given order divided by the number of streams in the next higher order, and it is a measure of the degree of branching within a stream network. T1 is defined as the product of mean bifurcation ratio (MBR) and total stream length (TSL). Lustig (1965) suggested it should be included for sediment yield simulation at southern California. In addition to the four well-acknowledged input parameters in debris yield prediction: watershed area, relief ratio, maximum one-hour rainfall intensity, and fire factor, the aforementioned six watershed geomorphic parameters provided by USACE are also included step by step in this study.

As a creative approach, three soil properties including soil erodibility factor (SEF), soil permeability rate (SP), and soil liquid limit (SLL) for each watershed are included as input parameters one by one for the modeling of unit debris yield in addition to the four basic input parameters. SEF is a key factor in the USLE

(Equation 2.1) and it is a measure of rock fragments susceptibility to be detached and moved by water. SP is defined as the average of the maximum (permh) and the minimum (perml) permeability rate (Equation 3.2) with the unit of inch per hour for the top soil layer. Another factor - SLL is the moisture content at which soil will transfer from plastic to liquid phase. Similarly, the SLL is the average of its maximum (llh) and minimum value (lll) of the top soil layer as defined in Equation (3.3).

$$\text{Permeability} = \frac{\text{permh} + \text{perml}}{2} \quad (3.2)$$

$$\text{Liquid Limit} = \frac{\text{llh} + \text{lll}}{2} \quad (3.3)$$

The procedure of the acquisition of these soil properties parameters summarized as follows. First, the upstream contributing area to each debris basin is delineated with the aid of Better Assessment Science Integrating Point & Nonpoint Sources (BASINS) software developed by US Environmental Protection Agency (USEPA). Based on Digital Elevation Model (DEM) in Economic and Social Research Institute (ESRI)'s grid format, BASINS software delineated upstream watershed collection area after the selection of a mask area and the location of debris basin or the outlet where the flow should contribute to. Both data can be manually added to the map or loaded from existing files. The delineation is further refined by using the known values of watersheds, for example, watershed area and relief ratio. The upstream collection area of Brand and Childs debris basin are shown in Figure 6 as an example. Soil data in the

format of ESRI shapefile is from State Soil Geographic (STATSGO) database developed by Natural Resources Conservation Service. The area with similar type of soil is classified into one map unit and one soil map unit includes up to 21 components and every component has a maximum of 6 soil layers. There are two Soil Interpretations Record tables required to join with the STASGO shapefile attributes table based on the Map Unit Identification Symbol (MUID). One is called “layer” which contains the soil attributes in terms of each soil layer such as SEF, permh, perml, llh, and llr, within each component; another is called “comp” which provides soil attributes in each component and the percentage of exposed area of each component within every soil map unit. Although the average method is the simplest to determine three soil characteristics for a soil map unit, it is not as reasonable as weighted average method (WAM). The WAM means the more

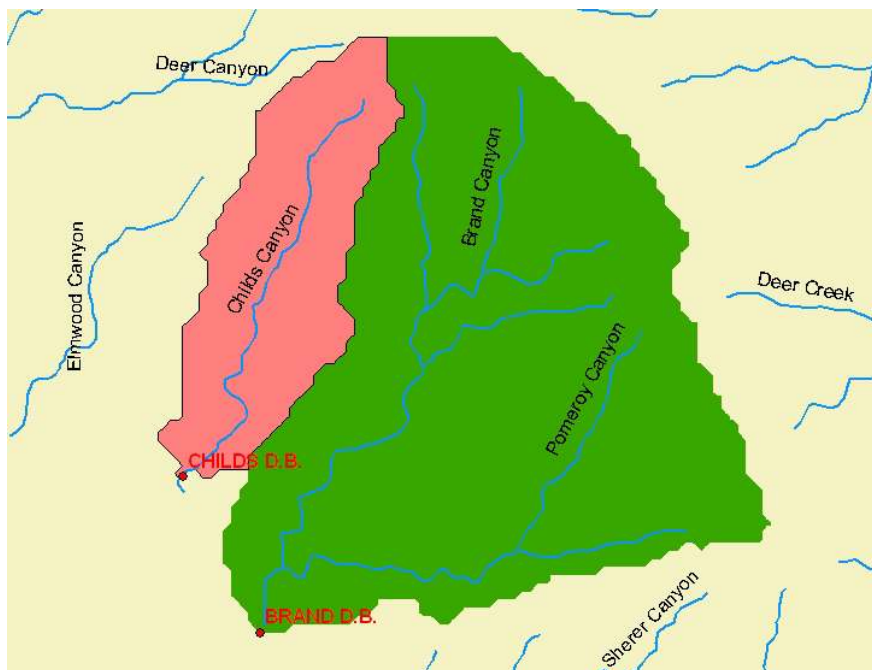


**Figure 6:** Upstream collection area for Brand and Childs debris basin

predominant of a soil component inside a soil map unit, the closer its values resemble the soil attributes values of the soil map unit. Most commonly a watershed includes more than one type of soil map unit, it is necessary to clip the soil attributes shapefile based on the watershed boundary and calculate the area of each soil map unit within the watershed. Finally, three soil factors for each watershed are determined by using WAM as well, i.e. proportioning their original values to the percentage of exposure of that soil map unit. The overlay of Brand and Childs Debris Basin watersheds and the soil layer is illustrated in Figure 7.

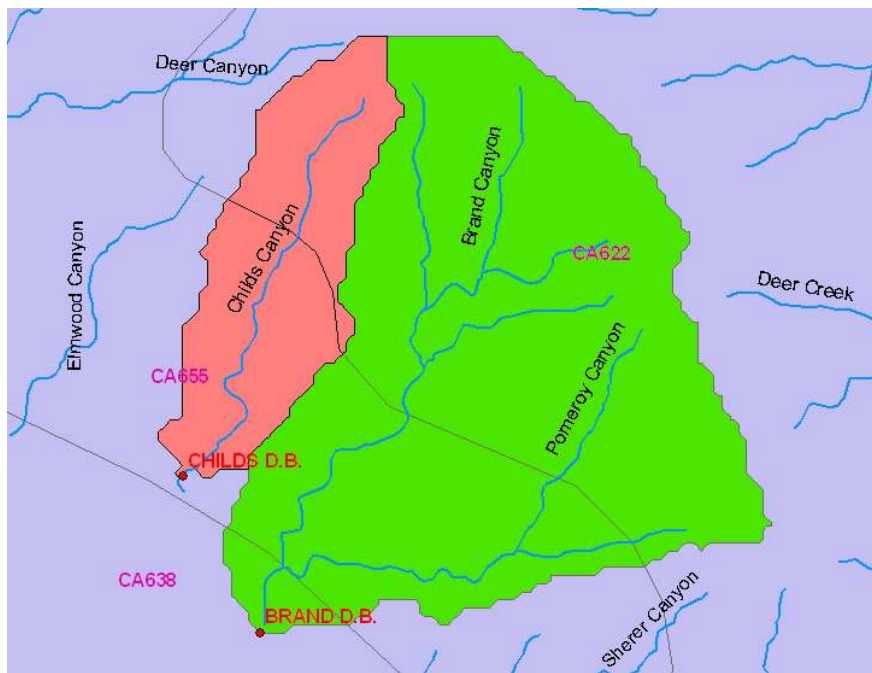


**Figure 7:** Overlay of soil layer and Brand and Childs debris basin watershed

### 3.2.2 Separation of Calibration and Validation Data

In general the whole data is divided into two sets: one set is for calibration or training data set, and the other set is for validation or testing data set. First an

ANN model is trained with the calibration data set, and then validation data set is provided to test the capability of the network to simulate new data. It was emphasized that the performance of ANN deteriorates seriously when the validation data set is outside the range of calibration data set (Flood and Kartam, 1994). Genetic Algorithm (GA) and Self-Organizing Map (SOM) were suggested by Bowden et al. (2002) as a solution to solve this problem. GA works in such a way that data is divided so as to minimize the statistical difference, i.e., mean and standard deviation, between calibration and validation data set. SOM clusters similar data records, or data records within a certain Euclidean distance, into one group. Thereafter, calibration and validation data sets are composed of data sampled from each cluster with similar statistical properties.

For the estimation of sequent debris yield, calibration and validation data are separated in the same way as in the MSDPM model (Pak, 2005), 300 data records for calibration and 30 for validation. For the unit debris yield simulation with watershed morphological parameters, approximately 15 percent of the whole data is randomly selected as validation data and the remainder 85% data is for calibration. Inspired by Bowden et al.'s (2002) study, subtractive clustering is used to separate calibration and validation data for unit debris yield collected from 80 smaller debris basins and 7 larger debris basins. This method 'find' cluster centers in a set of data by an iterative process of assigning all data within a certain radius of the cluster centers. Assuming all data points are clusters at the beginning, subtractive clustering method calculates the likelihood of each

data point to be a cluster. The data point with the maximum likelihood will be chosen as the first cluster, next, all the data points in the vicinity of the first center are removed, and then determine next cluster, repeat the same process until all data points are within the radius of the clusters. The radius for each data set is determined through modeling all the data by using fuzzy inference system. Since this fuzzy inference system classifies all the data into groups based on subtractive clustering method and then generates one fuzzy rule for each group of data, the radius is determined in such a way that training data error is the smallest and the structure of this fuzzy inference system is the simplest, i.e. less fuzzy rules. Generally, the clusters and data points furthest from the centers are selected for calibration and the data points in between are selected for validation.

### **3.2.3 Preprocessing of Data**

As suggested by Maier and Dandy (2000), calibration data for ANN should be standardized (i.e. a zero mean with unity standard deviation) to ensure all variables receive equal attention during training. It should also be scaled to a certain range to guarantee the outputs within the limit of the transfer function. For example, the range of logistic transfer function of the output layer is between 0 and 1, so the data should be generally scaled in the range 0.1-0.9 or 0.2-0.8 and “should avoid the area of extreme limits where too small weight updates can lead to flat spots in training” (Maier and Dandy, 2000).

If the mean square error (MSE) function is used as the measure of performance efficiency of neural network training, or the optimization of connection weights and biases, Fortin et al. (1997) stated that data needed to be normalized in order to obtain optimal result. In this study, all inputs and target output for ANN models are not only normalized, but also orthogonalized and uncorrelated with each other by using principal component analysis. Using singular value decomposition, those input variables that contributed less than 2% of the total variation, the sum of the square of the singular value divided by the column number of the calibration data set minus one, are eliminated (Demuth and Beale, 1998).

### **3.2.4 Determination of ANN Architecture**

ANN architecture is one of the most important and difficult tasks to be accomplished before start calibrating process. As introduced previously, it includes two parts: geometry of the network and internal parameters such as transfer function, the initial selection of connection weights and biases, epoch, error function, and so on.

#### **3.2.4.1 Geometry of A Neural Network**

The geometry of a neural network includes the selection of number of neuron on each layer and the number of hidden layer which are problem specific. Based on the review of some applications of ANN models with one hidden layer, the optimum number of neuron on hidden layer has been found to be less than

the number of inputs. Rogers and Dowla (1994) found the number of training samples has impact on network geometry. For example, the ratio of the number of training samples to the number of connection weights should be greater than 1, 2 (Masters, 1993), or even 10 (Weigend et. al., 1990). Compared with ANNs with more than one hidden layer, a neural network with one hidden layer requires less storage space and has higher processing speed, but its error surface is more complicated with more local minimum (Bebis and Georgiopoulos, 1994). ANNs with two hidden layers can learn the relation between inputs and outputs quickly (Plaut and Hinton, 1987) and have a remarkable ability to avoid local minima in the error surface. ANN with more than two hidden layers is seldomly used due to their low processing speed during training and testing. Flood and Kartam (1994) recommended two hidden layers as a starting point and they believed more hidden layer can provide more flexibility and enable approximation of complex functions with fewer connection weights in many situations. Without too many widely accepted guidelines, the trial-and-error method appears to be the only choice for determining the geometry.

As aforementioned, there are five input variables included to model sequent debris yield collected for 14 debris basins from 1984 to 2003. The number of input parameters varies from six to ten for forecasting unit debris yield for 36 debris basins from 1938 to 1983. There are four studied cases for this purpose. In the first case, six input parameters includes log transformed drainage area and relief ratio of the watershed, TSL, T1, logarithmic transformation of

rainfall intensity, and fire factor. In the second, third, and fourth case, DDM, ER and MBR, HI are included as input parameters step by step. 349 unit debris yield collected from 80 smaller debris basins are divided into five groups and each group of data is modeled with four basic input parameters such as log transformed drainage area and relief ratio, logarithmic values of maximum one hour precipitation, fire factor, and three soil attributes included one by one. For modeling seven larger debris basins, the four basic input parameters are maintained except the inclusion of peak discharge instead of maximum one hour precipitation. Peak discharge is believed to be more related to debris yield modeling but it is only available for larger watersheds. ANN models with a maximum of two hidden layers are calibrated to search for the best neural network geometry to estimate either sequent debris yield or unit debris yield. For the estimation of sequent debris yield, the number of hidden neuron varies from 6 to 14 for three-layered ANN models. The number of hidden neuron is from 5 to 21 when simulating unit debris yield with 10 inputs or less. After a neural network model is trained thousands of times, the best-fit connection weights and biases with the minimum calibration and validation error are saved for this neural network. The performance of all developed neural networks is compared to determine the best model for this studying case and meanwhile the effect of increasing hidden neurons on the network performance is analyzed. For both sequent debris yield and unit debris yield prediction, twenty-two four-layered ANN models are examined with different number of neurons on the first and the

second hidden layer, such as 3:1, 3:2, 3:3, 3:4, 4:1, 4:2, 4:3, 4:4, 4:5, 5:1, 5:2, 5:3, 5:4, 5:5, 5:6, 6:1, 6:2, 6:3, 6:4, 6:5, 6:6, and 6:7 (the first and second number indicate the number of the neuron on the first and second hidden layer, respectively). Pak and his colleague (2009) recommended that ANN models with two hidden layers are superior to neural networks with only one hidden layer. Therefore only ANN models with two hidden layers are selected for simulating unit debris yield collected from 7 larger debris basins.

### **3.2.4.2 Transfer Function**

Transfer function is applied to calculate the output of a neuron based on its incoming net input signal - the term inside the parentheses is a net input for neuron  $j$  on the hidden layer or the term inside the brackets is a net input for output neuron  $k$  in equation 3.1. The most commonly used transfer functions are sigmoid function, hyperbolic tangent function and linear function. The sigmoid function has the following form

$$f(n) = \frac{1}{1 + e^{-n}} \quad (3.4)$$

Where  $n$  is the net input,  $f(n)$  is the corresponding output of the neuron and it is in a range from 0 to 1. The hyperbolic tangent function is

$$f(n) = \tanh(n) = \frac{e^n - e^{-n}}{e^n + e^{-n}} \quad (3.5)$$

The linear function is simple; the output of the neuron equals to its net input.

Kaastra and Boyd (1995) demonstrated that a three-layered feed-forward neural network with sigmoid function for the hidden layer and linear for the output layer is capable of extrapolation beyond the range of calibration data. Kalman and Kwasny (1992) suggested that the hyperbolic tangent transfer function should be used for the hidden layer and linear function for the output layer that can approximate any function with a finite number of discontinuities. Referring to Maier and Dandy's paper in 1998, modeling results obtained using networks with hyperbolic tangent transfer function is slightly better than the results using logistic transfer function. Therefore, in this study, hyperbolic tangent function is chosen as the only transfer function for the hidden layer(s) of neural networks; and linear function is used as the transfer function for the output layer.

#### **3.2.4.3 Initial Selection of Connection Weights and Biases**

A traditional neural network is fully connected, in other words, neurons are only connected to neurons on the adjoining layers. The connection weight shows the strength between each two neurons, and its initial value can be zeroes, or any random numbers within the range of  $[0 \ 1]$  or  $[-1 \ 1]$  and has a significant impact on the performance of neural networks. It can also be applied to biases. Starting with different initial connection weights and biases, neural network should be trained for many times to reach the global minimum instead of local minimum in the error function surface. In this study, each neural network model is trained hundreds of times to start with different initial values.



### **3.2.5.1 BP Training Algorithm**

BP is one of the most widely used supervised training algorithms. It is composed of two directions of information flow: feed-forward and backward. During feed-forward pass, input vectors enter from the input layer and then flow through hidden layer and finally reach the output layer where outputs are computed based on the connection weights and biases, transfer functions, and the geometry of the network (Hagan, et al., 1996). The sum of squared error (SSE) between targets and outputs from the neural network is calculated, and the negative of the gradient vector of the error is propagated backwards toward the input layer to modify the connection weights and biases (Hagan, et al., 1996) based on Equation (3.6) and (3.7) that is called backward pass.

$$w_{i,j}^l(k+1) = w_{i,j}^l(k) - \alpha \frac{\partial E}{\partial w_{i,j}^l} \quad (3.6)$$

$$b_j^l(k+1) = b_j^l(k) - \alpha \frac{\partial E}{\partial b_j^l} \quad (3.7)$$

Where the superscript ( $l$ ) indicates the number of the layer, the first subscript ( $j$ ) describes  $j^{\text{th}}$  neuron on the current layer and the second subscripts represents the neuron  $i$  on the previous layer,  $\alpha$  is learning rate,  $k$  and  $k+1$  mean the  $k^{\text{th}}$  and  $(k+1)^{\text{th}}$  times that calibration data was presented to the network, and  $E$  is SSE. Although cubic and quadratic error functions are used sometimes, the SSE error function is the most commonly referenced because it is easy to calculate as well as its partial derivative with respect to connection weights and biases, penalizes

large errors, close to the heart of the normal distribution (Masters, 1993). SSE is formulated as follows.

$$SSE = \frac{1}{2} \sum_{s=1}^q \sum_{t=1}^p (Y_{st} - T_{st})^2 \quad (3.8)$$

In which  $q$  is the number of data pairs provided to train the ANN model during each epoch,  $p$  is the number of output neuron,  $Y$  is the estimated output by ANN, and  $T$  is target output.

### **3.2.5.2 Variations of BP Algorithm**

BP algorithm is criticized for its low training and convergence speed for some practical problems. As an improvement, the second order methods gain more and more popularity recently. For example, the classical Newton algorithm, one of the earlier developed second order methods, can be mathematically expressed as (Paris, et al., 1996):

$$W(k + 1) = W(k) - H^{-1} \nabla_{w_k} E \quad (3.9)$$

where, the first two terms are the new and old connection weights matrix,  $H^{-1}$  is the inverse of the Hessian matrix (Equation 3.10), and the last term is the gradient of the error at the  $k^{\text{th}}$  epoch.

$$H = \frac{\partial^2 E}{\partial^2 n^m} = \begin{bmatrix} \frac{\partial^2 E}{\partial n_1^m} & \frac{\partial^2 E}{\partial n_1^m \partial n_2^m} & \dots & \frac{\partial^2 E}{\partial n_1^m \partial n_{s^m}^m} \\ \frac{\partial^2 E}{\partial n_2^m \partial n_1^m} & \frac{\partial^2 E}{\partial n_2^m} & \dots & \frac{\partial^2 E}{\partial n_2^m \partial n_{s^m}^m} \\ \dots & \dots & \dots & \dots \\ \frac{\partial^2 E}{\partial n_{s^m}^m \partial x_1^m} & \frac{\partial^2 E}{\partial n_{s^m}^m \partial x_2^m} & \dots & \frac{\partial^2 E}{\partial n_{s^m}^m} \end{bmatrix} \quad (3.10)$$

Unfortunately, it is very complex and time-consuming to calculate the Hessian matrix for a feed-forward neural network. Therefore, a number of algorithms were proposed to approximate Hessian matrix in different ways. Levenberg-Marquardt (LM) algorithm (Hagan, et. al., 1996) is one of such improved algorithms, and connection weights and biases are updated following Equation 3.11.

$$W(k+1) = W(k) - [J^T J + \mu I]^{-1} J^T e \quad (3.11)$$

In which, J is Jacobian matrix which is the first derivatives of the network errors with respect to connection weights and biases,  $\mu$  is a scalar, I is identity matrix, and e is error matrix. Second-order methods have an order of two convergence speeds and require second order of the computational space. The latter is not a concern with the development of computer hardware. The LM algorithm is one of the fastest methods for training moderated-sized feed-forward neural networks and it is strongly recommended if there is no memory problem (Hagan, et. al.,

1996). Another algorithm is Bayesian Regulation BP (BRBP) algorithm which optimizes the connection weights and biases the same as LM algorithm, however, the performance function is a linear combination of SSE and connection weights and biases to reduce the risk of overfitting, or overtrained. Overfitting is a very common training problem and it has such a symptom that the estimation error of calibration data is small but the error of validation data is large. For comparison purpose, both training algorithms are used in this study.

Trained by either LM algorithm or BRBP algorithm, the generalization ability of neural networks also depends on some internal parameters such as epoch size, target goal, minimum gradient of training error, and maximum value of the scalar in Equation (3.11). The epoch size is the number of training samples for incremental training, and it is the number of times that calibration data is presented to train neural networks for batch training. Both algorithms belong to batch training. Epoch size is constant (i.e. 1000 or 10,000). Target goal is used to control the training process that means if a predefined target goal for calibration data is reached, the training is terminated and the architecture is saved for testing the validation data. Because the data are pre-processed between  $-1$  and  $1$ , so a lower target goal is used,  $1 \times 10^{-6}$ . The default values in Neural Network Toolbox of Matlab are used for minimum gradient of training error and maximum value of the scalar. To summarize, the training of a neural network will be stopped if any of the following goals is reached: (1) Epoch size, (2) Target goal, (3) Minimum gradient of training error, or (4) Maximum value of a scalar.

### 3.3 NFS and FNN Models

ANNs have been criticized for not helping in explaining the physics of hydrological process, and the lack of a standardized way to choose the architecture. Fuzzy logic system, addresses the linguistic, uncertainty and imprecise knowledge by using fuzzy sets for gradual qualities, and represents if-then rules by fuzzy antecedent and consequent parameters. Fuzzy logic system generally consists of five blocks as shown in Figure 8 (Jang, 1993), and it has been proved to be able to approximate any continuous function on a compact set to any accuracy (Buckley, 1993; Wang and Mendel, 1992).

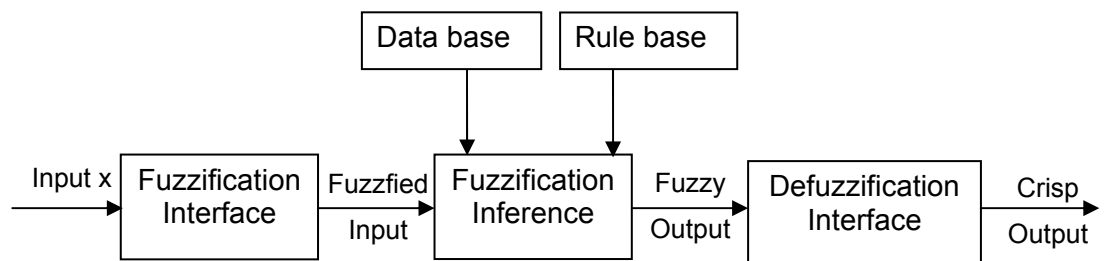


**Figure 8:** Basic configuration of fuzzy logic system

Through a fuzzification interface, crisp inputs are converted into fuzzified inputs or fuzzy singleton by using membership functions (i.e. triangular, trapezoidal, or Gaussian function). Data base includes membership function for antecedent fuzzy sets and rule base containing all fuzzy if-then rules for a practical problem. Employing fuzzy if-then rules from rule base, fuzzy inference generates a fuzzy output by a fuzzy reasoning method, e.g. minimum, product, etc. Finally, fuzzy output is transformed to crisp output through defuzzification interface by applying weighted average, or weighted sum method (Jang, 1993).

Fuzzy logic was first explored by Mamdani and Assilian (1975) for steam-engine control using fuzzy rules like ‘if  $x_1$  is  $F_1$ ,  $x_2$  is  $F_2$ , ... ,  $x_n$  is  $F_n$ , then  $y$  is  $Y$ ’ in which  $F_1$ ,  $F_2$ ,..., and  $F_n$  are called premise parameters and  $Y$  is consequent parameter. As an improvement, Takagi and Sugeno (1985), and Kang (TSK, 1988) introduced linear equations in the consequent part, for example, the fuzzy rule is ‘if  $x_1$  is  $F_1$ ,  $x_2$  is  $F_2$ , ... ,  $x_n$  is  $F_n$ , then  $y$  is  $c+a_1x_1+a_2x_2+\dots+a_nx_n$ ’ where  $c$ ,  $a_1$ ,  $a_2$ , ...,  $a_n$  are constants. Although TSK model was applied to many control and prediction problems, its lacking of learning methods for tuning the memberships to minimize output error limits its further application.

To overcome ‘black box’ behavior of ANNs and lack of formal tuning method of fuzzy logic system, researchers proposed two combined approaches: NFS and FNN. As an inventive approach in modeling sediment yield, ANFIS, one of the widely used NFSs, and GD-FNN, an improvement on traditional FNNs, are applied to estimate unit debris yield collected from 36 small debris basins within Los Angeles County in this study.

### **3.3.1 ANFIS Model**

ANFIS was developed by Jang in 1993 to generate “input-output mapping based on both human knowledge (fuzzy if-then rules) and stipulated input-output data pairs”. ANFIS employs either a combination of least-squares method and the BPGDM or only BPGDM to tune premise and consequent parameters. Figure 9 shows a simple ANFIS structure with two input variables ( $x$  and  $y$ ), one output,

and two fuzzy rules (Jang, 1993). Similar to ANN model, ANFIS composed of two passes, forward and backward. During forward pass, premise parameters are fixed, input data is entered from layer 1 and flows through layer 2, 3, and 4, and finally reach layer 5, defuzzification layer. ANFIS outputs are generated based on consequent parameters determined by using sequential least squares formulas (Equation 3.18) and outputs from the previous layer, and then the sum of squared errors between outputs and targets are calculated.

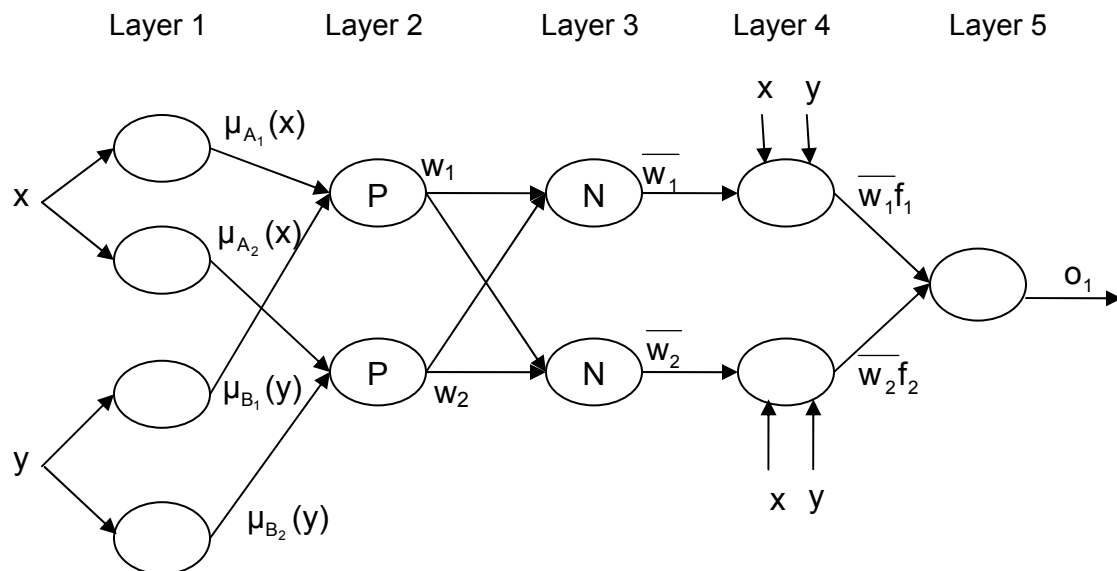


**Figure 9: An ANFIS Structure**

The working procedure of ANFIS model (Jang, 1993) is explained in details next.

Step 1 (layer 1 in Figure 9) is to calculate the matching degree of each input to a pre-specified membership function usually within a range of  $[0, 1]$ , for example, triangular-shaped function (Equation 3.12), trapezoidal-shaped function (Equation 3.13), Gaussian function (Equation 3.14), etc.

$$\mu_{A_i}(x) = \begin{cases} 0, & x < b_1 \\ \frac{x - b_1}{b_2 - b_1}, & b_1 \leq x \leq b_2 \\ \frac{b_3 - x}{b_3 - b_2}, & b_2 \leq x \leq b_3 \\ 0, & x \geq b_3 \end{cases} \quad (3.12)$$

$$\mu_{A_i}(x) = \begin{cases} 0, & x < a_1 \\ \frac{x - a_1}{a_2 - a_1}, & a_1 \leq x \leq a_2 \\ 1, & a_2 \leq x \leq a_3 \\ \frac{a_4 - x}{a_4 - a_3}, & a_3 \leq x \leq a_4 \\ 0, & x \geq a_4 \end{cases} \quad (3.13)$$

$$\mu_{A_i}(x) = \exp\left[-\frac{(x - c_i)^2}{\sigma_i^2}\right] \quad (3.14)$$

In Equation (3.12) three numbers  $b_1$ ,  $b_2$ , and  $b_3$ , inside triangular-shaped membership function are three corners of a triangle. Similarly, the number ( $a_1$ ,  $a_2$ ,  $a_3$ , and  $a_4$ ) indicates the location of four corners of a trapezoid in x-axis starting from the left bottom corner and going clockwise direction. ( $c_i, \sigma_i$ ) are the center and width of a Gaussian function. In fact, membership function can be any continuous function as long as it is piecewise differentiable (Jang, 1993).

Step 2 (layer 2 in Figure 9) is to compute the firing strength of a rule (Jang 1993), and it can be obtained by choosing products of outputs from the previous layer that can be expressed as

$$w_i = \mu_{A_i}(x) \times \mu_{B_i}(y) \quad i = 1, 2 \quad (3.15)$$

Step 3 (layer 3 in Figure 9) is to normalize the firing strength by the sum of all rules' firing strength as follows (Jang, 1993).

$$\overline{w}_i = \frac{w_i}{w_1 + w_2} \quad i = 1, 2 \quad (3.16)$$

Step 4 is to produce the output for each node in layer 4 by the product of normalized firing strength to fuzzy rule output implementing TSK model (i.e.  $f_i = r_i + p_i x + q_i y$  where  $r_i$ ,  $p_i$ , and  $q_i$  are consequent parameters) and the output is

$$\overline{O}_i = \overline{w}_i (r_i + p_i x + q_i y) \quad i = 1, 2 \quad (3.17)$$

The consequent parameters are determined by sequent least square formulas (Equation 3.18), a more efficient method for small numbers of linear parameters (Jang, 1993).

$$\begin{aligned} X_{k+1} &= X_k + S_{k+1} a_{k+1} (b_{k+1}^T - a_{k+1}^T X_k) \\ S_{k+1} &= S_k - \frac{S_k a_{k+1} a_{k+1}^T S_k}{1 + a_{k+1}^T S_k a_{k+1}} \quad k = 1, 2, \dots, n-1 \end{aligned} \quad (3.18)$$

In the equation,  $X$  is consequent parameter matrix with zeroes as initial values,  $S$  is covariance matrix and the initial value is the product of a large positive number and identity matrix,  $a_{k+1}$  is  $(k+1)^{\text{th}}$  row vector of input data matrix,  $b_{k+1}$  is the  $(k+1)^{\text{th}}$  element of target matrix, and  $n$  is the number of training data.

Step 5 is to calculate the overall output as a summation of all outputs from layer 4 (Jang, 1993).

$$\overline{O}_i = \frac{\sum_i w_i (r_i + p_i x + q_i y)}{\sum_i w_i} \quad i = 1, 2 \quad (3.19)$$

During backward pass, the first derivative of error function with respect to nodal outputs propagates backward from layer 5 to layer 1 while the consequent parameters are fixed but premise parameters are modified based on the GDM algorithm. Both premise and consequent parameters are iteratively adjusted during forward and backward passes in order to minimize difference between ANFIS outputs and target values. ANFIS is proved to be an effective modeling tool for nonlinear relationship, chaotic time series, and a number of practical problems.

ANFIS method demands some prior information such as input space partition and number of fuzzy rules and expert knowledge, and the trial-and-error method is necessary to find out the optimal structure if prior expert knowledge is not available.

### **3.3.2 GD-FNN Model**

In 2001, Wu et al. developed a generalized dynamic FNN (GD-FNN) approach implementing TSK fuzzy system which is capable of generating and deleting fuzzy rules automatically. The learning is hierarchical, on-line or adaptive as introduced in ANN section, and self-organizing. The width of Gaussian membership function are selected based on fuzzy  $\epsilon$  – completeness rather than random values or simple methods, and the number of fuzzy rule is not necessarily equivalent to the number of membership function for each input variable. The architecture of the GD-FNN model is illustrated in Figure 10.

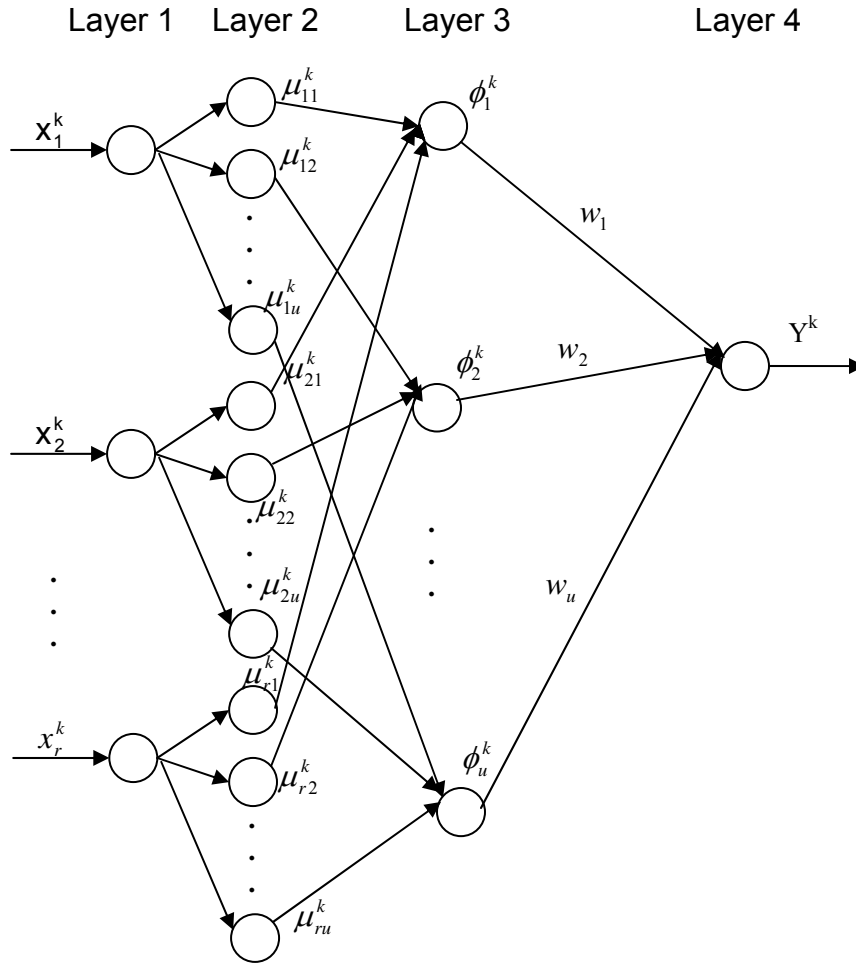


**Figure 10:** The architecture of the GD-FNN model

Layer 1 is input layer, the same as that in the neural network. In layer 2, crisp inputs are fuzzified by using Gaussian membership function (Wu et al., 2001) as follows.

$$\mu_{A_{ij}}(x_i) = \exp\left[-\frac{(x_i - c_{ij})^2}{\sigma_{ij}^2}\right] \quad (i=1, 2, \dots, r; j=1, 2, \dots, u) \quad (3.20)$$

Where  $r$  is the number of input variables,  $j$  is the number of fuzzy rules,  $c_{ij}$  and  $\sigma_{ij}$  are the center and width of Gaussian membership function for  $i^{\text{th}}$  input and  $j^{\text{th}}$

fuzzy rule. Using T-norm (product) as the method to calculate firing strength of each rule and introducing a new term – regularized Mahalanobis distance (md) (Wu et al., 2001), the output for the third layer can be expressed as

$$\varphi_j = \exp\left[-\sum_{i=1}^r \frac{(x_i - c_{ij})^2}{\sigma_{ij}}\right] = \exp[-md(j)^2] \quad (j=1, 2, \dots, u) \quad (3.21)$$

Based on TSK model, the output in the fourth layer is a weighted summation of outputs from the previous layer and results of fuzzy rules, and it is in the form of

$$y = \sum_{j=1}^u w_j * \varphi_j = \sum_{j=1}^u (k_{j0} + k_{j1}x_1 + \dots + k_{jr}x_r) * \varphi_j \quad (j=1, 2, \dots, u) \quad (3.22)$$

The above equation can be rewritten as follows,

$$Y = W\Phi \quad (3.23)$$

Where  $W = [k_{10} \dots k_{u0} \ k_{11} \dots k_{u1} \ k_{1r} \dots k_{ur}]_{1 \times (r+1)u}$ , and

$$\Phi = \begin{bmatrix} \varphi_{11} & \varphi_{12} & \dots & \varphi_{1n} \\ \dots & \dots & \dots & \dots \\ \varphi_{u1} & \varphi_{u2} & \dots & \varphi_{un} \\ \varphi_{11}x_{11} & \varphi_{12}x_{12} & \dots & \varphi_{1n}x_{1n} \\ \dots & \dots & \dots & \dots \\ \varphi_{u1}x_{11} & \varphi_{u2}x_{12} & \dots & \varphi_{un}x_{1n} \\ \dots & \dots & \dots & \dots \\ \varphi_{11}x_{r1} & \varphi_{12}x_{r2} & \dots & \varphi_{1n}x_{rm} \\ \dots & \dots & \dots & \dots \\ \varphi_{u1}x_{r1} & \varphi_{u2}x_{r2} & \dots & \varphi_{un}x_{rm} \end{bmatrix}_{(r+1)u \times n}$$

Using a computationally simple but efficient method - linear least squares (LLS) method, the consequent parameters are determined by  $W = T(\Phi^T\Phi)^{-1}\Phi^T$  where T is target matrix (Wu et al., 2001).

Two new parameters, desired accuracy ( $k_e$ ) and effective radius of the accommodation boundary ( $k_d$ ) are defined in equation (3.24) and (3.25), respectively. Both parameters gradually reduce as training continues because larger accommodation boundary and error index at the beginning promotes rough but global learning and fine learning begins when  $k_e$  and  $k_d$  reaches  $e_{\min}$  and  $d_{\min}$  (Wu et al., 2001).

$$k_e = \begin{cases} e_{\max}, & 1 < k < n/3 \\ \max(e_{\max} \times \beta^k, e_{\min}), & n/3 \leq k \leq 2n/3 \\ e_{\min}, & 2n/3 < k \leq n \end{cases} \quad (3.24)$$

$$k_d = \begin{cases} d_{\max} = \sqrt{\ln(1/\epsilon_{\min})}, & 1 < k < n/3 \\ \max(d_{\max} \times \gamma^k, d_{\min}), & n/3 \leq k \leq 2n/3 \\ d_{\min} = \sqrt{\ln(1/\epsilon_{\max})}, & 2n/3 < k \leq n \end{cases} \quad (3.25)$$

In the above two equations,  $e_{\max}$  = predefined maximum error,  $k$  = learning epoch,  $e_{\min}$  = desired accuracy,  $\beta$  is convergence constant and defined as

$\beta = \left(\frac{e_{\min}}{e_{\max}}\right)^{3/n}$ ,  $d_{\max}$  = largest length of input space,  $d_{\min}$  = smallest length of

interest, decay constant is  $\gamma = \left(\frac{d_{\min}}{d_{\max}}\right)^{3/n}$ ,  $\epsilon_{\max}$  = maximum value of fuzzy

$\epsilon$  – completeness, and  $\epsilon_{\min}$  = minimum value of fuzzy  $\epsilon$  – completeness, usually

0.5. Another big improvements in GD-FNN is the use of semiclosed fuzzy sets to satisfy  $\epsilon$  – completeness fuzzy rules, that is, for any input ( $x$ ) in the operating range ( $[a, b]$ ), there is at least one fuzzy rule so that firing strength is no less than

$\varepsilon$  (Wu et al., 2001). For one fuzzy set, the width of Gaussian membership function should be selected as

$$\sigma_1 = \begin{cases} \frac{|a-b|}{\sqrt{\ln(1/\varepsilon)}}, & |c_1 - a| \leq k_{mf}, \text{ or } |c_1 - b| \leq k_{mf} \\ \max\left(\frac{|c_1 - a|}{\sqrt{\ln(1/\varepsilon)}}, \frac{|c_1 - b|}{\sqrt{\ln(1/\varepsilon)}}\right), & |c_1 - a| > k_{mf} \ \& \ |c_1 - b| > k_{mf} \end{cases} \quad (3.26)$$

$c_1$  is center of Gaussian function, and  $k_{mf}$  is a predefined small constant for measuring the similarity of neighboring membership function. If there is more than one fuzzy rule, the newly generated Gaussian function width should be (Wu et al., 2001)

$$\sigma_j = \max\left(\frac{|c_{j-1} - c_j|}{\sqrt{\ln(1/\varepsilon)}}, \frac{|c_j - c_{j+1}|}{\sqrt{\ln(1/\varepsilon)}}\right), \quad \text{for any } x \in (c_{j-1}, c_{j+1}) \quad (3.27)$$

$c_{j-1}$  and  $c_{j+1}$  are two neighboring membership function centers.

During learning process, there are only four possible cases (Wu et al., 2001). The first case is when  $|e_k| > k_e$  and  $md_{\min} > k_d$ : a new fuzzy rule will be generated but whether a new membership should be added to a neuron depends on E-distance (ed) which is

$$ed_i = \left| x_i^k - x_{\min}, x_i^k - c_{i1}, \dots, x_i^k - c_{iu}, x_i^k - x_{\max} \right| \quad (3.28)$$

If  $\min(ed_i) > k_{mf}$ , a new membership should be created while the corresponding new center should be  $c_{i(u+1)} = x_i^k$  and equation (3.27) should be used for width. After a fuzzy rule is generated, its significance can be evaluated by Error Reduction Ratio (ERR) matrix which is derived as follows.

Rewrite equation (3.23) using T instead of Y,  $T = W\Phi + E^T$  where E is error matrix, and then transpose both sides of the equation (Wu et al., 2001), we have

$$T^T = \Phi^T W^T + E \Rightarrow D_{n \times 1} = H_{n \times (r+1)u} \theta_{(r+1)u \times 1} + E_{n \times 1} \quad (3.29)$$

If the row number in matrix H is greater than its column number, it can be decomposed into one orthogonal matrix (P) with the same size as H and one upper triangular matrix (N) as

$$H_{n \times (r+1)u} = P_{n \times (r+1)u} N_{(r+1)u \times (r+1)u} \quad (3.30)$$

Substitute Equation (3.30) into Equation (3.29),

$$D_{n \times 1} = P_{n \times (r+1)u} N_{(r+1)u \times (r+1)u} \theta_{(r+1)u \times 1} + E_{n \times 1} = P_{n \times (r+1)u} G_{(r+1)u \times 1} + E_{n \times 1} \quad (3.31)$$

The LLS solution of G is  $G_{(r+1)u \times 1} = (P^T P)^{-1} P^T D$  (Wu et al., 2001).

The sum of squares or energy D (Wu et al., 2001) is

$$DD^T = \sum_{m=1}^{(r+1)u} g_m^2 p_m^T p_m + E^T E \quad (3.32)$$

In equation (3.32),  $g_m$  is  $m^{\text{th}}$  row vector of matrix G, and  $p_m$  is  $m^{\text{th}}$  column vector of matrix P. The ERR matrix is given by (Wu et al., 2001)

$$\text{err}_m = \frac{(p_m^T D)^2}{p_m^T p_m D^T D} \quad (m = 1, 2, \dots, (r+1) * u) \quad (3.33)$$

ERR matrix represents the similarity of  $p_m$  and D. The matrix ERR is reorganized as  $\Delta_{(r+1) \times u} = (\rho_1 \ \rho_2 \ \dots \ \rho_u)$ . The relative significance of  $m^{\text{th}}$  neuron

can be evaluated by  $\eta_m = \sqrt{\frac{\rho_m^T \rho_m}{r+1}}$ . The larger the  $\eta_m$  is, the more important is the

$m^{\text{th}}$  neuron or the fuzzy rule (Wu et al., 2001). If  $\eta_m < k_{\text{err}}$ , the  $m^{\text{th}}$  neuron and corresponding fuzzy rule are delete where  $k_{\text{err}}$  is a predefined small positive constant.

If  $|e_k| > k_e$  and  $md_{\text{min}} \leq k_d$ , it indicates  $x_i^k$  can be covered by the adjacent fuzzy rule but performance is not satisfied. Therefore the width of the adjacent membership function should be updated (Wu et al., 2001) as

$$\sigma_{ij}^{\text{new}} = \begin{cases} \frac{k_s}{k_s + r^2(1-k_s)(B_{ij} - 1/r)^2} \sigma_{ij}^{\text{old}}, & B_{ij} = \frac{\text{err}_{ij}}{\sum_{m=2}^{r+1} \rho_j(m)} < 1/r \\ \sigma_{ij}^{\text{old}}, & \text{Otherwise} \end{cases} \quad (3.34)$$

$B_{ij}$  is a newly introduced parameter which represents the significance of  $i^{\text{th}}$  input variable in the  $j^{\text{th}}$  rule.  $K_s = 0.9$  was used by Wu et al. (2001). The change of width requires the modification of the consequent parameters by using  $W = T(\Phi^T \Phi)^{-1} \Phi^T$  as well.

For the remaining two cases:  $|e_k| \leq k_e$  and  $md_{\text{min}} \leq k_d$ , or  $|e_k| \leq k_e$  and  $md_{\text{min}} > k_d$ , only consequent parameters are required to adjust, or for the former case, do nothing. The whole procedure is outlined as a flow chart in Figure 11 (Wu et al., 2001).

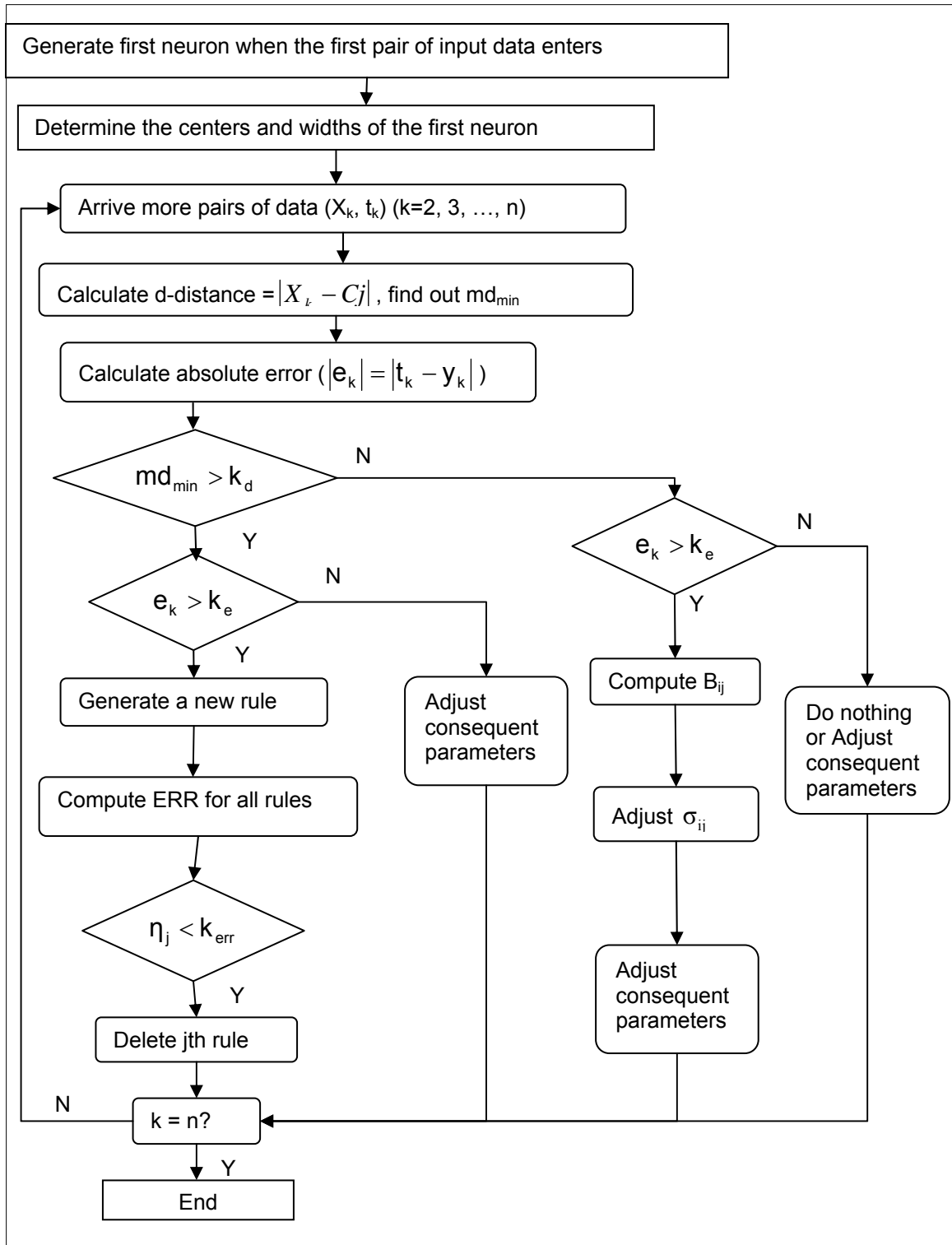


**Figure 11:** The flowchart of GD-FNN algorithm

For the unit debris yield estimation in this study, from Case 4 to 7, 85 percent data from the whole data set are presented to calibrate ANFIS, and calibrate GD-FNN model with one by one data record until running out of data. After training, the generated ANFIS and GD-FNN structure are saved and examined for its generalization capability for an independent set of validation data.

### **3.4 Sensitivity Analysis**

The study of the relative importance of input parameters on the generalization ability of an ANN model is referred to as sensitivity analysis. In this study, no more than two input parameters are included each step to examine their impacts on the performance of artificial intelligence models. Overall speaking, there are three studied cases for sequent debris yield estimation and twelve cases excluding those with soil characteristics as additional input parameters for modeling unit debris yield. ANN models are trained by different number of input parameters or different number of calibration data for all the fifteen studied cases and the detailed information is organized in Table 1. ANFIS and GD-FNN models are only applied to estimate unit debris yield in Case 4, 5, 6, and 7.

The neural network toolbox and the fuzzy logic toolbox in Matlab are very helpful for developing ANN and ANFIS models. Trial and error method is used to find out the best architecture of ANN and ANFIS. The computer codes for GD-

FNN model are created in this study following the general approach outlined in Wu et al.'s paper (2001). To evaluate the performance of all artificial intelligence models developed in this study, the mean square error (MSE) (Equation 3.35) and a regression analysis between the models predicted outputs and the measured debris values are used for both the validation data and calibration data.

$$\text{MSE} = \frac{1}{q \times p} \sum_{r=1}^q \sum_{k=1}^p (Y_{rk} - T_{rk})^2 \quad (3.35)$$

The parameters in the above equation are the same as those in equation (3.8).

The evaluation of network performance follows such a procedure: (1). compare the MSEs for both calibration and validation data sets; (2). compare the absolute difference between estimated and actual debris yield; (3). compare the correlation coefficients and the values of the slopes for the best linear regression lines. In general, the smaller the MSE is, the closer the correlation coefficient and the value of the slope are to unity, the more accurate is the model estimation.

**Table 1:** Summary of input parameters for each case

Output Case No.	Sequent Debris Yield			Unit Debris Yield											
	1	2	3	4 <sup>#</sup>	5 <sup>#</sup>	6 <sup>#</sup>	7 <sup>#</sup>	8	9	10	11	12	13	14	15
Input Parameter															
Watershed Area (A)	√	√	√	√	√	√	√	√	√	√	√	√	√	√	√
Relief Ratio (R <sub>r</sub> )	√	√	√	√	√	√	√	√	√	√	√	√	√	√	√
Max. 1-hr Rainfall Intensity (I)	√	√	√	√	√	√	√	√	√	√	√	√			
Total Rainfall Amount (P)	√	√	√												
Fire Factor (F)	√	√	√	√	√	√	√	√	√	√	√	√	√	√	√
Percentage of Burned Area (B <sub>p</sub> )			√												
Year after Last Wildfire Event (B <sub>y</sub> )			√												
No. of Antecedent Effective Storm (A <sub>p</sub> )			√												
Elongation Ratio (ER)						√	√								
Drainage Density (DDM)					√	√	√								
Hypsometric Index (HI)							√								
Total Stream Length (TSL)				√	√	√	√								
Mean Bifurcation Ratio (MBR)						√	√								
Transport Efficiency Factor (T <sub>1</sub> )				√	√	√	√								
Soil Erodibility Factor* (SEF)								√	√	√	√				
Soil Permeability* (SP)								√	√	√	√				
Soil Liquid Limit* (SLL)								√	√	√	√				
Peak Discharge (Q <sub>CSM</sub> )													√	√	√
Number of Calibration Data	300	244		170				58	61	55	62	63	48	52	54
Number of Validation Data	30			30				10	11	12	9	8	8	12	12

\* Three soil properties are added as input parameter one by one.

# Modeling methods include ANN, ANFIS, and GD-FNN.

## **Chapter 4: Presentation and Discussion of Results**

### **4.1 Estimation of Sequent Debris Yield**

Three sets of ANN models are developed to demonstrate their ability to estimate sequent sediment yield. The first set of ANN models is trained by 300 data with five input parameters including drainage area, watershed relief ratio, maximum one-hour rainfall intensity, total rainfall amount, and fire factor. These are the same parameters as used in a statistical model - MSDPM (Pak, 2005) except the logarithmic values of the first two input parameters and measured sediment yield is utilized in ANN models as targets rather than their estimated values by the MSDPM (Pak et al., 2009). The second set of ANN models are calibrated by the same input parameters but less data records. Data obtained at two debris basins (56 data records) before 1986 is excluded to study their effect on the neural networks performance. These data are believed to be less reliable than the more recent collected data because they were collected during a transition period when the collection agency changed. The last set of ANN models are trained by the aforementioned five input parameters, and three more input parameters: the percentage of the area that is burned by wildfire within the watershed, time after the last wildfire event in terms of year, and the number of the antecedent effective rainfall events. The number of training data records is the same as in the second case.

The calibration and validation data sets are the same as those used to create the MSDPM for comparison. Before start training the ANN models, both the inputs and the output target values are normalized, and the input vectors are uncorrelated by applying principal component analysis. Using singular value decomposition, those input variables that contributed less than 2% of the total variation are eliminated (Demuth and Beale, 1998).

#### **4.1.1 Case 1**

Trained by five input parameters, the number of hidden neuron of three-layer ANN models varies from 6 to 14. For four-layer ANN models, twenty-two groups of different geometries are examined and they are (3,1), (3,2), (3,3), (3,4), (4,1), (4,2), (4,3), (4,4), (4,5), (5,1), (5,2), (5,3), (5,4), (5,5), (5,6), (6,1), (6,2), (6,3), (6,4), (6,5), (6,6), and (6,7) (the first number indicates the number of neuron in the first hidden layer, and the second number is the number of the neuron in the second hidden layer). The training algorithm is BRBP algorithm to avoid overfitting problem. The training process will be terminated when epoch size reaches 1000, or error goal reaches  $1 \times 10^{-6}$ , or the minimum gradient of the error reaches  $1 \times 10^{-10}$ , or the default values of the rest internal parameters specified in Matlab. Transfer function for hidden layer(s) is hyperbolic tangent function, and linear function is for the output layer. The modeling results achieved by all ANN models are listed in Table 2.

**Table 2:** Summary of the performance of ANN models for Case 1

ANN Geometry	Validation Data Set			Calibration Data Set			Average MSE
	Slope	R	MSE	Slope	R	MSE	
5,6,1 (43)	0.900	0.952	0.33275	0.854	0.928	0.22255	0.27765
5,7,1 (50)	0.912	0.963	0.25377	0.885	0.943	0.17712	0.21544
5,8,1 (57)	1.070	0.995	0.23564	0.918	0.961	0.12287	0.17925
5,9,1 (64)	0.808	0.964	0.29863	0.931	0.966	0.10587	0.20225
5,10,1 (71)	0.786	0.957	0.38804	0.948	0.975	0.08004	0.23404
5,11,1 (78)	0.828	0.934	0.47781	0.938	0.97	0.09487	0.28634
5,12,1 (85)	0.938	0.946	0.38938	0.968	0.985	0.04860	0.21899
<b>5,13,1 (92)</b>	<b>0.829</b>	<b>0.981</b>	<b>0.21779</b>	<b>0.966</b>	<b>0.984</b>	<b>0.04929</b>	<b>0.13354</b>
5,14,1 (99)	0.786	0.948	0.39773	0.961	0.983	0.05509	0.22641
5,3,1,1 (24)	0.865	0.996	0.11163	0.956	0.978	0.06992	0.09078
5,3,2,1 (29)	0.830	0.992	0.17997	0.979	0.958	0.06622	0.12309
5,3,3,1 (34)	0.923	0.996	0.04711	0.973	0.986	0.04368	0.04539
5,3,4,1 (39)	0.924	0.996	0.05022	0.983	0.991	0.02751	0.03886
5,4,1,1 (31)	0.881	0.998	0.08878	0.996	0.998	0.00585	0.04731
5,4,2,1 (37)	0.910	0.997	0.05740	0.988	0.994	0.01963	0.03851
5,4,3,1 (43)	0.872	0.995	0.10707	0.997	0.999	0.00407	0.05557
5,4,4,1 (49)	1.020	0.998	0.01681	0.999	1.000	0.00112	0.00896
5,4,5,1 (55)	0.994	0.993	0.04827	1.000	1.000	0.00050	0.02439
5,5,1,1 (38)	0.964	1.000	0.00830	1.000	1.000	0.00037	0.00434
5,5,2,1 (45)	0.947	0.997	0.03108	0.999	1.000	0.00131	0.01619
5,5,3,1 (52)	0.927	0.995	0.05520	1.000	1.000	0.00014	0.02767
5,5,4,1 (59)	0.999	0.998	0.01204	1.000	1.000	0.00000	0.00602
5,5,5,1 (66)	0.968	0.995	0.03795	1.000	1.000	0.00003	0.01899
5,5,6,1 (73)	0.944	0.998	0.02658	1.000	1.000	0.00016	0.01337
5,6,1,1 (45)	0.923	0.999	0.03400	0.999	1.000	0.00139	0.01769
<b>5,6,2,1 (53)</b>	<b>0.972</b>	<b>0.996</b>	<b>0.02704</b>	<b>1.000</b>	<b>1.000</b>	<b>0.00020</b>	<b>0.01362</b>
5,6,3,1 (61)	0.971	0.995	0.03362	1.000	1.000	0.00007	0.01685
5,6,4,1 (69)	0.941	0.996	0.04085	1.000	1.000	0.00000	0.02043
5,6,5,1 (77)	0.915	0.988	0.10608	1.000	1.000	0.00002	0.05305
5,6,6,1 (85)	0.973	0.997	0.02212	1.000	1.000	0.00000	0.01106
5,6,7,1 (93)	0.992	0.996	0.02661	1.000	1.000	0.00000	0.01331

The first column in the table is the geometry of each neural network, for example, (5,6,1) is a network with five input neurons, six neurons on the hidden layer and one output neuron; and the number in the parenthesis after (5,6,1) (i.e. 43) is the number of connection weights and biases, or effective parameter of this network. The bolded row indicates the best geometry of ANN model with either one or two hidden layers. For example, the three-layer ANN model with 13

hidden neurons performs best among all the three-layered ANN models, and the neural network (5,6,2,1) achieves the lowest average MSE, best correlation coefficients and smallest percentage differences between measured and estimated debris yield. It is also true that this ANN model predicts debris yield more accurate than the remaining four-layered networks and all three-layered neural networks for both calibration and validation data.

The measured and estimated sediment yield by the best ANN model (5,6,2,1) and MSDPM are compared in Table 3. As seen from the table, the MSDPM predicts sediment yield within a range of a difference from -7.5% to 32.8% for the calibration data set compared with the field data, and the error bond is [-4.7%, 10.0%] by using the ANN model (5,6,2,1). It is seen that the ANN model prediction has smaller error bond for the calibration data set.

After calibration, both models are tested by the validation data set collected from the Brand debris basin and the Childs debris basin resulting from storm events between November 8, 2002 and April 2, 2003. For the Brand debris basin, the measured sediment yield is 81,358 m<sup>3</sup>, while the estimated sediment yield by the MSDPM is 75,935 m<sup>3</sup> and it is 69,401 m<sup>3</sup> by the ANN model. The difference between the estimated and measured values was 5,423 m<sup>3</sup> (-6.7%) for the MSDPM, and 11,957 m<sup>3</sup> (-14.7%) by the ANN model. It is obvious that this sediment yield is much larger than any of the sediment yield used for training. For the Childs debris basin, the measured sediment yield is 22,249 m<sup>3</sup>, while the estimated sediment yield is 20,355 m<sup>3</sup> by the MSDPM which underestimated the

sediment yield with a magnitude of 1,894 m<sup>3</sup> or -8.5%. ANN model prediction is 21,251 m<sup>3</sup> which is 998 m<sup>3</sup> (-4.5%) lower than the measured value. Both models underestimate sediment yield for the validation data and especially for the Brand debris basin by the ANN model. Figure 12 shows the linear regression results for both calibration and validation data sets. The solid line is the best linear regression line based on the data points whose x-value is the measured sediment yield, and the y-value is the predicted values by ANN model. The dashed 45 degree line is the perfect fit line.

**Table 3:** Summary of calibration and validation results by two models for Case1

	Debris Basin	Rr (m/km)	Area (ha)	Measured Dy (m <sup>3</sup> )	MSDPM Estimated Dy (m <sup>3</sup> )	Diffe <sup>1</sup> (%)	ANN Estimated Dy (m <sup>3</sup> )	Diffe <sup>2</sup> (%)
Calibration Data	Lannan Case 1	405.00	63.94	13,577	13,480	-0.71	13,340	-1.74
	Lannan Case 2	405.00	63.94	5,047	5,526	9.49	5,113	-1.30
	Kinneloa East	444.03	51.80	23,627	22,005	-6.87	23,474	-0.65
	Kinneloa West	475.84	52.21	33,261	30,751	-7.55	32,383	-2.64
	Rubio	280.06	329.2	17,001	17,830	4.88	17,038	0.22
	Bailey	337.07	153.8	22,948	23,501	2.41	22,965	0.07
	Sunny-side	475.80	5.212	1,239	1,282	3.47	1,181	-4.67
	Carriage House	433.99	7.689	1,710	2,007	17.4	1,824	6.69
	Auburn	521.71	41.28	8,364	8,942	6.91	8,604	2.87
	Fairoaks	60.013	54.63	1,847	1,748	-5.36	1,863	0.88
	West Ravine	286.76	63.94	9,331	11,276	20.84	9,706	4.02
	Big Briar	509.87	5.261	552	733	32.79	588	6.58
Hay	352.74	52.21	4,484	5,759	28.43	4,933	10.01	
Validation Data	Brand	280	267	81,358	75,935	-6.67	69,401	-14.70
	Childs	314	81	22,249	20,355	-8.51	21,251	-4.49

Diffe<sup>1</sup> - Difference between measured debris yield and the estimated values using MSDPM.

Diffe<sup>2</sup> - Difference between measured debris yield and the estimated values using ANN model

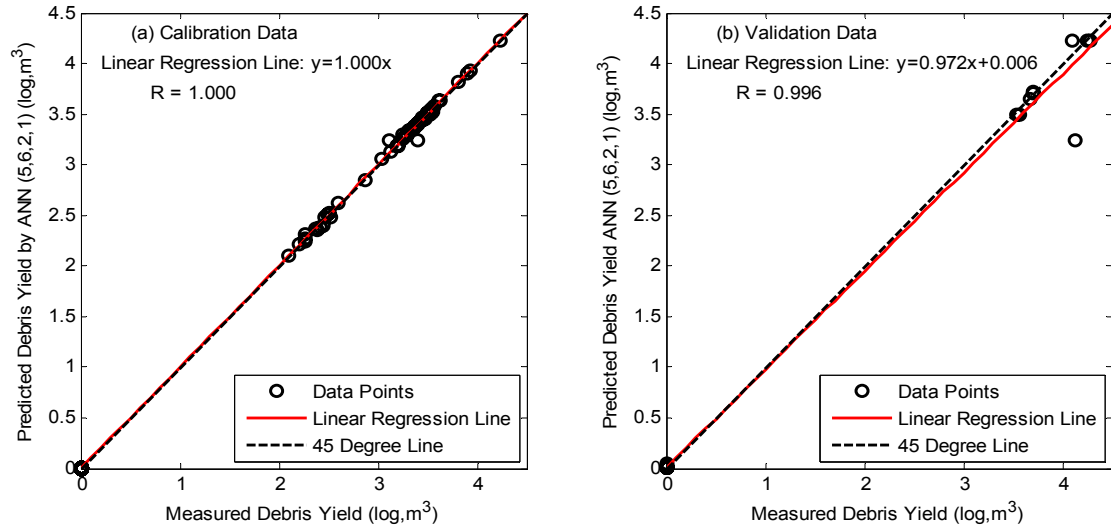


**Figure 12:** Linear regression analysis between measured and ANN model estimated debris yield (a) Calibration Data Set (b) Validation Data Set for Case 1

#### 4.1.2 Case 2

For the second set of ANN models, the data from Big Briar debris basin and Hay debris basin is removed from the calibration data. Therefore ANN models are trained by 244 data records and 5 input parameters while the data from Brand and Childs debris basin is still used for validation purpose. Internal parameters, transfer functions, training algorithm and neural network geometries are the same as those in the first case. Table 4 shows MSE and linear regression analysis results for all developed ANN models.

The ANN model with 13 neurons on the only hidden layer simulates debris yield with lowest average MSE among all three-layered networks. However, the optimal ANN model in this case has three and four neurons in the first and second hidden layer, respectively. It is able to predict debris yield with 0.00024

MSE for the calibration data and 0.00035 MSE for the validation data that outperformed the best neural network (5,6,2,1) in the first case. It suggests the removal of unreliable data does improve the modeling accuracy.

**Table 4:** Summary of the performance of ANN models for Case 2

ANN Geometry	Validation Data Set			Calibration Data Set			Average MSE
	Slope	R	MSE	Slope	R	MSE	
5,6,1 (43)	0.802	0.956	0.35516	0.896	0.948	0.18034	0.26775
5,7,1 (50)	0.847	0.985	0.24829	0.942	0.971	0.10075	0.17452
5,8,1 (57)	0.860	0.968	0.24267	0.911	0.957	0.15200	0.19734
5,9,1 (64)	0.955	0.961	0.28642	0.979	0.989	0.03745	0.16194
5,10,1 (71)	0.867	0.944	0.37904	0.951	0.977	0.08145	0.23025
5,11,1 (78)	0.986	0.964	0.26485	0.940	0.972	0.09743	0.18114
5,12,1 (85)	0.899	0.961	0.27403	0.939	0.973	0.09505	0.18454
<b>5,13,1 (92)</b>	<b>0.877</b>	<b>0.990</b>	<b>0.15869</b>	<b>0.968</b>	<b>0.980</b>	<b>0.05188</b>	<b>0.10528</b>
5,14,1 (99)	0.809	0.960	0.32019	0.969	0.986	0.04892	0.18456
5,3,1,1 (24)	0.884	0.996	0.08871	0.993	0.997	0.01210	0.05040
5,3,2,1 (29)	0.936	0.999	0.02310	0.97	0.985	0.05291	0.03800
5,3,3,1 (34)	0.992	1.000	0.00108	1.000	1.000	0.00013	0.00061
<b>5,3,4,1 (39)</b>	<b>1.004</b>	<b>1.000</b>	<b>0.00035</b>	<b>1.000</b>	<b>1.000</b>	<b>0.00024</b>	<b>0.00029</b>
5,4,1,1 (31)	0.886	0.996	0.08519	0.996	0.998	0.00638	0.04579
5,4,2,1 (37)	0.947	0.997	0.03338	0.999	1.000	0.00177	0.01757
5,4,3,1 (43)	0.986	1.000	0.00108	1.000	1.000	0.00003	0.00056
5,4,4,1 (49)	0.984	1.000	0.00166	1.000	1.000	0.00007	0.00087
5,4,5,1 (55)	0.984	1.000	0.00158	1.000	1.000	0.00003	0.00081
5,5,1,1 (38)	0.96	0.998	0.02322	1.000	1.000	0.00047	0.01184
5,5,2,1 (45)	0.988	1.000	0.00083	1.000	1.000	0.00010	0.00047
5,5,3,1 (52)	0.979	1.000	0.00377	1.000	1.000	0.00005	0.00191
5,5,4,1 (59)	0.997	0.999	0.00584	1.000	1.000	0.00000	0.00292
5,5,5,1 (66)	0.961	1.000	0.00947	1.000	1.000	0.00000	0.00473
5,5,6,1 (73)	0.964	0.998	0.02127	1.000	1.000	0.00000	0.01064
5,6,1,1 (45)	0.944	0.999	0.03140	0.999	1.000	0.00119	0.01629
5,6,2,1 (53)	0.967	1.000	0.00722	1.000	1.000	0.00001	0.00362
5,6,3,1 (61)	0.944	0.993	0.05600	1.000	1.000	0.00000	0.02800
5,6,4,1 (69)	0.952	0.999	0.01772	1.000	1.000	0.00000	0.00886
5,6,5,1 (77)	0.957	0.999	0.01312	1.000	1.000	0.00000	0.00656
5,6,6,1 (85)	0.995	0.997	0.01736	1.000	1.000	0.00000	0.00868
5,6,7,1 (93)	0.954	0.999	0.01409	1.000	1.000	0.00000	0.00704

Results of the best-performed ANN model (5,3,4,1), the field data, and the results using the MSDPM statistical model are presented in Table 5. The difference between the measured and the ANN predicted sediment yield for the

calibration data ranges from -4.22% to 15.96% while the minimum MSDPM prediction error is -7.55% and the maximum error is 20.84%. The ANN model performance for the validation data improves dramatically as compared with the first case. The predicted sediment yield for the Brand debris basin is 85,694 m<sup>3</sup> which is 5.33% greater than the measured value. The ANN model predicts sediment yield is 23,152 m<sup>3</sup> for the Childs Debris Basin which is 4.06% greater than the measured value.

**Table 5:** Summary of calibration and validation results by two models for Case 2

	Debris Basin	Rr (m/km)	Area (ha)	Measured Dy (m <sup>3</sup> )	MSDPM Estimated Dy (m <sup>3</sup> )	Diffe <sup>1</sup> (%)	ANN Estimated Dy (m <sup>3</sup> )	Diffe <sup>2</sup> (%)
Calibration Data	Lannan Case 1	405.00	63.94	13,577	13,480	-0.71	13,559	-0.13
	Lannan Case 2	405.00	63.94	5,047	5,526	9.49	5,522	9.41
	Kinneloa East	444.03	51.80	23,627	22,005	-6.87	22,668	-4.06
	Kinneloa West	475.84	52.21	33,261	30,751	-7.55	31,858	-4.22
	Rubio	280.06	329.2	17,001	17,830	4.88	17,210	1.23
	Bailey	337.07	153.8	22,948	23,501	2.41	22,772	-0.77
	Sunny-side	475.80	5.212	1,239	1,282	3.47	1,214	-2.00
	Carriage House	433.99	7.689	1,710	2,007	17.4	1,839	7.6
	Auburn	521.71	41.28	8,364	8,942	6.91	8,524	1.92
	Fairoaks	60.013	54.63	1,847	1,748	-5.36	1,866	1.04
	West Ravine	286.76	63.94	9,331	11,276	20.84	10,820	15.96
Validation Data	Brand	280	267	81,358	75,935	-6.67	85,694	5.33
	Childs	314	81	22,249	20,355	-8.51	23,152	4.06

Diffe<sup>1</sup> - Difference between measured debris yield and the estimated values using MSDPM.

Diffe<sup>2</sup> - Difference between measured debris yield and the estimated values using ANN model.

The correlation coefficients and the distribution of the estimated values as compared with measured debris yield are illustrated in Figure 13. As shown in

this figure, most data points are on the 45 degree line that indicates the estimated debris yield are very close to their measured values.

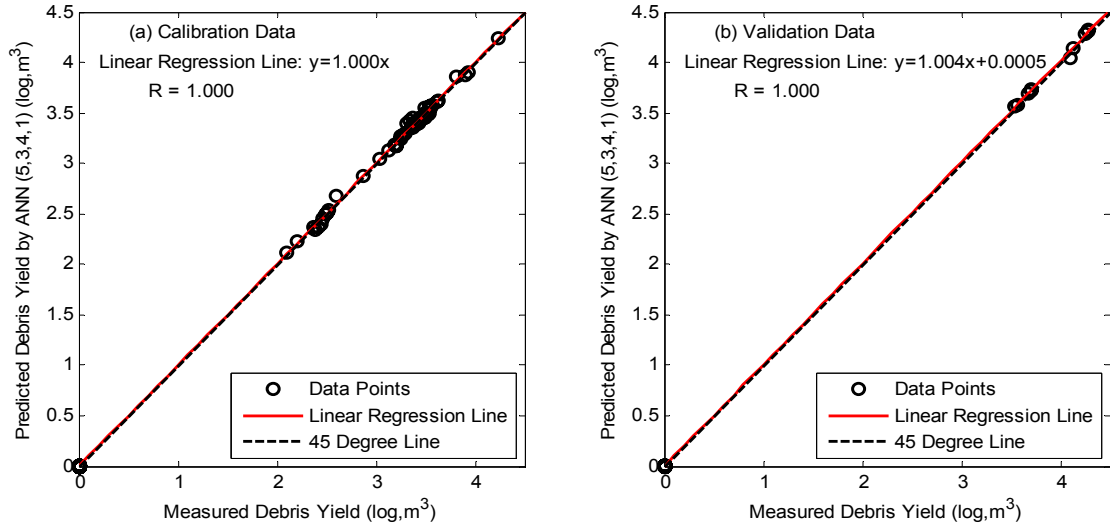


**Figure 13:** Linear regression analysis between measured and ANN model estimated debris yield (a) Calibration Data Set (b) Validation Data Set for Case 2

#### 4.1.3 Case 3

Three more input variables including the percentage of the area that was burned by wildfire within the watershed in the last 10 years, time after the last fire event in the terms of year, and the number of the antecedent effective rainfall event are included to research their impact on the performance of ANN models. As demonstrated in Equation 2.5, these three variables are key elements to compute the fire factor; in other words, fire factor already includes the effect of these variables. Trained by 244 calibration data and the same internal parameters as in the previous two cases, ANN modeling results are shown in Table 6.

**Table 6:** Summary of the performance of ANN models for Case 3

ANN Geometry	Validation Data Set			Calibration Data Set			Average MSE
	Slope	R	MSE	Slope	R	MSE	
8,6,1 (61)	0.829	0.965	0.27775	0.893	0.948	0.18203	0.22989
8,7,1 (71)	0.899	0.961	0.27695	0.898	0.951	0.17193	0.22444
8,8,1 (81)	0.903	0.959	0.28582	0.899	0.953	0.16381	0.22482
8,9,1 (91)	0.840	0.963	0.28402	0.936	0.970	0.10434	0.19418
8,10,1 (101)	0.829	0.963	0.37076	0.981	0.991	0.03184	0.20130
8,11,1 (111)	0.871	0.959	0.29522	0.942	0.974	0.09243	0.19383
8,12,1 (121)	0.783	0.968	0.28745	0.941	0.975	0.13112	0.20929
8,13,1 (131)	0.997	0.943	0.48064	0.939	0.974	0.09323	0.28694
<b>8,14,1 (141)</b>	<b>0.846</b>	<b>0.954</b>	<b>0.33568</b>	<b>0.987</b>	<b>0.995</b>	<b>0.01962</b>	<b>0.17765</b>
8,3,1,1 (33)	0.973	1.000	0.00450	1.000	1.000	0.00043	0.00246
<b>8,3,2,1 (38)</b>	<b>0.989</b>	<b>1.000</b>	<b>0.00074</b>	<b>1.000</b>	<b>1.000</b>	<b>0.00009</b>	<b>0.00083</b>
8,3,3,1 (43)	0.992	1.000	0.00107	1.000	1.000	0.00008	0.00115
8,3,4,1 (48)	0.991	1.000	0.00092	1.000	1.000	0.00027	0.00119
8,4,1,1 (43)	0.921	0.998	0.04489	0.999	0.999	0.00191	0.04681
8,4,2,1 (49)	0.900	0.996	0.07325	0.997	0.998	0.00548	0.07874
8,4,3,1 (55)	0.957	0.999	0.01333	1.000	1.000	0.00009	0.01342
8,4,4,1 (61)	0.979	1.000	0.00465	1.000	1.000	0.00000	0.00465
8,4,5,1 (67)	0.965	0.993	0.05155	1.000	1.000	0.00007	0.05162
8,5,1,1 (53)	0.901	0.996	0.07055	0.997	0.999	0.00468	0.07523
8,5,2,1 (60)	0.972	0.997	0.02318	1.000	1.000	0.00006	0.02324
8,5,3,1 (67)	0.954	0.997	0.02952	1.000	1.000	0.00016	0.02968
8,5,4,1 (74)	0.937	0.997	0.03924	1.000	1.000	0.00000	0.03925
8,5,5,1 (81)	0.990	0.998	0.01337	1.000	1.000	0.00002	0.01339
8,5,6,1 (88)	0.895	0.998	0.06938	1.000	1.000	0.00000	0.06938
8,6,1,1 (63)	0.991	0.997	0.02170	1.000	1.000	0.00001	0.02171
8,6,2,1 (71)	0.996	0.995	0.03419	1.000	1.000	0.00002	0.03421
8,6,3,1 (79)	0.933	0.997	0.03905	1.000	1.000	0.00000	0.03905
8,6,4,1 (87)	0.993	1.000	0.04678	1.000	1.000	0.00000	0.04678
8,6,5,1 (95)	0.996	0.986	0.09924	1.000	1.000	0.00000	0.09924
8,6,6,1 (103)	1.040	0.999	0.01538	1.000	1.000	0.00000	0.01538
8,6,7,1 (111)	0.942	0.999	0.02526	1.000	1.000	0.00000	0.02526

In this case, the neural network with 14 neurons achieves the best performance among all three-layered neural networks; however, the network with three and two neurons on the first and second hidden layer exhibits much better generalization ability. As seen from Table 6, the error bond of the calibration data is reduced but not as much as for the validation data. When overall considering results for the calibration and validation data, the modeling accuracy of ANN

model (8,3,2,1) is similarly as good as the best ANN model (5,3,4,1) in the second case. This is reasonable since three new input parameters have already been considered in the fire factor which is an input variable in all three cases.

#### 4.1.4 Discussion

Overall speaking, the performance of ANN model (8,3,2,1) is equivalently superior as the second ANN model (5,3,4,1) and both models are better than the first ANN model (5,6,2,1) (Table 7). This can be explained by a statistical goodness-of-fit index introduced by Gupta and Sorooshian (1985). The index is the ratio of the standard error estimate ( $S_e$ ), shown in Equation (4.1), to the standard deviation ( $S_y$ ) of the target values.

$$S_e = \sqrt{\frac{1}{\lambda} \sum_{l=1}^q \sum_{k=1}^p (Y_{lk} - T_{lk})^2} \quad (4.1)$$

where  $\lambda$  = degrees of freedom and is the difference between the number of calibration data and the number of connection weights and biases, and the remaining parameters are the same as defined in Equation (3.35). The smaller the ratio, the more accurate is the model prediction (Table 7). The ratio of the neural network (5,3,4,1) trained by 244 data is 0.01269 for the calibration data which is very close to the ratio for the ANN model (5,6,2,1) trained by 300 data, 0.01216. However, the ratio for the validation data, 0.00376, is much smaller than the ratio, 0.03033 obtained in the first case.

It seems that the removal of data from the Big Briar and Hay debris basin results in a significant improvement of ANN performance in the validation data. However, the inclusion of more input variables in the third case does not lead to better overall neural network performance since these three inputs are already considered in fire factor.

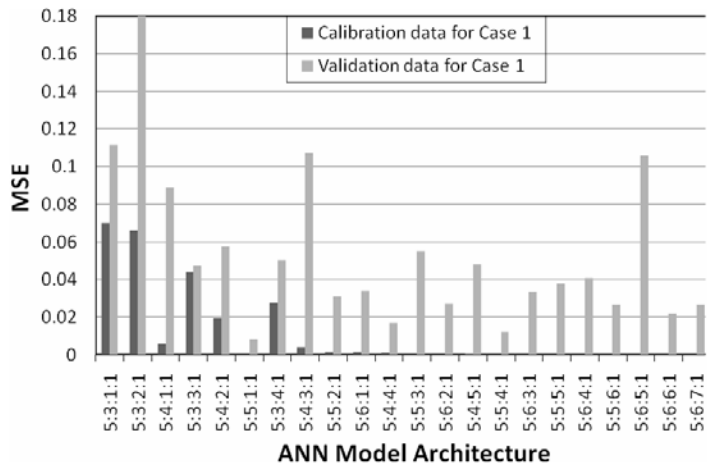
**Table 7:** Comparison of ANN models performance

Network Geometry	Validation Data set				Calibration Data Set			
	MSE	R	Slope	$S_e/S_y$	MSE	R	Slope	$S_e/S_y$
1 <sup>st</sup> ANN: (5,6,2,1)	0.02704	0.996	0.972	0.03033	0.00019	1.000	1.000	0.01216
2 <sup>nd</sup> ANN: (5,3,4,1)	0.00034	1.000	1.004	0.00376	0.00024	1.000	1.000	0.01269
3 <sup>rd</sup> ANN: (8,3,2,1)	0.00074	1.000	0.989	0.00550	0.00008	1.000	1.000	0.00749

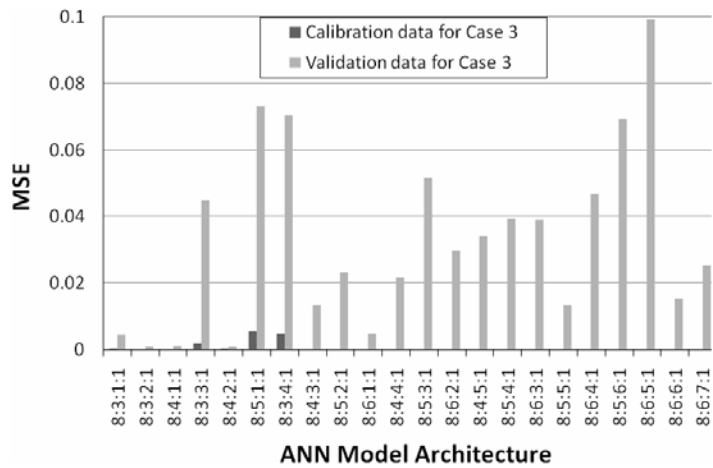
As seen from Table 2, 4 and 6, there appears to be an improvement on the modeling accuracy with an increase in the number of hidden neurons up to a certain point for three-layered ANN models. For example, the optimum performance is achieved when 13 neurons (5,13,1) are on the hidden layer for the first case and the second case, and 14 neurons (8,14,1) for the last case. The results indicate that the optimal number of neuron on the hidden layer is not only a function of the number of input parameters but also a function of the number of training samples.

With fewer connection weights and biases, the ANN models with two hidden layers have better generalization ability than the neural networks with one hidden layer. Although there is some variation in the generalization ability of the

networks with two hidden layers, referring to Figure 14, there appears to be such a trend that increasing the number of the neuron on the hidden layers improves the performance for the calibration data. However, there is no such trend for the validation data. In addition, it can be seen that as continued training with more neurons on the hidden layers, the prediction accuracy of the validation data is worsened - a sign of overfitting.



(a)



(b)

**Figure 14:** Calibration and validation mean square error for (a) Case 1 (b) Case 3

In the first case, the ratio of the number of the calibration data to the number of connection weights and biases is 5.66, as compared to 6.26 and 6.42, the ratios for the best-fit neural network models during the second and third test. It suggests that higher ratio of the number of calibration data to the number of connection weights and biases does not lead to a better simulation. As mentioned previously, ANN performance deteriorates when the validation data is out of the range of the calibration data. It is not the case in this study because the sediment yield collected from Brand debris basin are roughly 2.4 times greater than the maximum sediment yield used for training, the best prediction of debris yield achieved in the first set of ANN models are not accurate enough, but there is a ANN model within the second case provided desirable estimation.

#### **4.2 Estimation of Unit Debris Yield**

The modeling results of accumulated debris yield presented in the first three cases are promising that leads to further application of ANN technique to simulate debris yield per unit area resulting from a significant storm event in this study. ANN models are first developed to model unit debris yield collected between 1938 and 1983 from 36 small watersheds (i.e. area less than 3 square miles) within Los Angeles County. Another two artificial intelligence models – ANFIS and GD-FNN are also developed to estimate the unit debris yield using the same input variables and training samples for comparison purpose. Different numbers of input variables with a particular focus on six watershed morphological

parameters are selected to calibrate and validate these artificial intelligence models. One or two input parameters are added each step to find out their impact on the performance in order to determine the relative importance of the input parameters. A new input parameter is included in such a sequence - the least correlated to the output variable (unit debris yield) is the last one to be included.

USACE created an empirical equation (Equation 2.3) to describe the relation between unit debris yield and drainage area, relief ratio, precipitation and fire factor based on 349 data records collected between 1938 and 1983 at 80 small debris basins within Los Angeles County (USACE, 2000). The same data used by the USACE are modeled by using only ANN models trained by LM algorithm in this study. In order to reduce the modeling complexity, the data is split into five groups based on their upstream watersheds relief ratio. For example, data collected from watersheds with mild slope (i.e. from 58 m/km to 185 m/km) is arranged in the first group, second group consists of data from watersheds with steep slope (i.e. from 185 m/km to 250 m/km), third group is data from watersheds with steeper slope (i.e. from 250 m/km to 305 m/km), fourth group is data from watersheds with extreme steep slope (i.e. from 305 m/km to 375 m/km), and the fifth group is data from watershed with the steepest slope (i.e. from 375 m/km to 525 m/km). Three soil properties such as SEF, SP, and SLL are included as input variables one by one to the first four groups of unit debris yield data. They are not considered in the fifth group of data because all the watersheds in this group are within the same soil map unit.

The USACE also created three additional empirical equations to estimate unit debris yield collected from large watersheds with area from 10 to 25 square miles, or from larger watersheds with area between 25 and 50 square miles, or from much larger watersheds (i.e. area is within [50, 200] square miles). Three sets of ANN models are developed to simulate these unit debris yield data as well. To summarize, there are 12 studied cases (refer to Table 1) with different numbers of input variables and different numbers of training samples for estimating groups of unit debris yield classified either by relief ratio or area size of the upstream collection watershed.

#### **4.2.1 Case 4**

The process of transporting and collecting debris in a debris basin is very complicated and the relationship between unit debris yield and other parameters such as watershed area, relief ratio, watershed morphologic variables such as ER, DDM, HI, and MBR, rainfall information, and so on, is still under research. However, four parameters – drainage area ( $A$ ), watershed relief ratio ( $R_r$ ), rainfall intensity ( $I$ ), and fire factor ( $F$ ), (usually the first three parameters are log transformed), have long been proven as four basic input parameters for estimating unit debris yield induced by a significant storm event from a burned watershed. In addition to these four basic input parameters, Case 4 includes two more watershed morphologic parameters: total stream length (TSL) and transport

efficiency factor (T1) which is the product of mean bifurcation ratio (MBR) and total stream length (TSL).

Although there are 349 data records of unit debris yield available at small watersheds between 1938 and 1983 within Los Angeles County, only 200 data records are selected for modeling from Case 4 to 7 due to the lack of the required watershed morphologic parameters. 85 percent of the data, or 170 data records, are randomly chosen for calibrating three artificial intelligence models, with the remaining independent 15 percent of data (i.e. 30 data records) used for validation purpose. The data range for the first input parameter,  $\log A$  is [0.72, 2.98] hectare, the minimum and maximum values of  $\log R_r$  are 2.72 and 1.94 m/km, respectively, TSL is within the range of [2.43, 5.455], T1 is in a range of [1.51, 3.97],  $\log I$  ranges from 0.4 to 2.4 mm/hr, and F is from 3 to 6.5. There is only one output variable – unit debris yield whose logarithmic values are within a range of [2.37, 4.64] with the unit of cubic meter per square kilometer.

#### **4.2.1.1 ANN Model**

Before start the calibration process, input vectors are normalized first, uncorrelated with each other, and those input variables that contribute less than 2% of the total variation are removed. In this case, 39 ANN models with a maximum of two hidden layers are created and different numbers of neurons on hidden layers is evaluated. For neural networks with one hidden layer, the number of hidden neuron is within a range of [5 21]. Lack of guidelines for

determining the structure of neural networks with two hidden layers, twenty-two ANN models with different number of hidden neurons such as (3,1), (3,2), (3,3), (3,4), (4,1), (4,2), (4,3), (4,4), (4,5), (5,1), (5,2), (5,3), (5,4), (5,5), (5,6), (6,1), (6,2), (6,3), (6,4), (6,5), (6,6), and (6,7) are calibrated and validated for modeling unit debris yield. During training process, internal parameters selected as follows. Epoch size is 1000, and the desired error goal for training data is set as  $1 \times 10^{-6}$ . The transfer function is hyperbolic tangent for all hidden layers, and linear transfer function is applied for the output layer. Both BRBP and LM algorithm are employed to train ANN models, and the default values of the remaining internal parameters provided by Matlab are maintained.

Table 8 summarizes modeling results of all ANN models trained by the BRBP algorithm. The upper part of the table shows results obtained by using three-layered ANN models, and the bottom part is for four-layered ANN models. Among sixteen three-layered ANN models, the network (6,6,1) performs a little bit better than the other models because the MSE of the calibration data is relatively low and the validation data MSE is one of the lowest. With very little difference, the network (6,5,5,1) is better-performed than the remaining four-layered neural network models in terms of modeling accuracy. With lower errors and higher correlation coefficients for the calibration and the validation data, the neural network model (6,5,5,1) works better than the neural network with six neurons on the only hidden layer, and it also has better generalization ability than all the neural networks with one hidden layer in this case.

**Table 8:** Summary of the performances of ANN models trained by the BRBP algorithm for Case 4

ANN Geometry	Validation Data Set			Calibration Data Set			Average MSE
	Slope	R	MSE	Slope	R	MSE	
6,5,1 (41)	0.275	0.425	0.12000	0.381	0.647	0.13760	0.12880
<b>6,6,1 (49)</b>	<b>0.315</b>	<b>0.479</b>	<b>0.11149</b>	<b>0.368</b>	<b>0.638</b>	<b>0.14049</b>	<b>0.12599</b>
6,7,1 (57)	0.283	0.377	0.13528	0.400	0.669	0.13126	0.13327
6,8,1 (65)	0.298	0.479	0.10961	0.311	0.585	0.15549	0.13255
6,9,1 (73)	0.299	0.478	0.10992	0.313	0.587	0.15494	0.13243
6,10,1 (81)	0.312	0.474	0.11142	0.332	0.607	0.14955	0.13048
6,11,1 (89)	0.296	0.452	0.11571	0.377	0.646	0.13807	0.12689
6,12,1 (97)	0.315	0.477	0.11116	0.332	0.607	0.14954	0.13035
6,13,1 (105)	0.296	0.452	0.11576	0.377	0.647	0.13796	0.12686
6,14,1 (113)	0.296	0.452	0.11577	0.377	0.647	0.13792	0.12685
6,15,1 (121)	0.296	0.452	0.11578	0.377	0.647	0.13789	0.12683
6,16,1 (129)	0.257	0.372	0.13076	0.386	0.655	0.13551	0.13314
6,17,1 (137)	0.297	0.452	0.11578	0.377	0.647	0.13784	0.12681
6,18,1 (145)	0.297	0.452	0.11578	0.377	0.647	0.13782	0.12680
6,19,1 (153)	0.297	0.452	0.11578	0.377	0.647	0.13781	0.12679
6,20,1 (161)	0.297	0.452	0.11578	0.378	0.647	0.13779	0.12678
6,21,1 (169)	0.297	0.452	0.11578	0.378	0.647	0.13778	0.12678
6,3,1,1 (27)	0.313	0.513	0.10147	0.297	0.557	0.16251	0.13199
6,3,2,1 (32)	0.317	0.515	0.10132	0.299	0.560	0.16186	0.13159
6,3,3,1 (37)	0.317	0.515	0.10132	0.299	0.560	0.16183	0.13158
6,3,4,1 (42)	0.302	0.479	0.10901	0.329	0.596	0.15235	0.13068
6,4,1,1 (35)	0.302	0.436	0.12011	0.393	0.644	0.13802	0.12907
6,4,2,1 (41)	0.296	0.422	0.12344	0.400	0.651	0.13612	0.12978
6,4,3,1 (47)	0.364	0.512	0.10783	0.383	0.638	0.13998	0.12390
6,4,4,1 (53)	0.365	0.513	0.10766	0.383	0.638	0.14001	0.12383
6,4,5,1 (59)	0.348	0.510	0.10609	0.387	0.639	0.13947	0.12278
6,5,1,1 (43)	0.329	0.463	0.12050	0.442	0.683	0.12579	0.12315
6,5,2,1 (50)	0.420	0.516	0.11178	0.445	0.689	0.12419	0.11799
6,5,3,1 (57)	0.419	0.517	0.11149	0.445	0.689	0.12424	0.11787
6,5,4,1 (64)	0.419	0.517	0.11133	0.445	0.688	0.12427	0.11780
<b>6,5,5,1 (71)</b>	<b>0.427</b>	<b>0.554</b>	<b>0.10224</b>	<b>0.461</b>	<b>0.699</b>	<b>0.12090</b>	<b>0.11157</b>
6,5,6,1 (78)	0.427	0.553	0.10232	0.461	0.699	0.12086	0.11159
6,6,1,1 (51)	0.467	0.528	0.11498	0.447	0.693	0.12287	0.11892
6,6,2,1 (59)	0.459	0.530	0.11277	0.446	0.691	0.12360	0.11818
6,6,3,1 (67)	0.368	0.527	0.10486	0.458	0.698	0.12124	0.11305
6,6,4,1 (75)	0.368	0.525	0.10505	0.460	0.699	0.12072	0.11288
6,6,5,1 (83)	0.368	0.524	0.10521	0.462	0.701	0.12032	0.11277
6,6,6,1 (91)	0.368	0.523	0.10535	0.463	0.701	0.12003	0.11269
6,6,7,1 (99)	0.368	0.523	0.10546	0.464	0.702	0.11981	0.11264

It seems that the performance of all the ANN models trained by the BRBP algorithm is very poor. The LM training algorithm is applied to calibrate some of the four-layered neural networks to compare. Fifteen neural networks with two hidden layers are trained by the LM algorithm in this case and they are (4,3,4,1), (4,3,5,1), (4,3,6,1), (4,3,7,1), (4,4,2,1), (4,4,3,1), (4,4,4,1), (4,4,5,1), (4,4,6,1), (4,5,2,1), (4,5,3,1), (4,5,4,1), (4,5,5,1), (4,5,6,1), and (4,5,7,1). All internal parameters are the same as aforementioned. The modeling results of these ANN models are provided in Table 9.

**Table 9:** Summary of the performances of ANN models trained by the LM algorithm for Case 4

ANN Geometry	Validation Data Set			Calibration Data Set			Average MSE
	Slope	R	MSE	Slope	R	MSE	
6,3,4,1 (42)	0.579	0.562	0.12944	0.579	0.761	0.09923	0.11434
6,3,5,1 (47)	0.463	0.547	0.11155	0.588	0.767	0.09690	0.10423
6,3,6,1 (52)	0.290	0.428	0.11925	0.582	0.763	0.09842	0.10884
<b>6,3,7,1 (57)</b>	<b>0.547</b>	<b>0.703</b>	<b>0.07325</b>	<b>0.586</b>	<b>0.766</b>	<b>0.09742</b>	<b>0.08534</b>
6,4,2,1 (41)	0.430	0.426	0.15811	0.579	0.761	0.09924	0.12868
6,4,3,1 (47)	0.516	0.593	0.09834	0.598	0.773	0.09458	0.09646
6,4,4,1 (53)	0.528	0.626	0.09988	0.589	0.767	0.09685	0.09836
6,4,5,1 (59)	0.530	0.548	0.11856	0.643	0.802	0.08403	0.10130
6,4,6,1 (65)	0.636	0.650	0.09526	0.590	0.768	0.09654	0.09590
6,5,2,1 (50)	0.581	0.586	0.11260	0.587	0.766	0.09725	0.10492
6,5,3,1 (57)	0.584	0.615	0.10121	0.627	0.792	0.08784	0.09453
6,5,4,1 (64)	0.612	0.612	0.10677	0.656	0.810	0.08099	0.09388
6,5,5,1 (71)	0.443	0.543	0.10588	0.642	0.801	0.08439	0.09513
6,5,6,1 (78)	0.676	0.585	0.13455	0.701	0.837	0.07036	0.10245
6,5,7,1 (85)	0.474	0.521	0.12094	0.744	0.863	0.06021	0.09057

As seen from Table 9, the error for the calibration data is greatly reduced by using the LM training algorithm and it is also true for some validation data. The reason why all the networks trained by the BRBP algorithm provide poor modeling results particularly for the calibration data might be the training process

is terminated earlier to prevent overfitting. It is shown in Table 9 that the neural network (6,3,7,1) trained by the LM algorithm has a lower MSE for both the calibration data and the validation data than all the neural networks trained by the BRBP algorithm. To further evaluate the performance of these two neural networks, (6,5,5,1) trained by the BRBP algorithm and (6,3,7,1) trained by the LM algorithm, measured and estimated unit debris yield by two ANN models are plotted in Figure 15 and 16. The data points in Figure 16 especially in figure (b) distribute much closer to the 45 degree line than those in Figure 15. It also shows that the network (6,3,7,1) reduces the maximum difference between measured and estimated unit debris yield as compared to the network (6,5,5,1), particularly for the validation data. Therefore, neural networks trained by the LM training algorithm achieve much better modeling results than those trained by the BRBP algorithm in this case.

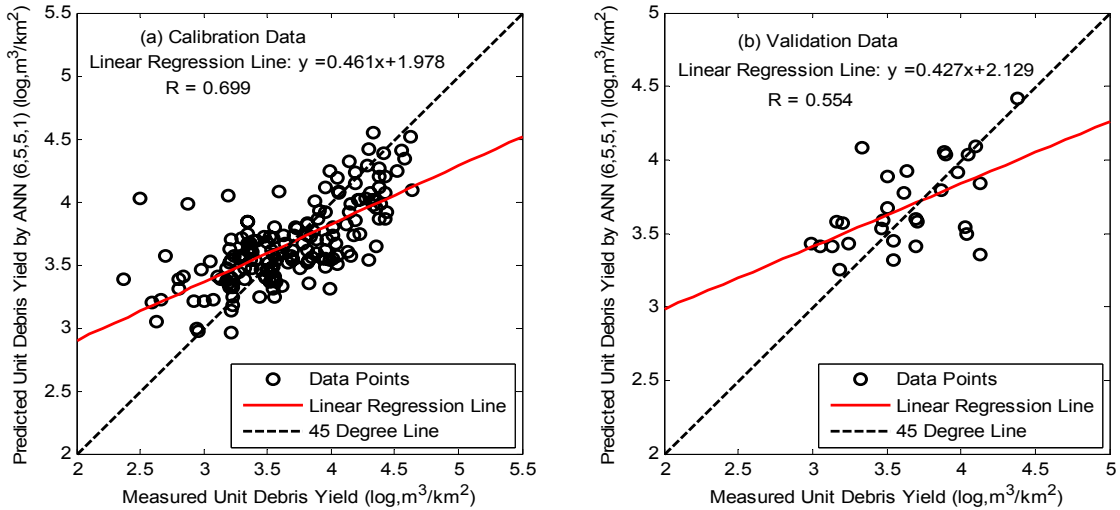


**Figure 15:** Linear regression analysis between measured and ANN model (BRBP) estimated debris yield (a) Calibration Data Set (b) Validation Data Set for Case 4

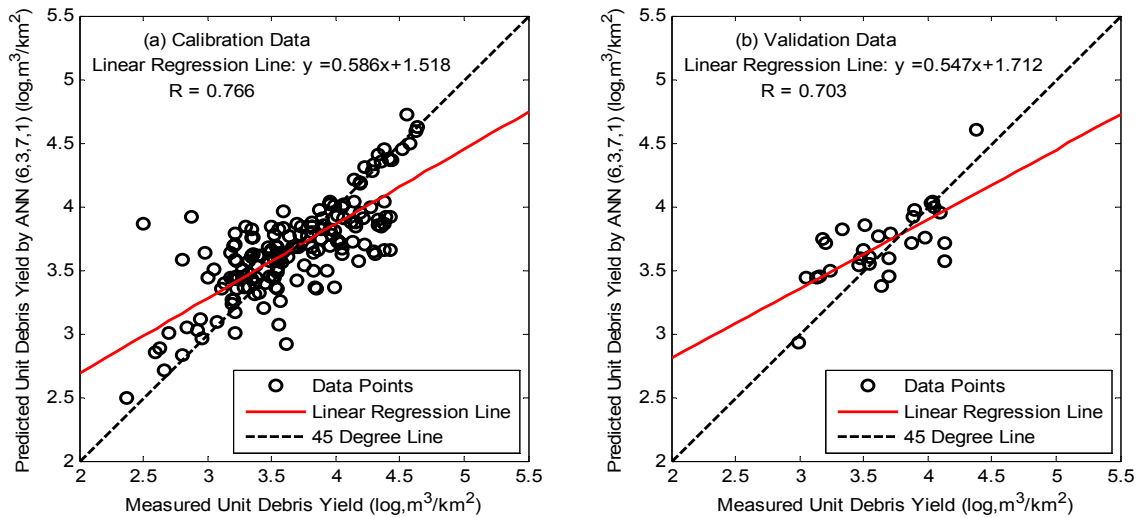


**Figure 16:** Linear regression analysis between measured and ANN model (LM) estimated debris yield (a) Calibration Data Set (b) Validation Data Set for Case 4

#### **4.2.1.2 ANFIS Model**

Fuzzy logic system can be interpreted by the use of fuzzy if-then rules that offers a possibility of the fusion of ANN technique and fuzzy logic system to overcome the ‘black box’ behavior of ANN models. Applying a combination of least-squares method and the BPGDM to adjust premise and consequent parameters, ANFIS (Jang, 1993) is one of the most commonly used NFS models. In this case, it is the second approach to predict unit debris yield.

Before the start of training in ANFIS, it is required to determine the number and type of membership function for each input variable and the number of fuzzy rule. If prior expert knowledge of the problem is available, they are easy to define; otherwise, trial-and-error method is the only choice for the determination of optimal partition of input space and the type of membership function, and the number of fuzzy rule. With the assumption that every input has the same kind of

membership function, a couple of membership functions including Gaussian function, triangular membership function, trapezoidal membership function, generalized bell-shaped membership function are employed. The default values of training error goal (i.e. 0), initial step size (i.e. 0.01), step size decrease rate (i.e. 0.9), and step size increase rate (i.e. 1.1) are used. All the ANFIS models are trained for 90 epochs. After varying the number and type of membership for six input parameters, it is found that the ANFIS model with two Gaussian membership functions for the first, fourth and fifth inputs, i.e.  $\log A$ ,  $T1$ , and,  $\log I$  is superior to other ANFIS models. The membership functions for these three inputs are sketched in Figure 17. The obtained eight fuzzy rules are summarized in Table 10.

**Table 10:** Summary of fuzzy rules for Case 4

No. of fuzzy rules	Premise Parameters			Consequent Parameters
	$\log A$	$T1$	$\log I$	
1	(0.889,1.076)	(1.409,0.385)	(0.423,0.963)	$t = -1.84-13.51\log A-8.742\log Rr+14.06TSL-4.785T1+1.809\log I+1.043F$
2	(0.889,1.076)	(1.409,0.385)	(2.433,0.659)	$t = -22.19+21.66\log A+28.43\log Rr-11.15TSL-2.738T1-18.32\log I-0.3263F$
3	(0.889,1.076)	(4.238,0.278)	(0.423,0.963)	$t = 71.57-21.99\log A-6.945\log Rr+1.497TSL-6.149T1-9.307\log I+0.6584F$
4	(0.889,1.076)	(4.238,0.278)	(2.433,0.659)	$t = -72.89+14.77\log A+22.12\log Rr+1.02TSL+10.95T1-20.15\log I+0.3679F$
5	(3.20,0.848)	(1.409,0.385)	(0.423,0.963)	$t = 105+66.77\log A+22.22\log Rr-68.06TSL-5.72T1+38.88\log I-2.494F$
6	(3.20,0.848)	(1.409,0.385)	(2.433,0.659)	$t = -45.56-99.13\log A-120.2\log Rr +59.58TSL+11.51T1+136.1\log I+1.062F$
7	(3.20,0.848)	(4.238,0.278)	(0.423,0.963)	$t = 4.722-13.92\log A+5.577\log Rr-0.9463TSL+8.574T1+7.51\log I-0.2279F$
8	(3.20,0.848)	(4.238,0.278)	(2.433,0.659)	$t = 57.21+12.89\log A-17.85\log Rr-5.202TSL-14.9T1+13.35\log I-0.3661F$

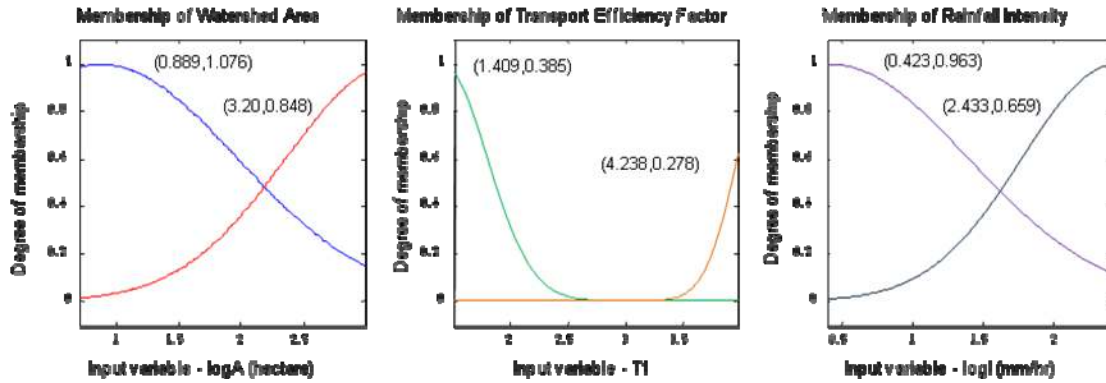


**Figure 17:** Membership functions for logA , T1, and logI (Case 4)

This ANFIS model is able to estimate 170 calibration data with a MSE of 0.1055 and 30 validation data with a MSE of 0.1125, and the correlation coefficients are 0.743 and 0.589 for those two data sets respectively. As graphed in Figure 18, many data points scatter far away from the 45 degree line, especially in figure (b). The ANFIS model performance for the calibration data is not satisfactory, and it is even worse for the validation data.

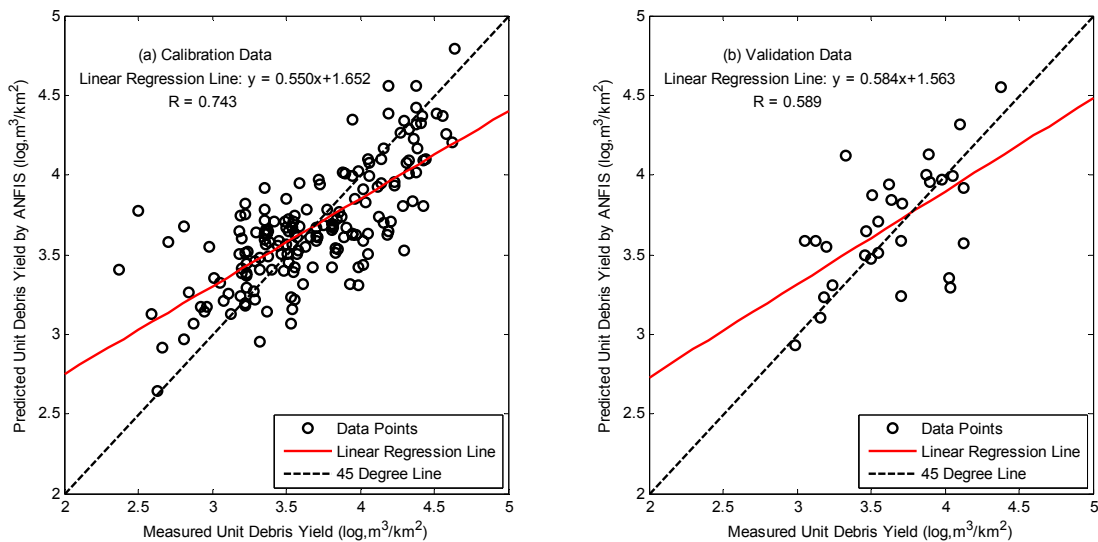


**Figure 18:** Linear regression analysis between measured and ANFIS model estimated debris yield (a) Calibration Data Set (b) Validation Data Set for Case 4

Compared to two best-fitted ANN models developed in this case, one is trained by the BRBP algorithm, and the other is trained by the LM algorithm, the ANFIS model is better performed than the neural network (6,5,5,1) trained by the BRBP algorithm and it is worse than the ANN model (6,3,7,1) trained by the LM algorithm.

#### **4.2.1.3 GD-FNN Model**

FNN model is the combination of ANN and fuzzy logic system in such a way that fuzzy methods are implemented in a neural network model for faster learning speed or better performance. The most common combination is using fuzzy subsets or a set of membership values of fuzzy sets as input signals and/or connection weights and/or outputs for neural networks (Mitra and Hayashi, 2000). The GD-FNN model is proposed by Wu et al. (2001) to implement TSK fuzzy system which is capable of recruiting and deleting fuzzy rules automatically. In addition, GD-FNN algorithm standardizes and improves the way to generate width for newly generated Gaussian membership function and to modify width for existing Gaussian functions as compared with previous FNN models, such as dynamic FNN models (Wu and Er, 2000).

In this case, GD-FNN model is applied to simulate unit debris yields based on 6 input parameters:  $\log A$ ,  $\log R_r$ , TSL, T1,  $\log I$ , and F. The optimal values of predefined parameters are found as follows.

$$\epsilon_{\min} = 0.5, \epsilon_{\max} = 0.8, e_{\max} = 5, e_{\min} = 0.002, k_{mf} = 0.65, k_s = 0.99, \text{ and } k_{err} = 0.002.$$

Two fuzzy rules are generated and they are in the form of:

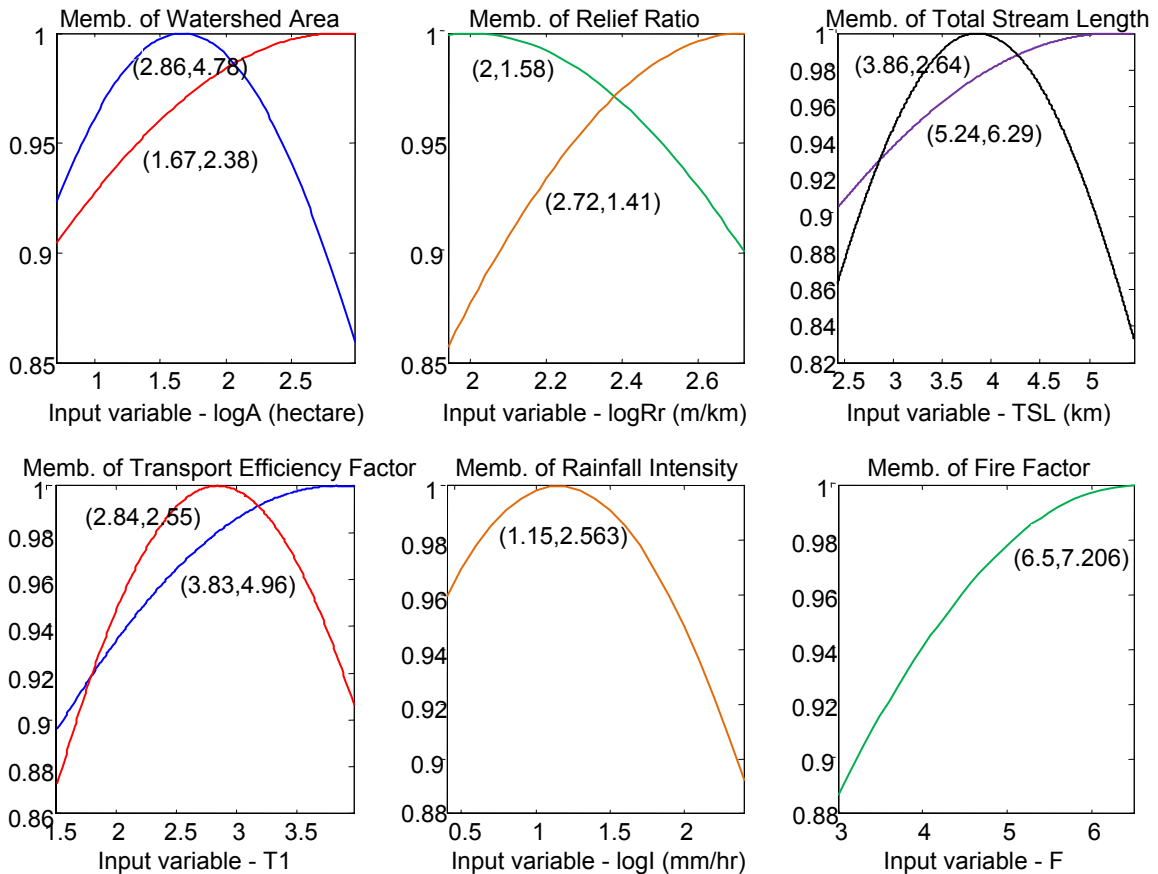
1st fuzzy rule: if logA is (2.86, 4.78), logR<sub>r</sub> is (2, 1.58), TSL is (5.25, 6.29), T1 is (3.83, 4.96), logI is (1.15, 2.563), and F is (6.5, 7.206), then

$$t = 9.346 + 0.194\log A + 2.396\log R_r - 3.614TSL + 3.330T1 - 0.976\log I - 0.454F$$

2nd fuzzy rule: if logA is (1.67, 2.38), logR<sub>r</sub> is (2.72, 1.41), TSL is (3.86, 2.64), T1 is (2.84, 2.55), logI is (1.15, 2.563), and F is (6.5, 7.06), then

$$t = -7.027 - 0.685\log A + 1.268\log R_r + 2.235TSL - 3.267T1 + 1.951\log I + 0.261F$$

The membership functions for six input variables are demonstrated in Figure 19.



(Memb. is the abbreviation of membership function).

**Figure 19:** Membership functions for input variables (Case 4)

The MSE of the estimated unit debris yield by the GD-FNN model is 0.1777 and 0.1057 for the calibration and the validation data, respectively. The correlation coefficient is only 0.501 for the calibration data, as illustrated in figure 20(a). It can be found that the GD-FNN model fails to predict a few unit debris yield data, and the estimation error for a single event is as large as 1.6. The correlation coefficient is 0.521 for the validation data, and it appears that the GD-FNN model estimates 10 data records to an acceptable level of accuracy and it either underestimates or overestimates the other 20 data points. The GD-FNN model has very poor generalization ability for both the calibration and validation data in this case. It has a similar performance as the ANFIS model for the validation data, but its performance for the calibration data is not comparable to the ANFIS model.

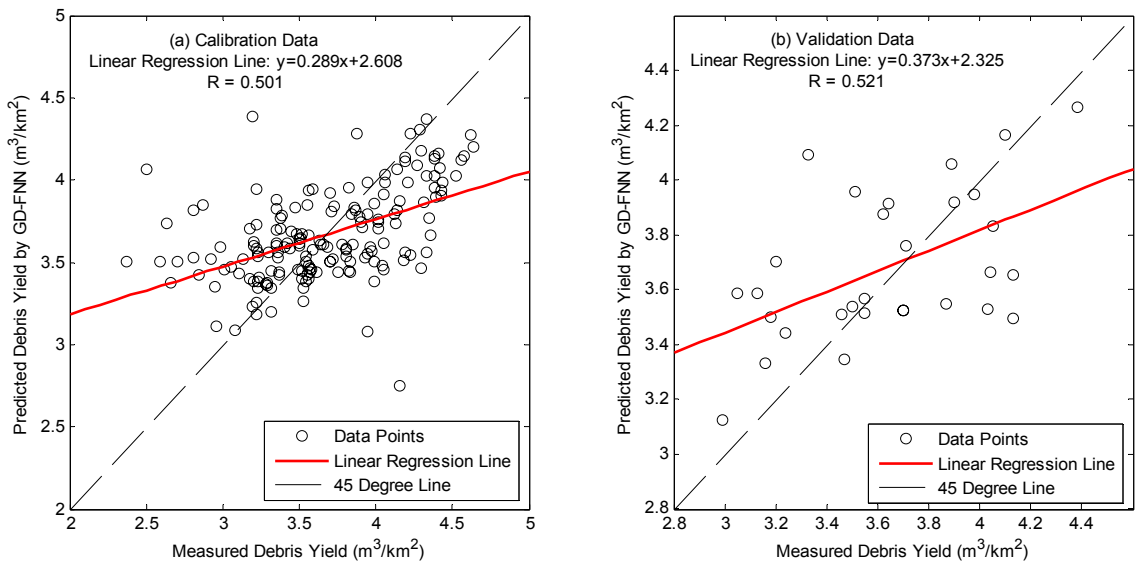


**Figure 20:** Linear regression analysis between measured and GD-FNN model estimated debris yield (a) Calibration Data Set (b) Validation Data Set for Case 4

### **4.2.2 Case 5**

The correlation coefficient between DDM and the measured unit debris yield data indicates it is the most highly related variable to the targets comparing with the other three watershed morphological parameters (i.e. ER, MBR, and HI) considered in this study. Therefore, it is included as additional input parameter in the fifth case. The artificial intelligence models in this case are trained by seven input parameters  $-\log A$ ,  $\log R_r$ , DDM, TSL, T1,  $\log l$ , and F. As aforementioned, 170 data records of unit debris yield are used for calibration and 30 data records are for validation.

#### **4.2.2.1 ANN Model**

The same preprocessing steps introduced previously are implemented first. Utilizing the same geometries and the same internal parameters as in Case 4, seventeen three-layered ANN models and twenty-two four-layered ANN models are developed. Every neural network is trained hundreds of times to start from different initial values of connection weights and biases, and during each time, their values are adjusted 1,000 times (i.e. epoch size) to produce the neural network outputs best approximating the targets. The best performance obtained by all the neural network models trained by the BRBP algorithm is presented in Table 11. Almost all the neural networks developed in this case have better performance for the validation data than for the calibration data. It is a result of balancing performance between the calibration and the validation data.

**Table 11:** Summary of the performances of ANN models trained by the BRBP algorithm for Case 5

ANN Geometry	Validation Data Set			Calibration Data Set			Average MSE
	Slope	R	MSE	Slope	R	MSE	
7,5,1 (46)	0.360	0.630	0.08668	0.314	0.597	0.15358	0.12013
7,6,1 (55)	0.478	0.545	0.10768	0.398	0.677	0.13016	0.11892
7,7,1 (64)	0.347	0.608	0.09204	0.319	0.601	0.15229	0.12216
7,8,1 (73)	0.344	0.600	0.09385	0.323	0.605	0.15124	0.12255
<b>7,9,1 (82)</b>	<b>0.474</b>	<b>0.547</b>	<b>0.10680</b>	<b>0.395</b>	<b>0.676</b>	<b>0.13038</b>	<b>0.11859</b>
7,10,1 (91)	0.333	0.626	0.09174	0.299	0.581	0.15792	0.12483
7,11,1 (100)	0.468	0.513	0.11809	0.439	0.708	0.11977	0.11893
7,12,1 (109)	0.387	0.646	0.08100	0.254	0.534	0.16991	0.12545
7,13,1 (118)	0.327	0.617	0.09342	0.302	0.583	0.15721	0.12531
7,14,1 (127)	0.387	0.646	0.08102	0.254	0.534	0.16990	0.12546
7,15,1 (136)	0.387	0.646	0.08103	0.254	0.535	0.16989	0.12546
7,16,1 (145)	0.320	0.603	0.09583	0.306	0.587	0.15621	0.12602
7,17,1 (154)	0.314	0.594	0.09677	0.306	0.586	0.15638	0.12658
7,18,1 (163)	0.317	0.596	0.09735	0.309	0.590	0.15534	0.12635
7,19,1 (172)	0.387	0.646	0.08106	0.254	0.535	0.16988	0.12547
7,20,1 (181)	0.311	0.589	0.09755	0.307	0.588	0.15598	0.12676
7,21,1 (190)	0.387	0.646	0.08107	0.254	0.535	0.16987	0.12547
7,3,1,1 (30)	0.443	0.580	0.09430	0.371	0.631	0.14301	0.11866
7,3,2,1 (35)	0.442	0.579	0.09414	0.373	0.631	0.14272	0.11843
7,3,3,1 (40)	0.415	0.592	0.09119	0.370	0.627	0.14399	0.11759
7,3,4,1 (45)	0.413	0.591	0.09130	0.370	0.627	0.14392	0.11761
7,4,1,1 (39)	0.412	0.576	0.09228	0.380	0.642	0.13969	0.11598
7,4,2,1 (45)	0.448	0.578	0.09349	0.386	0.644	0.13904	0.11627
7,4,3,1 (51)	0.445	0.576	0.09380	0.387	0.645	0.13862	0.11621
7,4,4,1 (57)	0.445	0.576	0.09391	0.388	0.646	0.13848	0.11619
7,4,5,1 (63)	0.389	0.572	0.09243	0.385	0.644	0.13902	0.11572
7,5,1,1 (48)	0.420	0.507	0.10981	0.406	0.668	0.13205	0.12093
7,5,2,1 (55)	0.378	0.504	0.10706	0.410	0.668	0.13164	0.11935
<b>7,5,3,1 (62)</b>	<b>0.394</b>	<b>0.502</b>	<b>0.10523</b>	<b>0.487</b>	<b>0.722</b>	<b>0.11387</b>	<b>0.10955</b>
7,5,4,1 (69)	0.503	0.546	0.10549	0.409	0.666	0.13248	0.11899
7,5,5,1 (76)	0.505	0.530	0.11058	0.454	0.699	0.12164	0.11611
7,5,6,1 (83)	0.375	0.503	0.10682	0.413	0.669	0.13142	0.11912
7,6,1,1 (57)	0.409	0.530	0.10093	0.407	0.672	0.13092	0.11592
7,6,2,1 (65)	0.512	0.570	0.10692	0.419	0.679	0.12860	0.11776
7,6,3,1 (73)	0.444	0.519	0.10857	0.424	0.682	0.12753	0.11805
7,6,4,1 (81)	0.443	0.518	0.10877	0.425	0.682	0.12745	0.11811
7,6,5,1 (89)	0.418	0.535	0.10059	0.415	0.674	0.12992	0.11526
7,6,6,1 (97)	0.442	0.517	0.10898	0.426	0.682	0.12738	0.11818
7,6,7,1 (105)	0.442	0.517	0.10904	0.426	0.682	0.12736	0.11820

The ANN model with nine neurons on the hidden layer is the best-performed one among all three-layered neural networks; and the neural network (7,5,3,1) is the best one among all the four-layered neural network models. The neural network (7,9,1) is capable of estimating 170 unit debris yield with 0.13038 MSE, one of the lowest errors achieved for the calibration data, 30 unit debris yield with 0.10680 MSE, one of the highest errors for the validation data. All the four-layered neural networks are calibrated more successfully with smaller errors than all the three-layered neural networks; however, the performance for the validation data is a little worse. The two neural networks, (7,9,1) and (7,5,3,1), have very similar performance for the calibration and the validation data; the latter network is selected as a better one with lower average MSE. The best linear regression line fits the data points with measured unit debris yield as abscissa and estimated unit debris yield as ordinate are shown in Figure 21. It appears that the neural network (7,5,3,1) seriously overestimates a dozen unit debris yield data records that results in a lower correlation coefficient for the calibration data, 0.722; and the performance of the validation data is even worse, the data points scatter far away from the 45 degree line and the correlation coefficient is only 0.502.

In order to improve the simulation accuracy, twelve four-layered neural networks are calibrated by the LM algorithm. The architecture of the ANN models with their best modeling results are listed in Table 12. The error of the calibration data is reduced to less than 0.1, meanwhile the validation data error is lowered to

0.07073 by a neural network (7,5,3,1). This network is considered to be the best-performed one with the lowest error for the validation data and a relatively lower error for the calibration data. All the neural networks trained by the LM algorithm provide more accurate modeling results for the calibration data and for most of the validation data than the ANN models trained by the BRBP algorithm. As seen from Figure 22(a), the performance for the calibration data improves with signs of lower error and higher correlation coefficient as compared with the same neural network trained by the BRBP (Figure 21(a)). This conclusion can also be applied for the validation data. In Figure 22(b), 30 validation data points are much closer to the 45 degree line than those in Figure 21(b), and a much higher correlation coefficient, 0.739, is achieved.

**Table 12:** Summary of the performances of ANN models trained by the LM algorithm for Case 5

ANN Geometry	Validation Data Set			Calibration Data Set			Average MSE
	Slope	R	MSE	Slope	R	MSE	
7,4,1,1 (39)	0.436	0.447	0.13553	0.583	0.764	0.09862	0.11708
7,4,2,1 (45)	0.406	0.509	0.09808	0.587	0.766	0.09777	0.09792
7,4,3,1 (51)	0.609	0.608	0.10806	0.625	0.791	0.08870	0.09838
7,4,4,1 (57)	0.493	0.625	0.07431	0.687	0.829	0.07410	0.07421
7,4,5,1 (63)	0.868	0.704	0.09339	0.664	0.815	0.07947	0.08643
7,4,6,1 (69)	0.544	0.627	0.08481	0.713	0.844	0.06792	0.07637
<b>7,5,3,1 (62)</b>	<b>0.721</b>	<b>0.739</b>	<b>0.07073</b>	<b>0.659</b>	<b>0.812</b>	<b>0.08062</b>	<b>0.07568</b>
7,5,4,1 (69)	0.445	0.520	0.10498	0.715	0.846	0.06741	0.08619
7,5,5,1 (76)	0.536	0.591	0.08736	0.706	0.840	0.06966	0.07851
7,5,6,1 (83)	0.563	0.578	0.09997	0.669	0.818	0.07841	0.08919
7,6,3,1 (73)	0.592	0.605	0.09183	0.719	0.848	0.06637	0.07910
7,6,4,1 (81)	0.781	0.654	0.10638	0.666	0.816	0.07899	0.09269

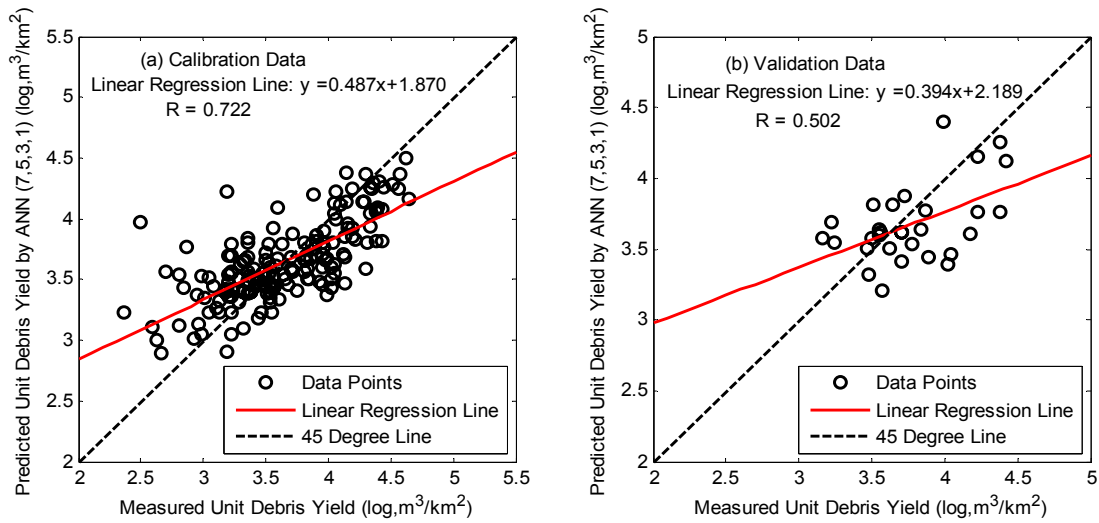


**Figure 21:** Linear regression analysis between measured and ANN model (BRBP) estimated debris yield (a) Calibration Data Set (b) Validation Data Set for Case 5

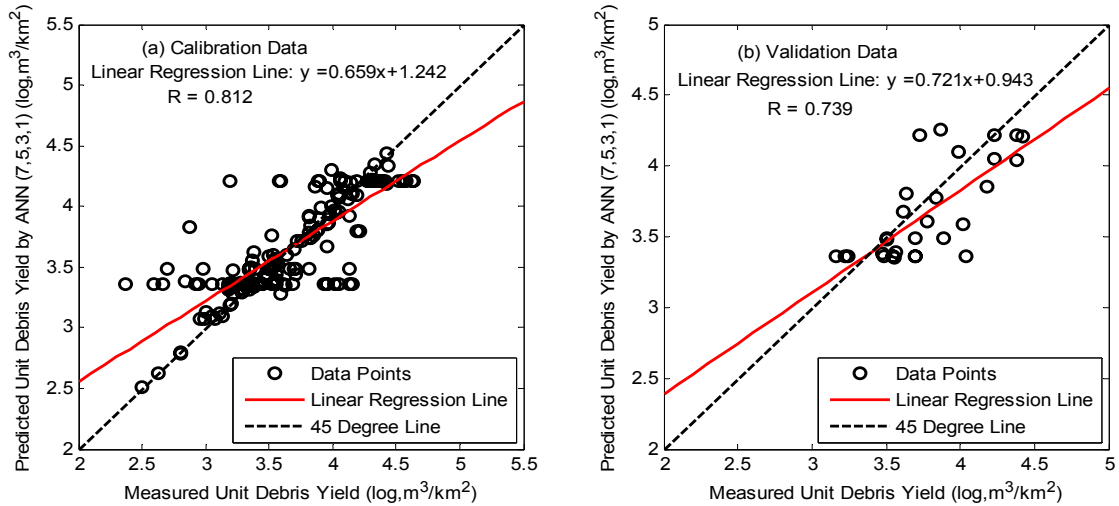


**Figure 22:** Linear regression analysis between measured and ANN model (LM) estimated debris yield (a) Calibration Data Set (b) Validation Data Set for Case 5

Compared with two best performed neural networks in Case 4, one trained by the BPBR algorithm and the other trained by the LM algorithm, the best neural networks (7,5,3,1) in this case trained either by the BPBR or the LM algorithm show some improvement on the modeling accuracy. It indicates that the DDM is an important input variable and should be included for the estimation.

#### 4.2.2.2 ANFIS Model

Following the same tuning procedure for the ANFIS model explained in Case 4, the best ANFIS model in this case creates eight fuzzy rules as listed in Table 13. There are two trapezoidal membership functions (Figure 23) for each of the first three inputs, i.e.  $\log A$ ,  $\log R_r$ , and DDM, and the membership values for the remaining parameters are equal to one as long as they are within their input ranges. The best ANFIS model is capable of estimating 170 data records of unit debris yield with a MSE of 0.1196 and 30 validation data records with a MSE of 0.1298.

**Table 13:** Summarization of fuzzy rules for Case 5

	Premise Parameters			Consequent Parameters
	$\log A$	$\log R_r$	DDM	
1	(-0.862, 0.042, 1.397, 2.255)	(1.394, 1.706, 2.175, 2.444)	(1.442, 1.616, 1.85, 2.031)	$f = -18.41+67.27\log A+44.31\log R_r-36.21\text{DDM}+58.57\text{TSL}-125.7\text{T1}-15.29\log I+6.893\text{F}$
2	(-0.862, 0.042, 1.397, 2.255)	(1.394, 1.706, 2.175, 2.444)	(1.871, 2.024, 2.312, 2.486)	$f = -8.98-46.22\log A-9.528\log R_r+7.439\text{DDM}-57.24\text{TSL}+148.3\text{T1}-12.29\log I-14.98\text{F}$
3	(-0.862, 0.042, 1.397, 2.255)	(2.174, 2.487, 2.954, 3.266)	(1.442, 1.616, 1.85, 2.031)	$f = 19.37+21.2\log A-19.11\log R_r+25.61\text{DDM}-7.97\text{TSL}+4.908\text{T1}+0.443\log I+0.2013\text{F}$
4	(-0.862, 0.042, 1.397, 2.255)	(2.174, 2.487, 2.954, 3.266)	(1.871, 2.024, 2.312, 2.486)	$f = 40.62+32.78\log A+15.51\log R_r+3.757\text{DDM}-2.286\text{TSL}-17.12\text{T1}+1.943\log I+0.14\text{F}$
5	(1.364, 2.301, 3.658, 4.562)	(1.394, 1.706, 2.175, 2.444)	(1.442, 1.616, 1.85, 2.031)	$f = -91.33-55.6\log A+51.17\log R_r-63.54\text{DDM}-1.724\text{TSL}+71.17\text{T1}-0.1917\log I-0.145\text{F}$
6	(1.364, 2.301, 3.658, 4.562)	(1.394, 1.706, 2.175, 2.444)	(1.871, 2.024, 2.312, 2.486)	$f = -41.63-11.52\log A-37.85\log R_r-44.87\text{DDM}-23.85\text{TSL}+69.89\text{T1}+24.99\log I+9.497\text{F}$
7	(1.364, 2.301, 3.658, 4.562)	(2.174, 2.487, 2.954, 3.266)	(1.442, 1.616, 1.85, 2.031)	$f = 11.38-17.59\log A+23.65\log R_r-44.77\text{DDM}+14.66\text{TSL}-3.129\text{T1}+0.887\log I+0.083\text{F}$
8	(1.364, 2.301, 3.658, 4.562)	(2.174, 2.487, 2.954, 3.266)	(1.871, 2.024, 2.312, 2.486)	$f = 207.2-64.57\log A-25.61\log R_r+100.1\text{DDM}+30.91\text{TSL}+16.14\text{T1}-1.627\log I+0.218\text{F}$

The best fit linear regression line for the data points with measured unit debris yield as x values and estimated values by the ANFIS model as y values

and their distribution are illustrated in Figure 24. It appears that the model is calibrated more successfully than the ANFIS model in Case 4; however, its performance for the validation data is still not acceptable (Figure 24(b)). Comparing to the two best ANN models in this case, the performance of the ANFIS model is very similar to the ANN model trained by the BRBP algorithm, but it is much worse than the ANN model trained by the LM algorithm.

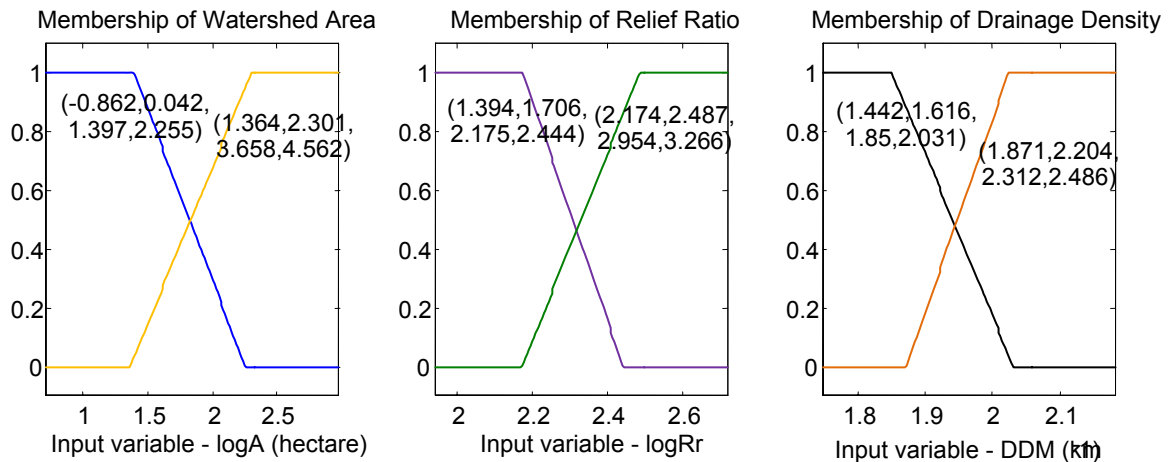


**Figure 23:** Membership functions for  $\log A$ ,  $\log R_r$ , and DDM (Case 5)

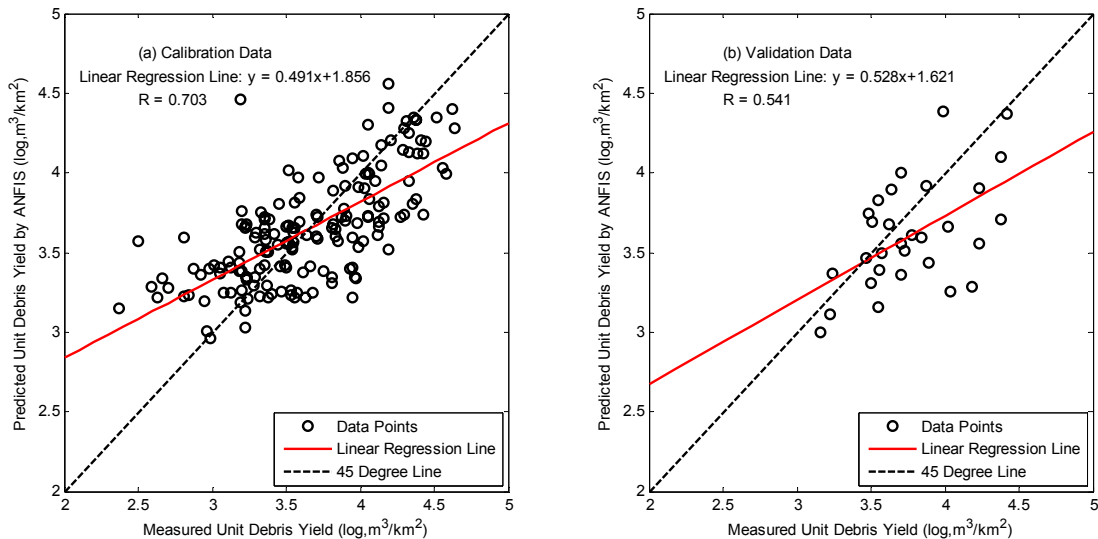


**Figure 24:** Linear regression analysis between measured and ANFIS model estimated debris yield (a) Calibration Data Set (b) Validation Data Set for Case 5

### **4.2.2.3 GD-FNN Model**

Using trial-and-error method, the values of predefined parameters are selected as  $\varepsilon_{\min} = 0.5$ ,  $\varepsilon_{\max} = 0.8$ ,  $e_{\max} = 5$ ,  $e_{\min} = 0.002$ ,  $k_{mf} = 0.55$ ,  $k_s = 0.99$ , and  $k_{err} = 0.002$ . The best fit GD-FNN model generates three fuzzy rules:

1st fuzzy rule: if  $\log A$  is (2.86, 4.78),  $\log R_r$  is (2, 1.46), DDM is (1.75, 0.81), TSL is (5.245, 5.664), T1 is (3.83, 4.91),  $\log I$  is (1.15, 2.63), and F is (6.5, 7.25), then

$$t = 10.807 - 4.089\log A + 5.145\log R_r - 7.465\text{DDM} + 1.275\text{TSL} + 0.546\text{T1} \\ + 1.377\log I - 0.398\text{F}$$

2nd fuzzy rule: if  $\log A$  is (1.91, 1.771),  $\log R_r$  is (2.72, 1.611), DDM is (1.75, 0.81), TSL is (3.974, 2.041), T1 is (3.25, 3.03),  $\log I$  is (1.15, 2.47), and F is (4.26, 3.49), then

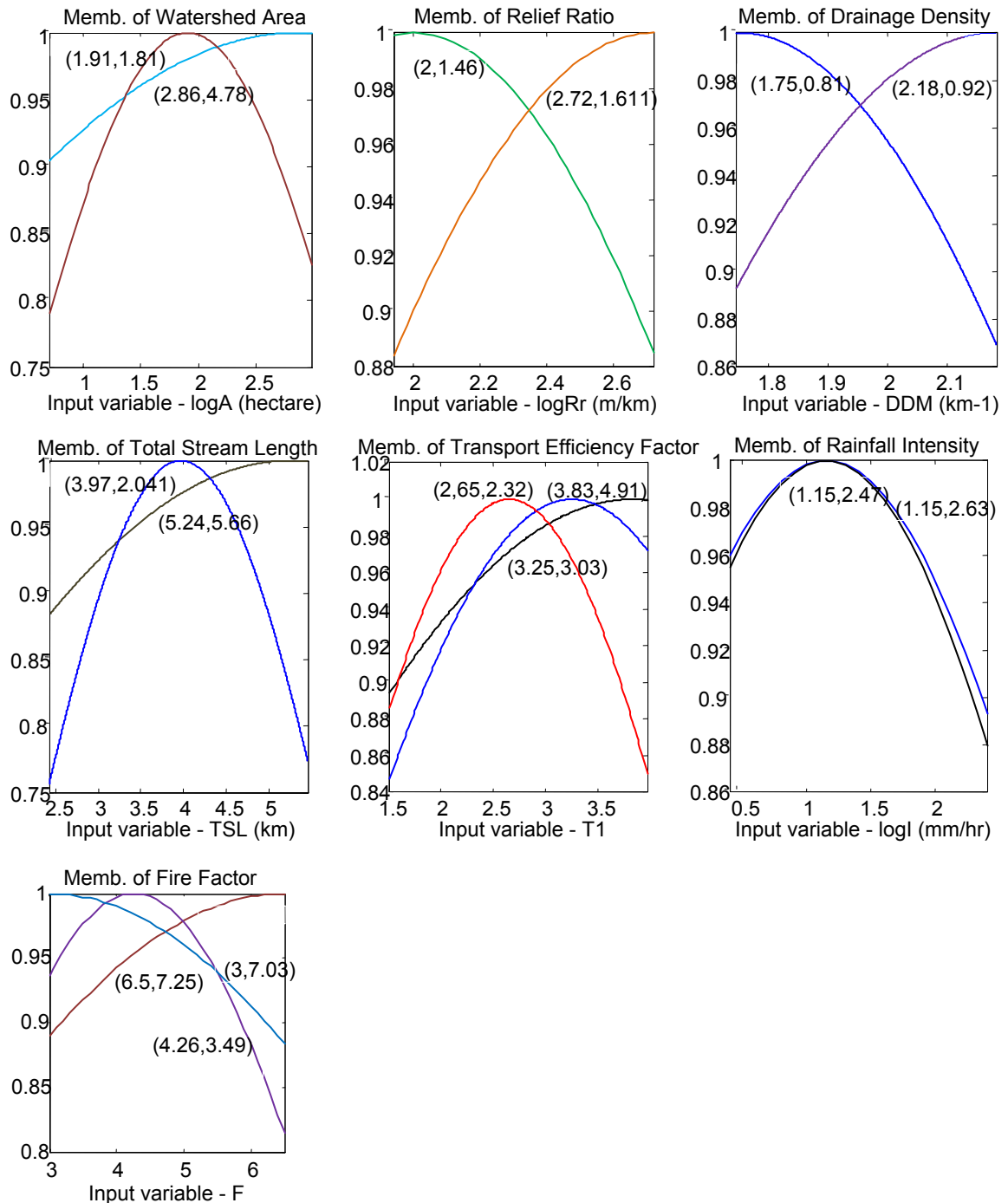
$$t = 56.844 - 10.760\log A - 5.822\log R_r - 18.339\text{DDM} + 1.876\text{TSL} + 3.141\text{T1} \\ - 2.858\log I - 0.426\text{F}$$

3rd fuzzy rule: if  $\log A$  is (1.91, 1.771),  $\log R_r$  is (2.72, 1.611), DDM is (2.18, 0.92), TSL is (3.974, 2.041), T1 is (2.65, 2.32),  $\log I$  is (1.15, 2.52), and F is (3, 7.03), then

$$t = -68.031 + 13.583\log A + 4.560\log R_r + 28.086\text{DDM} - 3.700\text{TSL} - 4.493\text{T1} \\ + 2.869\log I + 0.256\text{F}$$

This GD-FNN model consists of 7 neurons on the input layer, 3 neurons on the inference layer, and 1 neuron on the defuzzification layer. Each of  $\log A$ ,

$\log R_r$ , DDM, TSL, and  $\log l$  have two membership functions, and both T1 and F have three membership functions (Figure 25).



Memb. is the abbreviation of membership function.

**Figure 25:** Membership functions for each input variable (Case 5)

In this case, the best GD-FNN model is calibrated with a MSE of 0.1764 and a correlation coefficient of 0.507, and the MSE for the validation data is 0.1111 and the corresponding correlation coefficient is 0.569. It can be found that the calibration of the GD-FNN model is unsuccessful with a high error and very low correlation coefficient. Although the GD-FNN model achieves lower estimation error and higher correlation coefficient for the validation data, it estimates roughly 15 events seriously below their measured values as shown in Figure 26(b). The comparison between the GD-FNN model and other artificial intelligence models in this case shows it is the model with the least simulation accuracy for both the calibration and the validation data.

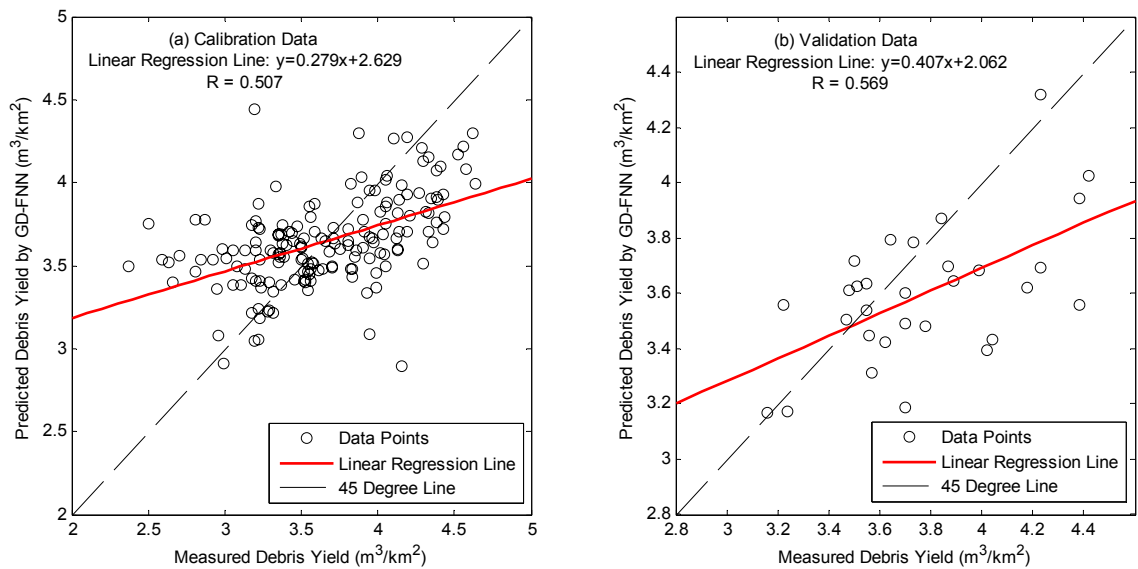


**Figure 26:** Linear regression analysis between measured and GD-FNN model estimated debris yield (a) Calibration Data Set (b) Validation Data Set for Case 5

### **4.2.3 Case 6**

Two new watershed morphological parameters, ER and MBR, are included as input parameters in this case. The data ranges of those two new input parameters are [1.45 1.97] for ER, and [2 3.04] for MBR. Nine input parameters included in this case are  $\log A$ ,  $\log R_r$ , ER, DDM, TSL, T1, MBR,  $\log l$ , and F.

#### **4.2.3.1 ANN Model**

Thirty-nine ANN models with either one or two hidden layer(s) are trained by the BRBP algorithm to find the most suitable neural network geometry for estimating unit debris yield in this case. Fifteen four-layered neural networks are also trained by the LM algorithm which promotes the modeling accuracy in the previous two cases. During training, the same internal parameters used in the preceding two cases are maintained. Both the calibration and validation data are preprocessed following the same procedure applied in Case 4 and 5.

The performance of all developed ANN models trained by the BRBP algorithm is given in Table 14. The neural network with 17 neurons on the only hidden layer is selected as the best one among all the three-layered neural networks with a relatively low MSE for both the calibration data and the validation data. This neural network provides equally performance for both the calibration and the validation data. The neural network with 4 neurons on both hidden layers is determined to be the best one among all the four-layered ANN models.

**Table 14:** Summary of the performances of ANN models trained by the BRBP algorithm for Case 6

ANN Geometry	Validation Data Set			Calibration Data Set			Average MSE
	Slope	R	MSE	Slope	R	MSE	
9,5,1 (56)	0.265	0.383	0.17877	0.462	0.725	0.10921	0.14399
9,6,1 (67)	0.207	0.352	0.17446	0.465	0.731	0.10750	0.14098
9,7,1 (78)	0.197	0.329	0.18056	0.486	0.749	0.10182	0.14119
9,8,1 (89)	0.276	0.378	0.18657	0.480	0.738	0.10494	0.14575
9,9,1 (100)	0.275	0.389	0.17942	0.467	0.728	0.10812	0.14377
9,10,1 (111)	0.277	0.390	0.17929	0.468	0.728	0.10799	0.14364
9,11,1 (122)	0.278	0.392	0.17869	0.468	0.729	0.10798	0.14334
9,12,1 (133)	0.357	0.503	0.14783	0.473	0.737	0.10553	0.12668
9,13,1 (144)	0.357	0.503	0.14781	0.474	0.737	0.10546	0.12663
9,14,1 (155)	0.356	0.503	0.14777	0.474	0.737	0.10542	0.12660
9,15,1 (166)	0.356	0.503	0.14773	0.474	0.737	0.10542	0.12657
9,16,1 (177)	0.356	0.503	0.14767	0.474	0.737	0.10542	0.12655
9,17,1 (188)	0.355	0.503	0.14760	0.474	0.737	0.10543	0.12651
9,18,1 (177)	0.355	0.495	0.15036	0.472	0.738	0.10545	0.12791
9,19,1 (188)	0.354	0.505	0.14748	0.409	0.684	0.12226	0.13487
9,20,1 (221)	0.354	0.505	0.14746	0.409	0.684	0.12225	0.13486
9,21,1 (232)	0.354	0.505	0.14744	0.409	0.684	0.12224	0.13484
9,3,1,1 (36)	0.394	0.528	0.14381	0.399	0.651	0.13075	0.13728
9,3,2,1 (41)	0.401	0.535	0.14210	0.399	0.653	0.13042	0.13626
9,3,3,1 (46)	0.402	0.537	0.14158	0.400	0.653	0.13028	0.13593
9,3,4,1 (51)	0.403	0.538	0.14136	0.400	0.653	0.13022	0.13579
9,4,1,1 (47)	0.321	0.490	0.14714	0.424	0.685	0.12118	0.13416
9,4,2,1 (53)	0.441	0.527	0.15497	0.424	0.682	0.12204	0.13850
9,4,3,1 (59)	0.450	0.529	0.15600	0.425	0.682	0.12180	0.13890
9,4,4,1 (65)	0.326	0.508	0.14208	0.449	0.696	0.11747	0.12978
9,4,5,1 (71)	0.316	0.478	0.15058	0.447	0.697	0.11718	0.13388
9,5,1,1 (58)	0.325	0.462	0.15931	0.497	0.736	0.10476	0.13204
9,5,2,1 (65)	0.299	0.379	0.19339	0.498	0.736	0.10465	0.14902
9,5,3,1 (72)	0.341	0.405	0.19212	0.531	0.756	0.09765	0.14489
9,5,4,1 (79)	0.237	0.359	0.18198	0.502	0.736	0.10453	0.14326
9,5,5,1 (86)	0.238	0.361	0.18135	0.502	0.735	0.10461	0.14298
9,5,6,1 (93)	0.346	0.477	0.15648	0.495	0.732	0.10579	0.13114
9,6,1,1 (69)	0.301	0.370	0.19897	0.541	0.768	0.09385	0.14641
9,6,2,1 (77)	0.260	0.345	0.19770	0.580	0.790	0.08581	0.14175
9,6,3,1 (85)	0.260	0.345	0.19768	0.579	0.790	0.08582	0.14175
9,6,4,1 (93)	0.382	0.464	0.17079	0.517	0.755	0.09861	0.13470
9,6,5,1 (101)	0.320	0.389	0.19440	0.546	0.769	0.09338	0.14389
9,6,6,1 (109)	0.321	0.389	0.19428	0.547	0.769	0.09337	0.14383
9,6,7,1 (117)	0.322	0.390	0.19420	0.547	0.769	0.09337	0.14378

As seen from Table 14, the neural networks with more than 72 effective parameters are capable of estimating 170 unit debris yield with smaller error (i.e. less than 0.10000), all these networks suffer from overfitting problem. The ANN model (9,17,1) estimates debris yield more accurately for the calibration data than the neural network model (9,4,4,1); however, the simulation is a little worse for the validation data. Considering the little difference in the average MSE of these two network models, it can be concluded that the (9,17,1) network is as good as the network (9,4,4,1). The unit debris yield simulated by the network (9,17,1) is plotted against their measured values in Figure 27 together with the best fit linear regression lines for those data points. Only six data points are very close to the 45 degree line in Figure 27(b) that explains why the correlation coefficient is only 0.503 for the validation data. Trained by the BRBP algorithm, even two 'best-performed' networks (9,17,1) and (9,4,4,1) are not able to simulate the calibration and validation data to a desirable level of accuracy.

Fifteen four-layered neural networks are also trained by the LM algorithm to compare the results. Table 15 shows the detailed network geometries and best modeling results for these fifteen neural network models. The network with five and four neurons on the first and the second hidden layer appears to be the best model with relatively better performance for the calibration and validation data thus achieving a best overall performance. The measured unit debris yield and the estimated values by this network are graphed in Figure 28. With much lower MSEs and higher correlation coefficients for the calibration and validation

data, this network is not only better performed than the network with the same geometry trained by the BRBP algorithm, but also better than the best network trained by the BRBP algorithm.

**Table 15:** Summary of the performances of ANN models trained by the LM algorithm for Case 6

ANN Geometry	Validation Data Set			Calibration Data Set			Average MSE
	Slope	R	MSE	Slope	R	MSE	
9,4,1,1 (47)	0.515	0.578	0.14382	0.579	0.761	0.09535	0.11958
9,4,2,1 (53)	0.597	0.650	0.12209	0.575	0.759	0.09619	0.10914
9,4,3,1 (59)	0.541	0.664	0.10914	0.599	0.774	0.09092	0.10003
9,4,4,1 (65)	0.420	0.578	0.12865	0.711	0.843	0.06555	0.09710
9,4,5,1 (71)	0.725	0.691	0.12328	0.684	0.827	0.07147	0.09737
9,4,6,1 (77)	0.602	0.647	0.13386	0.722	0.850	0.06292	0.09839
9,4,7,1 (83)	0.290	0.370	0.19464	0.625	0.791	0.08496	0.13980
9,5,3,1 (72)	0.466	0.674	0.10358	0.645	0.803	0.08032	0.09195
<b>9,5,4,1 (79)</b>	<b>0.516</b>	<b>0.649</b>	<b>0.11484</b>	<b>0.717</b>	<b>0.847</b>	<b>0.06417</b>	<b>0.08950</b>
9,5,5,1 (86)	0.765	0.672	0.14576	0.702	0.838	0.06744	0.10660
9,5,6,1 (93)	0.711	0.628	0.16161	0.810	0.900	0.04313	0.10237
9,5,7,1 (100)	0.376	0.527	0.15426	0.759	0.871	0.05461	0.10444
9,6,3,1 (85)	0.356	0.583	0.12638	0.601	0.775	0.09041	0.10840
9,6,4,1 (93)	0.511	0.562	0.16629	0.798	0.893	0.04582	0.10606
9,6,5,1 (101)	0.632	0.600	0.17172	0.849	0.922	0.03415	0.10294

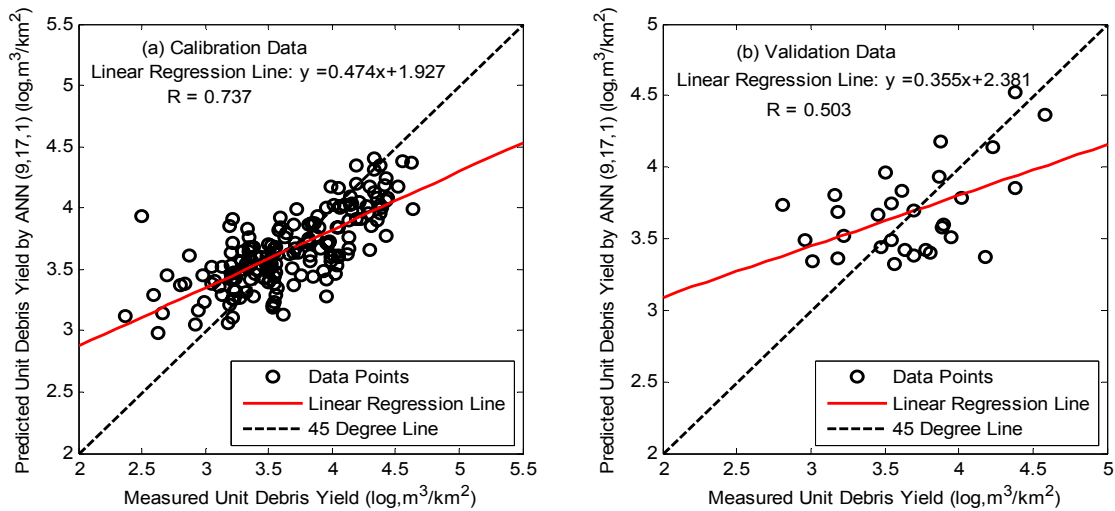


**Figure 27:** Linear regression analysis between measured and ANN model (BRBP) estimated debris yield (a) Calibration Data Set (b) Validation Data Set for Case 6

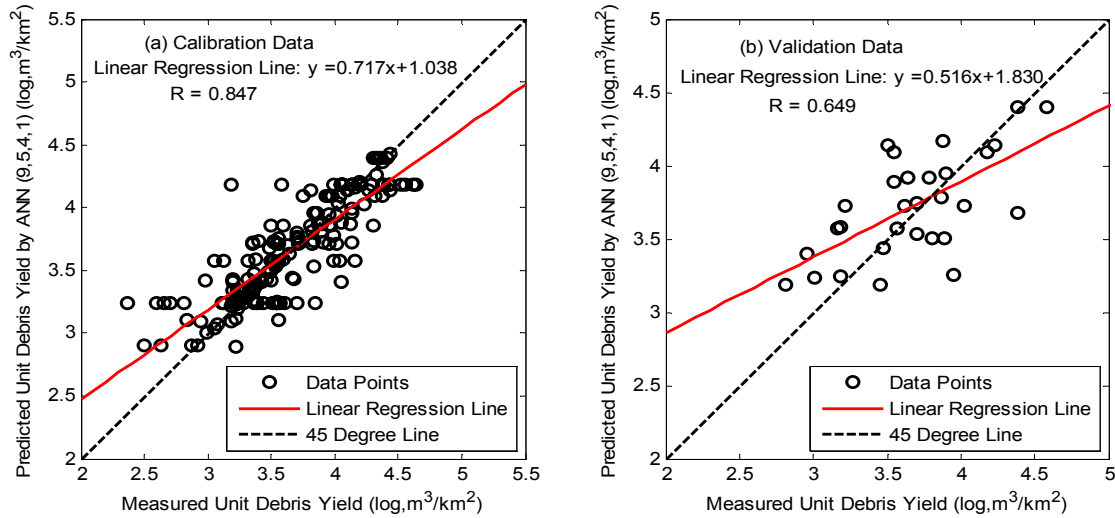


**Figure 28:** Linear regression analysis between measured and ANN model (LM) estimated debris yield (a) Calibration Data Set (b) Validation Data Set for Case 6

Compared with the two best-performed neural networks (7,5,3,1) in Case 5, one is trained by the BRBP algorithm and another is trained by the LM algorithm, errors and correlation coefficients obtained by the two best-performed networks in this case - (9,17,1) trained by the BRBP algorithm and (9,5,4,1) trained by the LM algorithm are much worse. It suggests that the inclusion of unimportant input variables such as ER and MBR introduces more error and makes the simulation deviate from the right direction.

#### **4.2.3.2 ANFIS Model**

For the simulation using ANFIS model in this case, the maximum number of membership functions for each input is four, and in order to create a same training environment as in Case 4 and 5, the same values for the remaining parameters such as epoch number, desired training data error goal, etc. are

maintained. To simplify the training process, same type of membership function is used for all input parameters. Among the four tested membership functions - Gaussian function, triangular membership function, trapezoidal membership function, generalized bell-shaped membership function, trapezoidal function is the best fit membership function for this case. Input spaces of logA and ER are partitioned into two subspaces (Figure 29) and the membership values of the other input parameters are always equal to one.

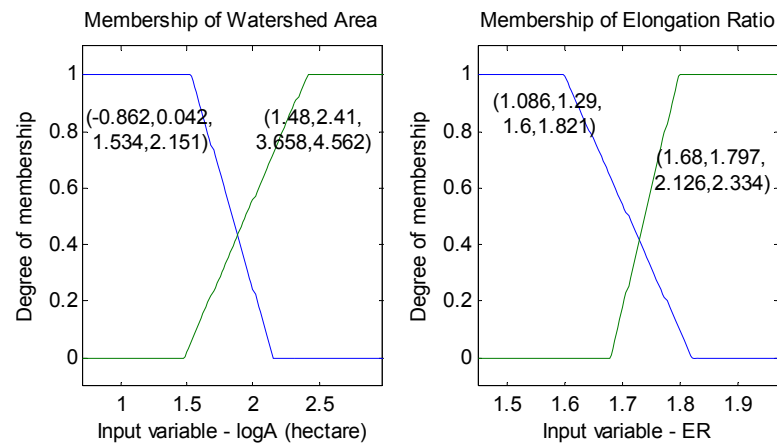


**Figure 29:** Membership functions for logA and ER (Case 6)

Consequently, four fuzzy rules are generated. The first fuzzy rule is: if logA is (-0.862 0.042 1.534 2.151), logR<sub>r</sub> is between 1.94 and 2.72, ER is (1.086 1.294 1.6 1.821), DDM is any value from 1.746 to 2.181, TSL can be any value within the range of [2.43 5.455], MBR is between 2 and 3.04, T1 is within the range of [1.51 3.97], logI is within [0.4 2.4], and F ranges from 3 to 6.5, then

$$t = 31.83 + 44.49\log A + 2.813\log R_r + 2.72ER + 91.18DDM - 85.56TSL - 94.13MBR + 94.7T1 - 1.096\log I + 0.2827F$$

The 2nd fuzzy rule is: if logA is (-0.862 0.042 1.534 2.151), ER is (1.68 1.797 2.126 2.334), and logR<sub>r</sub>, DDM, TSL, MBR, T1, logI, and F can be any value within their input ranges, then

$$t = -249.6 - 4.895\log A - 1.515\log R_r + 1.967ER - 17.52DDM + 91.49TSL + 139.4MBF - 141T1 + 2.058\log I + 0.1948F$$

The 3<sup>rd</sup> fuzzy rule is: if logA is (1.48 2.41 3.658 4.562), ER is (1.086 1.294 1.6 1.821), and the remaining seven input parameters can be any values as long as they are between their ranges, then

$$t = 358.6 - 109.1\log A + 5.683\log R_r - 4.706ER - 191DDM + 41.2TSL - 36.51MBR + 42.92T1 + 0.5869\log I - 0.0177F$$

The 4<sup>th</sup> fuzzy rule is: if logA is (1.48 2.41 3.658 4.562), ER is (1.68 1.797 2.126 2.334), and the remaining inputs are within their ranges, then

$$t = 70.8 + 12.68\log A - 1.929\log R_r - 0.4686ER + 22.57DDM - 36.12TSL - 50.39MBR + 47.2T1 + 0.3272\log I + 0.1628F$$

Figure 30 shows the measured unit debris yields and their simulated values by using the ANFIS model. The MSE for the calibration data is 0.1137 and the correlation coefficient is 0.706, and MSE for the validation data is 0.1579 and the correlation coefficient is 0.417. It performs much worse than the two best-performed ANN models in this case, one trained by the BRBP algorithm and the other trained by the LM algorithm, and it is also worse than the artificial intelligence models in Case 5. It suggests these two input parameters - ER and MBR should not be included for simulation.

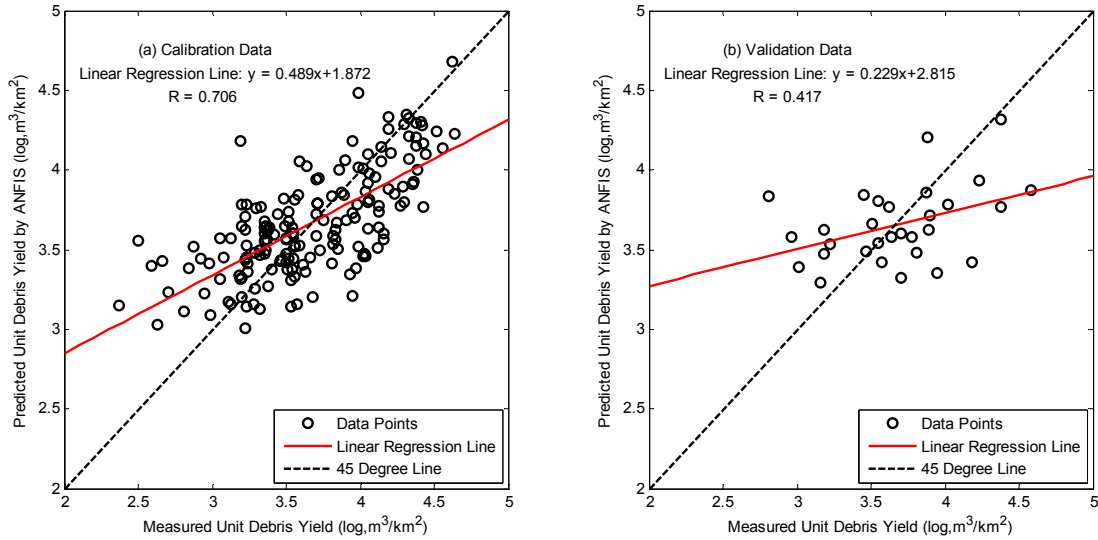


**Figure 30:** Linear regression analysis between measured and ANFIS model estimated debris yield (a) Calibration Data Set (b) Validation Data Set for Case 6

#### **4.2.3.3 GD-FNN Model**

The optimal values of seven predefined parameters required in the GD-FNN model are determined to be

$$\varepsilon_{\min} = 0.5, \varepsilon_{\max} = 0.8, e_{\max} = 5, e_{\min} = 0.002, k_{mf} = 0.65, k_s = 0.99, \text{ and } k_{err} = 0.002.$$

Two fuzzy rules procured from the GD-FNN model are listed.

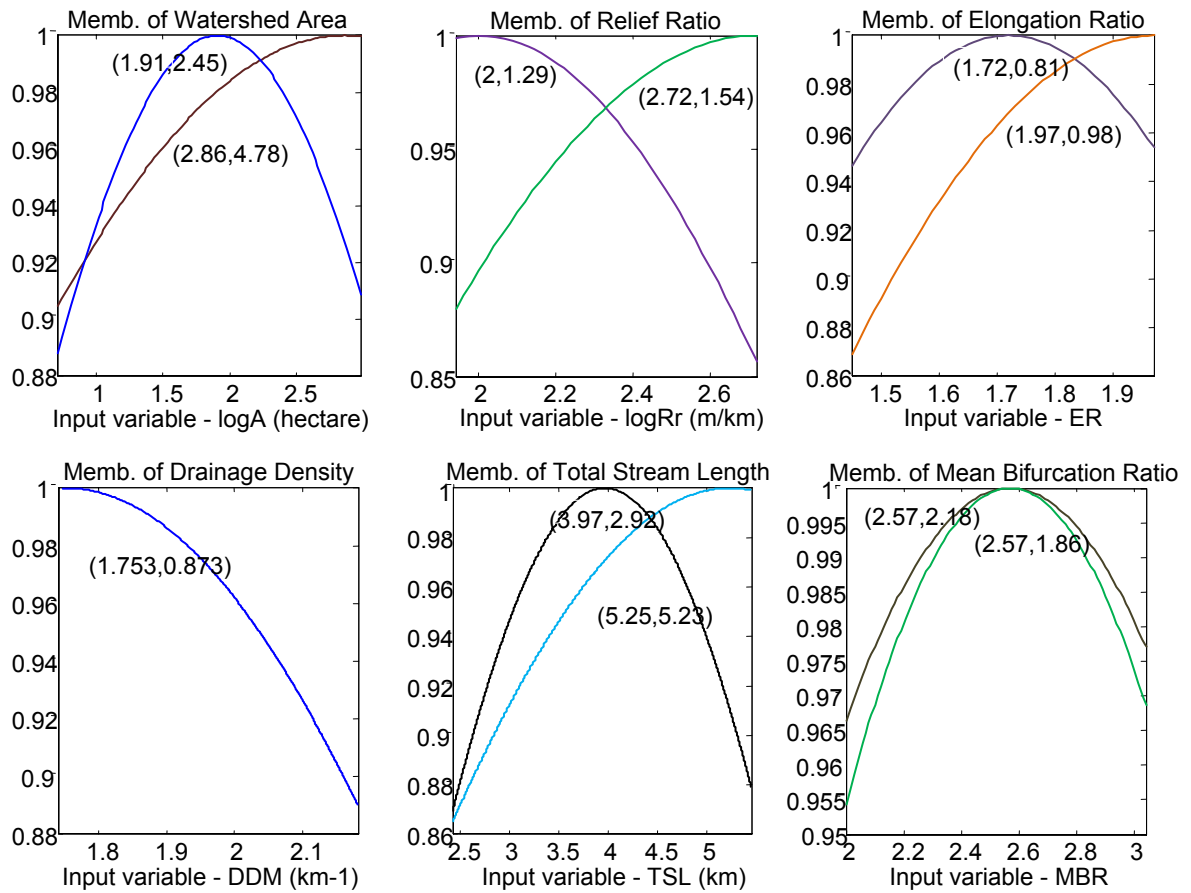
1st fuzzy rule: if  $\log A$  is (2.86, 4.78),  $\log R_r$  is (2, 1.29), ER is (1.72, 0.81), DDM is (1.753, 0.873), TSL is (5.25, 5.23), MBR is (2.57, 2.18), T1 is (3.83, 4.70),  $\log l$  is (1.18, 2.441), and F is (3.69, 5.79), then

$$t = 1.639 + 2.888\log A + 2.072\log R_r + 0.287ER + 11.491DDM - 3.284TSL + 0.823MBR - 2.283T1 - 1.654\log l - 0.070F$$

2nd fuzzy rule: if  $\log A$  is (1.91, 2.45),  $\log R_r$  is (2.72, 1.54), ER is (1.97, 0.98), DDM is (1.753, 0.873), TSL is (3.97, 2.92), MBR is (2.57, 1.86), T1 is (3.12, 3.10), is  $\log l$  (1.18, 2.441), and F is (6.5, 7.33), then

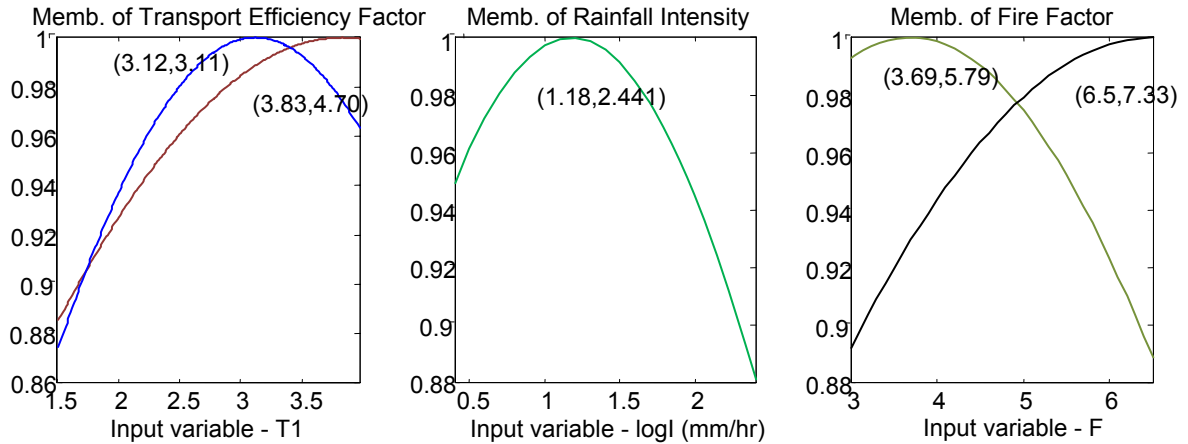
$$t = 10.690 - 4.347\log A + 6.291\log Rr + 3.028ER - 9.577DDM - 7.944TSL - 17.086MBR + 17.390T1 + 2.809\log l + 1.382F$$

The newly generated membership functions for 9 input parameters are plotted in Figure 31.



\*Memb. is the abbreviation of membership function.

**Figure 31:** Membership functions for input variables (Case 6)



\*Memb. is the abbreviation of membership function.

**Figure 31: (Continued)** Membership functions for input variables (Case 6)

This best fit GD-FNN model estimates the calibration data with a MSE of 0.1716 and the validation data with a MSE of 0.1233; and the corresponding correlation coefficients are 0.522 and 0.625 (Figure 32). This GD-FNN model is superior to the ANFIS model for the validation data; however, its performance for the calibration data is notorious.

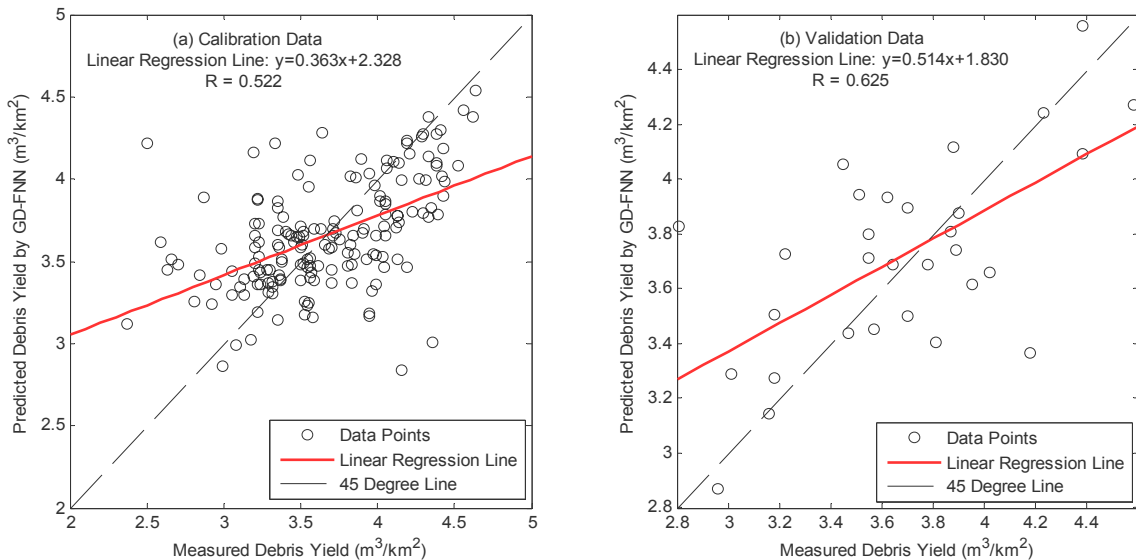


**Figure 32:** Linear regression analysis between measured and GD-FNN model estimated debris yield (a) Calibration Data Set (b) Validation Data Set for Case 6

#### **4.2.4 Case 7**

Hypsometric Index (HI), the relative height which divides the ground surface area into two equal parts, is considered as input parameter in this case. It is dimensionless and within a range of [1.38 1.79]. Therefore in this case, artificial intelligence models are trained by ten input parameters -  $\log A$ ,  $\log R_r$ , ER, DDM, TSL, T1, MBR,  $\log l$ , F, and HI.

##### **4.2.4.1 ANN Model**

Trained by the BRBP algorithm and the same internal parameters introduced in the previous three cases, seventeen three-layered neural networks and twenty-two four-layered neural networks are listed in Table 16. Also included in this table are their modeling results evaluated in terms of MSE, correlation coefficients, and the slopes of the best fitted linear regression lines. For three-layered ANN models, the errors of both the calibration and validation data vary within a very narrow range; the neural network with 17 neurons on the hidden layer has the best generalization ability with the relatively lower errors for both the calibration and the validation data. For four-layered neural networks, it is the network (10,5,5,1) that estimates the 30 validation data with the minimum error and its performance for the calibration data is acceptable. This network provides similar performance as the neural network (10,17,1) for the calibration data, however, the former one is more accurate for estimating the validation data. The debris yield estimated by the network (10,5,5,1) is compared with measured data

in Figure 33(a) and (b). In figure (a), quite a few data points are distributed far away from the 45 degree line that leads to a low correlation coefficient, 0.738, and the underestimation of a few validation data points worsens the performance of the neural network.

**Table 16:** Summary of the performances of ANN models trained by the BRBP algorithm for Case 7

ANN Geometry	Validation Data Set			Calibration Data Set			Average MSE
	Slope	R	MSE	Slope	R	MSE	
10,5,1 (61)	0.460	0.563	0.10591	0.423	0.699	0.11426	0.11008
10,6,1 (73)	0.507	0.530	0.12303	0.487	0.751	0.11414	0.11859
10,7,1 (85)	0.542	0.532	0.12591	0.519	0.772	0.11147	0.11869
10,8,1 (97)	0.501	0.518	0.12809	0.519	0.773	0.11224	0.12016
10,9,1 (109)	0.456	0.506	0.12285	0.534	0.786	0.10746	0.11515
10,10,1 (121)	0.573	0.554	0.12504	0.550	0.795	0.10647	0.11575
10,11,1 (133)	0.568	0.550	0.12619	0.552	0.797	0.10675	0.11647
10,12,1 (145)	0.568	0.550	0.12603	0.553	0.797	0.10655	0.11629
10,13,1 (157)	0.568	0.551	0.12591	0.554	0.798	0.10640	0.11616
10,14,1 (169)	0.576	0.552	0.12572	0.552	0.798	0.10629	0.11601
10,15,1 (181)	0.567	0.550	0.12589	0.555	0.798	0.10625	0.11607
10,16,1 (193)	0.567	0.550	0.12585	0.555	0.798	0.10620	0.11603
<b>10,17,1 (205)</b>	<b>0.566</b>	<b>0.550</b>	<b>0.12588</b>	<b>0.556</b>	<b>0.799</b>	<b>0.10615</b>	<b>0.11602</b>
10,18,1 (217)	0.531	0.548	0.12012	0.487	0.749	0.11296	0.11654
10,19,1 (229)	0.532	0.548	0.12016	0.487	0.749	0.11292	0.11654
10,20,1 (241)	0.540	0.512	0.13845	0.528	0.778	0.11600	0.12723
10,21,1 (253)	0.482	0.486	0.13892	0.505	0.764	0.11912	0.12902
10,3,1,1 (39)	0.506	0.607	0.11463	0.436	0.677	0.12836	0.12149
10,3,2,1 (44)	0.460	0.456	0.14427	0.478	0.715	0.11599	0.13013
10,3,3,1 (49)	0.409	0.526	0.10143	0.376	0.644	0.13916	0.12030
10,3,4,1 (54)	0.468	0.462	0.14382	0.479	0.714	0.11617	0.12999
10,4,1,1 (51)	0.495	0.602	0.09767	0.458	0.705	0.11957	0.10862
10,4,2,1 (57)	0.473	0.568	0.10477	0.449	0.705	0.11998	0.11238
10,4,3,1 (63)	0.505	0.577	0.10771	0.461	0.710	0.11796	0.11283
10,4,4,1 (69)	0.615	0.602	0.12071	0.531	0.753	0.10296	0.11184
10,4,5,1 (75)	0.616	0.602	0.12112	0.531	0.753	0.10298	0.11205
10,5,1,1 (63)	0.522	0.594	0.10814	0.504	0.741	0.10738	0.10776
10,5,2,1 (70)	0.612	0.604	0.14197	0.564	0.780	0.09343	0.11770
10,5,3,1 (77)	0.568	0.538	0.13490	0.575	0.786	0.09093	0.11291
10,5,4,1 (84)	0.526	0.557	0.13688	0.637	0.823	0.07695	0.10691
<b>10,5,5,1 (91)</b>	<b>0.512</b>	<b>0.615</b>	<b>0.09579</b>	<b>0.500</b>	<b>0.738</b>	<b>0.10842</b>	<b>0.10211</b>
10,5,6,1 (98)	0.516	0.570	0.11809	0.518	0.747	0.10525	0.11167
10,6,1,1 (75)	0.512	0.555	0.11329	0.521	0.762	0.10062	0.10695
10,6,2,1 (83)	0.642	0.550	0.14734	0.648	0.829	0.07451	0.11093

**Table 16, Continued**

ANN Geometry	Validation Data Set			Calibration Data Set			Average MSE
	Slope	R	MSE	Slope	R	MSE	
10,6,3,1 (91)	0.628	0.540	0.14907	0.648	0.828	0.07476	0.11192
10,6,4,1 (99)	0.627	0.539	0.14933	0.649	0.829	0.07454	0.11194
10,6,5,1 (107)	0.627	0.538	0.14948	0.650	0.829	0.07439	0.11194
10,6,6,1 (115)	0.494	0.536	0.13813	0.594	0.802	0.08518	0.11165
10,6,7,1 (123)	0.627	0.537	0.14967	0.650	0.829	0.07421	0.11194

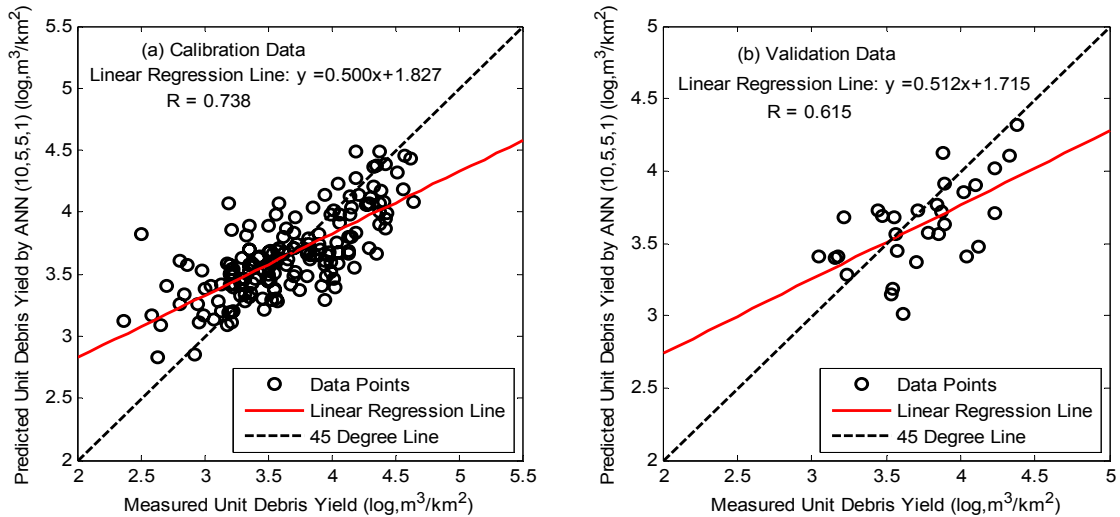


**Figure 33:** Linear regression analysis between measured and ANN model (BRBP) estimated debris yield (a) Calibration Data Set (b) Validation Data Set for Case 7

Twenty-two four-layered networks are trained by the LM algorithm to examine the possibility of improvement. The modeling results are summarized in Table 17. It appears that almost all neural networks trained by the LM algorithm are calibrated more successfully than the networks trained by the BRBP algorithm and the validation data error is reduced as well for many neural networks. Although the ANN model (10,3,4,1) is not the one with the lowest error for the calibration data, it fits best for the validation data and its performance for the calibration data is acceptable. It outperforms the best-performed network (i.e. 10,5,5,1) trained by the BRBP algorithm in this case.

**Table 17:** Summary of the performances of ANN models trained by the LM algorithm for Case 7

ANN Geometry	Validation Data Set			Calibration Data Set			Average MSE
	Slope	R	MSE	Slope	R	MSE	
<b>10,3,4,1 (54)</b>	<b>0.961</b>	<b>0.771</b>	<b>0.08031</b>	<b>0.661</b>	<b>0.813</b>	<b>0.08001</b>	<b>0.08016</b>
10,3,5,1 (59)	0.848	0.724	0.08558	0.608	0.780	0.09263	0.08910
10,3,6,1 (64)	0.561	0.577	0.11682	0.708	0.842	0.06890	0.09286
10,3,7,1 (69)	0.747	0.639	0.11212	0.632	0.796	0.08672	0.09942
10,4,1,1 (51)	0.852	0.700	0.10551	0.647	0.804	0.08348	0.09450
10,4,2,1 (57)	0.787	0.684	0.09440	0.629	0.793	0.08770	0.09105
10,4,3,1 (63)	0.534	0.586	0.09660	0.680	0.824	0.07569	0.08615
10,4,4,1 (69)	0.689	0.678	0.08585	0.667	0.817	0.07872	0.08229
10,4,5,1 (75)	0.676	0.639	0.10586	0.723	0.850	0.06541	0.08564
10,4,6,1 (81)	0.467	0.551	0.09889	0.716	0.846	0.06702	0.08295
10,5,1,1 (63)	0.699	0.646	0.10047	0.588	0.767	0.09743	0.09895
10,5,2,1 (70)	0.690	0.637	0.10062	0.656	0.810	0.08124	0.09093
10,5,3,1 (77)	0.521	0.541	0.11658	0.757	0.870	0.05734	0.08696
10,5,4,1 (84)	0.494	0.583	0.11510	0.748	0.865	0.05956	0.08733
10,5,5,1 (91)	0.507	0.542	0.12732	0.626	0.791	0.08846	0.10789
10,5,6,1 (98)	0.516	0.524	0.12304	0.591	0.769	0.09664	0.10984
10,6,1,1 (75)	0.976	0.714	0.11631	0.738	0.859	0.06196	0.08914
10,6,2,1 (83)	0.651	0.607	0.11117	0.707	0.841	0.06931	0.09024
10,6,3,1 (91)	0.716	0.619	0.11449	0.825	0.908	0.04139	0.07794
10,6,4,1 (99)	0.714	0.640	0.10585	0.856	0.925	0.03390	0.06988
10,6,5,1 (107)	0.702	0.635	0.11660	0.855	0.925	0.03430	0.07545
10,6,6,1 (115)	0.471	0.425	0.16220	0.803	0.896	0.04660	0.10440

Figure 34 is a plot of the measured unit debris yield versus their estimated values by using the network (10,3,4,1). Comparison between Figure 33 and 34 reveals a little improvement of performance in terms of the calibration data and significant improvement in the validation data by using the neural network (10,3,4,1) trained by the LM algorithm.

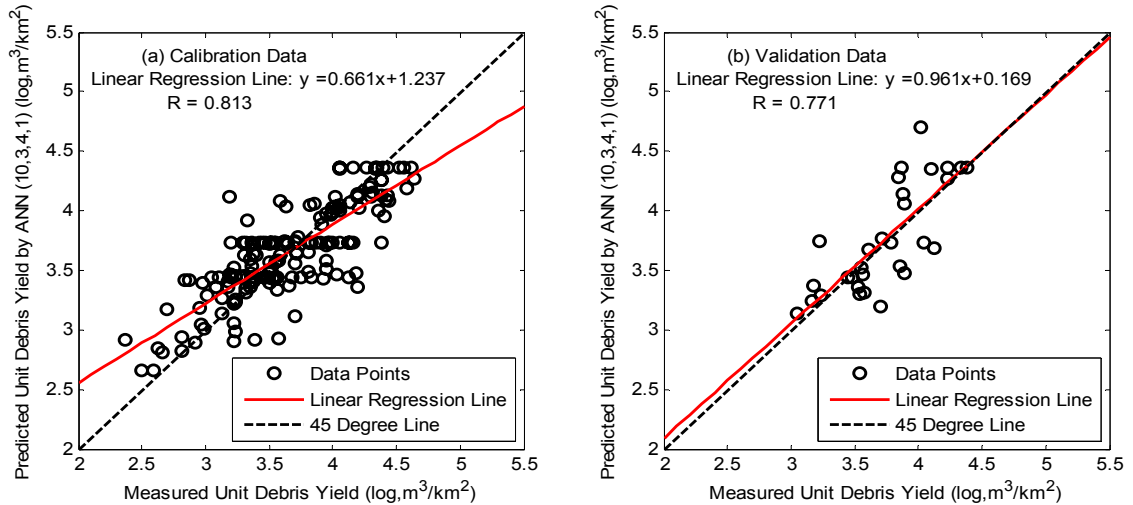


**Figure 34:** Linear regression analysis between measured and ANN model (LM) estimated debris yield (a) Calibration Data Set (b) Validation Data Set for Case 7

#### **4.2.4.2 ANFIS Model**

The number of membership function for each input variable of the ANFIS model varies from one to four but not equal to four at the same time due to the computation memory constraint. For example, if each input space is divided into two subspaces, the number of fuzzy rules will be  $2^{10}$ . With the assumption that every input variable uses the same kind of membership function, Gaussian function, triangular membership function, trapezoidal membership function, and generalized bell-shaped membership function are applied one by one. The best performance is obtained by using Gaussian membership function and both logA and TSL have two Gaussian membership functions (Figure 35). For the remaining eight input parameters, their membership values are always equal to one.

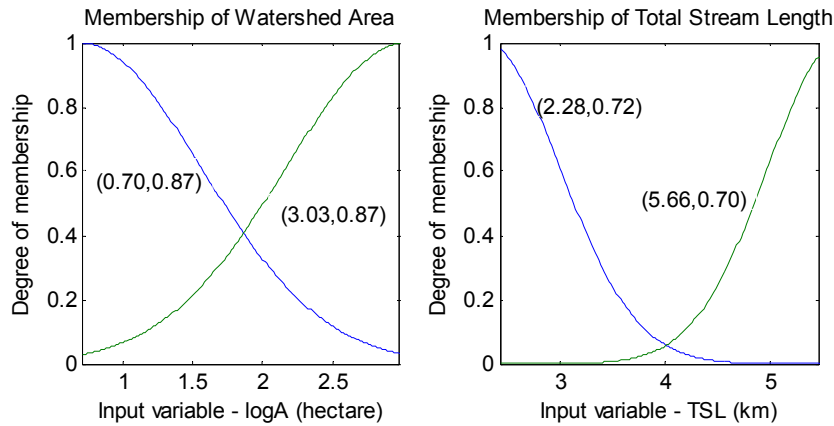


**Figure 35:** Membership functions for logA and TSL (Case 7)

The modeling results can be explained by four fuzzy if-then rules listed as follows.

1<sup>st</sup> fuzzy rule is: if logA is (0.698, 0.87) (the first and second values are the center and the width of a Gaussian function, respectively), TSL is within the range of (2.28 0.72), and the range of logR<sub>r</sub> is [1.94 2.72], ER is in a range of [1.45, 1.97], DDM is from 1.746 to 2.181, HI is within [1.38 1.79], MBR ranges from 2 to 3.04, T1 is within [1.51 3.97], logl is among the range [0.4 2.4], and F is between 3 and 6.5, then

$$t = 78.21 + 21.07\log A - 0.435\log R_r + 44.42ER - 23.48DDM - 45.51HI + 32.21TSL - 2.766MBR + 24.84T1 + 2.098\log l - 0.0464F$$

2<sup>nd</sup> fuzzy rule is: if logA is (0.698, 0.87), TSL is (5.66, 0.70), logR<sub>r</sub>, ER, DDM, MBR, T1, logl, and F can be any value within their input ranges, then

$$t = 268.2 - 45.24\log A - 18.16\log R_r + 15.99ER - 6.77DDM + 1.056HI - 47.65TSL - 78.35MBR + 77.73T1 + 3.68\log l + 0.5978F$$

3<sup>rd</sup> fuzzy rule is: if logA is (3.03, 0.87), TSL is (2.28, 0.72) and as long as the rest eight inputs are within their input ranges, then

$$t = 132.7 + 85.03\log A - 16.38\log R_r - 71.63ER + 41.45DDM + 65.62HI - 59.77TSL - 87.1MBR + 44.43T1 - 3.539\log l + 0.492F$$

4<sup>th</sup> fuzzy rule is: if logA is (3.03, 0.87), TSL is (5.66, 0.70), and the membership values for the remaining parameters are equal to one, then

$$t = -169.8 + 35.13\log A + 13.83\log R_r + 2.375ER + 41.55DDM - 13.45HI + 4.007TSL + 47.49MBR - 39.72T1 - 0.4258\log l - 0.1162F$$

The ANFIS model is capable of estimating the 170 calibration data with a MSE of 0.1247 and the 30 validation data with a MSE of 0.1007. The unit debris yield estimated by the ANFIS model is plotted versus their measured values in Figure 36(a) and (b). The comparison of the results between the ANFIS model and two best performed ANN models developed in this case indicates this ANFIS model is much worse in generalization ability.

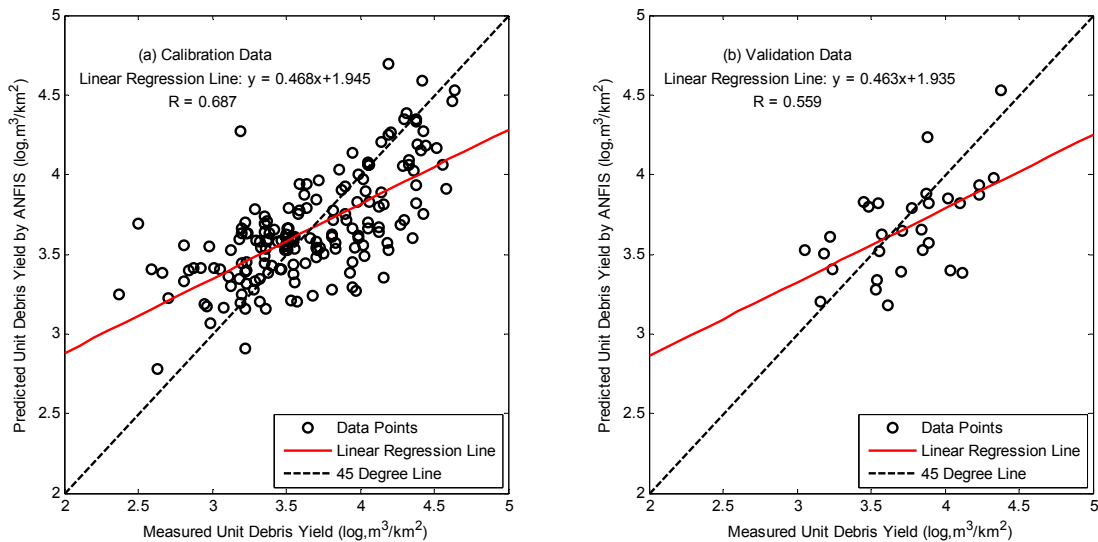


**Figure 36:** Linear regression analysis between measured and ANFIS estimated debris yield (a) Calibration Data Set (b) Validation Data Set for Case 7

#### **4.2.4.3 GD-FNN Model**

The best performed GD-FNN model for this case uses the following values of seven parameters.  $\varepsilon_{\min} = 0.5$ ,  $\varepsilon_{\max} = 0.8$ ,  $e_{\max} = 5$ ,  $e_{\min} = 0.002$ ,  $\varepsilon_{\min} = 0.5$ ,  $\varepsilon_{\max} = 0.8$ ,  $e_{\max} = 5$ ,  $e_{\min} = 0.002$ ,  $k_{mf} = 0.5$ ,  $k_s = 0.99$ ,  $k_{err} = 0.002$ . The errors for the calibration and the validation data set are 0.1919, and 0.0891, respectively. The correlation coefficients between estimated and measured unit debris yield is 0.493 for the calibration data and 0.641 for the validation data.

There are two fuzzy rules acquired from the GD-FNN model. The first fuzzy rule is: if  $\log A$  is (2.86, 4.78),  $\log R_r$  is (2, 1.58), ER is (1.72, 1.07), DDM is (1.753, 0.904), HI is (1.52, 0.831), TSL is (5.245, 6.0), MBR is (2.57, 2.104), T1 is (3.83, 4.903),  $\log I$  is (1.15, 2.595), and F is (6.5, 7.211), then

$$t = 203.467 - 10.329\log A + 2.214\log R_r - 6.054ER - 6.682DDM + 8.195HI \\ - 49.979TSL - 94.239MBR + 90.880T1 - 2.516\log I - 0.630F$$

The second fuzzy rule is: if  $\log A$  is (1.67, 2.42),  $\log R_r$  is (2.72, 1.62), ER is (1.97, 1.07), DDM is (1.753, 0.904), HI is (1.52, 0.831), TSL is (3.862, 2.926), MBR is (2.57, 2.104), T1 is (2.84, 2.734),  $\log I$  is (1.15, 2.595), and F is (6.5, 7.211), then

$$t = -166.271 + 2.976\log A + 1.800\log R_r + 7.421ER - 2.451DDM - 5.365HI \\ + 44.617TSL + 80.975MBR - 78.594T1 + 3.737\log I + 0.438F$$

Each of the five input variables (i.e.  $\log A$ ,  $\log R_r$ , ER, TSL, and T1) has two Gaussian membership functions; for the remaining five inputs, each only has one Gaussian membership function. They are plotted in Figure 37.

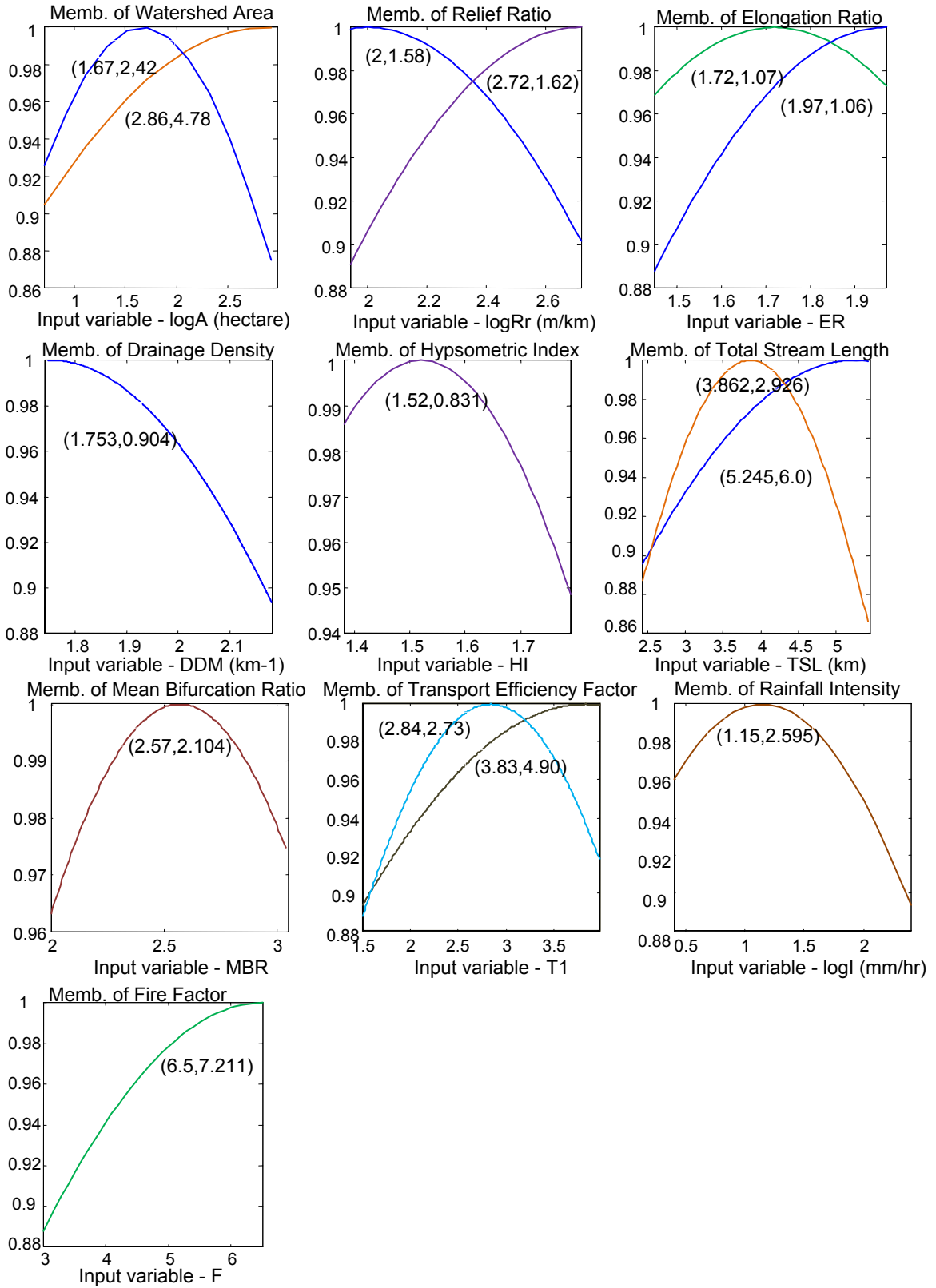


**Figure 37:** Membership functions for each input variable (Case 7)

The estimated unit debris yield by using the GD-FNN model is plotted versus their field collected values in Figure 38. Among all four artificial intelligence models created in this case, this GD-FNN model is more accurate for estimating 30 validation data records than the ANN model trained by the BRBP algorithm and the ANFIS model, however, its performance for the 170 calibration data is the worst.

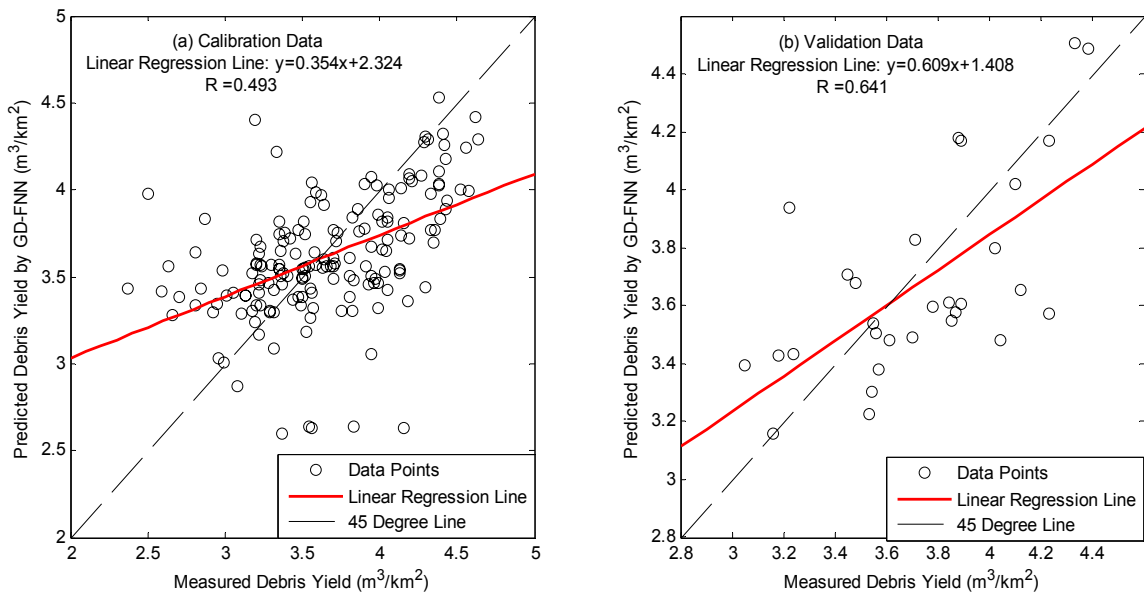


**Figure 38:** Linear regression analysis between measured and GD-FNN estimated debris yield (a) Calibration Data Set (b) Validation Data Set for Case 7

#### 4.2.5 Overall Discussion

The best performance of four artificial intelligence models from Case 4 to 7 is summarized in Table 18. There are two kinds of neural network models, the neural network on the top row is trained by the BRBP algorithm and the bottom network is trained by the LM algorithm, ANFIS, and GD-FNN model listed for

each case. From Case 4 to Case 7, equally considering the performance of artificial intelligence models for the calibration and the validation data, it is clear that ANN models trained by the LM algorithm estimate unit debris yields more accurately than ANN models trained by the BRBP algorithm, ANFIS models, and the GD-FNN models. The reason might be the LM training algorithm is more robust than the BRBP training algorithm, the combination of BPGDM and sequential least squares method employed by ANFIS model, and LLS method employed by the GD-FNN model. It is noteworthy that ANN models trained by the BRBP algorithm achieve similar performance as the ANFIS models and both models always work better than the GD-FNN models especially for the calibration data.

**Table 18:** The summary of all model performance from Case 4 to Case 7

Case No.	Model	Validation Data Set			Calibration Data Set		
		Slope	R	MSE	Slope	R	MSE
4	ANN (6,5,5,1)	0.427	0.554	0.1022	0.461	0.699	0.1209
	ANN (6,3,7,1)	0.547	0.703	0.0732	0.586	0.766	0.0974
	ANFIS	0.584	0.589	0.1125	0.550	0.743	0.1055
	GD-FNN	0.373	0.521	0.1057	0.289	0.501	0.1777
5	ANN (7,5,3,1)	0.394	0.502	0.1052	0.487	0.722	0.1139
	<b>ANN (7,5,3,1)</b>	<b>0.721</b>	<b>0.739</b>	<b>0.0707</b>	<b>0.659</b>	<b>0.812</b>	<b>0.0806</b>
	ANFIS	0.528	0.541	0.1298	0.491	0.703	0.1196
	GD-FNN	0.407	0.569	0.1111	0.279	0.507	0.1764
6	ANN (9,17,1)	0.355	0.503	0.1476	0.474	0.737	0.1054
	ANN (9,5,4,1)	0.516	0.649	0.1148	0.717	0.847	0.0642
	ANFIS	0.229	0.417	0.1579	0.489	0.706	0.1137
	GD-FNN	0.514	0.625	0.1233	0.363	0.522	0.1716
7	ANN (10,5,5,1)	0.512	0.615	0.0958	0.500	0.738	0.1084
	ANN (10,3,4,1)	0.961	0.771	0.0803	0.661	0.813	0.0800
	ANFIS	0.463	0.559	0.1007	0.468	0.687	0.1247
	GD-FNN	0.609	0.641	0.0891	0.354	0.493	0.1919

It appears that ANN models trained by the LM algorithm estimate unit debris yield more accurately not only for the calibration but also for the validation data than those networks trained by the BRBP algorithm. The reason might be the BRBP training algorithm terminates the calibration process too early to prevent overfitting problem hence the best modeling results cannot be achieved. It can be further proved by another sign –the validation data error varies in a very narrow range no matter how the neural network geometry is changed. The modeling results obtained through Case 4 to Case 7 strengths another finding from Case 1 to 3 and it is ANN models with two hidden layers have better generalization ability than those with one hidden layer.

As seen from Table 18, the network performance improves in Case 5 as compared with Case 4, improves in Case 7 as compared with Case 6, and the performance deteriorates seriously in Case 6. The major difference between these cases is the number of input parameters; Case 5 includes DDM as an additional input parameter and the remaining input parameters are the same as those in the Case 4; Case 6 is trained with two new input parameter: ER and MBR, as compared to Case 5; Case 7 has one more watershed morphological parameter, HI as compared with Case 6. The decrease of modeling errors in the Case 5 indicates the inclusion of parameter DDM improves the simulation accuracy. The inclusion of ER and MBR in Case 6 seriously worsens the generalization ability of neural network models. In Case 7, neural network performance for the validation data is enhanced dramatically due to the addition

of HI as a new input parameter as compared with Case 6. To summarize, DDM and HI are important input parameters for estimation of unit debris yield but ER and MBR are not important and should be eliminated for analysis.

#### **4.2.5 Case 8**

In this case, ANN technique is applied to estimate unit debris yield documented at 20 small debris basins within Los Angeles County from 1938 to 1983. The debris basins are Aliso, Big Dalton, Cassara, Emerald East, Fairoaks, Golf Course, Gould, Jasmine, La Tuna, LimeKiln, Lincoln, Linda Vista, Little Dalton, Ruby, Schwartz, Snowdrop, Sullivan, Turnbull, Wildwood, and Wilson and their location are graphically shown in Figure 3. They are classified into a same group because the relief ratio of their upstream collection watersheds ranges from 58 m/km to 185 m/km which is defined as mild slope in this study. 68 data records are available in this group; 58 of them are selected for calibration and 10 data records for validation by using subtractive clustering method. The data preprocessing consists of three steps: first, all the input and target values are normalized, secondly, input vectors are transferred to be uncorrelated, and finally any input variable that contributes than 2% of the total variation is removed. Four basic input parameters implemented in the debris estimation equation provided by USACE are log transformed watershed area, logarithmic relief ratio, logarithmic value of maximum one hour precipitation times 100, and fire factor. They are the input parameters used in Case 8(a); soil erodibility factor (SEF) is

included as an additional input parameter in Case 8(b), soil permeability rate (SP) in Case 8(c), and soil liquid limit (SLL) in Case 8(d).

#### **4.2.5.1 Case 8(a)**

Based on the finding that the LM training algorithm provides better modeling results than the BRBP training algorithm, ANFIS model, and GD-FNN model through Case 4 to 7, LM training algorithm is the only training algorithm used for the following eight cases. Neural network models with no more than two hidden layers are employed in this case. For three-layered neural networks, only six different geometries are created and they are (4, 4, 1), (4, 5, 1), (4, 6, 1), (4, 7, 1), (4, 8, 1), and (4, 9, 1). With a focus on neural network models with two hidden layers, twenty-five of them are generated for the estimation of unit debris yield and they are (4,2,3,1), (4,2,4,1), (4,2,5,1), (4,3,1,1), (4,3,2,1), (4,3,3,1), (4,3,4,1), (4,3,5,1), (4,3,6,1), (4,3,7,1), (4,4,1,1), (4,4,2,1), (4,4,3,1), (4,4,4,1), (4,4,5,1), (4,5,1,1), (4,5,2,1), (4,5,3,1), (4,6,1,1), (4,6,2,1), (4,6,3,1), (4,6,4,1), (4,6,5,1), (4,6,6,1), and (4,6,7,1). Hyperbolic tangent function is the only transfer function in use for hidden layers and linear function is for output layer. The training of the ANN models will be stopped when the epoch size reaches 10,000, or the calibration MSE reaches  $1 \times 10^{-6}$ , or the performance gradient is less than  $1 \times 10^{-10}$ , or the scalar ( $\mu$  in Equation 3.9) exceeds  $1 \times 10^{-10}$ . After the training process is over, the values of connection weights and biases are saved for the testing of 'unseen' data - validation data; and only the modeling results provided

by those connection weights and biases with the best performance for both calibration and validation data are listed in Table 19.

**Table 19:** Summary of the performances of ANN models for Case 8(a)

ANN Geometry	Validation Data Set			Calibration Data Set			Average MSE
	Slope	R	MSE	Slope	R	MSE	
4,4,1 (25)	0.830	0.635	0.16752	0.894	0.945	0.02247	0.09500
4,5,1 (31)	0.579	0.612	0.11972	0.819	0.905	0.03821	0.07897
4,6,1 (37)	0.528	0.717	0.09166	0.746	0.863	0.05386	0.07276
<b>4,7,1 (43)</b>	<b>0.691</b>	<b>0.733</b>	<b>0.09128</b>	<b>0.927</b>	<b>0.963</b>	<b>0.01549</b>	<b>0.05338</b>
4,8,1 (49)	0.968	0.725	0.23084	0.958	0.979	0.00893	0.11988
4,9,1 (55)	0.717	0.589	0.19424	0.995	0.997	0.00116	0.09770
4,2,3,1 (23)	0.374	0.626	0.09773	0.533	0.730	0.09893	0.09833
4,2,4,1 (27)	0.400	0.754	0.08360	0.690	0.831	0.06555	0.07458
4,2,5,1 (31)	0.405	0.528	0.12408	0.827	0.910	0.03652	0.08030
4,3,1,1 (21)	0.465	0.686	0.08787	0.628	0.793	0.07870	0.08328
4,3,2,1 (26)	0.495	0.731	0.07611	0.650	0.806	0.07406	0.07509
4,3,3,1 (31)	0.523	0.663	0.09181	0.822	0.907	0.03768	0.06475
4,3,4,1 (36)	0.618	0.753	0.07346	0.824	0.908	0.03718	0.05532
4,3,5,1 (41)	0.499	0.597	0.11732	0.843	0.918	0.03324	0.07528
<b>4,3,6,1 (46)</b>	<b>0.745</b>	<b>0.754</b>	<b>0.07869</b>	<b>0.915</b>	<b>0.957</b>	<b>0.01797</b>	<b>0.04833</b>
4,3,7,1 (51)	0.429	0.598	0.10473	0.893	0.945	0.02276	0.06374
4,4,1,1 (27)	0.567	0.571	0.14167	0.773	0.879	0.04794	0.09481
4,4,2,1 (33)	0.549	0.591	0.12254	0.735	0.858	0.05599	0.08926
4,4,3,1 (39)	0.299	0.346	0.18501	0.829	0.911	0.03618	0.11059
4,4,4,1 (45)	0.315	0.275	0.28585	0.946	0.973	0.01134	0.14859
4,4,5,1 (51)	0.894	0.614	0.21840	0.953	0.977	0.00971	0.11406
4,5,1,1 (33)	0.515	0.641	0.10582	0.795	0.891	0.04345	0.07464
4,5,2,1 (40)	0.754	0.592	0.17953	0.865	0.931	0.02836	0.10394
4,5,3,1 (47)	0.596	0.590	0.13400	0.832	0.912	0.03547	0.08473
4,6,1,1 (39)	0.498	0.493	0.16467	0.829	0.910	0.03623	0.10045
4,6,2,1 (47)	0.302	0.396	0.19567	0.888	0.943	0.02358	0.10962
4,6,3,1 (55)	0.747	0.591	0.19344	0.958	0.979	0.00888	0.10116
4,6,4,1 (63)	0.937	0.493	0.48483	0.994	0.997	0.00135	0.24309
4,6,5,1 (71)	1.006	0.759	0.13163	0.995	0.997	0.00112	0.06637
4,6,6,1 (79)	0.437	0.251	0.51999	0.995	0.997	0.00112	0.26055
4,6,7,1 (87)	0.386	0.356	0.23224	0.995	0.997	0.00112	0.11668

The neural network with seven hidden neurons is superior to the remaining three-layered networks because it achieved the lowest estimation error for the validation data and the performance for the calibration data is acceptable.

With the second lowest MSE for the validation data and acceptable error for the calibration data, the network with three and six neurons on the first and second hidden layer outperformed the other twenty-four four-layered neural networks. The performance of the latter network is slightly better than the previous network due to a better performance for the validation data. Therefore, the network (4,3,6,1) is chosen as the most suitable model for this case.

The modeling results obtained by the network (4,3,6,1) are evaluated by linear regression analysis as illustrated in Figure 39. In the left figure, there are five data points which are far away from the 45 degree line that descends the correlation coefficient to 0.957. In the right figure, none of the data points are on the 45 degree line, six are above the line and four are below. Hence the correlation coefficient is as low as 0.754 which indicates a non-satisfactory performance.

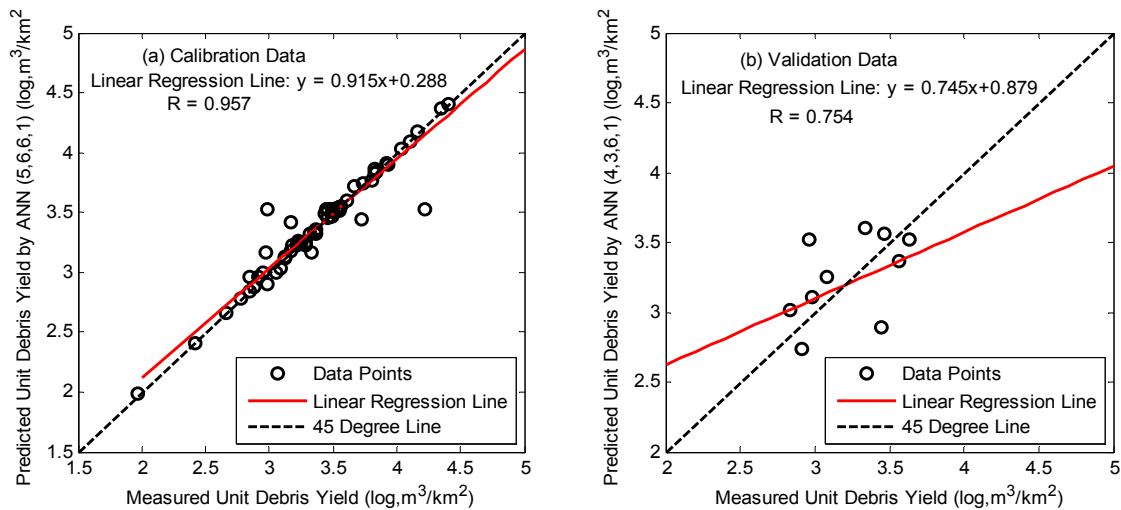


**Figure 39:** Linear regression analysis between measured and ANN model estimated debris yield (a) Calibration Data Set (b) Validation Data Set for Case 8(a) (Input Parameters: Watershed Area, Relief Ratio, Max. 1-hr Rainfall Intensity, and Fire Factor)

#### **4.2.5.2 Case 8 (b)**

As a key factor for the prediction of soil loss in Williams and Berndt's empirical equation (1972), SEF is the first soil property included for modeling unit debris yield. With four basic input variables, there are totally five input variables in this case. The internal parameters such as transfer function, training algorithm, calibration stopping criteria, and so on, are the same as in the previous case for comparison purpose. However, only four-layered neural network are developed in this case due to their better performance than the three-layered networks most of the time. Table 20 lists the modeling results of twenty-one ANN models such as (4,3,1,1), (4,3,2,1), (4,3,3,1), (4,3,4,1), (4,3,5,1), (4,3,6,1), (4,3,7,1), (4,4,2,1), (4,4,3,1), (4,4,4,1), (4,4,5,1), (4,5,1,1), (4,5,2,1), (4,5,3,1), (4,5,4,1), (4,6,1,1), (4,6,2,1), (4,6,3,1), (4,6,4,1), (4,6,5,1), and (4,6,6,1).

The network with six neurons on both hidden layers performs better than the other neural networks not only for the calibration data but also for the validation data. As seen from Figure 40(a), most data points stay on the 45 degree line and the correlation coefficient is 0.997, both of which indicate this neural network has excellent performance for the calibration data. The simulation of the validation data is not as good as that for the calibration data; the correlation coefficient for the validation data is only 0.762 because this network overestimates three unit debris yield data and underestimates one unit debris yield. However, the 10 data points are much closer to the 45 degree line than its distribution in Figure 39(b) using neural network (4,3,6,1) in the previous case.

**Table 20:** Summary of the performances of ANN models for Case 8(b)

ANN Geometry	Validation Data Set			Calibration Data Set			Average MSE
	Slope	R	MSE	Slope	R	MSE	
5,3,1,1 (24)	1.113	0.820	0.05008	0.675	0.822	0.06880	0.05944
5,3,2,1 (29)	0.564	0.664	0.05263	0.716	0.846	0.06003	0.05633
5,3,3,1 (34)	0.860	0.731	0.07241	0.820	0.906	0.03801	0.05521
5,3,4,1 (39)	0.373	0.495	0.07846	0.827	0.909	0.03664	0.05755
5,3,5,1 (44)	0.919	0.694	0.07376	0.951	0.975	0.01036	0.04206
5,3,6,1 (49)	0.640	0.702	0.08447	0.847	0.921	0.03228	0.05837
5,3,7,1 (54)	0.304	0.334	0.11784	0.970	0.985	0.00638	0.06211
5,4,2,1 (37)	0.130	0.213	0.09035	0.915	0.957	0.01794	0.05414
5,4,3,1 (43)	0.086	0.313	0.07731	0.862	0.929	0.02917	0.05324
5,4,4,1 (49)	0.541	0.642	0.07129	1.000	0.835	0.06395	0.06762
5,4,5,1 (55)	0.840	0.539	0.16118	0.898	0.948	0.02142	0.09130
5,5,1,1 (38)	0.741	0.715	0.06978	0.806	0.898	0.04107	0.05543
5,5,2,1 (45)	0.647	0.530	0.10233	0.771	0.878	0.04841	0.07537
5,5,3,1 (52)	0.459	0.605	0.05666	0.711	0.843	0.06123	0.05895
5,5,4,1 (59)	0.496	0.651	0.07168	0.839	0.916	0.03398	0.05283
5,6,1,1 (45)	0.215	0.166	0.19205	0.575	0.758	0.08990	0.14098
5,6,2,1 (53)	0.334	0.354	0.10059	0.815	0.903	0.03911	0.06985
5,6,3,1 (61)	0.604	0.482	0.11509	0.992	0.996	0.00179	0.05844
5,6,4,1 (69)	0.195	0.239	0.10365	0.696	0.834	0.06434	0.08400
5,6,5,1 (77)	0.663	0.465	0.14134	0.995	0.997	0.00112	0.07123
<b>5,6,6,1 (85)</b>	<b>0.798</b>	<b>0.762</b>	<b>0.04765</b>	<b>0.995</b>	<b>0.997</b>	<b>0.00112</b>	<b>0.02438</b>

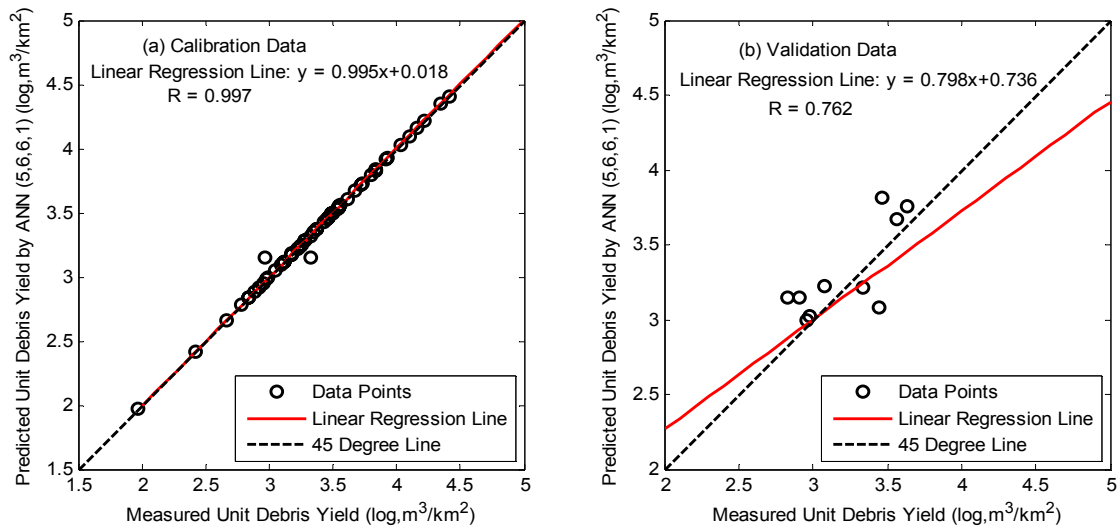


**Figure 40:** Linear regression analysis between measured and ANN model estimated debris yield (a) Calibration Data Set (b) Validation Data Set for Case 8(b) (Input Parameters: Watershed Area, Relief Ratio, Max. 1-hr Rainfall Intensity, Fire Factor, and Soil Erodibility Factor)

#### **4.2.5.3 Case 8 (c)**

With one more soil property - permeability rate (SP), this case includes six input parameters. Twenty-three ANN models with two hidden layers as shown in Table 21 are created for the simulation. Although four neural networks such as (6,3,7,1), (6,4,5,1), (6,6,5,1), (6,6,6,1) are calibrated more successfully than the network (6,4,3,1), their performance for the validation data is at least two times worse than that of the network (6,4,3,1). Overall considering the simulation accuracy for the calibration and validation data, the network (6,4,3,1) has the best generalization ability and the least number of effective parameters among the top five best-performed networks. The network estimates 58 unit debris yield data records with a very low error, 0.00508, and the 10 validated data with a MSE of 0.04651.

**Table 21:** Summary of the performances of ANN models for Case 8(c)

ANN Geometry	Validation Data Set			Calibration Data Set			Average MSE
	Slope	R	MSE	Slope	R	MSE	
6,3,1,1 (27)	0.861	0.853	0.06580	0.695	0.833	0.06462	0.06521
6,3,2,1 (32)	0.922	0.839	0.05141	0.775	0.880	0.04770	0.04955
6,3,3,1 (37)	1.054	0.797	0.05897	0.832	0.912	0.03562	0.04729
6,3,4,1 (42)	0.489	0.586	0.06765	0.816	0.903	0.03888	0.05327
6,3,5,1 (47)	0.409	0.662	0.04556	0.859	0.927	0.02985	0.03771
6,3,6,1 (52)	0.856	0.604	0.10786	0.957	0.979	0.00899	0.05843
6,3,7,1 (57)	0.854	0.663	0.13762	0.984	0.992	0.00330	0.07046
6,4,1,1 (35)	0.709	0.681	0.07014	0.789	0.888	0.04470	0.05742
6,4,2,1 (41)	0.536	0.636	0.06774	0.906	0.952	0.01995	0.04384
<b>6,4,3,1 (47)</b>	<b>0.756</b>	<b>0.772</b>	<b>0.04651</b>	<b>0.976</b>	<b>0.988</b>	<b>0.00508</b>	<b>0.02579</b>
6,4,4,1 (53)	0.417	0.432	0.09868	0.824	0.908	0.03725	0.06796
6,4,5,1 (59)	0.511	0.473	0.09668	0.993	0.996	0.00151	0.04909
6,5,1,1 (43)	1.047	0.692	0.10794	0.872	0.934	0.02699	0.06747
6,5,2,1 (50)	0.407	0.413	0.09349	0.920	0.959	0.01684	0.05517
6,5,3,1 (57)	0.695	0.662	0.05837	0.679	0.824	0.06791	0.06314
6,5,4,1 (64)	0.495	0.402	0.14407	0.907	0.952	0.01968	0.08188
6,5,5,1 (71)	0.850	0.697	0.09652	0.675	0.821	0.06888	0.08270

**Table 21.** (Continued)

<b>ANN Geometry</b>	<b>Validation Data Set</b>			<b>Calibration Data Set</b>			<b>Average MSE</b>
	<b>Slope</b>	<b>R</b>	<b>MSE</b>	<b>Slope</b>	<b>R</b>	<b>MSE</b>	
6,6,1,1 (51)	0.261	0.525	0.05962	0.608	0.780	0.08303	0.07133
6,6,2,1 (59)	0.625	0.587	0.07635	0.582	0.763	0.08840	0.08238
6,6,3,1 (67)	0.381	0.441	0.09794	0.918	0.958	0.01733	0.05764
6,6,4,1 (75)	0.618	0.727	0.06130	0.810	0.900	0.04022	0.05076
6,6,5,1 (83)	0.514	0.507	0.09177	0.995	0.997	0.00112	0.04644
6,6,6,1 (91)	0.849	0.707	0.09413	0.995	0.997	0.00112	0.04762

In Figure 41(a), all the data points are very close to the 45 degree line and a high correlation coefficient 0.998 is obtained. In Figure 41(b), most estimated unit debris yield are very close to their measured values except one data point where the measured unit debris yield is 3.45 cubic meter per square kilometer but the estimated value is 3.08 cubic meter per square kilometer. The correlation coefficient for the validation data is 0.772. Even with a higher correlation coefficient for the validation data, this network does not considered to be a better one than the best neural network model (5,6,6,1) in Case 8(b) not only because of worse performance for the calibration data but also a much higher error for a single event.

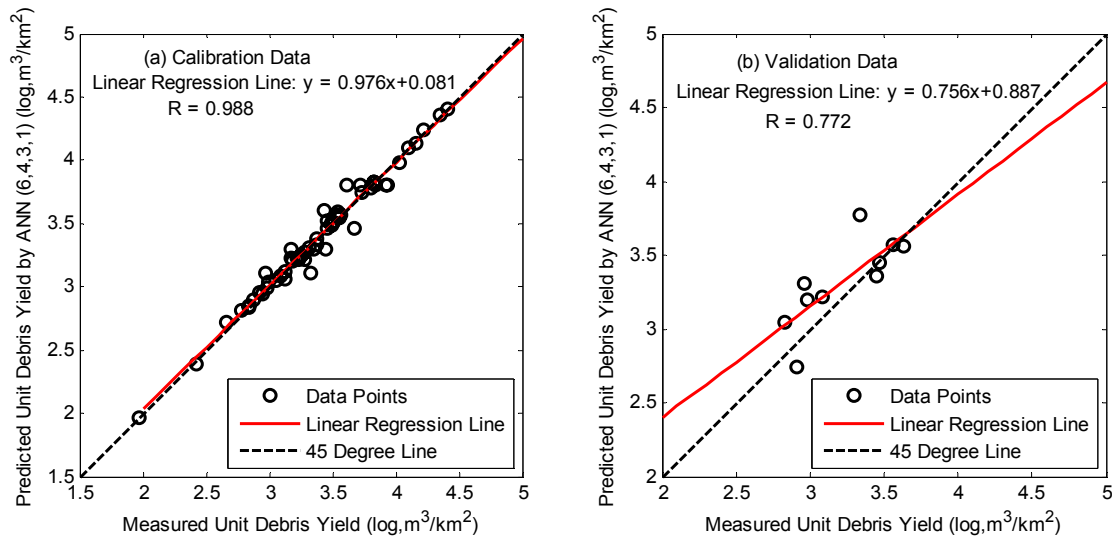


**Figure 41:** Linear regression analysis between measured and ANN model estimated debris yield (a) Calibration Data Set (b) Validation Data Set for Case 8(c) (Input Parameters: Watershed Area, Relief Ratio, Max. 1-hr Rainfall Intensity, Fire Factor, Soil Erodibility Factor, and Soil Permeability Rate)

#### **4.2.5.4 Case 8 (d)**

The last soil property considered in this study – soil liquid limit (SLL) is included as the seventh input parameter in Case 8(d). The other six input parameters are  $\log A$ ,  $\log R_r$ ,  $\log(I)$ ,  $F$ ,  $SEF$ , and  $SP$ . Twenty-four four-layered ANNs are trained by 58 data records first using the exactly same internal parameters as in the previous three cases and then tested by 10 data points. With the lowest average MSE and acceptable performance for the calibration and the validation data, the network (7,3,5,1) is the best-performed network in this case (Table 22).

**Table 22:** Summary of the performances of ANN models for Case 8(d)

ANN Geometry	Validation Data Set			Calibration Data Set			Average MSE
	Slope	R	MSE	Slope	R	MSE	
7,3,1,1 (30)	0.965	0.819	0.05614	0.697	0.835	0.06423	0.06018
7,3,2,1 (35)	0.754	0.746	0.04580	0.820	0.906	0.03808	0.04194

Table 22. Continued

ANN Geometry	Validation Data Set			Calibration Data Set			Average MSE
	Slope	R	MSE	Slope	R	MSE	
7,3,3,1 (40)	0.318	0.545	0.05750	0.859	0.927	0.02980	0.04365
7,3,4,1 (45)	0.548	0.846	0.06377	0.817	0.903	0.03919	0.05148
<b>7,3,5,1 (50)</b>	<b>0.465</b>	<b>0.734</b>	<b>0.04721</b>	<b>0.904</b>	<b>0.951</b>	<b>0.02039</b>	<b>0.03380</b>
7,3,6,1 (55)	0.367	0.466	0.08755	0.958	0.979	0.00891	0.04823
7,3,7,1 (60)	0.720	0.647	0.08083	0.783	0.885	0.04586	0.06334
7,4,1,1 (39)	1.154	0.845	0.07985	0.722	0.850	0.05873	0.06929
7,4,2,1 (45)	0.725	0.715	0.05654	0.701	0.837	0.06334	0.05994
7,4,3,1 (51)	0.575	0.556	0.09185	0.914	0.956	0.01823	0.05504
7,4,4,1 (57)	0.598	0.763	0.03683	0.708	0.842	0.06168	0.04925
7,4,5,1 (63)	0.832	0.588	0.12463	0.994	0.997	0.00123	0.06293
7,5,1,1 (48)	0.764	0.591	0.09532	0.689	0.830	0.06579	0.08056
7,5,2,1 (55)	0.726	0.754	0.07518	0.783	0.885	0.04587	0.06053
7,5,3,1 (62)	0.407	0.464	0.07734	0.982	0.992	0.00347	0.04040
7,5,4,1 (69)	0.425	0.630	0.06178	0.972	0.986	0.00582	0.03380
7,5,5,1 (76)	0.863	0.616	0.09969	0.872	0.934	0.02709	0.06339
7,6,1,1 (57)	0.427	0.850	0.03412	0.559	0.748	0.09337	0.06374
7,6,2,1 (65)	0.903	0.677	0.09648	0.940	0.969	0.01274	0.05461
7,6,3,1 (73)	0.731	0.591	0.09414	0.992	0.996	0.00170	0.04792
7,6,4,1 (81)	0.594	0.562	0.07588	0.738	0.859	0.05552	0.06570
7,6,5,1 (89)	0.654	0.652	0.05921	0.995	0.997	0.00112	0.03017
7,6,6,1 (97)	0.767	0.614	0.09514	0.995	0.997	0.00112	0.04813
7,6,7,1 (105)	0.626	0.581	0.08082	0.995	0.997	0.00112	0.04097

As seen from Figure 42, two data points within the calibration data set are deviated significantly from the 45 degree line resulting in a lower correlation coefficient - 0.951, and the three data points worsen the simulation accuracy of the validation data although the remaining seven data points fit in closely to the 45 degree line.

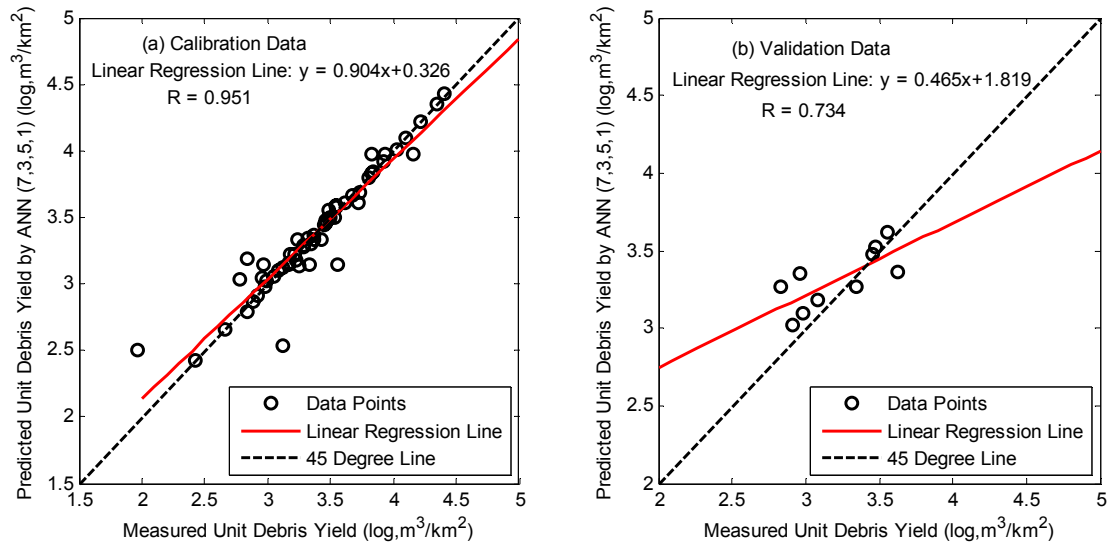


**Figure 42:** Linear regression analysis between measured and ANN model estimated debris yield (a) Calibration Data Set (b) Validation Data Set for Case 8(d) (Input Parameters: Watershed Area, Relief Ratio, Max. 1-hr Rainfall Intensity, Fire Factor, Soil Erodibility Factor, Soil Permeability Rate, and Soil Liquid Limit)

In Table 23, the best-performed ANN models for case 8(a), (b), (c), and (d) are presented and compared. The modeling results are compared to the USACE method (the last row in the table) as well. It is noticeable that the second ANN model (5,6,6,1) achieves the best modeling results for the calibration data. The second (5,6,6,1), third (6,4,3,1) and the fourth (7,3,5,1) neural network model have very similar performance for the validation data. However, both the second and the third neural network model achieve much lower MSE than the fourth neural network model. It can be concluded that the second and the third neural network model are superior to the first (4,3,6,1) and the fourth (7,3,5,1) neural network model. Since the only difference between these four cases is the number of input variables, the impact of three soil properties on ANN model performance can be summarized as follows: the addition of the SEF improves

the simulation accuracy but the SP and SLL do not contribute as much. Therefore, SEF is an important factor and should be included as an independent input variable in the future for estimating unit debris yield collected from small watershed with mild slope.

**Table 23:** Comparison of ANN models performance for Case 8

Case No.	Network Geometry	Validation Data Set			Calibration Data set			Average MSE
		Slope	R	MSE	Slope	R	MSE	
8(a)	(4,3,6,1)	0.745	0.754	0.07869	0.915	0.957	0.01797	0.04833
<b>8(b)</b>	<b>(5,6,6,1)</b>	<b>0.798</b>	<b>0.762</b>	<b>0.04765</b>	<b>0.995</b>	<b>0.997</b>	<b>0.00112</b>	<b>0.02438</b>
8(c)	(6,4,3,1)	0.756	0.772	0.04651	0.976	0.988	0.00508	0.02579
8(d)	(7,3,5,1)	0.465	0.734	0.04721	0.904	0.951	0.02039	0.03380
USACE		0.243	0.378	0.13790	0.139	0.258	0.22078	0.17934

The comparison also reveals that all these four neural networks are more accurate than the USACE (2000) empirical equation. To further clarify the modeling results between the second neural network (5,6,6,1) and the USACE method, the measured and estimated values by both methods are graphed in Figure 43 and the estimated values are compared one by one in Table 24. It is clear that the USACE data points (i.e. blue marks) scatter around the 45 degree line but ANN estimated data points (i.e. red circles) fit in closely to the line for both calibration and validation data sets. As seen from Table 24, for majority of the calibration data, this ANN model can estimate unit debris yield exactly as the measured values and it has a very small error range, [-0.18 0.18], but the errors between USACE estimated and measured values ranges from -1.01 and 1.14. For the validation data, the error range achieved by the ANN model is [-0.37

0.35] and it is [-0.52 0.70] by using USACE method. All the information leads to a conclusion that neural network technique is superior to the USACE method for estimating unit debris yield in Case 8.

**Table 24:** Measured, the USACE method, and ANN model (5,6,6,1) estimated unit debris yield for Case 8

Data	Debris Basin	Area (log, ha)	Rr (log, m/km)	Measured Unit Dy (log, m <sup>3</sup> /km <sup>2</sup> )	USACE Estimated Unit Dy (log, m <sup>3</sup> /km <sup>2</sup> )	Diffe <sup>1</sup>	ANN Estimated Unit Dy (log, m <sup>3</sup> /km <sup>2</sup> )	Diffe <sup>2</sup>
Calibration Data	Aliso	2.86	2	3.46	3.27	-0.19	3.46	0.00
	Big Dalton	2.83	2.08	2.84	3.38	0.54	2.84	0.00
		2.83	2.08	4.41	3.49	-0.92	4.41	0.00
		2.83	2.08	3.43	3.51	0.08	3.43	0.00
	Cassara	1.74	2.21	3.61	3.37	-0.24	3.61	0.00
		1.74	2.21	4.16	3.53	-0.63	4.16	0.00
	Emerald East	1.62	1.77	3.12	3.00	-0.12	3.12	0.00
		1.62	1.77	3.35	3.20	-0.15	3.35	0.00
		1.62	1.77	3.17	2.92	-0.25	3.17	0.00
	Fairoaks	1.74	1.78	2.66	2.72	0.06	2.66	0.00
		1.74	1.78	3.67	3.01	-0.66	3.67	0.00
		1.74	1.78	4.1	<b>3.09</b>	<b>-1.01</b>	4.10	0.00
	Golf Course	1.92	2.06	2.88	3.01	0.13	2.88	0.00
	Gould	2.09	2.16	3.73	3.43	-0.30	3.73	0.00
		2.09	2.16	3.49	3.48	-0.01	3.49	0.00
		2.09	2.16	3.84	3.27	-0.57	3.84	0.00
		2.09	2.16	3.92	3.31	-0.61	3.92	0.00
	Jasmine	1.42	2.1	3.49	2.87	-0.62	3.49	0.00
		1.42	2.1	3.5	3.03	-0.47	3.50	0.00
	La Tuna	3.14	1.94	3.17	3.24	0.07	3.17	0.00
		3.14	1.94	3.33	3.22	-0.11	<b>3.15</b>	<b>-0.18</b>
		3.14	1.94	2.97	3.22	0.25	<b>3.15</b>	<b>0.18</b>
		3.14	1.94	3.55	3.61	0.06	3.55	0.00
	LimeKiln	2.98	1.94	3.23	3.24	0.01	3.23	0.00
		2.98	1.94	2.99	3.58	0.59	2.99	0.00
		2.98	1.94	3.28	3.32	0.04	3.28	0.00
		2.98	1.94	3.53	3.63	0.10	3.53	0.00
	Lincoln	2.04	2.16	3.56	3.30	-0.26	3.56	0.00
		2.04	2.16	3.37	3.56	0.19	3.37	0.00
		2.04	2.16	4.03	3.44	-0.59	4.03	0.00
		2.04	2.16	2.95	3.21	0.26	2.95	0.00
		2.04	2.16	3.22	3.01	-0.21	3.22	0.00
		2.04	2.16	2.84	3.35	0.51	2.84	0.00

**Table 24, Continued**

Data	Debris Basin	Area (log, ha)	Rr (log, m/km)	Measured Unit Dy (log, m <sup>3</sup> /km <sup>2</sup> )	USACE Estimated Unit Dy (log, m <sup>3</sup> /km <sup>2</sup> )	Diffe <sup>1</sup>	ANN Estimated Unit Dy (log, m <sup>3</sup> /km <sup>2</sup> )	Diffe <sup>2</sup>	
Data	Linda Vista	1.98	2.21	3.12	3.27	0.15	3.12	0.00	
		1.98	2.21	1.97	<b>3.11</b>	<b>1.14</b>	1.97	0.00	
	Little Dalton	2.94	2.04	3.05	3.34	0.29	3.05	0.00	
		2.94	2.04	4.35	3.45	-0.90	4.35	0.00	
		2.94	2.04	4.22	3.63	-0.59	4.22	0.00	
	Ruby	1.86	2.22	3.54	3.47	-0.07	3.54	0.00	
		1.86	2.22	3.8	2.97	-0.83	3.80	0.00	
	Schwartz	1.84	2.15	3.93	3.39	-0.54	3.93	0.00	
		1.84	2.15	3.83	3.66	-0.17	3.83	0.00	
	Snowdrop	1.56	1.99	3.09	2.97	-0.12	3.09	0.00	
	Sullivan	2.79	1.8	3.32	3.45	0.13	3.32	0.00	
	Turnbill	2.41	2.03	2.42	3.00	0.58	2.42	0.00	
		2.41	2.03	2.98	3.27	0.29	2.98	0.00	
		2.41	2.03	3.46	3.58	0.12	3.46	0.00	
		2.41	2.03	3.45	3.49	0.04	3.45	0.00	
		2.41	2.03	2.92	3.99	1.07	2.92	0.00	
		2.41	2.03	3.28	3.20	-0.08	3.28	0.00	
	Wildwood	2.23	1.95	3.54	3.27	-0.27	3.54	0.00	
		2.23	1.95	3.37	3.26	-0.11	3.37	0.00	
		2.23	1.95	3.83	3.23	-0.60	3.83	0.00	
	Wilson	2.83	2.26	3.72	3.26	-0.46	3.72	0.00	
		2.83	2.26	2.78	3.56	0.78	2.78	0.00	
		2.83	2.26	3.25	3.63	0.38	3.25	0.00	
		2.83	2.26	3.24	3.72	0.48	3.24	0.00	
	Validation Data	Aliso	2.86	2	2.96	<b>3.66</b>	<b>0.70</b>	2.99	0.03
		Fairoaks	2.86	2	3.47	3.41	-0.06	<b>3.82</b>	<b>0.35</b>
		Golf Course	1.74	1.78	2.98	3.06	0.08	3.02	0.04
		LimeKiln	1.92	2.06	2.91	3.13	0.22	3.15	0.24
Little Dalton		2.98	1.94	3.08	3.24	0.16	3.22	0.14	
		2.94	2.04	2.83	3.37	0.54	3.15	0.32	
Ruby		2.94	2.04	3.63	3.49	-0.14	3.75	0.12	
Snowdrop		1.86	2.22	3.45	3.23	-0.22	<b>3.08</b>	<b>-0.37</b>	
Wildwood	1.56	1.99	3.34	<b>2.82</b>	<b>-0.52</b>	3.21	-0.13		

Diffe<sup>1</sup> - Difference between measured debris yield and the estimated values using the USACE method.

Diffe<sup>2</sup> - Difference between measured debris yield and the estimated values using ANN model.

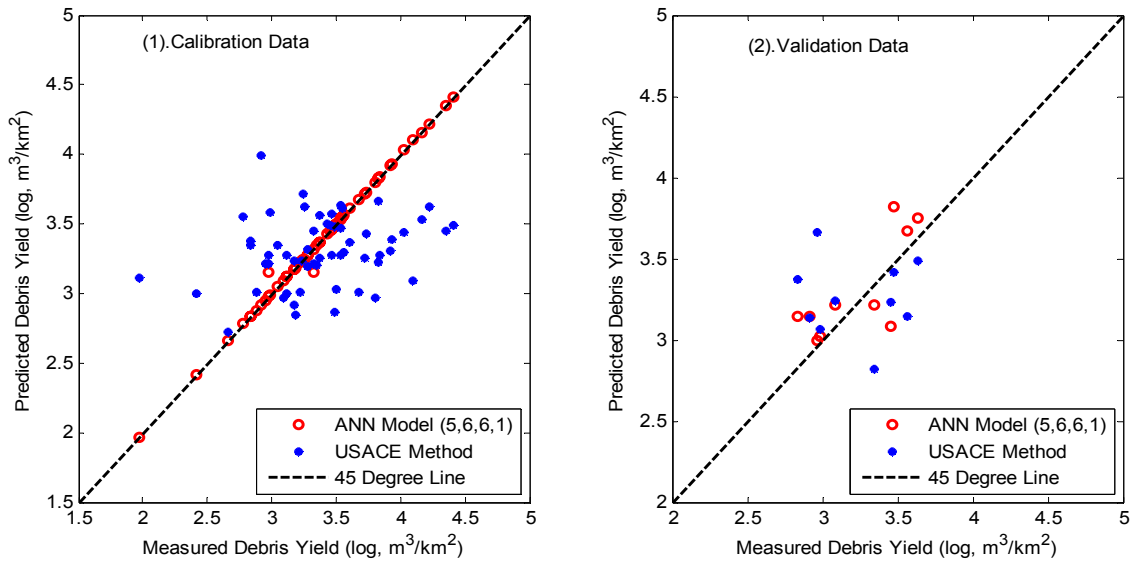


**Figure 43:** Comparison between measured USACE and the best ANN model (5,6,6,1) estimated unit debris yield for Case 8  
 (Input Parameters: Watershed Area, Relief Ratio, Max. 1-hr Rainfall Intensity, Fire Factor, Soil Erodibility Factor, Soil Permeability Rate, and Soil Liquid Limit)

#### 4.2.6 Case 9

Unit debris yield data studied in this case is collected from 20 debris basins including Beatty, Blanchard, Bluegum, Bradbury, Chamberlain, Cooks, Deer, Fieldbrook, Gordon, Haines, Halls, Laurel Ridge, May #2, Mull, Pickens, Santa Anita, Sawpit, Schoolhouse, Sierra Madre Dam, and Stetson debris basin (Figure 3). All these debris basins were built to collect debris yield from small watersheds with steep slope, from 185 m/km to 250 m/km. 71 unit debris yield data records collected between 1938 and 1983 are available for analysis. The calibration and validation data set are separated by using subtractive clustering method. 61 data records are applied for calibration and 11 data records for validation. The same preprocessing procedure aforementioned is implemented to

all the data. Similarly, there are four studied cases with Case 9. The first case is trained by four basic input variables – log transformed watershed area, logarithmic relief ratio, logarithmic value of maximum one hour precipitation times 100, and fire factor which are the exactly same as USACE (2000) included in their empirical equation (Equation 2.3). Three soil properties, SEF, SP, and SLL, are included as input variable step by step in the second, third, and fourth case to study their impact on the simulation.

#### **4.2.6.1 Case 9(a)**

For all ANN models with either one or two hidden layers developed in this case, there are four neurons in the input layer and only one neuron in the output layer representing unit debris yield. The number of hidden neurons varies from 4 to 10 for three-layered networks. For four-layered networks, twenty-two groups of different ANN geometries are evaluated and they are (3,1), (3,2), (3,3), (3,4), (3,5), (3,6), (4,1), (4,2), (4,3), (4,4), (4,5), (5,1), (5,2), (5,3), (5,4), (5,5), (6,1), (6,2), (6,3), (6,4), (6,5), and (6,6). All the networks are trained by the LM algorithm and the default values of most internal parameters are used except epoch size and the error goal for the calibration process. Transfer function is hyperbolic tangent function for all hidden layers and linear function for the output layer. Table 25 summarizes the performance of twenty-six neural networks created in this case.

There appears to be such a trend for three-layered neural networks that estimation error of the calibration data decreases and the error of the validation

**Table 25:** Summary of the performances of ANN models for Case 9(a)

ANN Geometry	Validation Data Set			Calibration Data Set			Average MSE
	Slope	R	MSE	Slope	R	MSE	
4,4,1 (25)	0.945	0.765	0.07587	0.691	0.831	0.09283	0.08435
4,5,1 (31)	0.774	0.777	0.05304	0.784	0.885	0.06506	0.05905
<b>4,6,1 (37)</b>	<b>0.641</b>	<b>0.817</b>	<b>0.06539</b>	<b>0.828</b>	<b>0.910</b>	<b>0.05177</b>	<b>0.05858</b>
4,7,1 (43)	0.727	0.743	0.07479	0.904	0.951	0.02871	0.05175
4,8,1 (49)	1.063	0.795	0.07853	0.908	0.953	0.02778	0.05316
4,9,1 (55)	0.798	0.643	0.11540	0.940	0.970	0.01793	0.06667
4,10,1 (61)	1.035	0.592	0.26597	0.997	0.998	0.00096	0.13346
4,3,1,1 (21)	0.533	0.540	0.12196	0.676	0.822	0.09752	0.10974
4,3,2,1 (26)	0.506	0.805	0.07181	0.763	0.874	0.07125	0.07153
4,3,3,1 (31)	0.734	0.757	0.05971	0.780	0.884	0.06579	0.06275
4,3,4,1 (36)	0.673	0.736	0.08227	0.794	0.891	0.06182	0.07204
4,3,5,1 (41)	0.653	0.736	0.07720	0.853	0.924	0.04370	0.06045
4,3,6,1 (46)	0.641	0.731	0.05808	0.688	0.830	0.09367	0.07587
4,4,1,1 (27)	0.873	0.759	0.09847	0.748	0.865	0.07579	0.08713
4,4,2,1 (33)	0.736	0.721	0.07297	0.797	0.893	0.06113	0.06705
4,4,3,1 (39)	0.938	0.757	0.08313	0.819	0.905	0.05441	0.06877
4,4,4,1 (45)	0.628	0.717	0.06901	0.876	0.936	0.03718	0.05310
4,4,5,1 (51)	0.283	0.418	0.11087	0.913	0.956	0.02604	0.06846
<b>4,5,1,1 (33)</b>	<b>1.001</b>	<b>0.832</b>	<b>0.06574</b>	<b>0.836</b>	<b>0.914</b>	<b>0.04935</b>	<b>0.05755</b>
4,5,2,1 (40)	1.030	0.801	0.07463	0.880	0.938	0.03599	0.05531
4,5,3,1 (47)	0.926	0.887	0.07556	0.914	0.956	0.02576	0.05066
4,5,4,1 (54)	0.512	0.711	0.05895	0.827	0.909	0.05198	0.05547
4,5,5,1 (61)	0.233	0.171	0.29139	0.977	0.988	0.00689	0.14914
4,6,1,1 (39)	0.844	0.721	0.09687	0.844	0.919	0.04697	0.07192
4,6,2,1 (47)	0.609	0.730	0.11011	0.852	0.923	0.04459	0.07735
4,6,3,1 (55)	0.420	0.625	0.07951	0.748	0.865	0.07568	0.07759
4,6,4,1 (63)	0.782	0.857	0.03204	0.703	0.839	0.08920	0.06062
4,6,5,1 (71)	0.622	0.485	0.16870	0.910	0.954	0.02699	0.09785
4,6,6,1 (79)	0.860	0.488	0.29830	1.000	1.000	0.00000	0.14915

data first decreases and then increases as more hidden neuron are included.

The network (4,6,1) provides reasonable performance for both the calibration data and the validation data among all three-layered neural networks. For the same reason, the network with five and one neuron on the first and second hidden layer is determined to be the most suitable network among the top four best-performed networks - (4,4,1,1), (4,5,1,1), (4,5,2,1) and (4,5,3,1). The two

neural network models - (4,6,1) and (4,5,1,1) achieve very similar performance. The latter one is selected to plot the estimated unit debris yield versus their actual values in Figure 44. It appears half a dozen data points scatter away from the 45 degree line in figure (a), and three data points in figure (b) do not fit in closely to the 45 degree line. The distribution of the data points suggests the simulation results obtained by the network (4,5,1,1) are acceptable for the validation data but not very desirable for the calibration data.

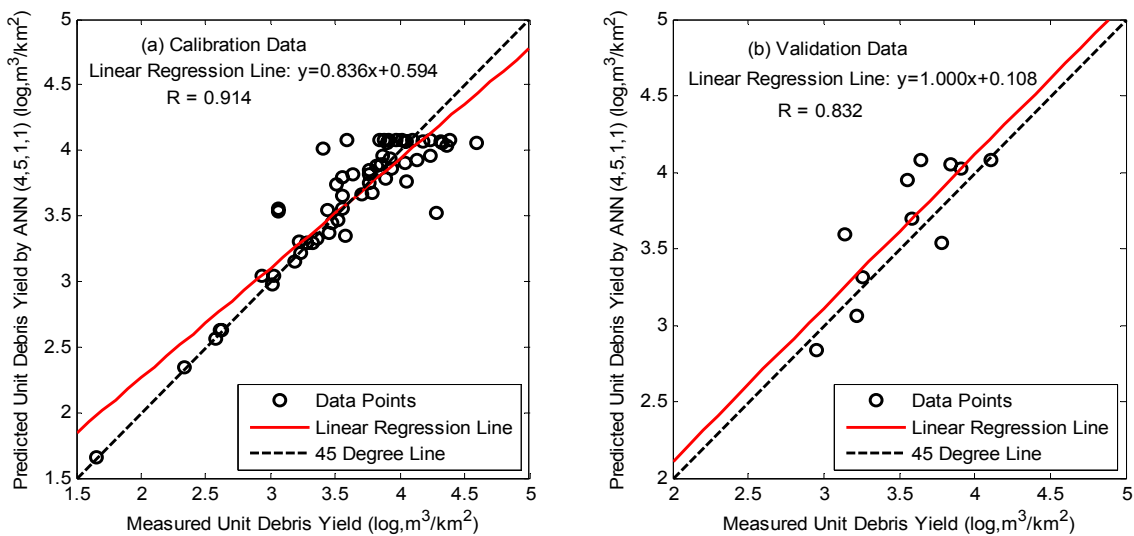


**Figure 44:** Linear regression analysis between measured and ANN model estimated debris yield (a) Calibration Data Set (b) Validation Data Set for Case 9(a) (Input Parameters: Watershed Area, Relief Ratio, Max. 1-hr Rainfall Intensit, and Fire Factor)

#### **4.2.6.2 Case 9(b)**

As shown in Figure 44, the best-performed neural network trained by four basic input variables cannot provide satisfactory results for the calibration data; therefore, SEF is included in the second case as an additional input variable to study the difference. Using the exactly same training algorithm and internal

parameters, twenty-three four-layered neural networks are calibrated by 61 data records with five input variables, and then the network with saved architecture is validated by 11 new data records. Table 26 lists the modeling results achieved by all the neural networks developed in this case.

**Table 26:** Summary of the performances of ANN models for Case 9(b)

ANN Geometry	Validation Data Set			Calibration Data Set			Average MSE
	Slope	R	MSE	Slope	R	MSE	
5,3,1,1 (24)	0.609	0.705	0.08518	0.682	0.826	0.09550	0.09034
5,3,2,1 (29)	0.518	0.718	0.05888	0.764	0.874	0.07083	0.06486
5,3,3,1 (34)	0.707	0.826	0.06230	0.795	0.892	0.06145	0.06188
5,3,4,1 (39)	0.395	0.702	0.08810	0.832	0.912	0.05059	0.06935
5,3,5,1 (44)	0.741	0.731	0.08655	0.911	0.954	0.02685	0.05670
5,3,6,1 (49)	0.809	0.810	0.07775	0.837	0.915	0.04905	0.06340
5,4,1,1 (31)	0.683	0.689	0.08909	0.836	0.914	0.04942	0.06925
5,4,2,1 (37)	0.797	0.785	0.06208	0.761	0.873	0.07173	0.06691
<b>5,4,3,1 (43)</b>	<b>0.747</b>	<b>0.780</b>	<b>0.06458</b>	<b>0.825</b>	<b>0.908</b>	<b>0.05270</b>	<b>0.05864</b>
5,4,4,1 (49)	0.759	0.629	0.11757	0.903	0.950	0.02913	0.07335
5,4,5,1 (55)	1.000	0.770	0.08973	0.794	0.891	0.06199	0.07586
5,4,5,1 (61)	1.047	0.865	0.11406	0.872	0.934	0.03853	0.07629
5,5,1,1 (38)	0.811	0.780	0.09908	0.873	0.934	0.03832	0.06870
5,5,2,1 (45)	0.625	0.742	0.05628	0.686	0.829	0.09414	0.07521
5,5,3,1 (52)	0.872	0.785	0.06183	0.796	0.892	0.06118	0.06150
5,5,4,1 (59)	1.107	0.826	0.08371	0.850	0.922	0.04518	0.06444
5,5,5,1 (66)	0.645	0.532	0.17606	0.919	0.959	0.02418	0.10012
5,6,1,1 (45)	0.686	0.633	0.09738	0.792	0.890	0.06251	0.07994
5,6,2,1 (53)	0.524	0.586	0.09306	0.798	0.893	0.06086	0.07696
5,6,3,1 (61)	0.665	0.784	0.11617	0.915	0.956	0.02559	0.07088
5,6,4,1 (69)	0.491	0.532	0.11190	0.674	0.821	0.09796	0.10493
5,6,5,1 (77)	0.404	0.445	0.14014	1.000	1.000	0.00000	0.07007
5,6,6,1 (85)	0.558	0.625	0.08117	0.730	0.855	0.08109	0.08113

As seen from table 26, it is as expected that the performance of most networks is better for the calibration data than for the validation data. The neural network (5,4,3,1) is the network with one of the lowest errors for the validation data and reasonable error for the calibration data. Although quite a few neural networks such as (5,3,5,1), (5,4,4,1), (5,5,5,1), and (5,6,5,1) are calibrated more

successfully than this network (5,4,3,1) but they are suffering from overfitting problem. In an effort to further clarify the modeling results, the linear regression results are plotted in Figure 45. In Figure 45(a), roughly ten data points scatter far away from the 45 degree line which leads to a relatively low correlation coefficient, 0.908. In Figure 45(b), only three unit debris yield are estimated accurately that explains why the correlation coefficient for the validation data is only 0.780. This network has similar performance for the calibration data as the best network (4,5,1,1) in the case (a), however, its performance for the validation data is worse. It suggests the inclusion of SEF as input parameter is not appropriate for the simulation of unit debris yield collected from small watersheds with steep slope.

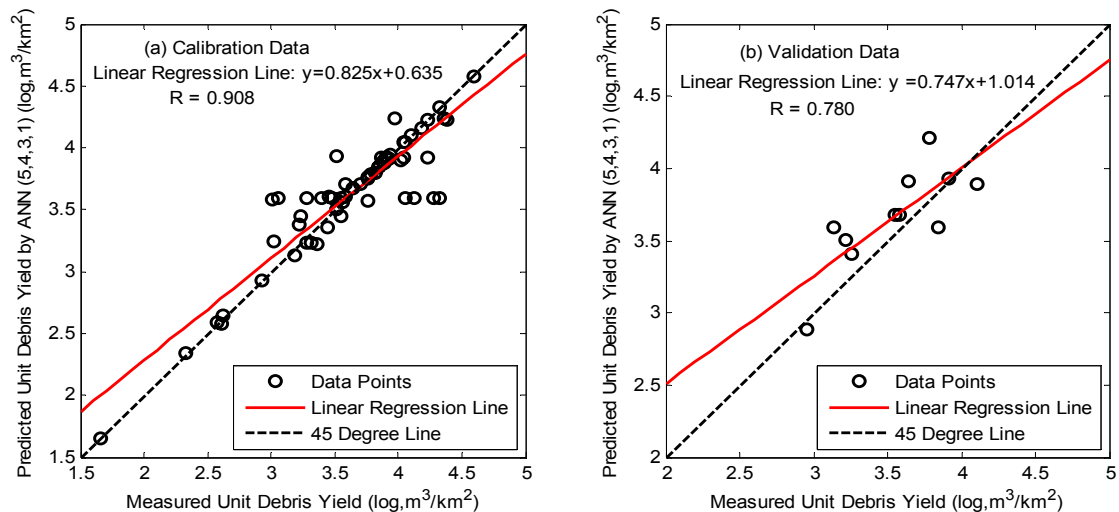


**Figure 45:** Linear regression analysis between measured and ANN model estimated debris yield (a) Calibration Data Set (b) Validation Data Set for Case 9(b) (Input Parameters: Watershed Area, Relief Ratio, Max. 1-hr Rainfall Intensity, Fire Factor, and Soil Erodibility Factor)

#### 4.2.6.3 Case 9(c)

Soil permeability rate (SP) is the new input parameter included in this case. All the four-layered neural networks have six neurons on the input layer, one neuron on the output layer, and twenty-two combinations of different numbers of hidden neurons; for example, if there are three neurons on the first hidden layer, then the number of the neuron on the second hidden layer varies from one to six; if there are either four, five or six neurons on the first hidden layer, the number of neuron on the second hidden layer is less than six. Table 27 lists the best modeling results for the twenty-two neural networks developed in this case.

**Table 27:** Summary of the performances of ANN models for Case 9(c)

ANN Geometry	Validation Data Set			Calibration Data Set			Average MSE
	Slope	R	MSE	Slope	R	MSE	
6,3,1,1 (27)	0.620	0.672	0.08833	0.770	0.878	0.06905	0.07869
6,3,2,1 (32)	0.536	0.794	0.07317	0.727	0.853	0.08202	0.07759
6,3,3,1 (37)	1.094	0.794	0.08466	0.837	0.915	0.04903	0.06684
6,3,4,1 (42)	0.756	0.840	0.09782	0.874	0.935	0.03775	0.06779
6,3,5,1 (47)	0.561	0.631	0.08223	0.779	0.883	0.06642	0.07433
6,3,6,1 (52)	0.837	0.816	0.07798	0.873	0.934	0.03819	0.05809
6,4,1,1 (35)	0.669	0.866	0.08958	0.855	0.925	0.04357	0.06658
6,4,2,1 (41)	0.529	0.605	0.09297	0.824	0.908	0.05300	0.07299
6,4,3,1 (47)	0.720	0.700	0.07690	0.699	0.836	0.09047	0.08368
6,4,4,1 (53)	0.963	0.890	0.07379	0.974	0.987	0.00801	0.04090
6,4,5,1 (59)	0.413	0.511	0.13018	0.897	0.947	0.03075	0.08046
6,5,1,1 (43)	0.513	0.596	0.11294	0.849	0.922	0.04532	0.07913
6,5,2,1 (50)	0.492	0.678	0.06721	0.748	0.865	0.07580	0.07150
6,5,3,1 (57)	1.045	0.764	0.09793	0.892	0.945	0.03233	0.06513
<b>6,5,4,1 (64)</b>	<b>1.005</b>	<b>0.838</b>	<b>0.06544</b>	<b>0.883</b>	<b>0.940</b>	<b>0.03504</b>	<b>0.05024</b>
6,5,5,1 (71)	1.098	0.760	0.11639	0.680	0.825	0.09620	0.10629
6,6,1,1 (51)	0.976	0.703	0.13975	0.749	0.865	0.07547	0.10761
6,6,2,1 (59)	0.749	0.584	0.13763	0.986	0.993	0.00429	0.07096
6,6,3,1 (67)	0.756	0.691	0.08235	0.807	0.899	0.05790	0.07012
6,6,4,1 (75)	0.339	0.287	0.20649	0.865	0.930	0.04068	0.12359
6,6,5,1 (83)	0.461	0.362	0.20292	1.000	1.000	0.00000	0.10146
6,6,6,1 (91)	0.377	0.316	0.21392	1.000	1.000	0.00000	0.10696

Although the neural network with four neurons on both hidden layers are calibrated more successfully than another neural network with five and four neurons on the first and second hidden layer, the latter network does not have overfitting problem because the MSE of the validation data MSE is on the same magnitude as the MSE of the calibration data. Another reason why the network (6,5,4,1) is chosen as the best-performed model is the validation data error is the least while the calibration data error is acceptable. The measured unit debris yield and their estimated values by the network (6,5,4,1) with the linear regression lines fitted for these data points are sketched in Figure 46. For the calibration data, the estimation of seven data records is out of line; for the validation data, the simulation of three data records is under expectation. The correlation coefficients are 0.940 and 0.838 for the calibration and validation

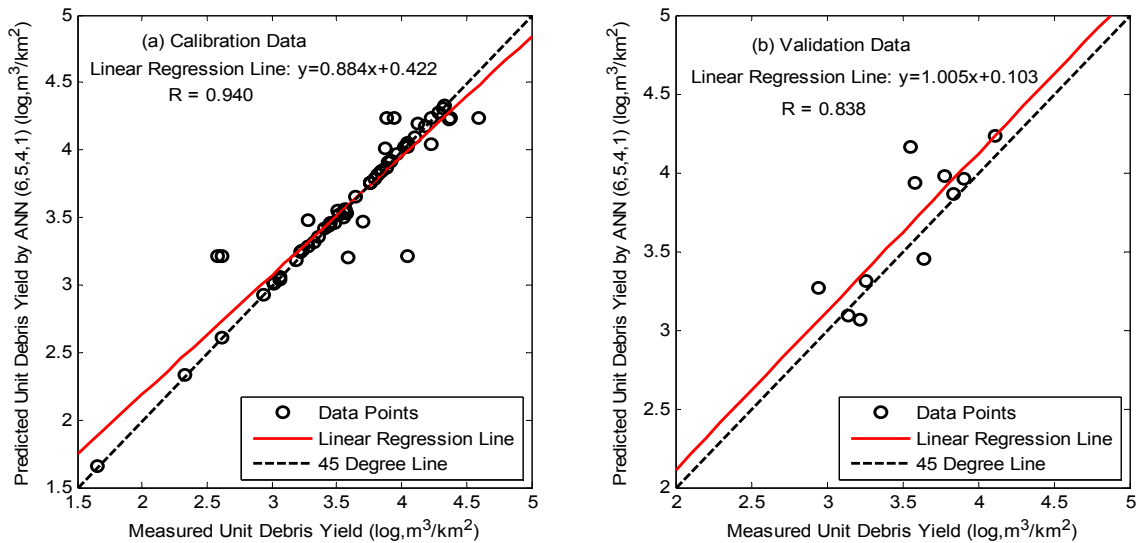


**Figure 46:** Linear regression analysis between measured and ANN model estimated debris yield (a) Calibration Data Set (b) Validation Data Set for Case 9(c) (Input Parameters: Watershed Area, Relief Ratio, Max. 1-hr Rainfall Intensity, Fire Factor, Soil Erodibility Factor, and Soil Permeability Rate )

data, respectively. Although the MSE for the validation data is very similar to that obtained by the network (5,4,3,1) in the preceding case, this neural network (6,5,4,1) is able to estimate 59 calibration data with a lower error and a higher correlation coefficient. It indicates the inclusion of SP enhances the simulation accuracy, in other words, SP is an important input variable in this case.

#### **4.2.6.4 Case 9(d)**

SLL is considered as the seventh input variable in this case. The variation of the number of neuron on hidden layers for the twenty-two ANN models with two hidden layers, the calibration and the validation data, training algorithm, and internal parameter are the same as those used in the Case 9(a), (b), and (c). The best performance obtained by each neural network is presented in Table 28. It appears two networks - (7,4,5,1) and (7,5,2,1) are calibrated very successfully especially the former one with the MSE as low as 0.01434, the validation results are very similar by using either neural network. The latter model (7,5,2,1) appears to more accurate with a lower error and a higher correlation coefficient.

**Table 28:** Summary of the performances of ANN models for Case 9(d)

ANN Geometry	Validation Data Set			Calibration Data Set			Average MSE
	Slope	R	MSE	Slope	R	MSE	
7,3,1,1 (30)	0.551	0.584	0.09413	0.708	0.841	0.08789	0.09101
7,3,2,1 (35)	0.770	0.686	0.08776	0.674	0.821	0.09814	0.09295
7,3,3,1 (40)	0.675	0.687	0.07355	0.810	0.900	0.05725	0.06540
7,3,4,1 (45)	0.814	0.781	0.09995	0.739	0.860	0.07843	0.08919
7,3,5,1 (50)	0.437	0.705	0.07446	0.870	0.933	0.03902	0.05674
7,3,6,1 (55)	0.245	0.419	0.11917	0.840	0.917	0.04767	0.08342
7,4,1,1 (39)	0.585	0.684	0.08821	0.852	0.923	0.04457	0.06639
7,4,2,1 (45)	0.501	0.575	0.09106	0.734	0.857	0.07986	0.08546
7,4,3,1 (51)	0.757	0.825	0.08011	0.791	0.889	0.06280	0.07146
7,4,4,1 (57)	0.628	0.576	0.12108	0.782	0.885	0.06541	0.09325

**Table 28.** Continued

ANN Geometry	Validation Data Set			Calibration Data Set			Average MSE
	Slope	R	MSE	Slope	R	MSE	
7,4,5,1 (63)	0.737	0.792	0.06293	0.952	0.976	0.01434	0.03863
7,5,1,1 (48)	0.756	0.644	0.11408	0.802	0.895	0.05960	0.08684
<b>7,5,2,1 (55)</b>	<b>0.544</b>	<b>0.812</b>	<b>0.05903</b>	<b>0.898</b>	<b>0.948</b>	<b>0.03055</b>	<b>0.04479</b>
7,5,3,1 (62)	0.856	0.803	0.06906	0.738	0.859	0.07876	0.07391
7,5,4,1 (69)	0.887	0.705	0.10282	0.757	0.870	0.07291	0.08787
7,5,5,1 (76)	0.455	0.347	0.21687	1.000	1.000	0.00000	0.10844
7,6,1,1 (57)	0.914	0.676	0.11956	0.933	0.966	0.02011	0.06984
7,6,2,1 (65)	0.866	0.760	0.10254	0.765	0.875	0.07071	0.08663
7,6,3,1 (73)	0.328	0.490	0.12624	0.738	0.859	0.07863	0.10243
7,6,4,1 (81)	0.492	0.471	0.14012	0.851	0.923	0.04475	0.09244
7,6,5,1 (89)	0.419	0.396	0.22456	1.000	1.000	0.00000	0.11228
7,6,6,1 (97)	0.426	0.544	0.15778	0.684	0.827	0.09504	0.12641

The measured values of 61 unit debris yield against their estimated values by the neural network (7,5,2,1) are plotted in Figure 47(a) and (b) is for 11 validation data. The distribution of the data points in Figure 47(a) indicates the network overestimates five unit debris yield data records and underestimates four unit debris yield data records. As a result, the correlation coefficient for the calibration data is 0.948. In Figure 47(b), 11 validation data points scatter around the 45 degree line, some are close to the line and some are a bit far; the correlation coefficient is 0.812. The performance for both the calibration and validation provided by this network is better than it of the network (6,5,4,1) in the case (c). It leads to such a conclusion that SLL is an important input variable for modeling unit debris yield at small watershed with steep slope.

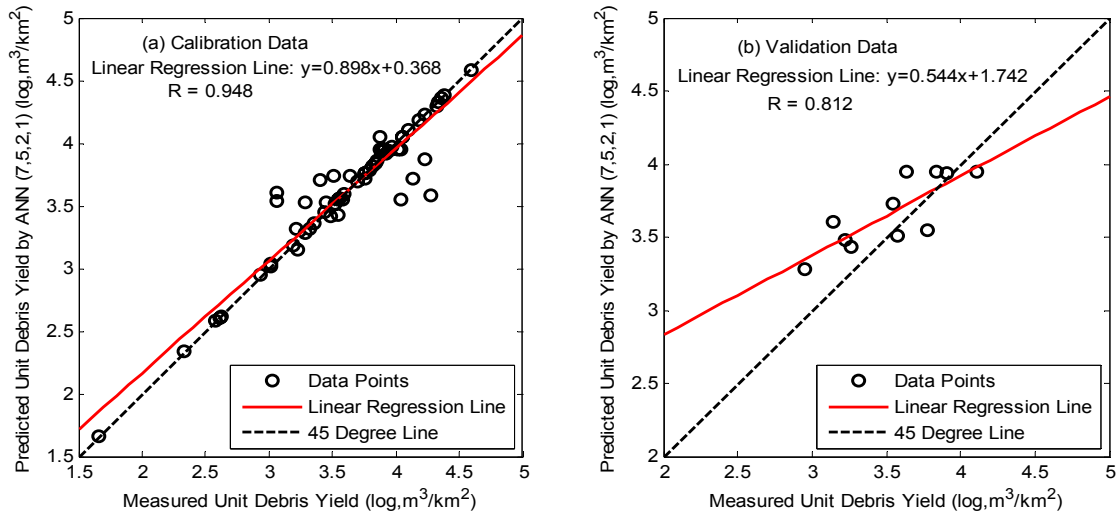


**Figure 47:** Linear regression analysis between measured and ANN model estimated debris yield (a) Calibration Data Set (b) Validation Data Set for Case 9(d) (Input Parameters: Watershed Area, Relief Ratio, Max. 1-hr Rainfall Intensity, Fire Factor, Soil Erodibility Factor, Soil Permeability Rate, and Soil Liquid Limit)

Table 29 itemizes all the best-performed neural network models from Case 9(a) to 9(d), and they are compared to the USACE method as well. It seems that there is no significant difference in the performance among all the neural network models, especially for the validation data. The first two ANN models have very similar performance, and the third and fourth neural networks are better-performed than the first two models. With the lowest errors for both data sets, the network (7,5,2,1) is chosen as the most suitable neural network model for Case 9. Since the major difference between each case is different number of input variable, the performance comparison among all cases leads to such a conclusion that SP and SLL are more important than SEF for the estimation of unit debris yield collected from small watersheds with steep slope.

**Table 29:** Comparison of ANN models performance for Case 9

Case Number	Network Geometry	Validation Data Set			Calibration Data set			Average MSE
		Slope	R	MSE	Slope	R	MSE	
9(a)	(4,5,1,1)	1.001	0.832	0.06574	0.836	0.914	0.04935	0.05755
9(b)	(5,4,3,1)	0.747	0.780	0.06458	0.825	0.908	0.05270	0.05864
9(c)	(6,5,4,1)	1.005	0.838	0.06544	0.883	0.940	0.03504	0.05024
<b>9(d)</b>	<b>(7,5,2,1)</b>	<b>0.544</b>	<b>0.812</b>	<b>0.05903</b>	<b>0.898</b>	<b>0.948</b>	<b>0.03055</b>	<b>0.04479</b>
USACE		0.404	0.677	0.06543	0.132	0.300	0.28514	0.17528

The first three neural networks and the USACE method achieve very similar performance for the validation data, however, the error for the calibration data is much less by using the neural network models. The fourth network (7,5,2,1) is more accurate than the USACE method not only for modeling the calibration data but also for modeling the validation data. The measured values of unit debris yield are presented together with their estimated values by the neural network (7,5,2,1) and the USACE method in Table 30. As seen from the table, the USACE method is able to estimate 61 unit debris yield within such an error range, [-0.94, 1.67] for the calibration data, and [-0.44, 0.49] for the validation data. The neural network (7,5,2,1) reduces the error range to [-0.70, 0.54] for the calibration data and [-0.23, 0.47] for the validation data. The results are plotted in Figure 48; red circles represent ANN model results and blue marks are for the USACE method estimations. In the left figure, the red circles gather very close to the 45 degree line while the blue marks scatter in the upper part of the figure. Those two methods are not at all comparable in terms of modeling accuracy for the calibration data. In the right figure, some neural network results

are better than the USACE method and some are worse; as aforementioned, the neural network (7,5,2,1) estimates 11 unit debris yield data records with a smaller error range.

**Table 30:** Measured, the USACE method, and the best ANN model (7,5,2,1) estimated unit debris yield for Case 9

Data	Debris Basin	Area (log, ha)	Rr (log, m/km)	Measured Unit Dy (log, m <sup>3</sup> /km <sup>2</sup> )	USACE Estimated Unit Dy (log, m <sup>3</sup> /km <sup>2</sup> )	Diffe <sup>1</sup>	ANN Estimated Unit Dy (log, m <sup>3</sup> /km <sup>2</sup> )	Diffe <sup>2</sup>
Calibration Data	Beatty	1.85	2.34	3.92	<b>2.97</b>	<b>-0.95</b>	3.92	0.00
	Blanchard	2.12	2.38	3.76	3.46	-0.30	3.72	-0.04
		2.12	2.38	4.02	3.93	-0.09	3.95	-0.07
		2.12	2.38	3.28	3.45	0.17	3.28	0.00
	Bluegum	1.69	2.37	4.23	3.86	-0.37	4.23	0.00
		1.69	2.37	3.22	3.39	0.17	3.31	0.09
		1.69	2.37	3.55	3.37	-0.18	3.42	-0.13
		1.69	2.37	4.1	3.69	-0.41	4.10	0.00
	Bradbury	2.25	2.39	3.48	3.52	0.04	3.42	-0.06
		2.25	2.39	3.45	3.60	0.15	3.53	0.08
		2.25	2.39	3.87	3.65	-0.22	4.05	0.18
		2.25	2.39	4.23	3.64	-0.59	3.88	-0.35
		2.25	2.39	4.13	3.52	-0.61	3.71	-0.42
	Chamberlain	1.02	2.32	3.36	3.13	-0.23	3.36	0.00
	Cooks	2.18	2.38	3.64	3.52	-0.12	3.74	0.10
		2.18	2.38	3.51	3.58	0.07	3.74	0.23
		2.18	2.38	3.06	3.37	0.31	<b>3.60</b>	<b>0.54</b>
		2.18	2.38	3.9	3.71	-0.19	3.95	0.05
		2.18	2.38	3.91	3.76	-0.15	3.95	0.04
	Deer	2.19	2.39	4.05	3.42	-0.63	4.05	0.00
		2.19	2.39	4.18	3.60	-0.58	4.18	0.00
		2.19	2.39	3.82	3.65	-0.17	3.82	0.00
		2.19	2.39	3.52	4.20	0.68	3.52	0.00
	Fieldbrook	1.96	2.31	2.62	3.36	0.74	2.62	0.00
		1.96	2.31	2.58	3.30	0.72	2.58	0.00
	Gordon	1.67	2.34	3.02	3.51	0.49	3.02	0.00
		1.67	2.34	1.66	<b>3.33</b>	<b>1.67</b>	1.66	0.00
	Halls	2.31	2.35	3.58	3.32	-0.26	3.55	-0.03
2.31		2.35	3.28	3.43	0.15	3.52	0.24	
2.31		2.35	3.06	3.38	0.32	3.54	0.48	
2.31		2.35	4.04	3.67	-0.37	3.95	-0.09	

**Table 30, Continued**

Data	Debris Basin	Area (log, ha)	Rr (log, m/km)	Measured Unit Dy (log, m <sup>3</sup> /km <sup>2</sup> )	USACE Estimated Unit Dy (log, m <sup>3</sup> /km <sup>2</sup> )	Diffe <sup>1</sup>	ANN Estimated Unit Dy (log, m <sup>3</sup> /km <sup>2</sup> )	Diffe <sup>2</sup>
Calibration Data	Halls	2.31	2.35	3.89	3.59	-0.30	3.93	0.04
		2.31	2.35	4.28	3.42	-0.86	<b>3.58</b>	<b>-0.70</b>
		2.31	2.35	4.59	3.68	-0.91	4.59	0.00
	Laurel Ridge	0.89	2.3	3.76	3.29	-0.47	3.76	0.00
	May #2	1.37	2.32	3.44	3.35	-0.09	3.45	0.01
		1.37	2.32	3.79	3.40	-0.39	3.78	-0.01
		1.37	2.32	3.97	3.50	-0.47	3.97	0.00
		1.37	2.32	4.05	3.11	-0.94	4.05	0.00
	Mull	1.59	2.38	3.32	3.52	0.20	3.32	0.00
	Pickens	2.6	2.29	3.84	3.58	-0.26	3.84	0.00
		2.6	2.29	2.93	3.36	0.43	2.95	0.02
		2.6	2.29	4.38	3.72	-0.66	4.38	0.00
		2.6	2.29	3.94	3.53	-0.41	3.94	0.00
	Sawpit	2.86	2.36	3.55	3.73	0.18	3.55	0.00
		2.86	2.36	4.32	3.73	-0.59	4.30	-0.02
		2.86	2.36	3.01	3.76	0.75	3.04	0.03
	School-house	1.86	2.36	3.59	3.74	0.15	3.59	0.00
		1.86	2.36	3.23	3.35	0.12	3.15	-0.08
		1.86	2.36	4.36	3.68	-0.68	4.36	0.00
	Santa Anita	2.65	2.28	3.56	3.69	0.13	3.56	0.00
		2.65	2.28	4.33	3.56	-0.77	4.33	0.00
		2.65	2.28	3.7	3.24	-0.46	3.70	0.00
		2.65	2.28	3.76	4.24	0.48	3.76	0.00
	Sierra Madre Dam	2.79	2.35	3.4	3.64	0.24	3.70	0.30
		2.79	2.35	2.33	3.25	0.92	2.33	0.00
		2.79	2.35	4.04	3.48	-0.56	3.55	-0.49
		2.79	2.35	2.61	3.84	1.23	2.61	0.00
		2.79	2.35	3.85	3.95	0.10	3.86	0.01
	Stetson	1.88	2.35	3.19	3.23	0.04	3.18	-0.01
	Validation Data	Bradbury	2.25	2.39	3.55	3.56	0.01	3.73
2.25			2.39	3.64	3.82	0.18	3.94	0.30
Cooks		2.18	2.38	4.11	3.98	-0.13	3.95	-0.16
Deer		2.19	2.39	3.84	<b>3.40</b>	<b>-0.44</b>	3.95	0.11
Haines		2.6	2.32	3.78	3.51	-0.27	<b>3.55</b>	<b>-0.23</b>
Halls		2.31	2.35	3.14	3.42	0.28	<b>3.61</b>	<b>0.47</b>
		2.31	2.35	3.91	3.64	-0.27	3.94	0.03
May #2		1.37	2.32	3.26	3.33	0.07	3.44	0.18
Pickens	2.6	2.29	2.95	<b>3.44</b>	<b>0.49</b>	3.29	0.34	

**Table 30, Continued**

Data	Debris Basin	Area (log, ha)	Rr (log, m/km)	Measured Unit Dy (log, m <sup>3</sup> /km <sup>2</sup> )	USACE Estimated Unit Dy (log, m <sup>3</sup> /km <sup>2</sup> )	Diffe <sup>1</sup>	ANN Estimated Unit Dy (log, m <sup>3</sup> /km <sup>2</sup> )	Diffe <sup>2</sup>
Validation Data	Sawpit	2.86	2.36	3.58	3.53	-0.05	3.51	-0.07
	School-house	1.86	2.36	3.22	3.24	0.02	3.48	0.26

Diffe<sup>1</sup> - Difference between measured debris yield and the estimated values using the USACE method.

Diffe<sup>2</sup> - Difference between measured debris yield and the estimated values using ANN model.

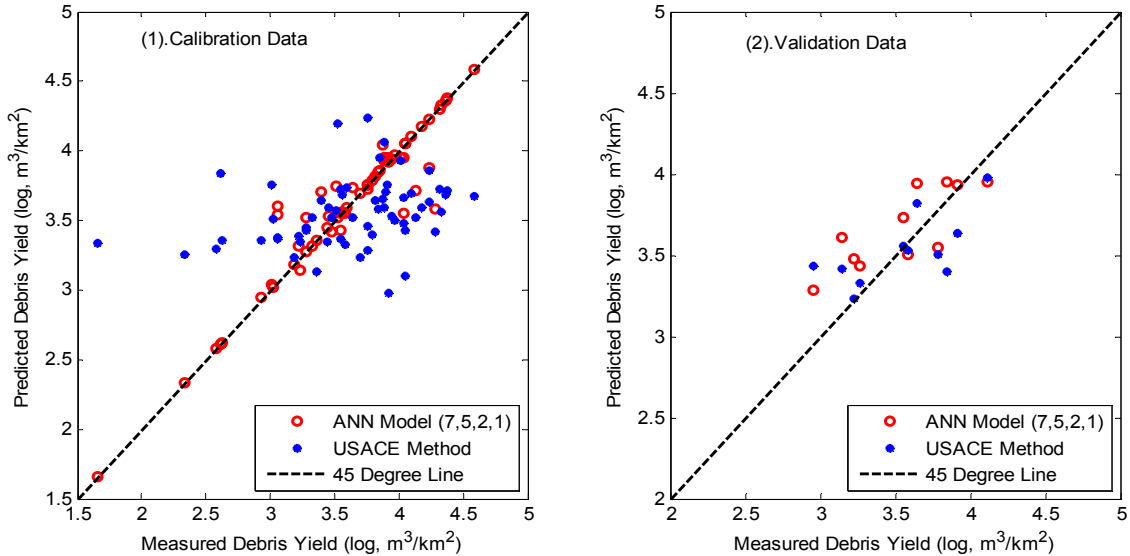


**Figure 48:** Comparison between measured, USACE, and the best ANN model (7,5,2,1) estimated unit debris yield for Case 9

(Input Parameters: Watershed Area, Relief Ratio, Max. 1-hr Rainfall Intensity, Fire Factor, Soil Erodibility Factor, Soil Permeability Rate, and Soil Liquid Limit)

#### 4.2.7 Case 10

Unit debris yield studied in this case was collected from fourteen debris basins including Brace, Brand, Dunsmuir, Engelwild, Fern, May #1, Morgan, Mullally, Rubio, Sierra Madre Villa, Snover, West Ravine, Winery, and Zachau debris basin (Figure 3). The upstream watershed area of these debris basins are less than 3 square miles and the watersheds slope is steeper (between 250 m/km and 305 m/km). Separated by subtractive clustering method, 55 unit debris

yield data records resulting from large storm events from 1938 and 1983 are used to calibrate the neural networks and the other 12 data records for validation. The first case is trained by four basic input variables -  $\log A$ ,  $\log R_r$ ,  $\log(I)$ , and  $F$  all of which are the exactly same as the USACE (2000) used in their empirical equation. Three newly developed soil properties such as SER, SP, and SLL, are considered as additional input variable in case (b), (c), and (d), respectively.

#### **4.2.7.1 Case 10(a)**

Trained by four input variables, six three-layered neural networks with four to nine neurons on the hidden layer are trained. Twenty-one four-layered networks are generated and their geometries are summarized as follows, if there are two neurons on the first hidden layer, the number of neuron on the second hidden layer might be from one to six; if the number of neuron on the first hidden layer is three, four, or five, the possible numbers of neuron on the second hidden layer are from one to five. All these networks are trained by the LM algorithm with hyperbolic tangent function as the transfer function for the hidden layers and linear function for the output layer.

Most three-layered neural networks suffer from overfitting problem (Table 31); for example, the validation data error of the last four three-layered networks is at least eight times greater than that of the calibration data. With a lower average MSE and relatively reasonable performance for the calibration and validation data, the network with five neurons on the hidden layer is superior to the remaining three-layered networks. However, the error of the validation data

achieved by this network (4,5,1) is considerable and it suggests this network is also overtrained. The performance of most of the four-layered neural networks is very similar to those of the three-layered neural networks except four of them - (4,3,3,1), (4,3,4,1), (4,3,5,1), (4,4,4,1). The ANN model (4,3,3,1) is selected to be the best-fit model since it has the lowest error for the validation data and acceptable error for the calibration data.

**Table 31:** Summary of the performances of ANN models for Case 10(a)

ANN Geometry	Validation Data Set			Calibration Data Set			Average MSE
	Slope	R	MSE	Slope	R	MSE	
4,4,1 (25)	0.523	0.598	0.18138	0.788	0.887	0.05258	0.11698
<b>4,5,1 (31)</b>	<b>0.673</b>	<b>0.659</b>	<b>0.17712</b>	<b>0.817</b>	<b>0.904</b>	<b>0.04531</b>	<b>0.11121</b>
4,6,1 (37)	0.412	0.527	0.19857	0.906	0.952	0.02321	0.11089
4,7,1 (43)	0.729	0.611	0.25526	0.878	0.937	0.03032	0.14279
4,8,1 (49)	0.743	0.601	0.26693	0.961	0.980	0.00972	0.13832
4,9,1 (55)	0.658	0.476	0.41372	0.990	0.995	0.00236	0.20804
4,2,1,1 (15)	0.371	0.6465	0.15724	0.386	0.622	0.15190	0.15457
4,2,2,1 (19)	0.564	0.808	0.09057	0.379	0.615	0.15384	0.12220
4,2,3,1 (23)	0.327	0.777	0.15641	0.520	0.721	0.11884	0.13762
4,2,4,1 (27)	0.641	0.686	0.15214	0.624	0.790	0.09314	0.12264
4,2,5,1 (31)	0.701	0.732	0.13155	0.632	0.795	0.09114	0.11134
4,2,6,1 (35)	0.791	0.727	0.17388	0.707	0.841	0.07264	0.12326
4,3,1,1 (21)	0.502	0.781	0.10627	0.433	0.658	0.14038	0.12332
4,3,2,1 (26)	0.621	0.743	0.11600	0.645	0.803	0.08797	0.10198
<b>4,3,3,1 (31)</b>	<b>0.663</b>	<b>0.831</b>	<b>0.08199</b>	<b>0.698</b>	<b>0.836</b>	<b>0.07474</b>	<b>0.07836</b>
4,3,4,1 (36)	0.653	0.738	0.12238	0.789	0.888	0.05226	0.08732
4,3,5,1 (41)	0.706	0.769	0.13598	0.924	0.961	0.01883	0.07740
4,4,1,1 (27)	0.594	0.763	0.13422	0.776	0.881	0.05546	0.09484
4,4,2,1 (33)	0.715	0.740	0.13450	0.666	0.816	0.08253	0.10851
4,4,3,1 (39)	0.784	0.737	0.14371	0.695	0.834	0.07542	0.10956
4,4,4,1 (45)	0.978	0.855	0.12662	0.879	0.938	0.02989	0.07826
4,4,5,1 (51)	0.729	0.558	0.33616	0.946	0.973	0.01333	0.17475
4,5,1,1 (33)	0.715	0.782	0.11506	0.617	0.786	0.09478	0.10492
4,5,2,1 (40)	0.585	0.629	0.17713	0.892	0.944	0.02683	0.10198
4,5,3,1 (47)	0.476	0.538	0.26901	0.984	0.992	0.00399	0.13650
4,5,4,1 (54)	0.229	0.320	0.27620	0.913	0.956	0.02154	0.14887
4,5,5,1 (61)	0.516	0.524	0.24792	0.908	0.953	0.02282	0.13537

The measured unit debris yield versus their estimated values by the neural network (4,3,3,1) is plotted in Figure 49. As illustrated in Figure 49(a), this ANN model appears to fail to predict some unit debris yield data that results in a very low correlation coefficient, 0.836, and a relatively high MSE, 0.07474. In figure (b), it can be found that this neural network estimates three validation data records very poorly although the remaining unit debris yield data is simulated well. It seems that this network provides the same level of performance for the calibration and the validation data sets with similar correlation coefficients and similar MSE. The reason why there are only eleven points shown in the figure (b) is because two points with the same measured and estimated values are overlapped. Overall speaking the performance of the network (4,3,3,1) is not satisfactory.

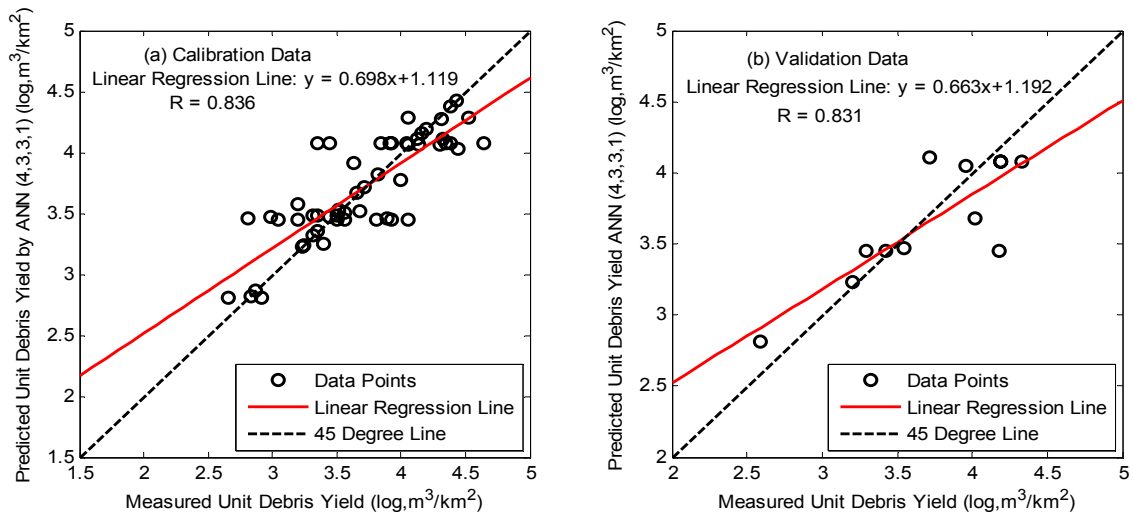


**Figure 49:** Linear regression analysis between measured and ANN model estimated debris yield (a) Calibration Data Set (b) Validation Data Set for Case 10(a) (Input Parameters: Watershed Area, Relief Ratio, Max. 1-hr Rainfall Intensity, and Fire Factor)

#### **4.2.7.2 Case 10(b)**

In addition to the four basic input variables, this case includes one more input variable - SEF. Twenty-two four-layered neural networks are trained to estimate the unit debris yield and their geometries and best modeling results are provided in Table 32. The neural network (5,4,1,1) achieves the lowest error (i.e. 0.06540) for the validation data, and it also provides good performance in terms of the calibration data (with a MSE of 0.03862). Although another neural network (5,5,2,1) appears to have a similar performance as then neural network (5,4,1,1), it is considered to be worse due to a slightly greater error for the validation data and a lower correlation coefficient.

**Table 32:** Summary of the performances of ANN models for Case 10(b)

ANN Geometry	Validation Data Set			Calibration Data Set			Average MSE
	Slope	R	MSE	Slope	R	MSE	
5,3,1,1 (24)	0.584	0.806	0.09736	0.598	0.773	0.09944	0.09204
5,3,2,1 (29)	0.597	0.880	0.07032	0.623	0.789	0.09341	0.08187
5,3,3,1 (34)	0.595	0.829	0.08638	0.621	0.788	0.09375	0.09006
5,3,4,1 (39)	0.909	0.789	0.12862	0.694	0.833	0.07573	0.10217
5,3,5,1 (44)	0.964	0.833	0.10898	0.832	0.912	0.04154	0.07526
5,3,6,1 (49)	0.687	0.725	0.13500	0.924	0.961	0.01876	0.07688
<b>5,4,1,1 (31)</b>	<b>0.891</b>	<b>0.893</b>	<b>0.06540</b>	<b>0.844</b>	<b>0.919</b>	<b>0.03862</b>	<b>0.05201</b>
5,4,2,1 (37)	0.841	0.809	0.10827	0.770	0.878	0.05689	0.08258
5,4,3,1 (43)	1.143	0.900	0.08795	0.862	0.928	0.03420	0.06108
5,4,4,1 (49)	0.572	0.779	0.11067	0.899	0.948	0.02496	0.06782
5,4,5,1 (55)	0.548	0.698	0.13137	0.602	0.776	0.09856	0.11496
5,5,1,1 (38)	0.772	0.858	0.09519	0.783	0.885	0.05379	0.07449
5,5,2,1 (45)	0.979	0.869	0.08035	0.902	0.950	0.02421	0.05228
5,5,3,1 (52)	0.517	0.673	0.14449	0.704	0.839	0.07320	0.10885
5,5,4,1 (59)	0.604	0.772	0.10914	0.613	0.783	0.09574	0.10244
5,5,5,1 (66)	0.511	0.517	0.24391	1.000	1.000	0.00000	0.12196
5,6,1,1 (45)	0.978	0.873	0.08785	0.835	0.914	0.04082	0.10244
5,6,2,1 (53)	0.642	0.784	0.10116	0.617	0.786	0.09470	0.09793
5,6,3,1 (61)	0.650	0.859	0.06975	0.772	0.879	0.05637	0.06306
5,6,4,1 (69)	1.019	0.873	0.09334	1.000	1.000	1.6E-09	0.04667
5,6,5,1 (77)	0.594	0.597	0.21362	1.000	1.000	2.3E-07	0.10681
5,6,6,1 (85)	0.697	0.784	0.10064	1.000	1.000	2.5E-07	0.05032

In Figure 50(a) for the calibration data, it shows the network (5,4,1,1) is able to predict most unit debris yield accurately but fail for a few data points which leads to a fair correlation coefficient – 0.919. However, with a relatively high correlation coefficient and the smallest error, this network is the best for modeling the validation data compared with the other neural networks. The error of the calibration data achieved by the network (5,4,1,1) is almost half of that obtained by the network (4,3,3,1) in the previous case and the error of the validation data error is also smaller than that of the network (4,3,3,1). The comparison between Table 31 and Table 32 shows that most neural networks trained in this case perform much better than the neural networks in case (a). All these signs indicate an improvement in the modeling accuracy due to the inclusion of SEF as an input parameter.

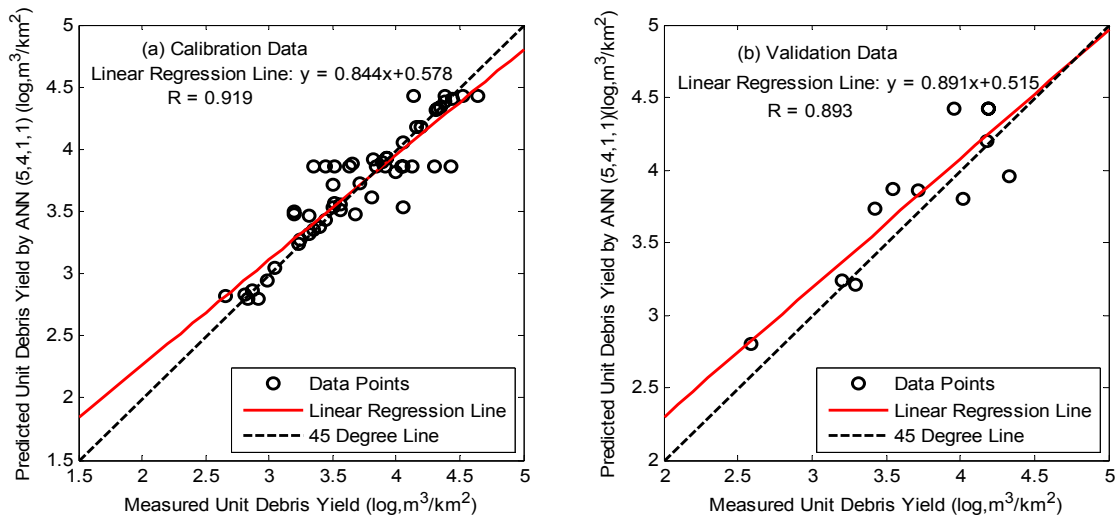


**Figure 50:** Linear regression analysis between measured and ANN model estimated debris yield (a) Calibration Data Set (b) Validation Data Set for Case 10(b) (Input Parameters: Watershed Area, Relief Ratio, Max. 1-hr Rainfall Intensity, Fire Factor, and Soil Erodibility Factor)

### 4.2.7.3 Case 10(c)

Twenty-two neural networks with no more than two hidden layers are trained in this case to estimate 67 unit debris yield based on six input parameters among which only the SP is the new parameter as compared with the previous case. As shown in Table 33, all these neural networks are calibrated very successfully with MSE less than 0.1 and some are even less than  $10^{-6}$ . Although the network (6,3,2,1) is not the one with the least MSE of the calibration data, it is the best-performed model when considering the performance for the validation data as well, in other words, it is the only ANN model without overfitting problem.

**Table 33:** Summary of the performances of ANN models for Case 10(c)

ANN Geometry	Validation Data Set			Calibration Data Set			Average MSE
	Slope	R	MSE	Slope	R	MSE	
6,3,1,1 (27)	0.773	0.837	0.08659	0.665	0.815	0.08300	0.08479
<b>6,3,2,1 (32)</b>	<b>0.743</b>	<b>0.857</b>	<b>0.06688</b>	<b>0.736</b>	<b>0.858</b>	<b>0.06525</b>	<b>0.06607</b>
6,3,3,1 (37)	0.795	0.826	0.09180	0.785	0.886	0.05317	0.07248
6,3,4,1 (42)	0.593	0.774	0.10151	0.739	0.860	0.06457	0.08304
6,3,5,1 (47)	0.814	0.837	0.08113	0.957	0.978	0.01075	0.04594
6,3,6,1 (52)	0.747	0.715	0.15584	0.942	0.971	0.01439	0.08511
6,4,1,1 (35)	0.747	0.812	0.09763	0.755	0.869	0.06068	0.07915
6,4,2,1 (41)	0.703	0.806	0.08922	0.674	0.821	0.08058	0.08490
6,4,3,1 (47)	0.897	0.847	0.09932	0.928	0.964	0.01771	0.05852
6,4,4,1 (53)	0.642	0.768	0.13466	0.905	0.951	0.02350	0.07908
6,4,5,1 (59)	0.741	0.656	0.22076	0.921	0.960	0.01939	0.12007
6,5,1,1 (43)	0.911	0.831	0.10470	0.916	0.957	0.02079	0.06275
6,5,2,1 (50)	0.760	0.808	0.09373	0.794	0.891	0.05103	0.07238
6,5,3,1 (57)	0.740	0.821	0.09751	0.900	0.949	0.02468	0.06110
6,5,4,1 (64)	0.378	0.455	0.23589	0.887	0.942	0.02792	0.13190
6,5,5,1 (71)	0.819	0.801	0.11580	1.000	1.000	2.5E-07	0.05790
6,6,1,1 (51)	1.230	0.895	0.10834	0.919	0.959	0.02006	0.06420
6,6,2,1 (59)	0.878	0.796	0.11585	0.794	0.891	0.05095	0.08340
6,6,3,1 (67)	0.865	0.896	0.07082	0.797	0.893	0.05033	0.06058
6,6,4,1 (75)	0.662	0.770	0.10486	0.951	0.975	0.01206	0.05846
6,6,5,1 (83)	0.260	0.252	0.48762	0.822	0.907	0.04407	0.26585
6,6,6,1 (91)	0.723	0.814	0.13402	1.000	1.000	1.1E-08	0.06701

The measured debris yield and the estimated values by the neural network (6,3,2,1) are plotted in Figure 51. As seen from Figure (a), four data records are seriously overestimated and six are underestimated by this neural network model (6,3,2,1) that results in a relatively high error – 0.06525 and a lower correlation coefficient – 0.858. All of signs indicate the neural network performance is not satisfactory for the calibration data. However, this neural network (6,3,2,1) is capable of estimating 12 unit debris yield never “seen” as well as the 55 unit debris yield for calibration. As shown in Figure 51(b), most of data points scatter closely to the 45 degree line and three data points stay on the line, and the correlation coefficient is 0.857. Overall considering its performance for the calibration and the validation data, this network is hardly a satisfactory model to estimate the unit debris yield collected from small watershed with steeper slope.

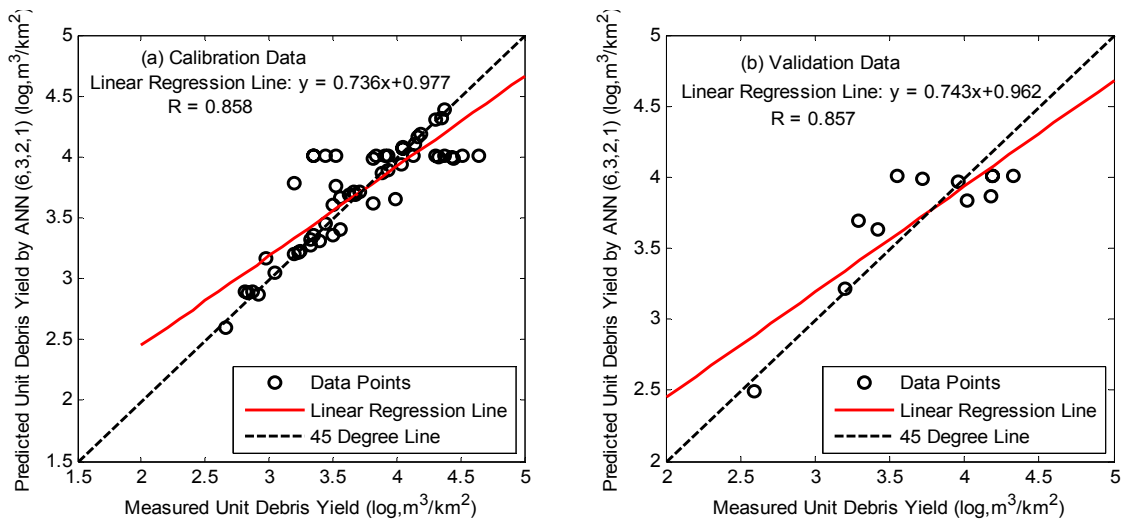


**Figure 51:** Linear regression analysis between measured and ANN model estimated debris yield (a) Calibration Data Set (b) Validation Data Set for Case 10(c) (Input Parameters: Watershed Area, Relief Ratio, Max. 1-hr Rainfall Intensity, Fire Factor, Soil Erodibility Factor, and Soil Permeability Rate)

#### **4.2.7.4 Case 10(d)**

With one more input variable, SLL, the ANN models in this case are trained by seven input parameters. The number of neurons on the hidden layers is the same as in the previous case, in other words, twenty-two ANN models with two hidden layers are trained and tested for estimating unit debris yield collected from small watersheds with steeper slope. As shown in Table 34, the neural network (7,5,3,1) acquires the lowest MSE for the validation data (i.e. 0.05385) and relatively small error for the calibration data (i.e. 0.03045). Most neural networks with more effective parameters than the network (7,5,3,1) have much smaller error for the calibration data but the error for the validation data is enormous. It suggests 62 connection weights and biases, or effective parameters included in the network (7,5,3,1) are enough for the simulation.

**Table 34:** Summary of the performances of ANN models for Case 10(d)

ANN Geometry	Validation Data Set			Calibration Data Set			Average MSE
	Slope	R	MSE	Slope	R	MSE	
7,3,1,1 (30)	0.551	0.768	0.11571	0.656	0.810	0.08503	0.10037
7,3,2,1 (35)	0.745	0.805	0.09432	0.680	0.825	0.07914	0.08673
7,3,3,1 (40)	0.901	0.846	0.08825	0.759	0.871	0.05968	0.07396
7,3,4,1 (45)	0.818	0.797	0.11880	0.817	0.904	0.04527	0.08203
7,3,5,1 (50)	0.601	0.769	0.12962	0.823	0.908	0.04362	0.08662
7,3,6,1 (55)	0.802	0.843	0.07584	0.900	0.949	0.02467	0.05026
7,4,1,1 (39)	0.696	0.763	0.11992	0.609	0.781	0.09669	0.10831
7,4,2,1 (45)	1.070	0.931	0.06537	0.618	0.786	0.09448	0.07993
7,4,3,1 (51)	0.754	0.842	0.07485	0.837	0.915	0.04029	0.05757
7,4,4,1 (57)	0.695	0.748	0.12684	0.720	0.849	0.06924	0.09804
7,4,5,1 (63)	1.243	0.905	0.10434	0.906	0.952	0.02319	0.06376
7,5,1,1 (48)	0.757	0.877	0.06741	0.645	0.803	0.08790	0.07765
7,5,2,1 (55)	0.668	0.749	0.11656	0.788	0.888	0.05249	0.08453
<b>7,5,3,1 (62)</b>	<b>0.816</b>	<b>0.887</b>	<b>0.05385</b>	<b>0.876</b>	<b>0.936</b>	<b>0.03045</b>	<b>0.04215</b>
7,5,4,1 (69)	0.714	0.731	0.13624	0.735	0.857	0.06558	0.10091
7,5,5,1 (76)	1.085	0.846	0.14330	1.000	1.000	8.5E-08	0.07165
7,6,1,1 (57)	0.910	0.843	0.08991	0.740	0.860	0.06437	0.07714

Table 34 Continued

ANN Geometry	Validation Data Set			Calibration Data Set			Average MSE
	Slope	R	MSE	Slope	R	MSE	
7,6,2,1 (65)	0.875	0.858	0.07953	0.722	0.849	0.06892	0.07423
7,6,3,1 (73)	0.844	0.819	0.09636	0.970	0.985	0.00751	0.05194
7,6,4,1 (81)	1.003	0.851	0.11958	0.650	0.806	0.08674	0.10316
7,6,5,1 (89)	0.675	0.704	0.17685	1.000	1.000	0.00064	0.08843
7,6,6,1 (97)	0.802	0.839	0.08857	0.997	0.999	0.00064	0.04460

The estimated and measured unit debris yield are plotted in Figure 52(a) and (b). It appears roughly six data records among the 55 calibration data are not simulated well, and there are two significant estimation errors within 12 validation data. The correlation coefficient for the calibration data is 0.936 which indicates a successful training and it is 0.887 for the validation data which is desirable for the validation data.

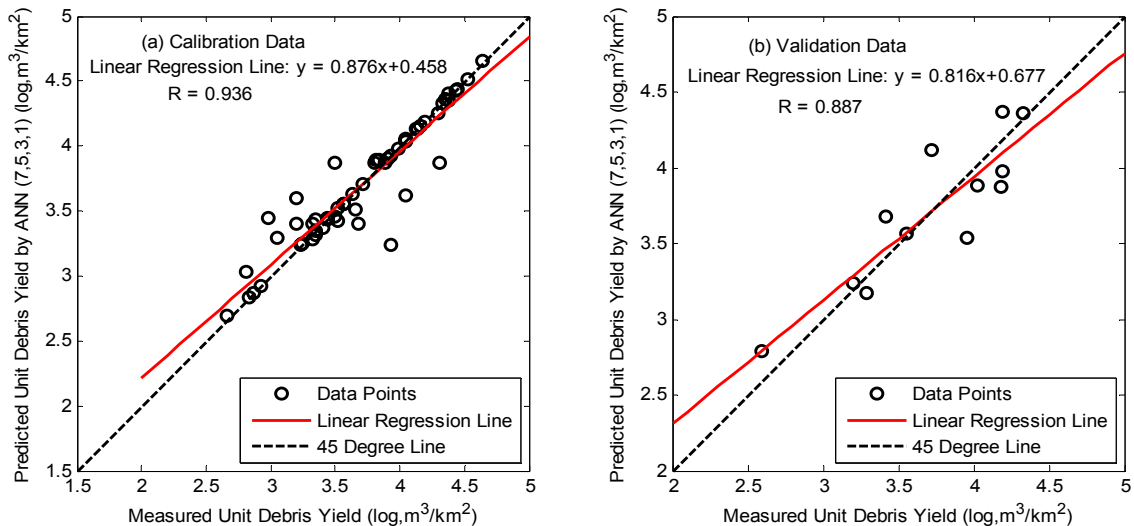


**Figure 52:** Linear regression analysis between measured and ANN model estimated debris yield (a) Calibration Data Set (b) Validation Data Set for Case 10(d) (Input Parameters: Watershed Area, Relief Ratio, Max. 1-hr Rainfall Intensity, Fire Factor, Soil Erodibility Factor, Soil Permeability Rate, and Soil Liquid Limit)

The best fitted neural networks for case 10(a), (b), (c), and (d) are organized in Table 35 with their modeling results evaluated in terms of MSEs,

correlation coefficients, and slopes of the linear regression lines. As aforementioned, all the internal parameters, training algorithm, and preprocessing procedures are the same during the training of neural network models developed for all the cases. The network (7,5,3,1) achieves the lowest errors for both the calibration and validation data, therefore, it is the most suitable neural network model for the estimation of unit debris yield for case 10. With lower error for both the calibration and the validation data, the second neural network (5,4,1,1) performs better than the first one (4,3,3,1) and the third one (6,3,2,1). Since the major difference between each case is the inclusion of different soil properties (i.e. SEF, SP, and SLL), the difference in the modeling results can be explained by SEF and SLL improve the estimation accuracy, but the inclusion of SP worsens the performance. In other words, both SEF and SLL are very important input parameters, especially SLL; but the SP does not appear to play an important role in the estimation of unit debris yield in Case 10.

**Table 35:** Comparison of ANN models performance for Case 10

Case Number	Network Geometry	Validation Data Set			Calibration Data set			Average MSE
		Slope	R	MSE	Slope	R	MSE	
10(a)	(4,3,3,1)	0.663	0.831	0.08199	0.698	0.836	0.07474	0.07836
10(b)	(5,4,1,1)	0.891	0.893	0.06540	0.844	0.919	0.03862	0.05201
10(c)	(6,3,2,1)	0.743	0.857	0.06688	0.736	0.858	0.06525	0.06607
<b>10(d)</b>	<b>(7,5,3,1)</b>	<b>0.816</b>	<b>0.887</b>	<b>0.05385</b>	<b>0.876</b>	<b>0.936</b>	<b>0.03045</b>	<b>0.04215</b>
USACE		0.328	0.642	0.15896	0.134	0.302	0.24098	0.19997

The last row in Table 35 is the modeling results obtained by using the USACE method (2000). With much lower errors and higher correlation

coefficients for the calibration and the validation data, all four neural networks are superior to the USACE method (2000) for the estimation of 67 unit debris yield in this case. The 67 measured and estimated unit debris yield data by the best-performed neural network (7,5,3,1) and the USACE method are presented in Table 36. As seen from the table, for the calibration data, the maximum difference between measured unit debris yield and the USACE estimated values is 0.98, an event occurred at Morgan debris basin, and the minimum difference is -1.28 collected at Fern debris basin. The maximum and minimum difference between measured and the neural network estimation are almost half of that of the USACE method and they are 0.47 and -0.69, two data records documented at May #1 debris basin. The USACE method simulates 12 unit debris yield data records for validation within [-0.68, 0.80] error range and the ANN model is capable of simulating all the validation data within a small error range, [-0.42, 0.40].

**Table 36:** Measured, the USACE method, and the best ANN model (7,5,3,1) estimated unit debris yield for Case 10

Data	Debris Basin	Area (log, ha)	Rr (log, m/km)	Measured Unit Dy (log, m <sup>3</sup> /km <sup>2</sup> )	USACE Estimated Unit Dy (log, m <sup>3</sup> /km <sup>2</sup> )	Diffe <sup>1</sup>	ANN Estimated Unit Dy (log m <sup>3</sup> /km <sup>2</sup> )	Diffe <sup>2</sup>
Calibration Data	Brand	2.43	2.45	3.5	3.62	0.12	3.87	0.37
		2.43	2.45	3.81	3.63	-0.18	3.87	0.06
		2.43	2.45	3.56	3.49	-0.07	3.56	0.00
		2.43	2.45	3.89	3.69	-0.20	3.87	-0.02
		2.43	2.45	3.71	3.77	0.06	3.71	0.00
		2.43	2.45	2.81	3.70	0.89	3.04	0.23
	Duns-muir	2.34	2.45	4.14	3.88	-0.26	4.13	-0.01
		2.34	2.45	4.44	3.81	-0.63	4.44	0.00
	Engle-wild	2.02	2.42	2.92	3.40	0.48	2.92	0.00
		2.02	2.42	4.52	4.00	-0.52	4.51	-0.01
		2.02	2.42	4.05	3.88	-0.17	4.05	0.00

Table 36, Continued

Data	Debris Basin	Area (log, ha)	Rr (log, m/km)	Measured Unit Dy (log, m <sup>3</sup> /km <sup>2</sup> )	USACE Estimated Unit Dy (log, m <sup>3</sup> /km <sup>2</sup> )	Diffe <sup>1</sup>	ANN Estimated Unit Dy (log m <sup>3</sup> /km <sup>2</sup> )	Diffe <sup>2</sup>
Calibration Data	Fern	1.91	2.41	3.63	3.54	-0.09	3.63	0.00
		1.91	2.41	3.4	3.48	0.08	3.36	-0.04
		1.91	2.41	3.32	3.15	-0.17	3.28	-0.04
		1.91	2.41	2.66	3.28	0.62	2.70	0.04
		1.91	2.41	3.82	3.62	-0.20	3.89	0.07
		1.91	2.41	4.16	<b>2.88</b>	<b>-1.28</b>	4.16	0.00
	May #1	2.27	2.48	3.5	3.61	0.11	3.46	-0.04
		2.27	2.48	3.66	3.66	0.00	3.51	-0.15
		2.27	2.48	3.05	3.40	0.35	3.29	0.24
		2.27	2.48	2.98	3.59	0.61	<b>3.45</b>	<b>0.47</b>
		2.27	2.48	3.93	3.37	-0.56	<b>3.24</b>	<b>-0.69</b>
		2.27	2.48	4.35	3.87	-0.48	4.36	0.01
		2.27	2.48	3.35	4.14	0.79	3.32	-0.03
	Morgan	2.27	2.48	3.35	3.66	0.31	3.35	0.00
		2.19	2.44	3.32	3.55	0.23	3.40	0.08
		2.19	2.44	3.2	3.60	0.40	3.40	0.20
		2.19	2.44	3.68	3.58	-0.10	3.40	-0.28
	Mullally	2.19	2.44	2.87	<b>3.85</b>	<b>0.98</b>	2.87	0.00
		1.95	2.45	3.84	3.67	-0.17	3.89	0.05
		1.95	2.45	3.44	3.66	0.22	3.44	0.00
		1.95	2.45	3.84	3.67	-0.17	3.89	0.05
	Rubio	1.95	2.45	3.44	3.66	0.22	3.44	0.00
		2.52	2.45	3.2	3.67	0.47	3.60	0.40
		2.52	2.45	3.24	3.27	0.03	3.25	0.01
		2.52	2.45	4.05	3.64	-0.41	3.62	-0.43
		2.52	2.45	4.19	3.70	-0.49	4.19	0.00
	Sierra Madre Villa	2.52	2.45	3.56	3.83	0.27	3.56	0.00
		2.58	2.43	4.38	3.59	-0.79	4.35	-0.03
	Snover	2.58	2.43	4.31	3.55	-0.76	3.87	-0.44
		1.74	2.4	3.52	3.39	-0.13	3.52	0.00
		1.74	2.4	4.04	3.47	-0.57	4.03	-0.01
		1.74	2.4	4.33	3.61	-0.72	4.33	0.00
	West Ravine	1.74	2.4	4.43	3.59	-0.84	4.43	0.00
		1.81	2.46	4.05	3.49	-0.56	4.06	0.01
		1.81	2.46	4.3	3.49	-0.81	4.25	-0.05
		1.81	2.46	3.23	3.40	0.17	3.23	0.00
Winery	1.81	2.46	4.64	4.05	-0.59	4.65	0.01	
	1.67	2.44	3.52	3.53	0.01	3.42	-0.10	
	1.67	2.44	3.91	3.61	-0.30	3.91	0.00	
		1.67	2.44	4.13	3.48	-0.65	4.13	0.00

**Table 36, Continued**

Data	Debris Basin	Area (log, ha)	Rr (log, m/km)	Measured Unit Dy (log, m <sup>3</sup> /km <sup>2</sup> )	USACE Estimated Unit Dy (log, m <sup>3</sup> /km <sup>2</sup> )	Diffe <sup>1</sup>	ANN Estimated Unit Dy (log m <sup>3</sup> /km <sup>2</sup> )	Diffe <sup>2</sup>	
Calibration	Winery	1.67	2.44	3.35	3.58	0.23	3.44	0.09	
		1.67	2.44	3.44	3.34	-0.10	3.44	0.00	
Data	Zachau	1.96	2.45	3.99	3.47	-0.52	3.98	-0.01	
		1.96	2.45	4.38	3.99	-0.39	4.40	0.02	
Validation	Brace	1.88	2.44	3.55	3.80	0.25	3.57	0.02	
	Brand	2.43	2.45	4.18	<b>3.50</b>	<b>-0.68</b>	3.87	-0.31	
	Duns-muir	2.34	2.45	4.19	4.05	-0.14	3.97	-0.22	
	Engle-wild	2.02	2.42	3.96	3.63	-0.33	<b>3.54</b>	<b>-0.42</b>	
	Data	Fern	1.91	2.41	4.02	3.53	-0.49	3.88	-0.14
			1.91	2.41	2.59	<b>3.39</b>	<b>0.80</b>	2.79	0.20
	May #1	2.27	2.48	3.29	3.29	0.00	3.17	-0.12	
	Rubio	2.52	2.45	3.42	3.59	0.17	3.67	0.25	
	Snover	1.74	2.4	3.72	3.53	-0.19	<b>4.12</b>	<b>0.40</b>	
	West Ravine	1.81	2.46	3.2	3.40	0.20	3.23	0.03	
Zachau	1.96	2.45	4.33	3.81	-0.52	4.36	0.03		
	1.96	2.45	4.19	4.16	-0.03	4.37	0.18		

Diffe<sup>1</sup>- Difference between measured debris yield and the estimated values using the USACE method.

Diffe<sup>2</sup>- Difference between measured debris yield and the estimated values using ANN model.

The measured unit debris yield and their estimated values by the network model (7,5,3,1) and the USACE method are illustrated in Figure 53. As shown in Figure (a), most red circles, ANN model estimation, are on the 45 degree line; while the blue marks, the USACE method estimation, scatter far away from the line. In Figure 53(b), the red circles are much closer to the 45 degree line than the blue marks. The comparison between the error ranges and the plot clearly shows the application of neural network technique for the estimation of unit debris yield is more advantageous.

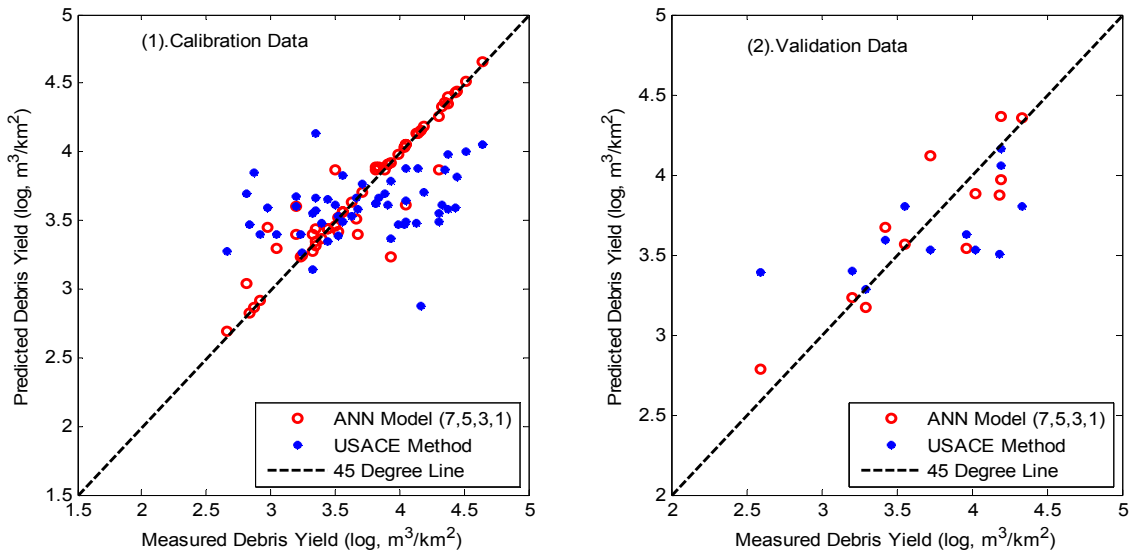


**Figure 53:** Comparison between measured, USACE, and the best ANN model (7,5,3,1) estimated unit debris yield for Case 10  
(Input Parameters: Watershed Area, Relief Ratio, Max. 1-hr Rainfall Intensity, Fire Factor, Soil Erodibility Factor, Soil Permeability Rate, and Soil Liquid Limit)

#### 4.2.8 Case 11

71 cleanup data records of unit debris yield from thirteen small debris basins collected during 46 years starting from 1938 are of particular interest in this case. These thirteen small debris basins are Bailey, Childs, Cloudcraft, Elmwood, Harrow, Hay, Hillcrest, Hook West, Las Flores, Maddock, Sturtevant, Sunset, and Ward debris basin. The reason why these thirteen debris basins are grouped together is because their upstream collection watersheds have an extreme steep slope - their relief ratios are between 305 m/km and 375 m/km. 9 data records are selected by subtractive clustering method and saved for validation and the remaining 62 data records are used for calibration. Altogether there are four studied cases trained by different number of input variables in Case 11: 4 basic input variables are considered in case (a), 4 basic input

variables and one soil property, SEF, are used in case (b), 4 basic input variables and two soil properties, SEF and SP, are in case (c), and 4 basic input variables and three soil properties, SEF, SP, and SLL, are in case (d).

#### **4.2.8.1 Case 11(a)**

The first case within case 11 is trained by four primary variables, similar to the cases 8, 9, and 10, - log transformed watershed area and relief ratio, logarithmic value of maximum one hour precipitation times 100, and fire factor. Seven three-layered neural networks and twenty-two four-layered neural networks are trained to estimate unit debris yield. For three-layered neural network, the number of neurons on the hidden layer is from four to ten. It is more complicated for neural networks with two hidden layers. If there are two, three or five neurons on the first hidden layer, the number of neuron on the second hidden layer varies from one to six; if there are four neurons on the first hidden layer, the number of neuron on the second hidden layer is no more than five. The training algorithm is the LM algorithm. Hyperbolic tangent function is the transfer function for all hidden layers and linear function is used for output layer. The values of other internal parameters are the same as what are used in the cases 8, 9, and 10.

Table 37 shows the modeling results evaluated in terms of MSE and linear regression analysis for twenty-nine neural networks developed in this case. Among seven three-layered neural networks, the one with eight hidden neurons appears to be the best one with a lowest average MSE and it does not have

overfitting problem. When compared with four-layered neural networks, it is worse than the best-performed neural network with two hidden layers. With relatively low error for both the calibration and the validation data set, the ANN model (4,5,5,1) is the best model for this case.

**Table 37:** Summary of the performances of ANN models for Case 11(a)

ANN Geometry	Validation Data Set			Calibration Data Set			Average MSE
	Slope	R	MSE	Slope	R	MSE	
4,4,1 (25)	0.752	0.637	0.07973	0.682	0.826	0.08423	0.08198
4,5,1 (31)	0.676	0.576	0.10120	0.787	0.887	0.05637	0.07878
4,6,1 (37)	0.755	0.555	0.11993	0.827	0.910	0.04567	0.08280
4,7,1 (43)	0.963	0.553	0.18271	0.919	0.959	0.02139	0.10205
<b>4,8,1 (49)</b>	<b>0.776</b>	<b>0.641</b>	<b>0.08052</b>	<b>0.947</b>	<b>0.973</b>	<b>0.01412</b>	<b>0.04732</b>
4,9,1 (55)	1.012	0.589	0.19152	0.959	0.979	0.01089	0.10120
4,10,1 (61)	1.109	0.678	0.14680	0.997	0.999	0.00073	0.07377
4,2,2,1 (19)	0.411	0.512	0.07176	0.591	0.769	0.10833	0.09005
4,2,3,1 (23)	0.768	0.676	0.06703	0.661	0.813	0.08954	0.07829
4,2,4,1 (27)	0.317	0.511	0.07730	0.646	0.803	0.09380	0.08555
4,2,5,1 (31)	0.342	0.408	0.08759	0.832	0.912	0.04453	0.06606
4,2,6,1 (35)	0.739	0.603	0.09680	0.690	0.831	0.08198	0.08939
4,3,1,1 (21)	0.724	0.601	0.08576	0.574	0.757	0.11283	0.09929
4,3,2,1 (26)	0.352	0.688	0.04910	0.537	0.733	0.12260	0.08585
4,3,3,1 (31)	0.931	0.771	0.05331	0.589	0.767	0.10877	0.08104
4,3,4,1 (36)	0.486	0.409	0.12308	0.871	0.933	0.03425	0.07867
4,3,5,1 (41)	0.890	0.813	0.03766	0.750	0.866	0.06622	0.05194
4,3,6,1 (46)	0.718	0.706	0.05179	0.818	0.905	0.04788	0.04983
4,4,1,1 (27)	0.759	0.619	0.09320	0.627	0.792	0.09859	0.09590
4,4,2,1 (33)	0.732	0.516	0.13328	0.702	0.838	0.07885	0.10607
4,4,3,1 (39)	0.314	0.457	0.10761	0.599	0.774	0.10609	0.10685
4,4,4,1 (45)	0.599	0.453	0.13527	0.907	0.953	0.02454	0.07991
4,4,5,1 (51)	0.593	0.552	0.08700	0.921	0.960	0.02099	0.05400
4,5,1,1 (33)	0.938	0.670	0.09525	0.711	0.844	0.07627	0.08576
4,5,2,1 (40)	0.766	0.505	0.17136	0.765	0.875	0.06211	0.11674
4,5,3,1 (47)	0.799	0.764	0.05472	0.744	0.862	0.06786	0.06129
4,5,4,1 (54)	0.579	0.632	0.05980	0.771	0.878	0.06047	0.06014
<b>4,5,5,1 (61)</b>	<b>0.695</b>	<b>0.665</b>	<b>0.06174</b>	<b>0.949</b>	<b>0.974</b>	<b>0.01339</b>	<b>0.03756</b>
4,5,6,1 (68)	1.182	0.549	0.29111	0.999	0.999	0.00032	0.14572

The 62 calibration data points are graphed in Figure 54(a) with measured unit debris yield as their abscissa and the simulated values by the neural network

(4,5,5,1) as their ordinates. For the validation data in figure (b), only three data points are very close to the 45 degree line, one data point is very far away from the line, and the remaining five data points are in between. The correlation coefficient is as high as 0.974 for the calibration data and it is only 0.665 for the validation data. With such a poor performance for the validation data, the neural network (4,5,5,1) trained by four input variables is not an efficient network to simulate the unit debris yield collected from small watersheds with extreme steep slope.

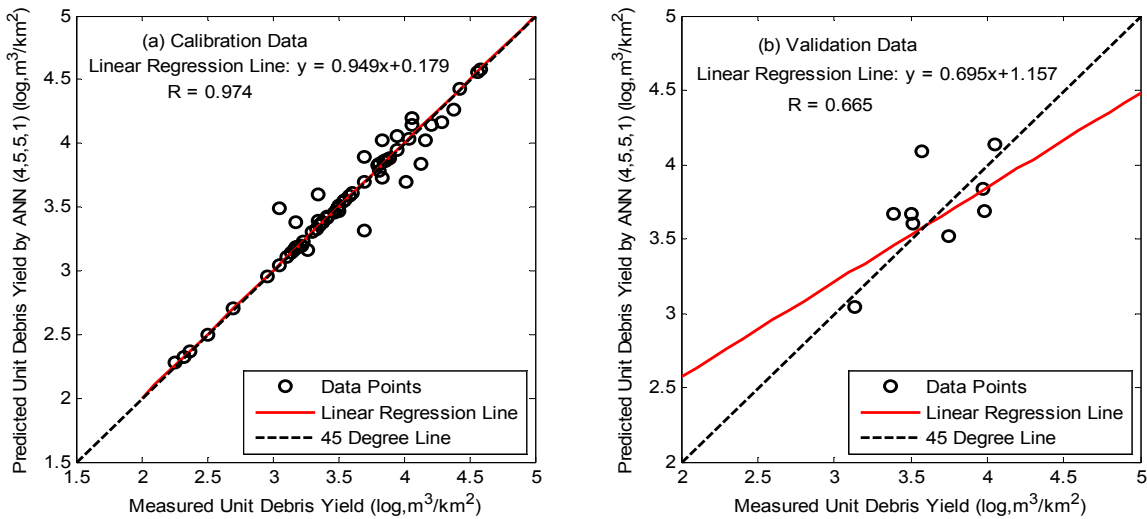


**Figure 54:** Linear regression analysis between measured and ANN model estimated debris yield (a) Calibration Data Set (b) Validation Data Set for Case 11(a) (Input Parameters: Watershed Area, Relief Ratio, Max. 1-hr Rainfall Intensity, and Fire Factor)

#### 4.2.8.2 Case 11(b)

In addition to the four primary input variables, SEF is included as the fifth input variable in this case. Only four-layered neural networks are trained for the simulation of unit debris yield. The geometries of the neural network are very

similar to those used in the preceding cases and they are listed as follows, (5,3,1,1), (5,3,2,1), (5,3,3,1), (5,3,4,1), (5,3,5,1), (5,3,6,1), (5,4,1,1), (5,4,2,1), (5,4,3,1), (5,4,4,1), (5,4,5,1), (5,5,1,1), (5,5,2,1), (5,5,3,1), (5,5,4,1), (5,5,5,1), (5,6,1,1), (5,6,2,1), (5,6,3,1), (5,6,4,1), (5,6,5,1), and (5,6,6,1). Each of the twenty-two neural networks are trained hundreds of times to start from different initial connection weights and biases to avoid local minimum, the best modeling results obtained by all the neural networks are included in Table 38. It seems all the networks are calibrated and validated very successfully, with errors less than 0.1 except one network (5,5,5,1). It is a dramatic improvement compared with the previous case. Among all the neural network models, the network with four neurons on both hidden layers has the lowest error for the validation data, 0.02363, the lowest average error as well, 0.02542, and high correlation coefficients, 0.947 for the calibration data and 0.870 for the validation data. It is the best-performed neural network model for this case.

**Table 38:** Summary of the performances of ANN models for Case 11(b)

ANN Geometry	Validation Data Set			Calibration Data Set			Average MSE
	Slope	R	MSE	Slope	R	MSE	
5,3,1,1 (24)	0.636	0.641	0.06136	0.654	0.809	0.09154	0.07645
5,3,2,1 (29)	0.410	0.584	0.07339	0.699	0.836	0.07977	0.07658
5,3,3,1 (34)	0.921	0.772	0.06511	0.787	0.887	0.05646	0.06078
5,3,4,1 (39)	0.199	0.355	0.08845	0.767	0.876	0.06170	0.07507
5,3,5,1 (44)	0.430	0.581	0.05932	0.934	0.966	0.01752	0.03842
5,3,6,1 (49)	0.598	0.600	0.07828	0.856	0.925	0.03822	0.05825
5,4,1,1 (31)	0.565	0.571	0.08307	0.742	0.861	0.06823	0.07565
5,4,2,1 (37)	0.412	0.539	0.06573	0.794	0.891	0.05464	0.06018
5,4,3,1 (43)	0.610	0.562	0.08312	0.906	0.952	0.02472	0.05392
<b>5,4,4,1 (49)</b>	<b>0.894</b>	<b>0.870</b>	<b>0.02363</b>	<b>0.897</b>	<b>0.947</b>	<b>0.02720</b>	<b>0.02542</b>
5,4,5,1 (55)	0.371	0.627	0.05546	0.642	0.801	0.09477	0.07512
5,5,1,1 (38)	0.750	0.716	0.05446	0.732	0.855	0.07104	0.06275
5,5,2,1 (45)	0.761	0.786	0.06578	0.876	0.936	0.03294	0.04936

**Table 38, Continued**

ANN Geometry	Validation Data Set			Calibration Data Set			Average MSE
	Slope	R	MSE	Slope	R	MSE	
5,5,3,1 (52)	0.794	0.727	0.05350	0.895	0.946	0.02772	0.04061
5,5,4,1 (59)	0.942	0.727	0.06787	0.985	0.992	0.00397	0.03592
5,5,5,1 (66)	0.528	0.478	0.10354	0.979	0.990	0.00545	0.05449
5,6,1,1 (45)	0.700	0.679	0.07426	0.795	0.892	0.05425	0.06426
5,6,2,1 (53)	0.843	0.770	0.06049	0.891	0.944	0.02881	0.04465
5,6,3,1 (61)	0.758	0.930	0.01696	0.856	0.925	0.03823	0.02760
5,6,4,1 (69)	0.517	0.543	0.07590	0.999	0.999	0.00032	0.03811
5,6,5,1 (77)	0.663	0.681	0.05923	0.999	0.999	0.00032	0.02978
5,6,6,1 (85)	0.749	0.678	0.06417	0.999	0.999	0.00032	0.03225

62 measured unit debris yield data records used for calibration are plotted against their estimated values by the network (5,4,4,1) in Figure 55(a), and 9 validation data records for validation are in figure (b). Among 62 calibration data, roughly six data points distribute far away from the 45 degree line. Compared with the neural network (4,5,5,1) in the case (a), this neural network (5,4,4,1) is trained less efficiently for the calibration data. However, it has much better generalization ability for the validation data as seen from the Figure 55(b), almost all the data points are very close to the 45 degree line. The MSE of the validation data achieved by the network (5,4,4,1) is roughly one third of the error obtained by the neural network (4,5,5,1) in case (a), but the MSE for the calibration data in this case is almost two times greater than that of the MSE in the previous case. Overall speaking, this network (5,4,4,1) is better performed than the previous one (4,5,5,1).

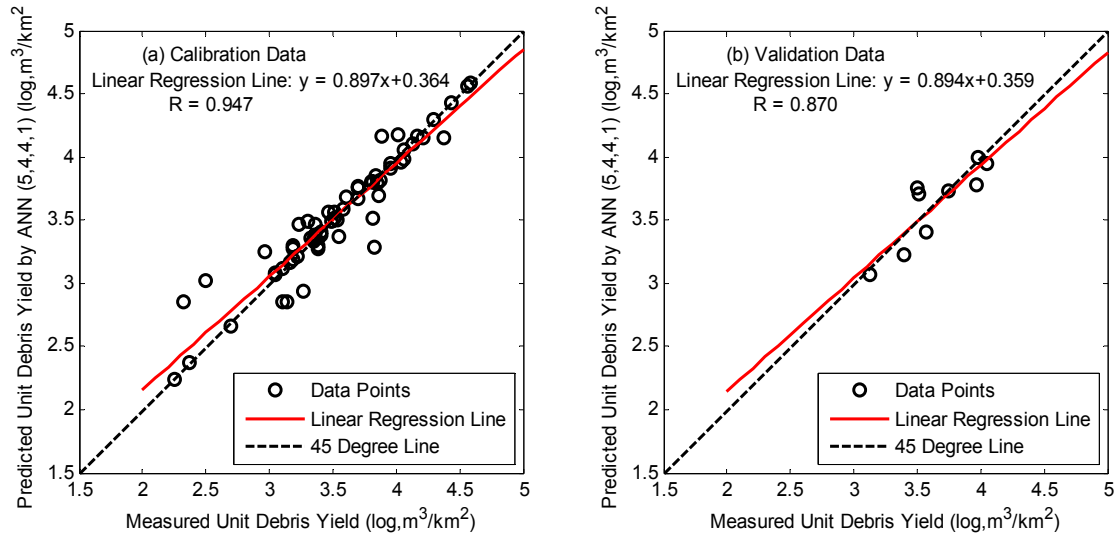


**Figure 55:** Linear regression analysis between measured and ANN model estimated debris yield (a) Calibration Data Set (b) Validation Data Set for Case 11(b) (Input Parameters: Watershed Area, Relief Ratio, Max. 1-hr Rainfall Intensity, Fire Factor, and Soil Erodibility Factor)

#### **4.2.8.3 Case 11(c)**

The geometries of the twenty-two neural network models are the same as those used in the previous case except the number of neurons on the input layer is six in this case. The modeling results of all the twenty-two neural networks are listed in Table 39. As seen from the table, the neural network (6,6,1,1) achieves the lowest error for the validation data, i.e. 0.01243, and a very high correlation coefficient, 0.942; meanwhile, its performance for the calibration data is acceptable with a low MSE of 0.01287 and a correlation coefficient of 0.975. Obviously it is the best neural network for this case.

**Table 39:** Summary of the performances of ANN models for Case 11(c)

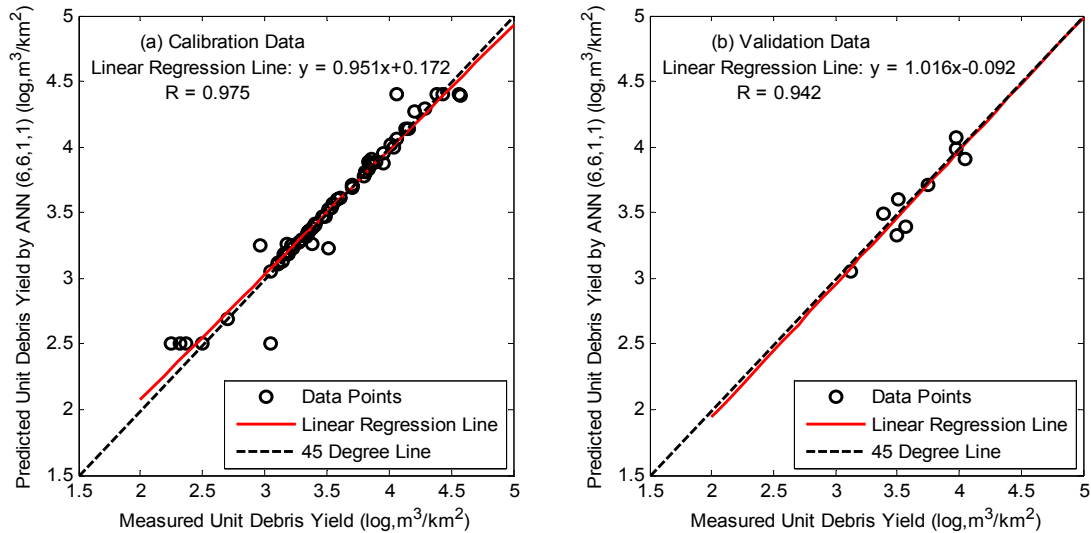
ANN Geometry	Validation Data Set			Calibration Data Set			Average MSE
	Slope	R	MSE	Slope	R	MSE	
6,3,1,1 (27)	0.542	0.526	0.09878	0.661	0.813	0.08981	0.09429
6,3,2,1 (32)	0.431	0.548	0.06463	0.691	0.831	0.08187	0.07325

Table 39, Continued

ANN Geometry	Validation Data Set			Calibration Data Set			Average MSE
	Slope	R	MSE	Slope	R	MSE	
6,3,3,1 (37)	0.770	0.709	0.05448	0.796	0.892	0.05397	0.05422
6,3,4,1 (42)	1.151	0.880	0.03633	0.776	0.881	0.05931	0.04782
6,3,5,1 (47)	0.532	0.640	0.05467	0.832	0.912	0.04432	0.04950
6,3,6,1 (52)	0.515	0.532	0.07767	0.956	0.978	0.01171	0.04469
6,4,1,1 (35)	0.454	0.433	0.11242	0.865	0.930	0.03563	0.07402
6,4,2,1 (41)	1.591	0.890	0.09027	0.872	0.934	0.03382	0.06205
6,4,3,1 (47)	0.874	0.652	0.09163	0.918	0.958	0.02170	0.05667
6,4,4,1 (53)	0.904	0.863	0.02781	0.881	0.938	0.03159	0.02970
6,4,5,1 (59)	0.537	0.487	0.10306	0.871	0.933	0.03421	0.06864
6,5,1,1 (43)	0.932	0.718	0.07231	0.698	0.835	0.07994	0.07613
6,5,2,1 (50)	0.478	0.610	0.09459	1.000	0.971	0.01535	0.05497
6,5,3,1 (57)	0.853	0.832	0.03893	0.865	0.930	0.03576	0.03735
6,5,4,1 (64)	0.518	0.476	0.09790	0.970	0.985	0.00798	0.05294
6,5,5,1 (71)	0.576	0.572	0.07459	0.999	0.999	0.00032	0.03746
<b>6,6,1,1 (51)</b>	<b>1.016</b>	<b>0.942</b>	<b>0.01243</b>	<b>0.951</b>	<b>0.975</b>	<b>0.01287</b>	<b>0.01265</b>
6,6,2,1 (59)	0.728	0.781	0.03707	0.778	0.882	0.05877	0.04792
6,6,3,1 (67)	0.600	0.580	0.07225	1.000	0.999	0.00032	0.03628
6,6,4,1 (75)	0.532	0.495	0.09638	0.999	0.999	0.00032	0.04835
6,6,5,1 (83)	0.574	0.671	0.04975	0.959	0.979	0.01089	0.03032
6,6,6,1 (91)	1.176	0.879	0.03893	0.999	0.999	0.00032	0.01963

The estimated unit debris yield by the network (6,6,1,1) are graphically compared with their measured values in Figure 56. As seen from Figure 56(a), three unit debris yield data are overestimated and two unit debris yield data are underestimated but not to a great extent. In Figure 56(b), the unit debris yield data estimated by the neural network (6,6,1,1) are very close to their actual values. The neural network (6,6,1,1) has a remarkable performance for the calibration data and the validation data. The errors achieved by the network (6,6,1,1) in this case are about one half of the errors obtained by the network (5,4,4,1) in the previous case, therefore, this network (6,6,1,1) is more accurate than the previous neural network (5,4,4,1) for the simulation. The only

explanation is that the inclusion of SP as an additional input variable advances the network performance dramatically.



**Figure 56:** Linear regression analysis between measured and ANN model estimated debris yield (a) Calibration Data Set (b) Validation Data Set for Case 11(c) (Input Parameters: Watershed Area, Relief Ratio, Max. 1-hr Rainfall Intensity, Fire Factor, Soil Erodibility Factor, and Soil Permeability Rate)

#### **4.2.8.4 Case 11(d)**

It is the SLL that is included as the additional variable in the case (d). The neural network architectures and all the internal parameters are the same as what are utilized in the previous two cases. Table 40 presents all the neural networks with their best modeling results. The network with five neurons on the first hidden layer and three neurons on the second hidden layer is capable of simulating the nine validation data with the lowest MSE, 0.04953, meanwhile the MSE of the calibration data is one of the lowest, 0.00273. This neural network has a much better performance for the calibration data than for the validation data. The correlation coefficient of the calibration data is 0.995 which is very

desirable, and as shown in Figure 57(a), the simulation of the 62 unit debris yield data by the neural network (7,5,3,1) is very accurate. However, in Figure 57(b), three data points are on the 45 degree line, two data points are above the line and four data points are below the line. In contrast with the calibration data, the validation data has a much bigger error and a much lower correlation coefficient, 0.726; all of which indicates the network (7,5,3,1) is poorly-performed for the validation data.

**Table 40:** Summary of the performances of ANN models for Case 11(d)

ANN Geometry	Validation Data Set			Calibration Data Set			Average MSE
	Slope	R	MSE	Slope	R	MSE	
7,3,1,1 (30)	0.735	0.611	0.10014	0.700	0.837	0.07943	0.08978
7,3,2,1 (35)	0.554	0.616	0.06231	0.850	0.922	0.03979	0.05105
7,3,3,1 (40)	0.533	0.544	0.07893	0.850	0.922	0.03965	0.05929
7,3,4,1 (45)	0.781	0.746	0.07438	0.804	0.897	0.05187	0.06313
7,3,5,1 (50)	0.578	0.617	0.06958	0.878	0.937	0.03237	0.05098
7,3,6,1 (55)	0.721	0.605	0.08371	0.917	0.958	0.02196	0.05283
7,4,1,1 (39)	0.799	0.637	0.08306	0.756	0.870	0.06444	0.07375
7,4,2,1 (45)	0.854	0.704	0.06641	0.811	0.901	0.05001	0.05821
7,4,3,1 (51)	0.751	0.586	0.09740	0.968	0.984	0.00840	0.05290
7,4,4,1 (57)	0.453	0.605	0.09198	0.981	0.991	0.00494	0.04846
7,4,5,1 (63)	0.531	0.504	0.09073	0.913	0.955	0.02308	0.05691
7,5,1,1 (48)	0.518	0.530	0.09442	0.710	0.843	0.07679	0.08561
7,5,2,1 (55)	0.857	0.659	0.08323	0.915	0.957	0.02252	0.05287
<b>7,5,3,1 (62)</b>	<b>0.636</b>	<b>0.726</b>	<b>0.04953</b>	<b>0.990</b>	<b>0.995</b>	<b>0.00273</b>	<b>0.02613</b>
7,5,4,1 (69)	0.742	0.682	0.06489	0.997	0.999	0.00074	0.03281
7,5,5,1 (76)	0.476	0.473	0.09510	0.999	0.999	0.00032	0.04771
7,6,1,1 (57)	0.581	0.620	0.08967	0.656	0.810	0.09093	0.09030
7,6,2,1 (65)	0.503	0.513	0.09374	0.741	0.862	0.06815	0.08094
7,6,3,1 (73)	1.185	0.830	0.06200	0.998	0.999	0.00043	0.03122
7,6,4,1 (81)	0.571	0.612	0.06728	0.871	0.933	0.03425	0.05076
7,6,5,1 (89)	0.717	0.636	0.07144	0.999	0.999	0.00032	0.03588
7,6,6,1 (97)	1.021	0.724	0.08469	0.999	0.999	0.00032	0.04251

Compared with the best-performed neural network (6,6,1,1) in the previous case, although the error for the calibration data is much lower obtained

by using the network (7,5,3,1) in this case, the error for the validation data is four times greater than that of the previous neural network. It leads to such a conclusion that the performance deteriorates with the inclusion of SLL as the seventh input variable for the unit debris yield simulation collected from small watersheds with extreme steep slope.

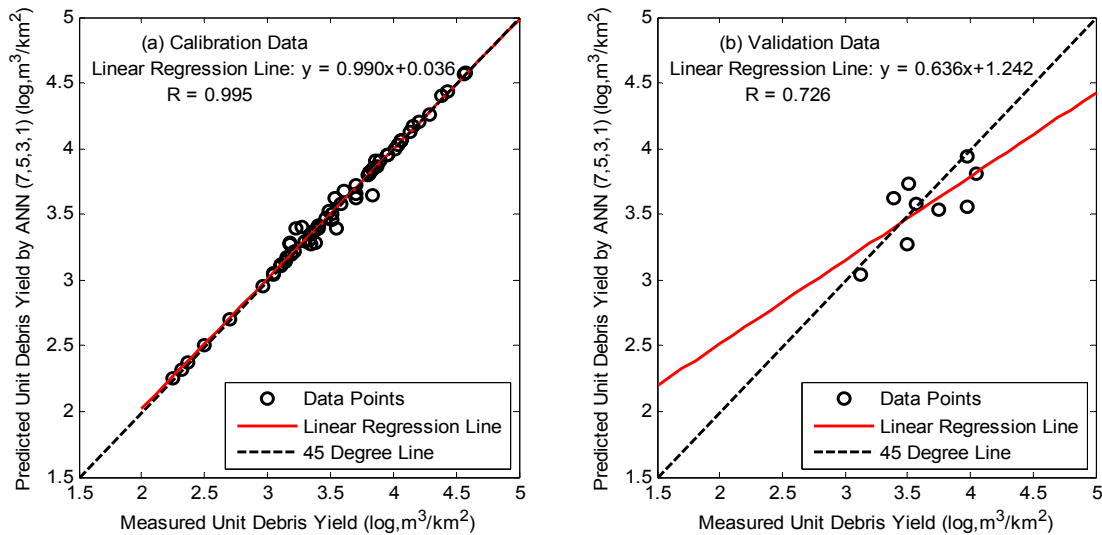


**Figure 57:** Linear regression analysis between measured and ANN model estimated debris yield (a) Calibration Data Set (b) Validation Data Set for Case 11(d) (Input Parameters: Watershed Area, Relief Ratio, Max. 1-hr Rainfall Intensity, Fire Factor, Soil Erodibility Factor, Soil Permeability Rate, and Soil Liquid Limit)

The best-performed neural networks for four cases are summarized in Table 41. With the lowest errors for the calibration and validation data, the neural network (6,6,1,1) developed in case (c) superior to the other three neural network models. The second neural network model (5,4,4,1) shows some improvement on the first neural network model (4,5,5,1), and so does the third neural network (6,6,1,1). Although the last network (7,5,3,1) seems to be the best model for the calibration data, it provides a very poor performance for the validation data. The

first neural network trained with the least input variables is the worst model when overall considering the performance of the calibration and the validation data.

**Table 41:** Comparison of ANN models performance for Case 11

Case Number	Network Geometry	Validation Data Set			Calibration Data set			Average MSE
		Slope	R	MSE	Slope	R	MSE	
11(a)	(4,5,5,1)	0.695	0.665	0.06174	0.949	0.974	0.01339	0.03756
11(b)	(5,4,4,1)	0.894	0.870	0.02363	0.897	0.947	0.02720	0.02542
<b>11(c)</b>	<b>(6,6,1,1)</b>	<b>1.016</b>	<b>0.942</b>	<b>0.01243</b>	<b>0.951</b>	<b>0.975</b>	<b>0.01287</b>	<b>0.01265</b>
11(d)	(7,5,3,1)	0.636	0.726	0.04953	0.990	0.995	0.00273	0.02613
USACE		0.164	0.069	0.08904	0.369	0.135	0.24542	0.16723

The major difference between each case is the number of input variables and neural network architecture and the internal parameters are the same through all the training process. The different modeling results can be explained by the roles that the three soil properties play. For example, SP is the most important soil property, the SEF is not as important as SP, but SLL is the one that has a worse impact on the simulation. Therefore, these six input variables, drainage area, relief ratio, maximum one hour precipitation, fire factor, SEF, and SP, should all be included for the estimation of unit debris yield collected at debris basins from small watersheds with extreme steep slope.

The 71 measured unit debris yield and their estimated values by the USACE method and the neural network model (6,6,1,1) are given in Table 42. Among all the calibration data, the biggest error between the measured unit debris yield and the USACE estimation is 1.36, an event recorded at Maddock debris basin. There is a data record at Las Flores debris basin which is seriously

underestimated by the USACE method with an error of 0.71. Most unit debris yield data records estimated by the ANN model are very accurate except two events; one is at Ward debris basin, ANN overestimates the unit debris yield with an error of 0.34; another is at Hillcrest debris basin, the unit debris yield is underestimated with an error of 0.55. For the validation data, the estimated unit debris yield by the USACE method are within such an error range [-0.34, 0.56], but the neural network technique reduces the range to [-0.17, 0.10].

**Table 42:** Measured, the USACE method, and the best ANN model (6,6,1,1) estimated unit debris yield for Case 11

Data	Debris Basin	Area (log, ha)	Rr (log, m/km)	Measured Unit Dy (log, m <sup>3</sup> /km <sup>2</sup> )	USACE Estimated Unit Dy (log, m <sup>3</sup> /km <sup>2</sup> )	Diffe <sup>1</sup>	ANN Estimated Unit Dy (log, m <sup>3</sup> /km <sup>2</sup> )	Diffe <sup>2</sup>
Calibration Data	Bailey	2.19	2.53	3.18	3.77	0.59	3.27	0.09
		2.19	2.53	3.05	3.69	0.64	3.06	0.01
		2.19	2.53	3.38	3.77	0.39	3.27	-0.11
		2.19	2.53	3.16	3.29	0.13	3.18	0.02
		2.19	2.53	3.7	3.67	-0.03	3.69	-0.01
		2.19	2.53	3.84	3.83	-0.01	3.88	0.04
		2.19	2.53	4.58	4.14	-0.44	4.39	-0.19
		2.19	2.53	4.13	3.76	-0.37	4.14	0.01
		2.19	2.53	4.04	3.52	-0.52	4.00	-0.04
	Childs	1.91	2.5	3.61	3.45	-0.16	3.61	0.00
		1.91	2.5	3.36	3.57	0.21	3.36	0.00
		1.91	2.5	3.55	3.63	0.08	3.57	0.02
		1.91	2.5	3.23	3.43	0.20	3.23	0.00
		1.91	2.5	3.33	3.83	0.50	3.32	-0.01
		1.91	2.5	3.89	3.84	-0.05	3.89	0.00
	Cloud-craft	1.74	2.49	3.41	3.80	0.39	3.40	-0.01
		1.74	2.49	2.96	3.60	0.64	3.25	0.29
		1.74	2.49	3.51	3.66	0.15	3.23	-0.28
	Elm-wood	1.91	2.55	3.7	3.60	-0.10	3.70	0.00
		1.91	2.55	3.54	3.47	-0.07	3.54	0.00
		1.91	2.55	4.06	3.90	-0.16	4.06	0.00
	Harrow	2.05	2.52	3.35	3.69	0.34	3.35	0.00
		2.05	2.52	3.18	3.46	0.28	3.20	0.02
		2.05	2.52	3.87	3.84	-0.03	3.87	0.00
		2.05	2.52	4.56	4.10	-0.46	4.40	-0.16

Table 42, Continued

Data	Debris Basin	Area (log, ha)	Rr (log, m/km)	Measured Unit Dy (log, m <sup>3</sup> /km <sup>2</sup> )	USACE Estimated Unit Dy (log, m <sup>3</sup> /km <sup>2</sup> )	Diffe <sup>1</sup>	ANN Estimated Unit Dy (log, m <sup>3</sup> /km <sup>2</sup> )	Diffe <sup>2</sup>
Calibration Data	Hay	1.72	2.55	3.81	3.69	-0.12	3.81	0.00
		1.72	2.55	3.85	3.56	-0.29	3.86	0.01
		1.72	2.55	3.35	3.69	0.34	3.34	-0.01
		1.72	2.55	3.36	3.61	0.25	3.36	0.00
		1.72	2.55	3.3	3.65	0.35	3.29	-0.01
		1.72	2.55	3.11	3.38	0.27	3.10	-0.01
		1.72	2.55	3.51	3.55	0.04	3.52	0.01
		1.72	2.55	4.43	3.73	-0.70	4.40	-0.03
	Hill-crest	1.96	2.52	3.27	3.73	0.46	3.27	0.00
		1.96	2.52	3.83	3.65	-0.18	3.83	0.00
		1.96	2.52	2.25	3.56	1.31	2.50	0.25
		1.96	2.52	3.05	3.59	0.54	<b>2.50</b>	<b>-0.55</b>
	Hook West	1.65	2.51	3.8	3.62	-0.18	3.78	-0.02
	Las Flores	2.07	2.52	3.7	3.58	-0.12	3.71	0.01
		2.07	2.52	3.86	3.71	-0.15	3.91	0.05
		2.07	2.52	4.21	3.83	-0.38	4.27	0.06
		2.07	2.52	4.02	3.68	-0.34	4.02	0.00
		2.07	2.52	3.95	<b>3.24</b>	<b>-0.71</b>	3.87	-0.08
	Mad-dock	1.85	2.56	3.81	3.68	-0.13	3.81	0.00
		1.85	2.56	2.7	3.59	0.89	2.69	-0.01
		1.85	2.56	2.5	<b>3.86</b>	<b>1.36</b>	2.50	0.00
	Sturtevant	0.89	2.56	3.11	3.42	0.31	3.11	0.00
		0.89	2.56	3.41	3.56	0.15	3.42	0.01
		0.89	2.56	3.14	3.64	0.50	3.13	-0.01
		0.89	2.56	2.32	3.49	1.17	2.50	0.18
	Sunset	2.06	2.49	3.38	3.62	0.24	3.38	0.00
		2.06	2.49	3.47	3.73	0.26	3.47	0.00
		2.06	2.49	3.95	3.59	-0.36	3.96	0.01
		2.06	2.49	3.58	4.21	0.63	3.60	0.02
		2.06	2.49	2.37	3.53	1.16	2.50	0.13
	Ward	1.5	2.51	4.06	3.71	-0.35	<b>4.40</b>	<b>0.34</b>
		1.5	2.51	3.49	3.43	-0.06	3.47	-0.02
		1.5	2.51	3.22	3.55	0.33	3.25	0.03
1.5		2.51	4.29	3.94	-0.35	4.29	0.00	
1.5		2.51	4.38	3.76	-0.62	4.40	0.02	
1.5		2.51	4.16	3.67	-0.49	4.14	-0.02	
1.5		2.51	3.19	4.11	0.92	3.18	-0.01	
2.19		2.53	3.5	3.63	0.13	3.33	-0.17	
2.19		2.53	3.51	3.80	0.29	3.60	0.09	

**Table 42, Continued**

Data	Debris Basin	Area (log, ha)	Rr (log, m/km)	Measured Unit Dy (log, m <sup>3</sup> /km <sup>2</sup> )	USACE Estimated Unit Dy (log, m <sup>3</sup> /km <sup>2</sup> )	Diffe <sup>1</sup>	ANN Estimated Unit Dy (log, m <sup>3</sup> /km <sup>2</sup> )	Diffe <sup>2</sup>
Validation Data	Bailey	2.19	2.53	3.13	<b>3.69</b>	<b>0.56</b>	3.06	-0.07
		2.19	2.53	3.5	3.63	0.13	3.33	-0.17
		2.19	2.53	3.51	3.80	0.29	3.60	0.09
	Childs	1.91	2.5	3.98	3.73	-0.25	4.07	0.09
	Mad-dock	1.85	2.56	3.57	3.55	-0.02	<b>3.40</b>	<b>-0.17</b>
		1.85	2.56	3.97	3.67	-0.30	3.98	0.01
	Elm-wood	1.91	2.55	3.39	3.66	0.27	<b>3.49</b>	<b>0.10</b>
		1.91	2.55	4.05	3.85	-0.20	3.91	-0.14
	Ward	1.5	2.51	3.75	<b>3.41</b>	<b>-0.34</b>	3.71	-0.04

Diffe<sup>1</sup>- Difference between measured debris yield and the estimated values using the USACE method.

Diffe<sup>2</sup>- Difference between measured debris yield and the estimated values using ANN model.

Figure 58 on the next page is provided as a more direct means to compare the results achieved by these two methods. In both figures, the red circles – ANN estimation follow to the 45 degree line while the blue marks representing the USACE estimation spread out in the area. All these findings lead to a conclusion that the neural network is more accurate for the estimation of unit debris yield than the USACE method in Case 11.

#### 4.2.9 Case 12

The studied unit debris yield in this case was collected from thirteen small debris basins including Auburn, Big Briar, Carriage House, Carter, Cloud Creek, Hook East, Kinneloa East, Kinneloa West, Lannan, Pinelawn, Shields, Startfall, and Sunnyside debris basin (Figure 3). The upstream collection watersheds of these debris basins all have the steepest slope, or the relief ratios are between 375 m/km and 525 m/km. 71 data records of unit debris yield collected from 1938 and 1983 are available. They are separated by subtractive clustering method into

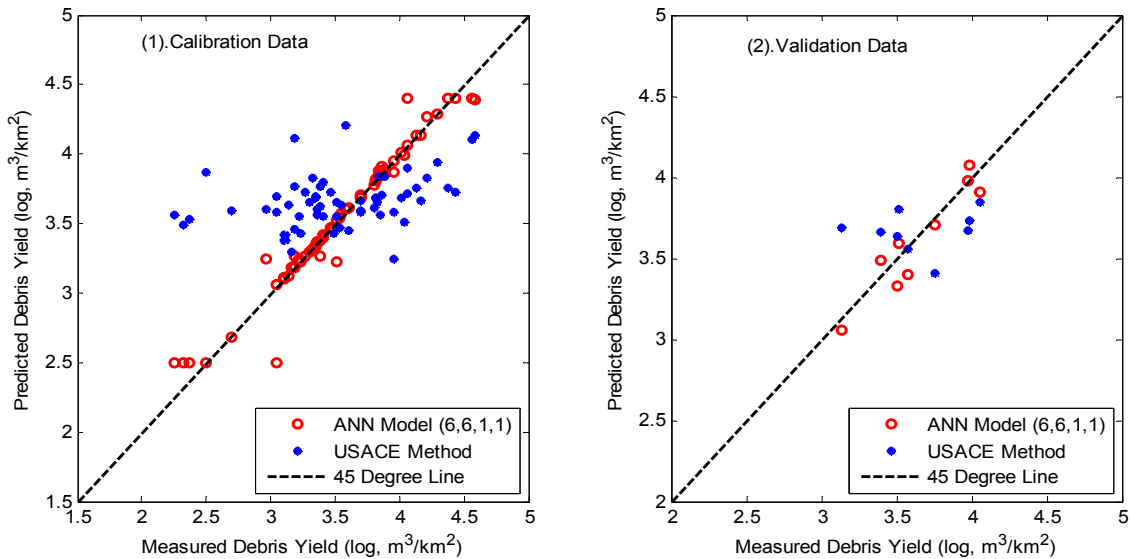


**Figure 58:** Comparison between measured, USACE, and the best ANN model (6,6,1,1) estimated unit debris yield for Case 11  
 (Input Parameters: Watershed Area, Relief Ratio, Max. 1-hr Rainfall Intensity, Fire Factor, Soil Erodibility Factor, and Soil Permeability Rate)

calibration (i.e. 63 data records) and validation data (i.e. 8 data records). The initiative is to study the impact of three soil properties including SEF, SP, and SLL on the unit debris yield estimation similar to Case 8, 9, 10, and 11. However, all the debris basins within this case are located within the same soil unit; in other words, the values of these soil properties are the same for all the debris basins. Therefore, only four basic input variables - log transformed watershed area, logarithmic relief ratio, logarithmic value of maximum one hour precipitation times 100, and fire factor are used to train neural network models to estimate unit debris yield.

Eight neural networks with one hidden layer are calibrated by 63 unit debris yield data and then 8 validation data are applied to check their capability for modeling new data. As shown in Table 43, the neural network with six

neurons on the hidden layer achieves the best performance with the lowest average MSE and comparable performance for the calibration and the validation data. Twenty-four four-layered neural networks are created and the most suitable neural network model appears to be the network (4,6,3,1). This neural network (4,6,3,1) appears to be more successfully trained than the network (4,6,1) with a much lower error for the calibration data and the performance for the validation data is improved as well. The MSE for the calibration data is as low as 0.00493 which is about 34 times less than the MSE obtained by using the USACE method (Table 43); the MSE of the validation data simulated by the same network is roughly one third of the error using the USACE method. It is true that all the four-layered neural networks developed in this case are superior to the USACE method for estimating the 71 unit debris yield.

**Table 43:** Summary of the performances of ANN models for Case 12

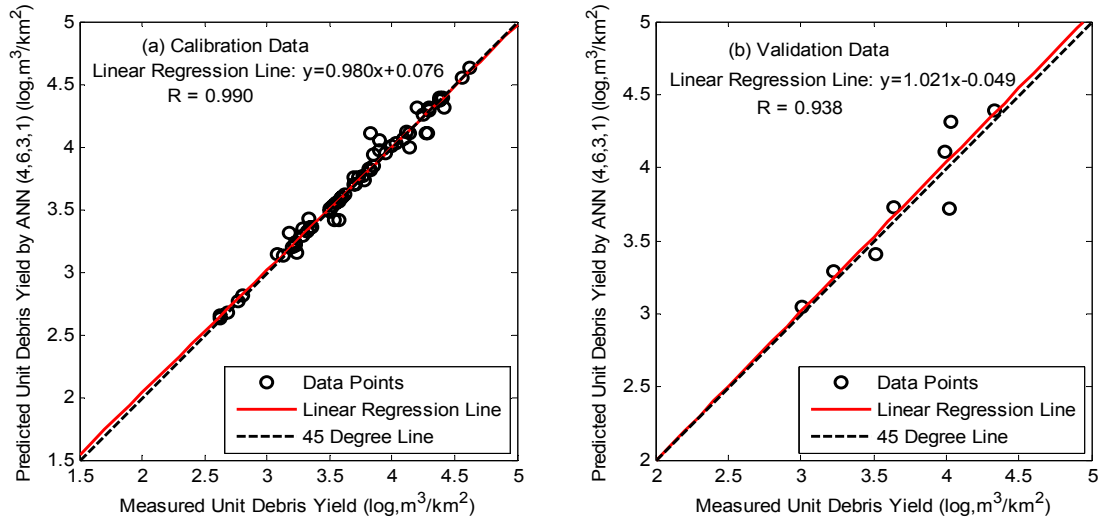
ANN Geometry	Validation Data Set			Calibration Data Set			Average MSE
	Slope	R	MSE	Slope	R	MSE	
4,4,1 (25)	0.871	0.915	0.02916	0.667	0.817	0.07987	0.05452
4,5,1 (31)	0.914	0.941	0.03543	0.833	0.913	0.04003	0.03773
<b>4,6,1 (37)</b>	<b>0.982</b>	<b>0.916</b>	<b>0.03405</b>	<b>0.860</b>	<b>0.927</b>	<b>0.03359</b>	<b>0.03382</b>
4,7,1 (43)	1.161	0.907	0.05757	0.907	0.953	0.02223	0.03990
4,8,1 (49)	1.017	0.870	0.06032	0.914	0.956	0.02055	0.04043
4,9,1 (55)	0.806	0.725	0.11361	0.980	0.990	0.00477	0.05919
4,10,1 (61)	0.915	0.833	0.08043	1.000	1.000	0.00008	0.04025
4,11,1 (67)	0.573	0.574	0.18988	1.000	1.000	0.00012	0.09500
4,3,1,1 (21)	0.673	0.753	0.08189	0.767	0.876	0.05594	0.06891
4,3,2,1 (26)	0.594	0.769	0.07983	0.846	0.920	0.03696	0.05839
4,3,3,1 (31)	0.675	0.882	0.04854	0.832	0.912	0.04032	0.04443
4,3,4,1 (36)	0.814	0.860	0.04859	0.907	0.952	0.02234	0.03547
4,3,5,1 (41)	0.810	0.827	0.06186	0.923	0.962	0.01806	0.03996
4,3,6,1 (46)	1.222	0.924	0.06087	0.944	0.971	0.01354	0.03721
4,4,1,1 (27)	0.976	0.871	0.05500	0.791	0.890	0.05009	0.05255
4,4,2,1 (33)	0.958	0.923	0.04362	0.841	0.917	0.03820	0.04091
4,4,3,1 (39)	1.025	0.890	0.04933	0.858	0.926	0.03401	0.04167

Table 43, Continued

ANN Geometry	Validation Data Set			Calibration Data Set			Average MSE
	Slope	R	MSE	Slope	R	MSE	
4,4,4,1 (45)	0.689	0.773	0.07393	0.891	0.944	0.02621	0.05007
4,4,5,1 (51)	0.927	0.884	0.04372	0.974	0.987	0.00630	0.02501
4,4,6,1 (57)	0.922	0.902	0.03634	0.966	0.983	0.00804	0.02219
4,5,1,1 (33)	0.986	0.913	0.03786	0.751	0.867	0.05970	0.04878
4,5,2,1 (40)	1.009	0.927	0.03458	0.886	0.941	0.02741	0.03099
4,5,3,1 (47)	0.866	0.939	0.02457	0.928	0.963	0.01720	0.02089
4,5,4,1 (54)	0.810	0.919	0.02794	0.943	0.971	0.01365	0.02080
4,5,5,1 (61)	1.019	0.925	0.03119	0.985	0.992	0.00368	0.01744
4,5,6,1 (68)	0.762	0.866	0.05540	0.975	0.988	0.00579	0.03060
4,6,1,1 (39)	1.182	0.966	0.03368	0.870	0.933	0.03111	0.03240
4,6,2,1 (47)	0.741	0.938	0.02660	0.949	0.974	0.01215	0.01937
<b>4,6,3,1 (55)</b>	<b>1.021</b>	<b>0.938</b>	<b>0.02635</b>	<b>0.979</b>	<b>0.990</b>	<b>0.00493</b>	<b>0.02668</b>
4,6,4,1 (63)	0.901	0.866	0.05791	0.952	0.976	0.01155	0.03473
4,6,5,1 (71)	1.360	0.946	0.06217	1.000	1.000	2.6E-08	0.03109
4,6,6,1 (79)	0.774	0.919	0.02927	1.000	1.000	3.8E-08	0.01464
USACE	0.866	0.439	0.07304	0.571	0.229	0.16939	0.12122

The 63 unit debris yield estimated by the network (4,6,3,1) are plotted in Figure 59(a) against their measured values. All the data points stay very close to the 45 degree line that results in a desirable correlation coefficient, 0.990. The 8 validation data points are plotted in Figure 59(b) which shows that all of them are very close to the 45 degree line except one data point, and the correlation coefficient is as high as 0.938. It is evident that not only the calibration of the neural network (4,6,3,1) but also the validation are very successful.

The estimated unit debris yield by the USACE method and the neural network (4,6,3,1) are listed and compared in Table 44. The first 63 data records are the calibration data and 8 validation data are in succession. The maximum difference between the USACE estimation and the measured unit debris yield is [-0.84, 1.08] for the calibration data and [-0.22, 0.60] for the validation data; the



**Figure 59:** Linear regression analysis between measured and ANN model estimated debris yield (a) Calibration Data Set (b) Validation Data Set for Case 12 (Input Parameters: Watershed Area, Relief Ratio, Max. 1-hr Rainfall Intensity, and Fire Factor)

maximum difference between the measured and the ANN model (4,6,3,1) estimation is [-0.18, 0.28] for the calibration data and it is [-0.30, 0.28] for the validation data.

**Table 44:** Measured, the USACE method and the best ANN model (4,6,3,1) estimated unit debris yield for Case 12

Data	Debris Basin	Area (log, ha)	Rr (log, m/km)	Measured Unit Dy (log, m <sup>3</sup> /km <sup>2</sup> )	USACE Estimated Unit Dy (log, m <sup>3</sup> /km <sup>2</sup> )	Diffe <sup>1</sup>	ANN Estimated Unit Dy (log, m <sup>3</sup> /km <sup>2</sup> )	Diffe <sup>2</sup>
Calibration Data	Auburn	1.62	2.72	3.78	3.78	0.00	3.73	-0.05
		1.62	2.72	3.9	3.85	-0.05	4.05	0.15
		1.62	2.72	3.57	3.71	0.14	3.56	-0.01
		1.62	2.72	3.62	3.84	0.22	3.62	0.00
		1.62	2.72	3.24	3.67	0.43	3.15	-0.09
		1.62	2.72	4.38	4.15	-0.23	4.39	0.01
		1.62	2.72	3.7	3.61	-0.09	3.76	0.06
		1.62	2.72	4.38	3.85	-0.53	4.36	-0.02
	Big Briar	0.72	2.71	3.33	3.53	0.20	3.43	0.10
		0.72	2.71	3.57	3.57	0.00	3.42	-0.15
	Carriage House	0.89	2.64	4.42	3.97	-0.45	4.31	-0.11
		0.89	2.64	3.9	3.72	-0.18	3.97	0.07
	Carter	1.5	2.69	3.95	3.74	-0.21	3.95	0.00
		1.5	2.69	3.13	3.51	0.38	3.13	0.00

Table 44, Continued

Data	Debris Basin	Area (log, ha)	Rr (log, m/km)	Measured Unit Dy (log, m <sup>3</sup> /km <sup>2</sup> )	USACE Estimated Unit Dy (log, m <sup>3</sup> /km <sup>2</sup> )	Diffe <sup>1</sup>	ANN Estimated Unit Dy (log, m <sup>3</sup> /km <sup>2</sup> )	Diffe <sup>2</sup>
Calibration Data	Carter	1.5	2.69	3.73	3.81	0.08	3.75	0.02
		1.5	2.69	3.53	3.52	-0.01	3.53	0.00
		1.5	2.69	3.22	3.80	0.58	3.21	-0.01
		1.5	2.69	2.81	3.67	0.86	2.81	0.00
		1.5	2.69	3.2	3.74	0.54	3.20	0.00
		1.5	2.69	4.27	3.90	-0.37	4.10	-0.17
		1.5	2.69	3.71	3.78	0.07	3.70	-0.01
	Cloud Creek	0.72	2.72	3.82	3.66	-0.16	3.82	0.00
		0.72	2.72	4.14	3.93	-0.21	4.11	-0.03
		0.72	2.72	4.12	3.75	-0.37	4.12	0.00
		0.72	2.72	3.5	3.70	0.20	3.49	-0.01
		0.72	2.72	2.63	3.61	0.98	2.65	0.02
	Hook East	1.67	2.6	3.55	3.44	-0.11	3.55	0.00
		1.67	2.6	3.59	3.68	0.09	3.59	0.00
		1.67	2.6	4.39	3.82	-0.57	4.38	-0.01
		1.67	2.6	4.62	4.08	-0.54	4.63	0.01
	Kinneloa East	1.72	2.65	4.3	4.08	-0.22	4.29	-0.01
		1.72	2.65	3.29	3.49	0.20	3.28	-0.01
	Kinneloa West	1.72	2.68	3.95	3.97	0.02	3.95	0.00
		1.72	2.68	3.54	3.65	0.11	3.42	-0.12
		1.72	2.68	3.7	3.77	0.07	3.70	0.00
		1.72	2.68	3.83	3.67	-0.16	3.81	-0.02
		1.72	2.68	4.41	4.10	-0.31	4.39	-0.02
		1.72	2.68	3.32	3.50	0.18	3.32	0.00
		1.72	2.68	3.99	3.52	-0.47	4.01	0.02
	Lannan	1.81	2.61	3.6	3.62	0.02	3.60	0.00
		1.81	2.61	3.23	3.82	0.59	3.23	0.00
		1.81	2.61	4.03	3.78	-0.25	4.03	0.00
		1.81	2.61	3.08	3.66	0.58	3.14	0.06
	Pine-lawn	0.72	2.65	3.85	3.61	-0.24	3.94	0.09
		0.72	2.65	4.14	3.66	-0.48	3.99	-0.15
		0.72	2.65	4.2	4.06	-0.14	4.31	0.11
		0.72	2.65	4.25	3.59	-0.66	4.26	0.01
		0.72	2.65	3.36	3.28	-0.08	3.36	0.00
	Shields	0.89	2.7	3.29	3.50	0.21	3.35	0.06
		0.89	2.7	4.29	3.95	-0.34	<b>4.11</b>	<b>-0.18</b>
		0.89	2.7	3.85	3.62	-0.23	3.85	0.00
		0.89	2.7	3.83	4.12	0.29	<b>4.11</b>	<b>0.28</b>
		0.89	2.7	3.5	3.65	0.15	3.51	0.01
		0.89	2.7	4.56	<b>3.72</b>	<b>-0.84</b>	4.55	-0.01
0.89		2.7	2.77	3.40	0.63	2.76	-0.01	
Startfall	1.53	2.61	3.6	3.40	-0.20	3.60	0.00	
	1.53	2.61	4.3	4.01	-0.29	4.31	0.01	

**Table 44, Continued**

Data	Debris Basin	Area (log, ha)	Rr (log, m/km)	Measured Unit Dy (log, m <sup>3</sup> /km <sup>2</sup> )	USACE Estimated Unit Dy (log, m <sup>3</sup> /km <sup>2</sup> )	Diffe <sup>1</sup>	ANN Estimated Unit Dy (log, m <sup>3</sup> /km <sup>2</sup> )	Diffe <sup>2</sup>
Calibration Data	Startfall	1.53	2.61	3.35	3.74	0.39	3.35	0.00
		1.53	2.61	2.63	<b>3.71</b>	<b>1.08</b>	2.63	0.00
		1.53	2.61	3.77	4.18	0.41	3.77	0.00
		1.53	2.61	4.09	3.78	-0.31	4.06	-0.03
	Sunny-side	0.72	2.68	2.69	3.66	0.97	2.67	-0.02
Validation Data	Auburn	1.62	2.72	3.64	3.78	0.14	3.73	0.09
		1.62	2.72	4.02	3.81	-0.21	<b>3.72</b>	<b>-0.30</b>
	Carter	1.5	2.69	4.33	<b>4.11</b>	<b>-0.22</b>	4.39	0.06
		1.5	2.69	3.01	<b>3.61</b>	<b>0.60</b>	3.05	0.04
	Cloud	0.72	2.72	3.99	4.10	0.11	4.11	0.12
	Kinneloa East	1.72	2.65	3.52	3.62	0.10	3.41	-0.11
	Pine-lawn	0.72	2.65	4.03	3.87	-0.16	<b>4.31</b>	<b>0.28</b>
	Shields	0.89	2.7	3.23	3.47	0.24	3.29	0.06

Diffe<sup>1</sup>- Difference between measured debris yield and the estimated values using the USACE method.

Diffe<sup>2</sup>- Difference between measured debris yield and the estimated values using ANN model

Figure 60 offers a more direct means to compare those results. For both the calibration and the validation data, red circles, ANN estimations, scatter much closer to the 45 degree line than the blue marks, the USACE predictions. All the comparison indicates that ANN is more accurate than the USACE method for the estimation of the unit debris yield collected from small watershed with the steepest slope in this case.

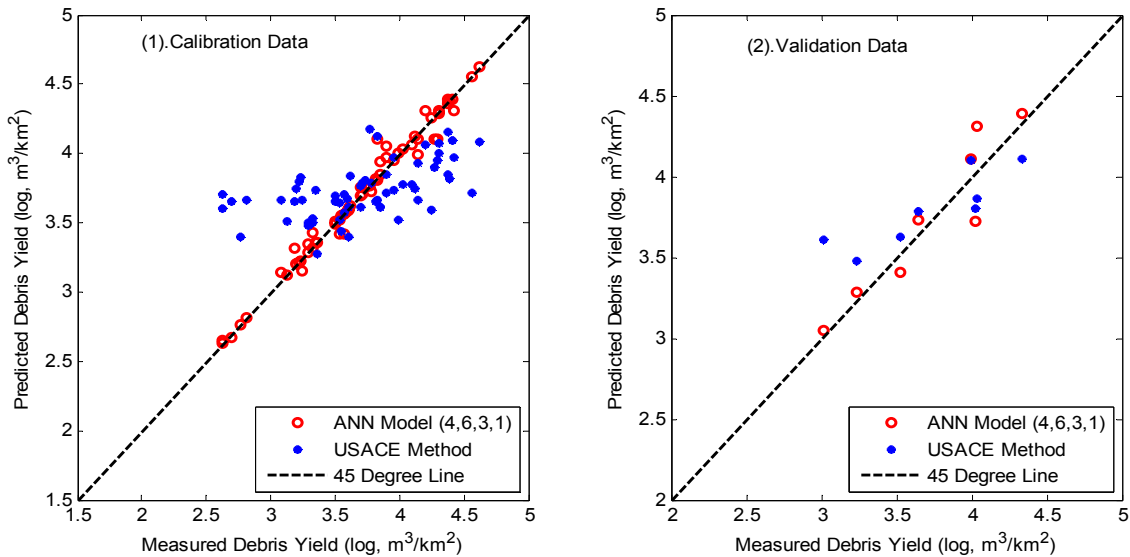


**Figure 60:** Comparison between measured, USACE, and the best ANN model (4,6,3,1) estimated unit debris yield for Case 12  
(Input Parameters: Watershed Area, Relief Ratio, Max. 1-hr Rainfall Intensity, and Fire Factor)

#### 4.2.10 Case 13

The USACE (2000) developed an empirical equation (Equation 4.1) for estimating unit debris yield from watershed with area between 10 and 25 miles.

$$\log D_y = 0.88(\log Q) + 0.48(\log RR) + 0.06(\log A) + 0.20(FF) \quad (4.1)$$

In this equation,  $D_y$  is unit debris yield in cubic yards per square mile,  $RR$  is relief ratio with unit of ft/mile,  $Q$  is unit peak discharge with the unit of  $\text{ft}^3/\text{s}/\text{mi}^2$ ,  $A$  is watershed area in acre, and  $FF$  is non-dimensional fire factor. The equation was developed based on 57 data records collected from Santa Anita Dam and San Dimas Gate Dam debris basin (Figure 4) from 1938 to 1983. To provide a comparison with the ANN modeling result, the same data is applied to train neural network models for the estimation of unit debris yield. Before start

training ANN models, 48 data records are selected for calibration and the remaining 9 data for validation using subtractive clustering method. Before presenting these data to ANN models, both the input and target values are normalized, the input vectors are transformed to be uncorrelated, and those input variables that contributed less than 2% of the total variation are eliminated. The LM training algorithm is the only training algorithm used and the default values of most internal parameters are used except epoch size and the calibration data error goal. 10,000 is chosen as the epoch size and the calibration process will be stopped when the error reaches  $10^{-6}$ . The hyperbolic tangent function is the only transfer function for the hidden layers and linear function is for the output layer.

Randomly started with a neural network with four and three neurons on the first and the second hidden layer, the results are very remarkable. The MSE for the calibration data is 0.00607 and it is 0.00761 for the validation data. The correlation coefficients are 0.994 for the calibration data and 0.991 for the validation data. Not only are the correlation coefficients close to one but also the slopes of the linear regression lines. As seen from Figure 61, all the data points are very close to the 45 degree line and the linear regression lines are almost coincide with the 45 degree line. All these signs indicate this neural network is perfect for modeling unit debris yield collected from larger watersheds. Therefore, it is not necessary to train other neural networks.

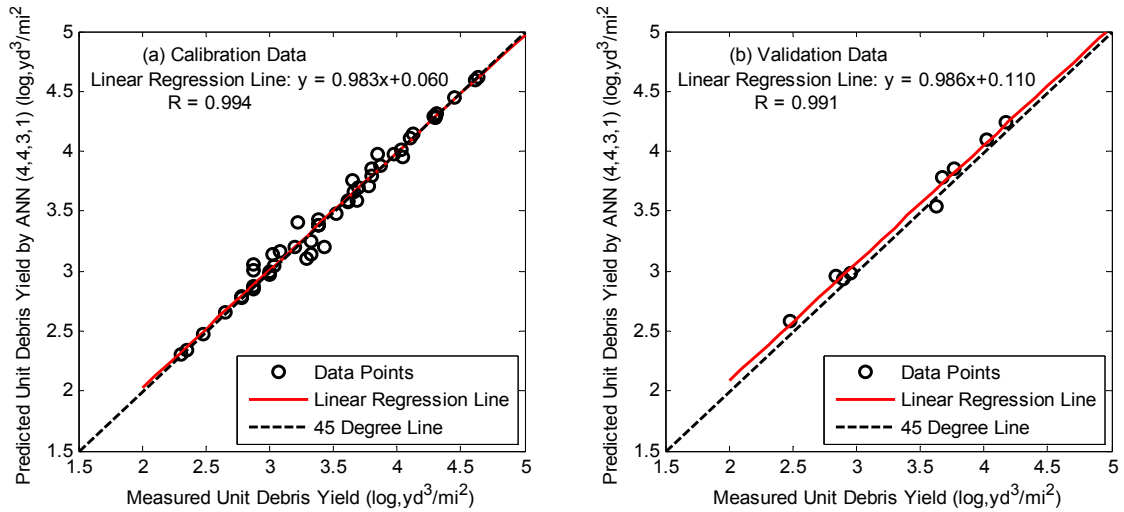


**Figure 61:** Linear regression analysis between measured and ANN model estimated debris yield (a) Calibration Data Set (b) Validation Data Set for Case 13

Among 48 calibration data, 28 of them were collected from Santa Anita Dam debris basin and the remaining 20 data records were from San Dimas Gate Dam debris basin. For the calibration data, the USACE method estimates those data within the following error range:  $[-0.06, 0.83]$ , (Table 45), and the MSE is 0.11417; the error range achieved by the neural network (4,4,3,1) is  $[-0.22, 0.44]$ , and the MSE is much smaller, 0.00607. Although the lower limit of the error bound of the neural network is worse than that of the USACE method, as seen from Figure 62(a), the USACE overestimates almost all data and some of them are overestimated to a large extent. The validation data consist of 3 data records from Santa Anita debris basin and 6 data records from San Dimas Gate Dam debris basin. The estimated and measured values of the 9 validation data are plotted in Figure 62(b). It appears that the USACE method also overestimates most of the validation data with a MSE of 0.12664. As seen from figure (b), ANN model data points are clustered around the 45 degree line but almost all of the

USACE data points are above the line. For the validation data, the lower limit of the error bound for both the USACE method and the neural network is -0.09, however, the upper limit of the error bound for the USACE method is 0.65, and it is only 0.12 for the neural network. With much lower errors and smaller error ranges, the ANN model (4,4,3,1) is superior to the USACE method.

**Table 45:** Measured, the USACE method, and the best ANN model (4,4,3,1) estimated unit debris yield for Case 13

Data	Debris Basin	Area (mi <sup>2</sup> )	Rr (ft/mi)	Measured Dy (log, yd <sup>3</sup> /mi <sup>2</sup> )	USACE Estimated Unit Dy (log, yd <sup>3</sup> /mi <sup>2</sup> )	Diffe <sup>1</sup>	ANN Estimated Unit Dy (log, yd <sup>3</sup> /mi <sup>2</sup> )	Diffe <sup>2</sup>
Calibration Data	Santa Anita Dam	10.8	871.0	2.87	3.28	0.41	3.01	0.14
		10.8	871.0	2.87	3.38	0.51	3.05	0.18
		10.8	871.0	2.87	3.15	0.28	2.85	-0.02
		10.8	871.0	2.87	3.24	0.37	2.88	0.01
		10.8	871.0	3.02	3.51	0.49	3.14	0.12
		10.8	871.0	2.65	3.11	0.46	2.66	0.01
		10.8	871.0	3.65	4.05	0.40	3.76	0.11
		10.8	871.0	3.69	3.90	0.21	3.59	-0.10
		10.8	871.0	3.62	3.90	0.28	3.58	-0.04
		10.8	871.0	3.8	4.15	0.35	3.86	0.06
		10.8	871.0	3.85	4.22	0.37	3.98	0.13
		10.8	871.0	4.04	4.26	0.22	3.96	-0.08
		10.8	871.0	4.64	4.60	-0.04	4.62	-0.02
		10.8	871.0	4.61	4.68	0.07	4.60	-0.01
		10.8	871.0	3.38	3.87	0.49	3.44	0.06
		10.8	871.0	3.29	3.42	0.13	3.11	-0.18
		10.8	871.0	3.43	3.53	0.10	<b>3.21</b>	<b>-0.22</b>
		10.8	871.0	3.52	4.09	0.57	3.48	-0.04
		10.8	871.0	3.22	<b>4.05</b>	<b>0.83</b>	3.41	0.19
		10.8	871.0	3.61	4.27	0.66	3.59	-0.02
		10.8	871.0	2.35	2.88	0.53	2.35	0.00
		10.8	871.0	3.78	4.15	0.37	3.72	-0.06
		10.8	871.0	4.13	4.16	0.03	4.14	0.01
		10.8	871.0	3.8	3.83	0.03	3.80	0.00
10.8	871.0	3.32	3.71	0.39	3.14	-0.18		
10.8	871.0	2.78	3.51	0.73	2.78	0.00		
10.8	871.0	4.3	4.41	0.11	4.29	-0.01		
10.8	871.0	4.31	4.65	0.34	4.31	0.00		

**Table 45, Continued**

Data	Debris Basin	Area (mi <sup>2</sup> )	Rr (ft/mi)	Measured Dy (log, yd <sup>3</sup> /mi <sup>2</sup> )	USACE Estimated Unit Dy (log, yd <sup>3</sup> /mi <sup>2</sup> )	Diffe <sup>1</sup>	ANN Estimated Unit Dy (log, yd <sup>3</sup> /mi <sup>2</sup> )	Diffe <sup>2</sup>
Calibration Data	San Dimas Gate Dam	16.2	501.2	3.87	3.91	0.04	<b>4.31</b>	<b>0.44</b>
		16.2	501.2	3	3.08	0.08	2.98	-0.02
		16.2	501.2	3.08	3.24	0.16	3.16	0.08
		16.2	501.2	2.78	3.02	0.24	2.78	0.00
		16.2	501.2	4.03	4.02	-0.01	4.01	-0.02
		16.2	501.2	4.1	4.15	0.05	4.11	0.01
		16.2	501.2	3	3.04	0.04	3.00	0.00
		16.2	501.2	3.04	3.06	0.02	3.04	0.00
		16.2	501.2	3.38	3.60	0.22	3.38	0.00
		16.2	501.2	3.32	3.32	0.00	3.25	-0.07
		16.2	501.2	3.98	4.20	0.22	3.98	0.00
		16.2	501.2	4.45	<b>4.39</b>	<b>-0.06</b>	4.45	0.00
		16.2	501.2	2.48	2.85	0.37	2.48	0.00
		16.2	501.2	3.66	3.80	0.14	3.66	0.00
		16.2	501.2	3.2	3.61	0.41	3.20	0.00
		16.2	501.2	3.38	3.47	0.09	3.38	0.00
		16.2	501.2	2.3	2.68	0.38	2.30	0.00
		16.2	501.2	3.7	3.96	0.26	3.70	0.00
16.2	501.2	4.29	4.59	0.30	4.30	0.01		
16.2	501.2	4.3	4.32	0.02	4.30	0.00		
Validation Data	Santa Anita Dam	10.8	871.0	2.95	3.25	0.30	2.99	0.04
		10.8	871.0	3.67	4.12	0.45	3.78	0.11
		10.8	871.0	2.48	<b>3.13</b>	<b>0.65</b>	2.59	0.11
	San Dimas Gate Dam	16.2	501.2	2.84	3.07	0.23	<b>2.96</b>	<b>0.12</b>
		16.2	501.2	4.02	4.19	0.17	4.10	0.08
		16.2	501.2	3.63	3.61	-0.02	<b>3.54</b>	<b>-0.09</b>
		16.2	501.2	4.17	<b>4.08</b>	<b>-0.09</b>	4.24	0.07
16.2	501.2	3.76	4.07	0.31	3.85	0.09		
16.2	501.2	2.9	3.39	0.49	2.93	0.03		

Diffe<sup>1</sup> - Difference between measured debris yield and the estimated values using the USACE method.

Diffe<sup>2</sup> - Difference between measured debris yield and the estimated values using ANN model.

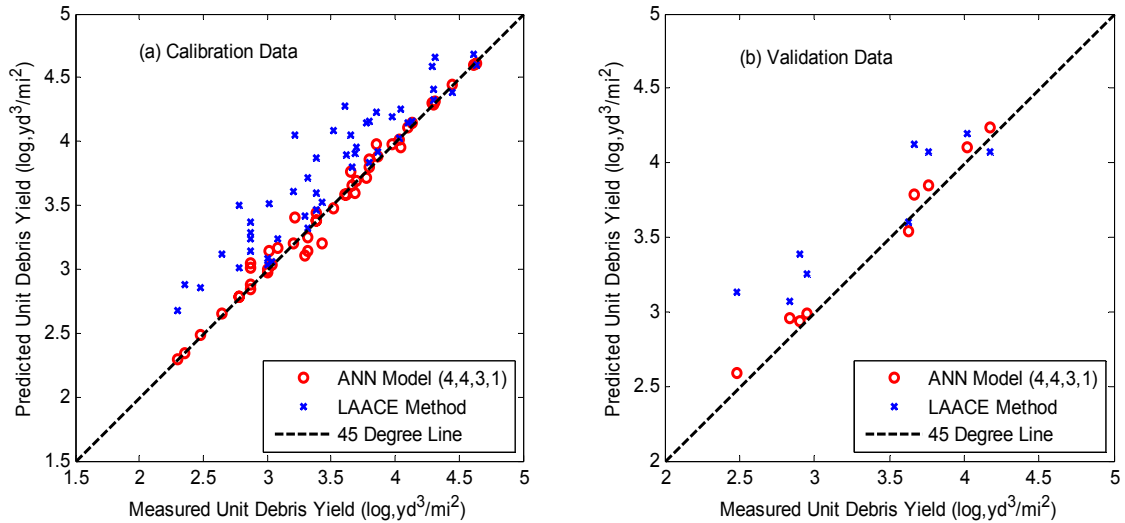


**Figure 62:** Comparison between measured, USACE, and the best ANN model (4,4,3,1) estimated unit debris yield for Case 13

#### 4.2.11 Case 14

There is another empirical equation (Equation 4.2) formulated by the USACE (2000) for estimating unit debris yield collected from watershed with area between 25 and 50 square miles.

$$\log Dy = 0.94(\log Q) + 0.32(\log RR) + 0.14(\log A) + 0.17(FF) \quad (4.2)$$

Every parameter within the equation is the same as in Equation 4.1 and the only difference between those two equations is the coefficients. This equation is developed based on 22 data records documented at Pacoima Dam debris basin, 20 records at Devil's Gate Dam debris basin, and 22 records at Cogswell Dam debris basin (Figure 4). These 64 data records are separated into two data sets, one for calibration and the other for validation by using subtractive clustering method. The calibration data consists of 19 data records from Pacoima

Dam debris basin, 16 data records from Devil's Gate Dam debris basin, and 17 data records from Cogswell Dam debris basin. The remaining 12 data records are saved for validation purpose.

Before training the ANN models, the same procedure to preprocess the data such as normalization, removal of the correlation between input vectors if there is any, and reduction of input dimensions are implemented. The LM training algorithm is the only training algorithm used. The internal parameters such as epoch size, calibration data error goal, transfer function, and so on are identical to those in Case 13. Only a few neural networks are calibrated and an excellent performance is achieved before long by a neural network with four and five neurons on the first and second hidden layer. The network is capable of estimating 52 calibration data with 0.00200 MSE and 12 validation data with 0.00998 MSE, and the correlation coefficient is 0.996 for the calibration data (Figure 63(a)) and 0.987 for the validation data (Figure 63(b)). The correlation coefficients and the slopes of the linear regression lines are very close to one that indicates this neural network is a perfect model for estimating unit debris yield collected from watersheds area ranging from 25 and 50 square miles.

The 64 measured and estimated unit debris yield by the USACE method and the neural network (4,5,5,1) are listed in Table 46 and they are compared graphically in Figure 64. For the calibration data, the USACE can estimate the 52 unit debris yield with a small MSE, 0.07786, and a small error range, [-0.70, 0.55], however the neural network (4,4,5,1) reduces the error to 0.00200 and

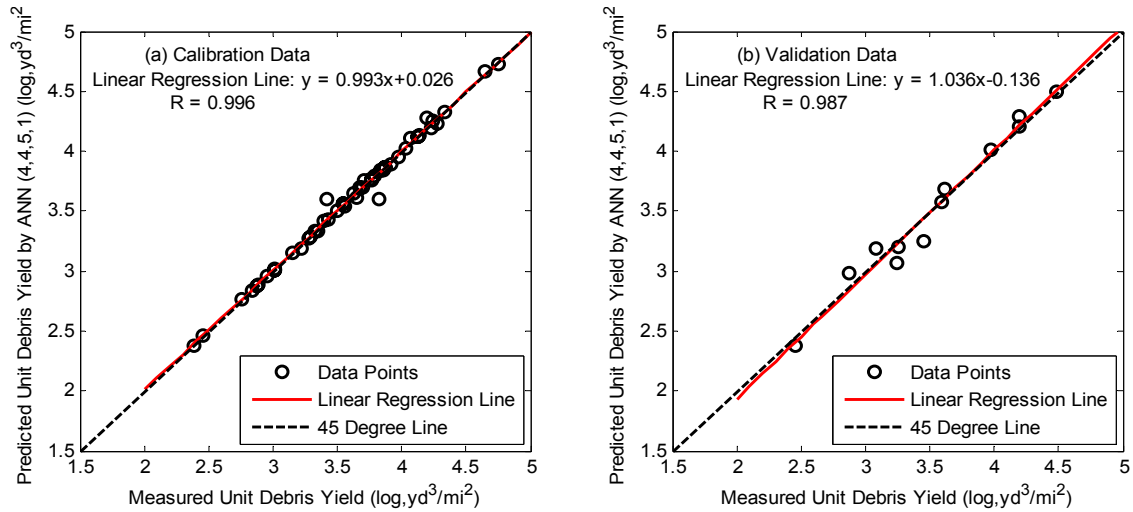


**Figure 63:** Linear regression analysis between measured and ANN model estimated debris yield (a) Calibration Data Set (b) Validation Data Set for Case 14

shortens the error range to [-0.22, 0.18]. It is also true for the validation data; the error range of the estimation by the USACE method is [-0.38, 0.49], and the MSE is 0.072161; the neural network model (4,4,5,1) lowers the error range to [-0.12, 0.20], and the MSE is only 0.00998. It appears that this neural network model (4,4,5,1) is much better-performed than the USACE method. It can be further demonstrated in Figure 64; the blue marks envelop the red circles in both figure (a) and (b) with the dashed 45 degree line. As a final conclusion, neural network model is more suitable than the USACE method for the estimation of unit debris yield from larger watershed with area between 25 and 50 square miles.

**Table 46:** Measured, the USACE method, and the best ANN model (4,4,5,1) estimated unit debris yield for Case 14

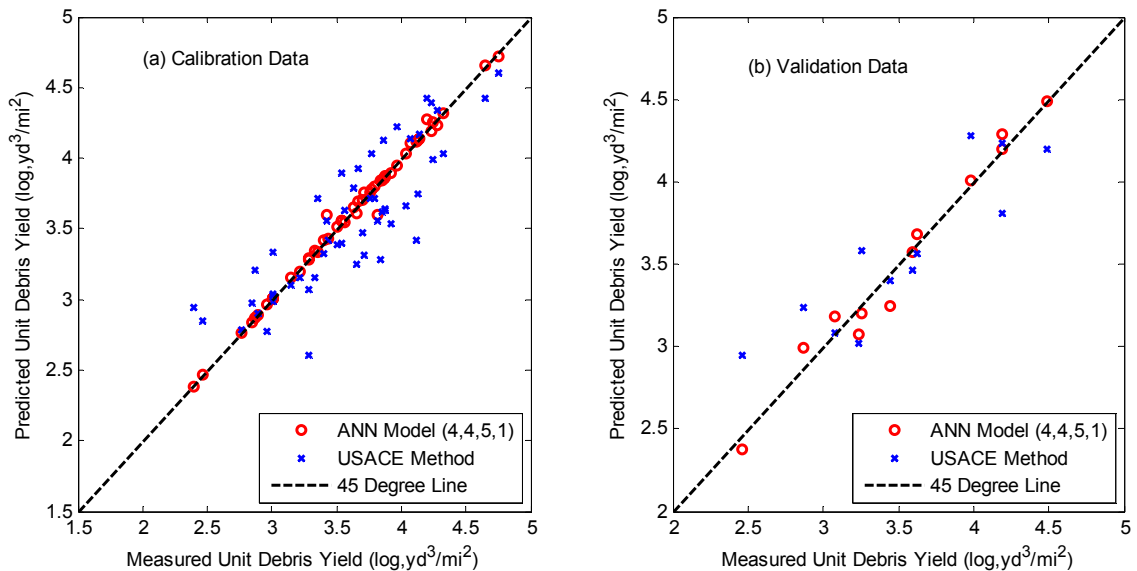
Data	Debris Basin	Area (mi <sup>2</sup> )	Rr (ft/mi)	Measured Dy (log, yd <sup>3</sup> /mi <sup>2</sup> )	USACE Estimated Unit Dy (log, yd <sup>3</sup> /mi <sup>2</sup> )	Diffe <sup>1</sup>	ANN Estimated Unit Dy (log, yd <sup>3</sup> /mi <sup>2</sup> )	Diffe <sup>2</sup>
Calibration Data	Pacoima Dam	28.2	223.9	3.70	3.47	-0.23	3.70	0.00
		28.2	223.9	3.71	3.31	-0.40	3.76	0.05
		28.2	223.9	3.87	3.63	-0.24	3.87	0.00

Table 46, Continued

Data	Debris Basin	Area (mi <sup>2</sup> )	Rr (ft/mi)	Measured Dy (log, yd <sup>3</sup> /mi <sup>2</sup> )	USACE Estimated Unit Dy (log, yd <sup>3</sup> /mi <sup>2</sup> )	Diffe <sup>1</sup>	ANN Estimated Unit Dy (log, yd <sup>3</sup> /mi <sup>2</sup> )	Diffe <sup>2</sup>
Calibration Data	Pacoima Dam	28.2	223.9	3.92	3.54	-0.38	3.90	-0.02
		28.2	223.9	3.65	3.25	-0.40	3.61	-0.04
		28.2	223.9	3.84	3.28	-0.56	3.84	0.00
		28.2	223.9	3.79	3.72	-0.07	3.80	0.01
		28.2	223.9	3.43	3.42	-0.01	3.43	0.00
		28.2	223.9	3.01	3.03	0.02	3.01	0.00
		28.2	223.9	2.96	2.77	-0.19	2.96	0.00
		28.2	223.9	2.76	2.78	0.02	2.76	0.00
		28.2	223.9	3.28	3.07	-0.21	3.28	0.00
		28.2	223.9	4.24	3.99	-0.25	4.25	0.01
		28.2	223.9	4.12	<b>3.42</b>	<b>-0.70</b>	4.12	0.00
		28.2	223.9	3.01	3.04	0.03	3.01	0.00
		28.2	223.9	4.14	4.17	0.03	4.14	0.00
		28.2	223.9	3.76	3.72	-0.04	3.76	0.00
		28.2	223.9	3.29	2.61	-0.68	3.29	0.00
	28.2	223.9	2.84	2.97	0.13	2.84	0.00	
	Devil's Gate Dam	31.9	331.1	3.50	3.39	-0.11	3.51	0.01
		31.9	331.1	3.54	3.40	-0.14	3.56	0.02
		31.9	331.1	3.42	3.56	0.14	<b>3.60</b>	<b>0.18</b>
		31.9	331.1	3.82	3.56	-0.26	<b>3.60</b>	<b>-0.22</b>
		31.9	331.1	3.22	3.15	-0.07	3.20	-0.02
		31.9	331.1	3.40	3.32	-0.08	3.42	0.02
		31.9	331.1	3.33	3.15	-0.18	3.34	0.01
		31.9	331.1	4.28	4.34	0.06	4.23	-0.05
		31.9	331.1	4.07	4.14	0.07	4.11	0.04
		31.9	331.1	4.65	4.42	-0.23	4.66	0.01
		31.9	331.1	3.87	3.64	-0.23	3.86	-0.01
		31.9	331.1	4.03	3.66	-0.37	4.03	0.00
		31.9	331.1	4.13	3.75	-0.38	4.13	0.00
		31.9	331.1	3.85	3.62	-0.23	3.84	-0.01
		31.9	331.1	3.63	3.79	0.16	3.65	0.02
	31.9	331.1	4.33	4.03	-0.30	4.32	-0.01	
	Cogswell Dam	39.2	426.6	3.97	4.22	0.25	3.95	-0.02
		39.2	426.6	3.86	4.13	0.27	3.85	-0.01
		39.2	426.6	3.77	4.03	0.26	3.78	0.01
		39.2	426.6	4.20	4.42	0.22	4.28	0.08
		39.2	426.6	4.23	4.39	0.16	4.19	-0.04
		39.2	426.6	2.87	3.21	0.34	2.87	0.00
		39.2	426.6	3.01	3.33	0.32	3.01	0.00
		39.2	426.6	3.01	2.99	-0.02	3.01	0.00
		39.2	426.6	2.89	2.90	0.01	2.89	0.00

**Table 46, Continued**

Data	Debris Basin	Area (mi <sup>2</sup> )	Rr (ft/mi)	Measured Dy (log, yd <sup>3</sup> /mi <sup>2</sup> )	USACE Estimated Unit Dy (log, yd <sup>3</sup> /mi <sup>2</sup> )	Diffe <sup>1</sup>	ANN Estimated Unit Dy (log, yd <sup>3</sup> /mi <sup>2</sup> )	Diffe <sup>2</sup>
Calibration Data	Cogswell Dam	39.2	426.6	3.15	3.10	-0.05	3.15	0.00
		39.2	426.6	2.39	<b>2.94</b>	<b>0.55</b>	2.38	-0.01
		39.2	426.6	2.46	2.85	0.39	2.47	0.01
		39.2	426.6	3.54	3.90	0.36	3.56	0.02
		39.2	426.6	3.35	3.71	0.36	3.33	-0.02
		39.2	426.6	3.67	3.93	0.26	3.69	0.02
		39.2	426.6	3.56	3.63	0.07	3.55	-0.01
Validation Data	Pacoima Dam	28.2	223.9	3.62	3.56	-0.06	3.68	0.06
		28.2	223.9	3.08	3.08	0.00	3.18	0.10
		28.2	223.9	4.49	4.20	-0.29	4.49	0.00
	Cogswell Dam	39.2	426.6	3.98	4.28	0.30	4.01	0.03
		39.2	426.6	2.87	3.24	0.37	<b>2.99</b>	<b>0.12</b>
		39.2	426.6	2.46	<b>2.95</b>	<b>0.49</b>	2.38	-0.08
		39.2	426.6	3.26	3.58	0.32	3.20	-0.06
	Devil's Gate Dam	39.2	426.6	3.45	3.40	-0.05	<b>3.25</b>	<b>-0.20</b>
		31.9	331.1	3.59	3.46	-0.13	3.57	-0.02
		31.9	331.1	3.24	3.02	-0.22	3.07	-0.17
		31.9	331.1	4.19	4.23	0.04	4.29	0.10
		31.9	331.1	4.19	<b>3.81</b>	<b>-0.38</b>	4.20	0.01



**Figure 64:** Comparison between measured, USACE, and the best ANN model (4,4,5,1) estimated unit debris yield for Case 14

#### 4.2.12 Case 15

The last empirical equation (Equation 4.3) developed by the USACE (2000) is for predicting the unit debris yield at watershed with area ranging from 50 to 200 square miles.

$$\log Dy = 1.02(\log Q) + 0.23(\log RR) + 0.16(\log A) + 0.13(FF) \quad (4.3)$$

Every term in this equation is the same as introduced in Equation 4.1 and 4.2. The equation was formulated based on 66 unit debris yield data records; 36 data records were documented at Big Tujunga Dam debris basin and the rest 30 is from San Gabriel Dam debris basin (Figure 4).

The subtractive clustering method is applied to divide the whole data into two groups; one is for calibration and the other is for validation. There are 54 data records within the calibration data set and 12 data records within the validation data set. The data is preprocessed to be normalized and uncorrelated before presenting to neural network for training. A neural network with four and five neurons on the first and second hidden layer is trained by the LM training algorithm while all the internal parameters are the same as in Case 13 and 14. This network is capable of simulating the 54 calibration data with 0.00324 MSE and the 12 validation data with 0.00765 MSE. The data points with measured unit debris yield as x value and estimated unit debris yield as y value are plotted in Figure 65 along with their linear regression line. In Figure 65(a), the correlation coefficient of the calibration data is 0.996 and the slope of the linear regression line is 0.993; both of which are very close to one. As plotted in Figure 65(b), the

validation data has a high correlation coefficient – 0.987, and a high slope of the linear regression line – 0.974. Because two data points overlap in figure (b), thus, only 11 data points are shown in the figure. Further considering the distribution of the data points in these figures, the neural network (4,4,5,1) is a very well-trained model for estimating the unit debris yield collected from larger watersheds with area between 50 square miles and 200 square miles.

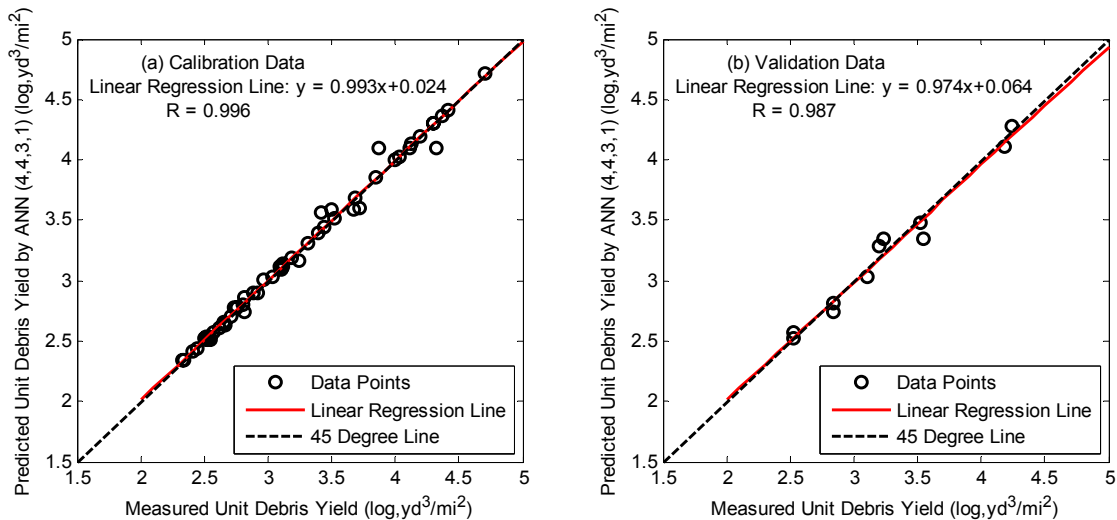


**Figure 65:** Linear regression analysis between measured and ANN model estimated debris yield (a) Calibration Data Set (b) Validation Data Set for Case 15

The 66 unit debris yield data records with their collection basin name, area, relief ratio, measured, and estimated values by the USACE method and the neural network (4,4,5,1) are presented in Table 47. For the calibration data, the error range between measured and the estimated unit debris yield by the USACE method is  $[-0.36, 0.51]$ , and the MSE is 0.03245; the MSE achieved by the neural network is ten times smaller, 0.00324, and the error range is  $[-0.22, 0.23]$ . Regarding the validation data, the MSEs are 0.01296 and 0.00764 accomplished

by the USACE method and the neural network, respectively; the error range is [-0.14, 0.29] by using the USACE empirical equation, and it is [-0.21, 0.12] by using the network. Figure 66 is provided as a more direct means to compare the results obtained by using these two methods. In figure (a), the red circles scatter much closer to the 45 degree line than the blue marks; in figure (b), all symbols stay very close to the 45 degree line except one blue mark that seriously deteriorates the USACE method performance. All the comparisons lead to conclusion that ANN technique is more accurate than the USACE method for estimating unit debris yield from larger watersheds with area between 50 and 200 square miles.

**Table 47:** Measured, the USACE method, and the best ANN model (4,4,5,1) estimated unit debris yield for Case 15

Data	Debris Basin	Area (mi <sup>2</sup> )	Rr (ft/mi)	Measured Dy (log, yd <sup>3</sup> /mi <sup>2</sup> )	USACE Estimated Unit Dy (log, yd <sup>3</sup> /mi <sup>2</sup> )	Diffe <sup>1</sup>	ANN Estimated Unit Dy (log, yd <sup>3</sup> /mi <sup>2</sup> )	Diffe <sup>2</sup>
Calibration Data	Big Tujunga Dam	82.0	288.4	2.55	2.52	-0.03	2.52	-0.03
		82.0	288.4	2.57	2.54	-0.03	2.58	0.01
		82.0	288.4	2.50	2.58	0.08	2.53	0.03
		82.0	288.4	2.44	2.51	0.07	2.43	-0.01
		82.0	288.4	2.65	2.63	-0.02	2.66	0.01
		82.0	288.4	2.71	2.68	-0.03	2.71	0.00
		82.0	288.4	2.33	2.31	-0.02	2.34	0.01
		82.0	288.4	2.52	2.54	0.02	2.53	0.01
		82.0	288.4	2.52	2.50	-0.02	2.52	0.00
		82.0	288.4	2.41	2.41	0.00	2.42	0.01
		82.0	288.4	2.67	2.72	0.05	2.63	-0.04
		82.0	288.4	2.89	3.20	0.31	2.89	0.00
		82.0	288.4	2.80	3.10	0.30	2.80	0.00
		82.0	288.4	2.76	3.06	0.30	2.78	0.02
		82.0	288.4	3.19	3.28	0.09	3.19	0.00
		82.0	288.4	3.52	3.52	0.00	3.51	-0.01
		82.0	288.4	3.42	3.56	0.14	3.56	0.14
82.0	288.4	3.72	3.65	-0.07	3.60	-0.12		
82.0	288.4	3.09	3.10	0.01	3.11	0.02		

Table 47, Continued

Data	Debris Basin	Area (mi <sup>2</sup> )	Rr (ft/mi)	Measured Dy (log, yd <sup>3</sup> /mi <sup>2</sup> )	USACE Estimated Unit Dy (log, yd <sup>3</sup> /mi <sup>2</sup> )	Diffe <sup>1</sup>	ANN Estimated Unit Dy (log, yd <sup>3</sup> /mi <sup>2</sup> )	Diffe <sup>2</sup>
Calibration Data	Big Tujunga Dam	82.0	288.4	2.92	2.92	0.00	2.90	-0.02
		82.0	288.4	3.24	3.22	-0.02	3.16	-0.08
		82.0	288.4	4.11	4.17	0.06	4.10	-0.01
		82.0	288.4	3.87	4.11	0.24	<b>4.10</b>	<b>0.23</b>
		82.0	288.4	4.32	4.00	-0.32	<b>4.10</b>	<b>-0.22</b>
		82.0	288.4	4.37	4.40	0.03	4.37	0.00
		82.0	288.4	3.12	3.04	-0.08	3.14	0.02
		82.0	288.4	2.82	2.83	0.01	2.86	0.04
		82.0	288.4	2.52	2.39	-0.13	2.52	0.00
	82.0	288.4	3.68	3.92	0.24	3.69	0.01	
	161.6	436.5	3.50	3.38	-0.12	3.59	0.09	
	161.6	436.5	3.40	3.40	0.00	3.40	0.00	
	161.6	436.5	3.67	3.38	-0.29	3.59	-0.08	
	161.6	436.5	3.44	3.15	-0.29	3.44	0.00	
	161.6	436.5	4.19	4.07	-0.12	4.19	0.00	
	161.6	436.5	4.00	4.09	0.09	4.00	0.00	
	161.6	436.5	4.30	4.34	0.04	4.30	0.00	
	161.6	436.5	4.13	<b>3.77</b>	<b>-0.36</b>	4.13	0.00	
	161.6	436.5	4.03	3.80	-0.23	4.03	0.00	
	161.6	436.5	4.41	4.34	-0.07	4.41	0.00	
	161.6	436.5	2.81	2.72	-0.09	2.74	-0.07	
	161.6	436.5	2.73	2.77	0.04	2.77	0.04	
	161.6	436.5	2.97	2.87	-0.10	3.01	0.04	
	161.6	436.5	2.51	2.62	0.11	2.54	0.03	
	161.6	436.5	2.54	2.96	0.42	2.54	0.00	
	161.6	436.5	2.65	3.06	0.41	2.65	0.00	
	161.6	436.5	3.03	<b>3.54</b>	<b>0.51</b>	3.03	0.00	
	161.6	436.5	3.31	3.17	-0.14	3.31	0.00	
	161.6	436.5	4.71	4.60	-0.11	4.71	0.00	
161.6	436.5	3.11	2.89	-0.22	3.10	-0.01		
161.6	436.5	3.12	2.90	-0.22	3.12	0.00		
161.6	436.5	2.62	2.52	-0.10	2.60	-0.02		
161.6	436.5	2.34	2.33	-0.01	2.34	0.00		
161.6	436.5	3.85	3.86	0.01	3.85	0.00		
161.6	436.5	4.30	4.30	0.00	4.30	0.00		
Validation Data	Big Tujunga Dam	82.0	288.4	2.52	2.57	0.05	2.57	0.05
		82.0	288.4	2.52	2.54	0.02	2.52	0.00
		82.0	288.4	2.84	<b>3.13</b>	<b>0.29</b>	2.82	-0.02
		82.0	288.4	3.52	3.45	-0.07	3.48	-0.04
		82.0	288.4	3.23	3.28	0.05	<b>3.35</b>	<b>0.12</b>
		82.0	288.4	4.18	4.16	-0.02	4.11	-0.07

**Table 47, Continued**

Data	Debris Basin	Area (mi <sup>2</sup> )	Rr (ft/mi)	Measured Dy (log, yd <sup>3</sup> /mi <sup>2</sup> )	USACE Estimated Unit Dy (log, yd <sup>3</sup> /mi <sup>2</sup> )	Diffe <sup>1</sup>	ANN Estimated Unit Dy (log, yd <sup>3</sup> /mi <sup>2</sup> )	Diffe <sup>2</sup>
Validation Data	San Gabriel Dam	161.6	436.5	3.55	3.43	-0.12	<b>3.34</b>	<b>-0.21</b>
		161.6	436.5	4.24	4.13	-0.11	4.28	0.04
		161.6	436.5	2.84	<b>2.70</b>	<b>-0.14</b>	2.74	-0.10
		161.6	436.5	3.20	3.08	-0.12	3.28	0.08
		161.6	436.5	3.10	3.08	-0.02	3.03	-0.07

Diffe<sup>1</sup> - Difference between measured debris yield and the estimated values using the USACE method.

Diffe<sup>2</sup> - Difference between measured debris yield and the estimated values using ANN model.

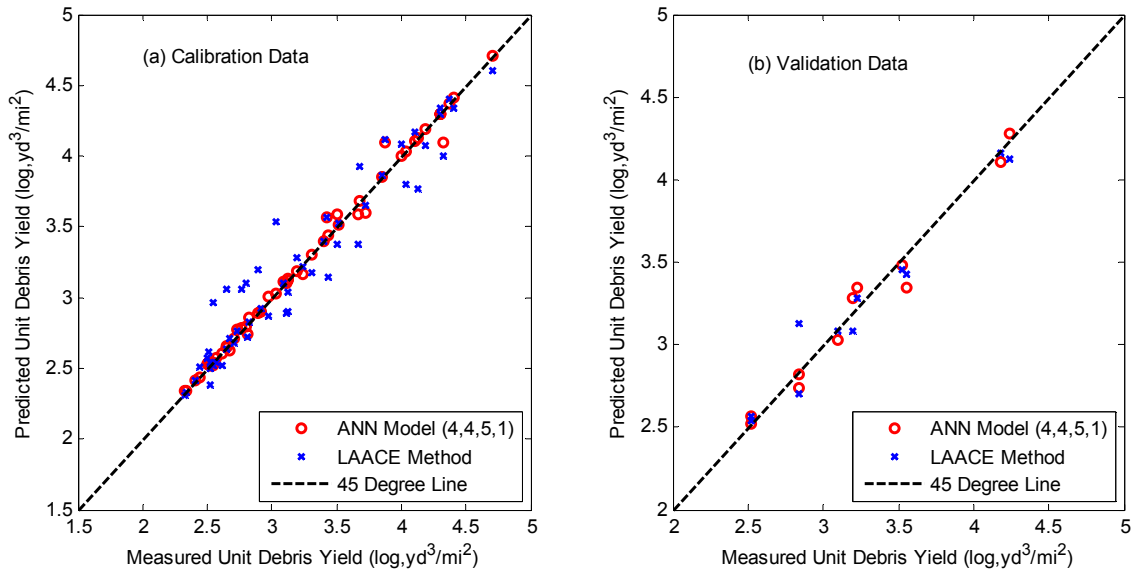


**Figure 66:** Comparison between measured, USACE, and the best ANN model (4,4,5,1) estimated unit debris yield for Case 15

## Chapter 5: Summary and Conclusion

### 5.1 Summary and Conclusion

The feasibility of applying Artificial Neural Network (ANN) models for accurately estimating accumulated debris yields resulting from wildfire and a series of storm events for 14 debris basins from 1984 to 2003 within Los Angeles County are examined in this study. The first set of ANN models are trained by 300 training samples with five input parameters such as drainage area, watershed relief ratio, maximum one-hour rainfall intensity, total rainfall amount, and fire factor. The second set of ANN models are trained by the same number of input parameter but with less training samples, i.e. 244, after the removal of some questionable data records. The third set has the same number of training samples as the second one but more input parameters such as the percentage of the area that was burned by wildfire within the watershed in the last 10 years, time after the last fire event, and the number of the antecedent effective rainfall event. The comparison of the estimate error of sequent debris yield among the first three best-performed ANN models indicates the performance of the third ANN model (8,3,2,1) is equivalently good as the second ANN model (5,3,4,1). Both models are superior to the first ANN model (5,6,2,1). With errors as little as  $8.5 \times 10^{-4}$  and correlation coefficients as high as 1.000, all these three ANN models achieve the desired level of accuracy. The first best-performed ANN model (5,6,2,1) is capable of estimating 12 data records of accumulated debris

yield more accurate than the MSDPM (Pak, 2005) statistical model and worse in 3 data records. The best-fit ANN model (5,3,4,1) among all the second set of ANN models is capable of predicting sediment yields with higher accuracy than the MSDPM statistical model. The inclusion of three additional input variables in the third ANN model does not lead to a better overall performance. In addition, the results reinforce the theory that the smaller the ratio between the standard error estimate ( $S_e$ ) and the standard deviation ( $S_y$ ) of the target values, the better is the modeling accuracy.

Four artificial intelligence models including one set of ANN models trained by the Bayesian Regulation Backpropagation (BRBP) algorithm, one set of ANN models trained by the Levenberg-Marquardt (LM) algorithm, Adaptive-Network-Based Fuzzy Inference System (ANFIS) model, and Generalized Dynamic Fuzzy Neural Network (GD-FNN) model are applied to simulate unit debris yield collected from 36 small debris basins with upstream drainage area less than 3 square miles from 1938 to 1983 within Los Angeles County. The relative importance of four watershed morphological parameters such as elongation ratio, drainage density, hypsometric index, and mean bifurcation ratio are analyzed. The comparison of modeling accuracy among four sets of models trained by different numbers of input parameters reveals that both the drainage density and the hypsometric index are important input parameters but the elongation ratio and the mean bifurcation ratio are not important and should be eliminated for modeling unit debris yield.

349 unit debris yield data records documented at 80 small debris basins from 1938 to 1983 within Los Angeles County are classified into five groups based on the relief ratios of their watersheds, and each group of data is modeled by only ANN models trained by the LM algorithm based on four input parameters (i.e. log transformed watershed area, logarithmic relief ratio, logarithmic value of maximum one hour precipitation times 100, and fire factor).

Three soil properties like soil erodibility factor, permeability rate, and liquid limit are included as input parameter one by one to study their impact on the simulation. The only exception is the fifth group of data because all the watersheds are within the same soil map unit; in other words, the values of three soil properties are identical for all the watersheds. This study demonstrates that ANN models achieve satisfactory modeling results and their performance is improved by the inclusion of some soil properties compared with the original models trained by only four basic input parameters. For example, the inclusion of soil erodibility factor enhances the ANN models performance on the estimation of unit debris yield collected from small watersheds with mild slope (i.e. relief ratio is between 58 m/km and 185 m/km); but the permeability rate and liquid limit do not contribute as much. However, the modeling of unit debris yield collected from small watershed with steep slope (i.e. relief ratio is between 185 m/km and 250 m/km) appears to be more successful when soil permeability rate and liquid limit are included as input parameters. The modeling results achieved by ANN models trained with additionally two soil properties - soil erodibility factor and liquid limit

especially with the latter parameter are more accurate for estimating unit debris yield collected from small watersheds with steeper slope, (i.e. relief ratio is between 250 m/km and 305 m/km). Soil permeability rate is the most important soil property for simulating unit debris yield from small watersheds with extreme steep slope (i.e. relief ratio is between 305 m/km and 375 m/km), soil erodibility factor is fair, but liquid limit is the one that has a worse impact on the simulation. An ANN model is capable of estimating unit debris yield data from small watershed with the steepest slope (i.e. relief ratio is between 375 m/km and 525 m/km) with higher accuracy even without soil properties as input parameters. The comparison between all the best-fit ANN models and the modeling results obtained by using the empirical equation developed by the USACE (2000) indicates that the training and testing accuracy of the ANN models is comparatively higher than that of the USACE method.

ANN technique is further applied to estimate unit debris yield collected from large watersheds with area between 10 and 25 square miles based on four input parameters, relief ratio, unit peak discharge, watershed area, and fire factor; the same data used by the USACE to create their regression equation. A randomly selected four-layered ANN model is able to reproduce most unit debris yield very close to their measured values and the simulation accuracy for the validation data is as good as that of the calibration data. The USACE also developed another two empirical equations; one is for debris basins with larger watersheds (i.e. area is in the range of 25-50 square miles), and the other is for

debris basins from much larger watersheds with area ranging from 50 to 200 square miles. A few randomly selected ANN models are trained by the same data and excellent modeling results are achieved even without the need of searching among a number of ANN models. The accuracy of unit debris yield predicted by the ANN models is significantly higher than that of the USACE regression equations.

Through the training of thousands of neural network models in this study, a number of major findings regarding the neural network geometry can be drawn as follows.

1. There appears to be an improvement on the modeling accuracy with an increase in the number of hidden neurons up to a certain point for three-layered ANN models. Although there is some variation in the generalization ability of the networks with two hidden layers, there appears to be such a trend that increasing the number of the neuron in the hidden layers improves the performance meanwhile it increases the risk of overfitting. The best ANN model is the one with balanced performance between the calibration and validation data.
2. The ANN models with two hidden layers have better generalization ability than the neural networks with one hidden layer most of the time. This finding strongly recommends using ANN models with two hidden layers as a start for modeling any practical problems.

3. The simulation results indicate that the optimal number of neuron in the hidden layer is not only a function of the number of input parameters but also a function of the number of training samples.
4. Based on the results from Case 4 to Case 7, the neural networks trained by the LM algorithm always achieve smaller errors and higher correlation coefficients than the ANN models trained by the BRBP algorithm. The reason might be the early termination of the calibration process to prevent overfitting by the BRBP algorithm. The modeling results also show ANN models trained by the LM algorithm are more accurate than both the ANFIS and the GD-FNN model because the LM training algorithm is more robust than the combination of back-propagation gradient descent method and sequential least squares method employed by ANFIS model and Linear Least Squares method employed by the GD-FNN model. It is noteworthy that ANN models trained by the BRBP algorithm achieve similar performance as the ANFIS models and both models always work better than the GD-FNN models especially for the calibration data.
5. Another important finding is more training samples do not necessarily improve neural network modeling efficiency. Higher ratio of the number of calibration data to the number of connection weights and biases does not lead to a better simulation. This study also demonstrates that the addition of more input parameters does not necessarily enhance the neural network performance.

6. The selection calibration and validation data plays a very important role in the neural network modeling success. As a novel approach, the clustering subtractive method used for the separation of calibration and validation in eight studied cases appears to be a better alternative than the random separation. Some studies reported that ANN performance deteriorates when the validation data is out of the range used for the calibration data. It is not the case in this study because the sediment yield collected from Brand Debris basin in the first three cases are roughly 2.4 times greater than the maximum sediment yield used for training, the best prediction of sediment yield achieved by an ANN model in the first case are not accurate enough, but there is an ANN model within the second case provided more desirable estimations.
7. ANN models are viable tools for estimating sediment yield resulting from a series of storm event or from a significant storm event. This study shows that ANN models provide higher accuracy than the MSDPM statistical model for the accumulated debris yield and they are also superior to four regression equations prepared by the USACE for estimating unit debris yield for watersheds with area ranging from 0.1 mi<sup>2</sup> to 3 mi<sup>2</sup>, and from 10 mi<sup>2</sup> to 200 mi<sup>2</sup>. The capability of ANN models to accurately predict sequent and unit debris yield worth its time-consuming training process and its easy application for future event is another advantage.

## **5.2 Recommendation for Future Study**

The modeling of unit debris yield collected from large watersheds (i.e. area is from 10 square miles to 200 square miles) is more successful than the modeling of unit debris yield from small watersheds (i.e. area is less than 3 square miles), the reason is the inclusion of unit peak discharge as input parameter for large watersheds. As we all know, peak discharge is highly related to debris yield but it is only collected at large watershed. For small watersheds, a well-acknowledged runoff simulation tool, Hydrologic Engineering Center – Hydrologic Modeling System (HEC-HMS) can be applied to estimate peak discharge. It might be a good approach to further improve estimation accuracy of unit debris yield collected from small watersheds.

## References

Abbott, M.B., Bathurst, J.C., Cunge, J.A., O'Connell, P. E., and Rasmussen, J. (1986a) "An Introduction of European Hydrological System-SystPme Hydrologique Europeen, 'SHE', 1: History and philosophy of a physically-based, distributed modeling system." *Journal of Hydrology*, Vol.87, No. 1-2, p45-59.

Abbott, M.B., Bathurst, J.C., Cunge, J.A., O'Connell, P.E. and Rasmussen, J., (1986b). "An introduction to the European Hydrological System-Systemme Hydrologique Europeen, 'SHE', 2: Structure of a physically-based, distributed modelling system." *Journal of Hydrology*, Vol.87, No. 1-2, p61-77.

ASCE Task Committee on Application of Artificial Neural Networks in Hydrology (2000, a) "Artificial Neural Networks in Hydrology: I. Preliminary Concepts", *Journal of Hydrologic Engineering*, Vol. 5, No. 2, April 2000, p115-123

ASCE Task Committee on Application of Artificial Neural Networks in Hydrology (2000, b) "Artificial Neural Networks in Hydrology: II. Hydrologic Applications", *Journal of Hydrologic Engineering*, Vol. 5, No. 2, April 2000, p124-137

Beasley, D. B., Huggins, L. F. and Monke, E. J. (1980). "ANWERS: a Model for Watershed Planning", *Trans., American Society of Agricultural Engineers*, Vol.23, p938-944

Bebis, G., Georgiopoulos, M. (1994). "Feed-Forward Neural Networks: Why Network Size is So Important", *IEEE Potentials* October/November, p27-31

Bennett, J. P. (1974). "Concepts of Mathematical Modeling of Sediment Yield", *Water Resources Research*, Vol.10, No.3, p485-492

Buckley, J. J. (1993). "Sugeno Type Controllers are Universal Controllers", *Fuzzy Sets System*, Vol.53, p299-303

Chang, N. B., Chen, H. W., and Ning, S. K. (2001). "Identification of River Water Quality using the Fuzzy Synthetic Evaluation Approach", *Journal of Environmental Management*, Vol.63, No.3, p293-305

Chau, K. W., Wu, C. L., and Li, Y. S. (2005). "Comparison Of Several Flood Forecasting Models In Yangtze River", *Journal of Hydrological Engineering*, Vol.10, No.6, p485-491

Chaves, P. and Kojiri, T. (2007). "Deriving Reservoir Operational Strategies Considering Water Quantity and Quality Objectives by Stochastic Fuzzy Neural Networks", *Advances in Water Resources*, in press

Coppola, E. Jr., Szidarovszky, F., Poulton, M. and Charles, E. (2003). "Artificial Neural Network Approach for Predicting Transient Water Levels in a Multilayered Groundwater System under Variable State, Pumping, and Climate Conditions", *Journal of Hydrologic Engineering*, Vol.8, No.6, p348-360

Dayhoff, Judith E. (1990). "Neural Network Architectures: An Introduction".

Deka, P. and Chandramouli, V. (2005). "Fuzzy Neural Network Model for Hydrologic Flow Routing", *Journal of Hydrologic Engineering*, Vol.10, No.4, p302-314

Doten, C. O., Bowling, L. C., Lanini, J. S., Maurer, E. P., and Lettenmaier, D. P. (2006). "A Spatially Distributed Model for the Dynamic Prediction of Sediment Erosion and Transport in Mountainous Forested Watersheds", *Water Resources Research*, Vol.42,

Bowden, G. J., Maier, H. R., and Dandy, G. C. (2002). "Optimal Division of Data for Neural Network Models in Water Resources Applications", *Water Resources Research*, Vol.38, No.2, from p2-1 to p2-11

Ferrell, W. R. (1959). "Debris Reduction Studies for Mountain Watersheds", Los Angeles County Flood Control District, Rept.; p164

Flood, I., and Kartam, N. (1994). "Neural Networks in Civil Engineering. 1. Principles and Understanding", Journal of Computing in Civil Engineering, Vol.8, No.2, p131-148

Fortin, V., Ouarda, T. B. M. J., and Bobee, B. (1997). "Comment on 'The Use Of Artificial Neural Networks for the Prediction of Water Quality Parameters' by H.R. Maier And G.C. Dandy", Water Resources Research, Vol.33, No.10, p2423-2424

Gupta, S. K., and Solomon, S. I. (1977a). "Distributed Numerical Model for Estimating Runoff and Sediment Discharge of Ungauged Rivers. 1. The Information System". Water Resources Research, Vol.13, No.3, p613-618

Gupta, S. K., and Solomon, S. I. (1977b). "Distributed Numerical Model for Estimating Runoff and Sediment Discharge of Ungauged Rivers. 2. Model Development". Water Resources Research, Vol.13, No.3, p619-629

Hagan, M. T., Demuth, H. B., and Beale, M. (1996). "Neural Network Design"

Half. A. H., Half, H. M., and Azmoodeh, M. (1993). "Predicting Runoff From Rainfall Using Neural Networks, Proc.", Engineering Hydrology, ASCE, New York, p760-765

Holtan, H. N. (1961). "A Concept for Infiltration Estimates in Watershed Engineering", ARS-41-51, Agricultural Research Services, USDA, p25

Huggins, L. F., and Monke, E. J. (1966). "The Mathematical Simulation of the Hydrology of Small Watersheds", Technical Report 1, Water Resources Research Center, Purdue University, West Lafayette, IN. p130

Jain, A., and Indurthy, S. K. V. P. (2003). "Comparative Analysis of Event-based Rainfall-runoff Modeling Techniques - Deterministic, Statistical, and Artificial Neural Networks", Technical Notes, Journal of Hydrologic Engineering, Vol.8, No.2, p93-98

Jain, S. K., and Chalisgaonkar, D. (2000). "Setting Up Stage-discharge Relations Using ANN", Journal of Hydrologic Engineering, Vol.5, No.4, p428-433

Jang, J. R. (1993). "ANFIS: Adaptive-Network-Based Fuzzy Inference System", IEEE Transactions on Systems, Man, and Cybernetics, Vol.23, No.3, p665-685

Kaastra, I., and Boyd, M. S. (1995). "Forecasting Futures Trading Volume Using Neural Networks", Journal of Futures Markets, Vol.15, No.8, p953-970

Kalman B. L., and Kwasny, S. C. (1992). "Why Tanh Choosing a Sigmoidal Function", In: Proceedings of the International Joint conference on Neural Networks, Baltimore, MD IEEE, New York

Kişi, Ö. (2007). "Streamflow Forecasting Using Different Artificial Neural Network Algorithms", Journal of Hydrologic Engineering, Vol.12, No.5, p532-539

Kitanidis, P. K., and Bras, R. L. (1980a). "Adaptive Filtering Through Detection of Isolated Transient Errors in Rainfall-runoff Models", Water Resources Research, Vol.16, No.4, p740-748

Kitanidis, P. K., and Bras, R. L. (1980b). "Real-time Forecasting with a Conceptual Hydrological Model, 1.Analysis of Uncertainty", Water Resources Research, Vol.16, No.6, p1025-1033

Kothyari, U. C., Tiwari, A. K., and Singh, R. (1996). "Temporal Variation of Sediment Yield", J. of Hydrological Engineering, Vol.1, No.4, p169-176

Kothyari, U. C., Tiwar, A. K., and Singh, R. (1997). "Estimation of Temporal Variation of Sediment Yield from Small Catchments through the Kinematic Method", Journal of Hydrology, Vol.203, p39-57

Lee, H. Y., Lin, Y. T., and Chiu, Y. J. (2006). "Quantitative Estimation of Reservoir Sedimentation form Three Typhoon Events", Journal of Hydrologic Engineering, Vol.11, No.4, p362-370

Los Angeles County of Department of Public Works (1993). "Sedimentation Manual", Hydraulic/Water Conservation Division, June, 1993

Los Angeles County of Department of Public Works (2005). "Los Angeles Hydrologic Report"

Lustig, L. K. (1965). "Sediment Yield of the Castaic Watershed, Western Los Angeles County, California: a Quantitative Geomorphic Approach", USGS. Prof. Paper 422-f, Washington, D.C.

Maier, H. R. and Dandy, G. C. (1996). "The Use of Artificial Neural Networks for the Prediction of Water Quality Parameters", Water Resources Research, Vol. 32, No. 4, April 1996, p1013-1022

Maier, H. R. and Dandy, G. C. (1998). "The Effect of Internal Parameters and Geometry on the Performance of Back-Propagation Neural Networks: An Empirical Study", Environmental Modeling & Software, Vol. 13, 1998, p193-209

Maier, H. R. and Dandy, G. C. (2000). "Neural Networks for the Prediction and Forecasting of Water Resources Variables: A Review of Modeling Issues and Applications", Environmental Modeling & Software, Vol. 15, 2000, p101-124

Mamdani, E.H. and Assilian, S. (1975). "An experiment in Linguistic Synthesis with a Fuzzy Logic Controller," International Journal of Man-Machine Studies, Vol. 7, No. 1, pp. 1-13

Mainali, A. P. and Rajaratnam, N. (1991). "Hydraulics of Debris Flows a Review", Water Resources Engineering Report (WRE 91-2), Department of Civil Engineering, University of Alberta

Masters, T. (1993). "Practical Neural Network Recipes in C++", Academic Press, San Diego, CA

McCulloch, W. and Pitts, W. (1943). "A Logical Calculus Of The Ideas Immanent In Nervous Activity", Bulletin of Mathematical Biophysics, Vol.5, p115-133

McGee, W.J. (1897). "Sheetflood Erosion: Geological Society of America Bulletin, 8, p87-112

Mitra, S., and Hayashi, Y. (2000). "Neuro-Fuzzy Rule Generation: Survey in Soft Computing Framework", IEEE Trans. Neural Network, Vol.11, No.3, p748-768

Morisawa, M. (1957). "Accuracy of Determination of Stream Lengths from Topographic Maps", Amer. Geophys. Union Trans., Vol.38, No.1, p86-88

Pak, J. H. (2005). "A Real-time Debris Prediction Model (USCDMP) Incorporating Wildfire and Subsequent Storm Events", Ph.D. dissertation

Pak, J. H. and Lee, J. J. (2008). "A Statistical Debris Prediction Model Incorporating the Effect of Wildfires and Subsequent Storm Events", Journal of American Water Resources Association, Vol.44, Issue.3, p689-699

Pak, J. H., Kou, Z., Kwon, H. J., and Lee, J. J. (2009). "Predicting Debris Yield from Burned Watersheds: Comparison of Statistical and Artificial Neural Network Models", Journal of American Water Resources Association, Vol.45, Issue 1, p210-223

Paris, R., Di Claudio, E. D., Orlandi, G., and Rao, B. D. (1996). "A Generalized Learning Paradigm Exploiting the Structure of Feed-Forward Neural Networks", IEEE Transactions on Neural Networks, Vol.7, No.6, p1451-1460

Plaut, D. C. and Hinton, G. E. (1987). "Learning Sets Of Filters Using Back-Propagation", Computer Speech Language 2, p35-61

Raghuwanshi, N. S., Singh, R., and Reddy, L. S. (2006). "Runoff and Sediment Yield Modeling Using Artificial Neural Networks: Upper Siwane River, India", Journal of Hydrologic Engineering, Vol.11, No.1, p71-79

Ray, C. and Klindworth, K. K. (1996). "Use of Artificial Neural Networks for Agricultural Chemical Assessment of Rural Private Wells", Proc., North Am. Water and Environmental. Conf., ASCE, New York, p1687-1692

Rogers, L. L. and Dowla, F. U. (1994). "Optimization Of Groundwater Remediation Using Artificial Neural Networks With Parallel Solute Transport Modeling", Water Resources Research, Vol.30, No.2, p457-481

Rumelhart, D. E. and McClelland, J. L. (1986). "Parallel Distributed Processing: Explorations in the Microstructure of Cognition", Vol.1, Cambridge, MA, MIT Press

Scott, K. M. and Williams, R. P. (1978). "Erosion and Sediment Yield in the Transverse Ranges, Southern California", USGS Prof. Paper 1030, Washington, D.C.

Schigidi, A. and Garcia, L. A. (2003). "Parameter Estimation in Groundwater Hydrology Using Artificial Neural Networks", Journal of Computing in Civil Engineering, Vol. 17, No. 4, p281-289

Sorooshian, S., Duan, Q. and Gupta, V.K. (1993). "Calibration of Rainfall-runoff Models: Application of Global Optimization to the Sacramento Soil Moisture Accounting Model", Water Resources Research, Vol.29, No.4, p1185-1194

Strahler, A. N. (1957). "Quantitative Analysis of Watershed Geomorphology", Amer. Geophys. Union Trans., Vol.38, p913-920

Tatum, F. E. (1963). "A New Method of Estimating Debris-storage Requirements for Debris Basins," Proceedings, Federal Inter-Agency Sedimentation Conference, Jackson, MS, 28 January-1 February 1963, US Department of Agriculture, Agriculture Research Service Miscellaneous Publication No. 970, Paper No. 89, pp 886-898

Takagi, T. and Sugeno, M., (1985). "Fuzzy Identification of Systems and its Applications to Modeling and Control," IEEE Transactions on Systems, Man, and Cybernetics, Vol.15, p116-132

Tayfur, G., Ozdemir, S., and Singh, V.P. (2003). "Fuzzy Logic Algorithm for Runoff-induced Sediment Transport from Bare Soil Surface", Advances in Water Resources, Vol.26, p1249-1256

Tokar, A. S., and Markus, M. (2000). "Precipitation-runoff Modeling Using Artificial Neural Networks and Conceptual Models", Journal of Hydrologic Engineering, Vol.5, No.2, p156-161

US Army Corps of Engineers, Los Angeles District (USACE, 2000). "Debris Method", Los Angeles District Method for Prediction of debris yield

Weigend, A. S., D. E. Rumelhart, and B. A. Huberman (1990). "Predicting The Future: A Connectionist Approach", Int. J. Neural Syst., Vol.1, No.3, p193-209

Wigmosta, M. S., Vail, L. W., and Lettenmarier, D. P. (1994). "A Distributed Hydrology-Vegetation Model for Complex Terrain", Water Resources Research, Vol.30, p1665-1669

William, J. R. and Berndt, H. D. (1972). "Sediment Yield Computed with Universal Equation", Journal of Hydrologic Engineering, Proc., ASCE, Vol.98, p2087-2098

Wu, S. Q., and Er, M. J. (2000). "Dynamic Fuzzy Neural Networks – a Novel Approach to Function Approximation", IEEE Transactions on Systems, Man, and Cybernetics, Vol.30, No.2, p358-364

Wu, T. H., Hall, J. A., and Bonta, J. V. (1993). "Evaluation of Runoff and Erosion Models", Journal of Irrigation and Drainage Engineering, Vol.119, No.4, p364-382